AD-769 237

RADIATIVE TRANSFER MODEL OF A PYROTECHNIC FLAME

Bernard E. Douda

Naval Ammunition Depot
Crane, Indiana

26 September 1973

DISTRIBUTED BY:

NTIS
National Technical Information Service
U. S. DEPARTMENT OF COMMERCE
5285 Port Royal Road, Springfield Va. 22151

UNCLASSIFIED

RDTR NO. 258
26 SEPTEMBER 1973

AD 769237

RADIATIVE TRANSFER MODEL OF A PYROTECHNIC FLAME

APPROVED FOR PUBLIC RELEASE; DISTRIBUTION UNLIMITED

PREPARED BY

RESEARCH AND DEVELOPMENT DEPARTMENT

NAVAL AMMUNITION DEPOT, CRANE, INDIANA

Reproduced by
NATIONAL TECHNICAL
INFORMATION SERVICE
U S Department of Commerce
Springfield VA 22151

UNCLASSIFIED

UNCLASSIFIED

Security Classification

ii

DOCUMENT CONTROL DATA - R & D

(Security classification of title, body of abstract and indexing annotation must be entered when the overall report is classified)

1. ORIGINATING ACTIVITY (Corporate author) Naval Ammunition Depot Crane, Indiana 47522	2a. REPORT SECURITY CLASSIFICATION UNCLASSIFIED
	2b. GROUP

3. REPORT TITLE

RADIATIVE TRANSFER MODEL OF A PYROTECHNIC FLAME

4. DESCRIPTIVE NOTES (Type of report and inclusive dates)

PhD Thesis

5. AUTHOR(S) (First name, middle initial, last name)

Bernard E. Douda

6. REPORT DATE 26 September 1973	7a. TOTAL NO. OF PAGES ~~175~~ 186	7b. NO. OF REFS 24
8a. CONTRACT OR GRANT NO. AIRTASK AIR310310C/159A/3R02402002	9a. ORIGINATOR'S REPORT NUMBER(S) RDTR No. 258	
b. PROJECT NO.		
c.	9b. OTHER REPORT NO(S) (Any other numbers that may be assigned this report)	
d.		

10. DISTRIBUTION STATEMENT

APPROVED FOR PUBLIC RELEASE; DISTRIBUTION UNLIMITED

11. SUPPLEMENTARY NOTES	12. SPONSORING MILITARY ACTIVITY Naval Air Systems Command Washington, D. C. 20360

13. ABSTRACT

A two-line radiative transfer model of a pyrotechnic illuminating flare flame was formulated and validated. The model is capable of predicting the spectral radiant flux of different illuminating flares from known system variables such as formula, size, and ambient pressure, these having been varied over a wide range. This was done without introducing assumptions which require ad hoc modifications of the model to describe different flares.

Relative radiant power spectra are presented of the flames from three different pyrotechnic flare formulas burning at ambient pressures of 760, 630, 300, 225, 150, 75, 30 and 6 torr. The sodium concentration in the flare formulas varies by a factor of 10 between each formula. The experimental spectra of these illuminating flare flames show the magnitude of sodium D line broadening as a function of ambient pressure and sodium atom density in the flame.

A set of theoretical spectra, computed using the two-line radiative transfer model, are presented for comparison with the experimental spectra. The correlation between theoretical and experimental spectra shows that an LTE radiative transfer model is useful for prediction of radiant power spectra of magnesium-alkali nitrate flares, or, alternatively, these flares are a predictable laboratory model radiative transfer system.

DD FORM 1473 (PAGE 1)

UNCLASSIFIED

Security Classification

0102-014-6600

UNCLASSIFIED
Security Classification

14 KEY WORDS	LINK A ROLE	LINK A WT	LINK B ROLE	LINK B WT	LINK C ROLE	LINK C WT
Flame						
Illuminating flare						
Pyrotechnics						
Magnesium						
Sodium nitrate						
Spectra						
Radiant power						

DD FORM 1 NOV 65 1473 (BACK)
(PAGE 2)

UNCLASSIFIED
Security Classification

RADIATIVE TRANSFER MODEL

OF A PYROTECHNIC FLAME

BY

BERNARD EDWARD DOUDA

Submitted to the Faculty of the Graduate School
in partial fulfillment of the requirements
for the degree of Doctor of Philosophy
in the Department of Chemistry
Indiana University
October, 1973

V

September 24, 1973

To the Dean and Faculty of the Graduate School:

We, the undersigned members of the Faculty of the Graduate School and members of the Ph.D. Committee appointed for the examination of Bernard E. Douda, examined him on Monday, September 24, 1973.

It is hereby certified that he has successfully passed the examinations in major and minor subjects.

We recommend Mr. Douda for the Degree Doctor of Philosophy.

Chairman _____
(Research Adviser)

_____

_____

_____

September 24, 1973

This is to certify that the thesis submitted by Bernard Edward Douda has been accepted by the Ph.D. Advisory Committee as satisfactory in partial fulfillment of the requirements for the Ph.D. degree.

Chairman _____
E. J. Blair, Research Adviser

_____
G. E. Ewing

_____
D. A. McQuarrie

_____
R. A. D. Wentworth

ABSTRACT

A two-line radiative transfer model of a pyrotechnic illuminating flare flame was formulated and validated. The model is capable of predicting the spectral radiant flux of different illuminating flares from known system variables such as formula, size, and ambient pressure, these having been varied over a wide range. This was done without introducing assumptions which require *ad hoc* modifications of the model to describe different flares.

To solve the transfer equation for observed radiant intensity, the flame is represented by a model whose main characteristics are (a) the flame is a homogeneous gaseous atmosphere with plane-parallel stratification, (b) the gas consists of inert molecules plus sodium atoms which can be excited to the $^2P_{\frac{1}{2}}$ or $^2P_{\frac{3}{2}}$ level, (c) there is local thermodynamic equilibrium governed by the local temperature, (d) the temperature gradient can be represented by a parabola whose vertex is at the center of the flame, (e) the dispersion profile and number density of sodium atoms have average values, inside the flame, that are independent of depth, and (f) the individual line dispersion profile is replaced with a two-line function to simultaneously describe the spectral distribution of both of the sodium D lines.

The parameters of the radiative transfer theory were supplied from calculated thermodynamic properties of the flare. Optical thickness as a function of position in the flame was determined using

computed sodium atom densities and physical flame size was obtained photographically. A flame temperature gradient was constructed numerically as a function of temperature in the flame using the computed adiabatic temperature at the flame center and the boundary. The two-line dispersion profile was constructed as a function of line broadening. The magnitude of the broadening was computed *a priori*.

Relative radiant power spectra are presented of the flames from three different pyrotechnic flare formulas burning at ambient pressures of 760, 630, 300, 225, 150, 75, 30 and 6 torr. The sodium concentration in the flare formulas varies by a factor of 10 between each formula. The experimental spectra of these illuminating flare flames show the magnitude of sodium D line broadening as a function of ambient pressure and sodium atom density in the flame.

A set of theoretical spectra, computed using the two-line radiative transfer model, are presented for comparison with the experimental spectra. The correlation between theoretical and experimental spectra shows that an LTE radiative transfer model is useful for prediction of radiant power spectra of magnesium-alkali nitrate flares, or, alternatively, these flares are a predictable laboratory model radiative transfer system.

ACKNOWLEDGEMENTS

The author wishes to sincerely thank, Professor Edward J. Bair, Indiana University for his guidance and assistance during this research problem. His frequent encouragement was an important part in the progress of the work and his counsel contributed significantly to the development of the researcher.

Thanks are also due to Professor H. R. Johnson, Department of Astronomy, Indiana University and Dr. D. G. Hummer, Joint Institute of Laboratory Astrophysics, Boulder, Colorado for many helpful discussions and comments. Special thanks are due to Mrs. Sondra Williams for typing the manuscript.

The understanding of my wife, Marjorie, and my family is especially appreciated.

Finally, the financial support of Naval Air Systems Command, Research Administration Office, Dr. H. Rosenwasser, is gratefully acknowledged.

B.E.D.

TABLE OF CONTENTS

	Page
INTRODUCTION	1
EXPERIMENTAL	4
Measurement Parameters	4
Experimental Apparatus	5
Data Collection	6
Physical Flame Depth	6
Wavelength Calibration	6
Radiant Power Determination	7
Data Averaging	10
Results	11
DETERMINATION OF THERMODYNAMIC PARAMETERS	14
THEORETICAL	16
The Radiative Transfer Equation	16
Justification for LTE Assumption	20
Construction of 2-line Voigt Function	24
Superposition of Broadening Mechanisms	25
Voigt Function a Parameter	26
Optical Thickness	30
Radial Temperature Profile in Flame	30
DISCUSSION	32
REFERENCES	36
APPENDICES	54
A. Relative Power Spectra of All Flares Tested	55
B. Derivation and Integration of Radiative Transfer Equation	136
C. Program LTE4 to Solve Radiative Transfer Equation	143

INDEX OF FIGURES

Figure		Page
1.	A schematic of the experimental set-up	42
2.	Illuminating Flare Flame Spectra at 760, 630, 300, and 225 torr	44
3.	Illuminating Flare Flame Spectra at 150, 75, 30, and 6 torr	46
4.	Theoretical Φ and experimentally measured Φ' flare relative radiant power as a function of pressure	48
5.	Theoretical ΔW_R and experimentally measured $\Delta W_R'$ widths as a function of pressure	50
6.	Theoretical $\Delta W_{\frac{1}{2}}$ and experimentally measured $\Delta W_{\frac{1}{2}}'$ half-widths as a function of pressure	52
A1-A80	Relative power spectra of all flares tested	56-135
B1.	Model of flame as homogeneous gaseous atmosphere with plane-parallel stratification	142

INDEX OF TABLES

Table		Page
I.	Flare formulations	39
II.	Flare mean burning time, sodium atom number density, and adiabatic flame temperature	40
III.	Values of the source function $S(\tau)$ as a function of depth τ	41

INTRODUCTION

The purpose of this research is to characterize the mechanism responsible for the large luminous efficacy of the magnesium-sodium nitrate pyrotechnic flare and to determine whether radiative transfer theory predicts the spectral radiant power of different illuminating f[illegible] with large variations of system variables such as formula, flare diameter, and ambient pressure.

Preliminary research[1] showed that the major component of the emission from magnesium-sodium nitrate flares is a continuous spectrum, called the sodium resonance-line continuum. The emission occurs in a broad but variable region on either side of the sodium resonance lines. The resonance-line continuum from large flares at atmospheric pressure extends for several hundred angstroms more or less symmetrically about the sodium D lines, which are strongly reversed. The spectrum can be characterized by a parameter, $\Delta W_R = |\lambda_{max} - \lambda_R|$, the difference between the sodium D_2 line wavelength λ_R and the wavelength of maximum spectral flux density λ_{max} located on the short wavelength side of the sodium D_2 line. The value of ΔW_R increases with increasing size of flare and increasing ambient pressure. The resonance-line continuum is many orders of magnitude greater than can be attributed to any simple consideration of Doppler or Lorentz effects, suggesting that some other mechanism, such as that provided by radiative transfer theory, must give rise to the resonance-line continuum. Understanding the

origin of the resonance-line continuum appears at this point to be the key to a more quantitative understanding of the radiant flux from magnesium-sodium nitrate flares.

Further research[2] compared the energy radiated by the sodium resonance-line continuum with the energy of the flare reaction to further characterize the mechanism that gives rise to this continuum. Additionally, an observed high-resolution radiant power emission spectrum from a 10.8 cm diameter flare at atmospheric pressure was compared to a spectrum predicted by radiative transfer of emission from sodium-D lines. The Hummer and Rybicki formalism[3] was used to solve the radiative transfer equation. The flare flame was represented by a model in which the flame is an isothermal atmosphere and the Planck function, Voigt function, and deexcitation probability γ have average values, inside the flame, that are independent of optical depth τ where γ is the probability per collision that an emitter will be deexcited by the collision. The doublet sodium D lines at 589.0 and 589.6 nm were taken to be a single line with an oscillator strength of unity. This model yielded reasonable agreement between the computed spectrum and the experimental spectrum of a 10.8 cm diameter flare with high sodium atom density burning at atmospheric pressure. However, the model is incapable of predicting the spectral distribution of the D lines as a resolved doublet with each of the D_1 and D_2 lines strongly reversed at line center as occurs in low pressure-low sodium atom number density flames.

Furthermore, the defects caused by this and the isothermal assumption were somewhat arbitrarily mitigated by treating γ as an adjustable parameter. To overcome these deficiencies, a more detailed model was needed which included provision for a temperature gradient distributed radially through the flare flame, for treatment of the D lines as a doublet, and for determining all parameters of the theory from ambient flare conditions with no parameters to be adjusted.

The purpose of the present research is to formulate and validate a two-line model of the pyrotechnic illuminating flare flame capable of predicting the spectral radiant flux of different illuminating flares from known system variables such as formula, size, and ambient pressure, these having been varied over a wide range, and to do this without introducing assumptions which require *ad hoc* modifications of the model to describe different flares. To do this we shall first present experimental radiant power spectra of three different flare formulas burned at eight different ambient pressures, then describe the determination of thermodynamic parameters; namely, sodium atom number density and adiabatic flame temperature, and finally compare the experimental spectra with radiant power spectra obtained theoretically using a two-line radiative transfer model of the flame at local thermodynamic equilibrium containing a temperature profile distributed radially through the flame.

EXPERIMENTAL

The spectral radiant intensity of illuminating flames fluctuates considerably due to normal variables of the flare manufacturing process. Flare combustion also becomes increasingly more irregular as the ambient pressure is reduced. The sodium concentration in the flare formula and the ambient pressure were chosen to cover a wide range to make variability of the flare radiative output small compared to changes due solely to sodium concentration and ambient pressure. The effect of sodium concentration and ambient pressure changes is therefore completely unambiguous even in the presence of relatively large flare output fluctuations.

Measurement Parameters

Each of three different illuminating composition formulas was tested at 8 levels of pressure; namely 760, 630, 300, 225, 150, 75, 30 and 6 torr. For each pressure-formula combination, the burning time, flame size, and relative spectral radiant power distribution in the visible region were recorded.

The test flares were composed of 50 g of a magnesium-sodium nitrate-binder mixture compressed into 3.3 cm i.d. by 5.5 cm long paper tubes, having formulas shown in Table I. Formula groups 1, 2, and 3 are nearly stoichiometric mixtures, the sodium nitrate in groups 2 and 3 being .1 and .01 of group 1 respectively. Stoichiometry

was maintained in groups 2 and 3 by addition of potassium nitrate chosen because it reacts with magnesium at about the same rate as sodium nitrate and because of its low-emissivity in the neighborhood of the sodium D lines, the region of interest for these studies.

Experimental Apparatus

Fig. 1 shows the experimental arrangement. The test flares F were positioned inside a 6 m^3 vacuum chamber, centered between windows W_1 and W_2, the flares burning cigarette fashion with the flame projecting upward. Simultaneously, as each flare burned, the camera viewed the flame through window W_2 and plate glass G to record flame size. The grating spectrograph was used to record the spectral distribution of the flame through aperture A, window W_1, and mirror M. The burning duration Δt was measured with a stopwatch. Table II contains flare burning time averages $\overline{\Delta t}$. A He-Ne CW laser and Ar ion pulse laser were used to maintain alignment of the spectrograph with the flare and to provide wavelength calibration points.

A 3m Jarrell Ash Model JA-78 spectrograph using a 30 micron entrance slit and fitted with a tracking camera was positioned to view a 3 cm wide by 5 cm high region of the flame defined by A on the flare axis centered on a point about 3 cm above the burning surface. The optical path was changed 90° by a retractable front

surface plane mirror M between the slits S and window W_1. Kodak Linagraph Shellburst 35 mm film with typical usable range of 400 to 700 nm was exposed to the flare for a known time period chosen to provide film transmittance in the range 0.2 to 0.8 in the vicinity of the sodium D lines, the region of maximum interest.

Data Collection

Physical Flame Depth

Each flame was photographed with a 35 mm camera using Kodak Plus-X film through an ND2 neutral density filter at f/4 lens stop for 1/125 sec. The exposure settings and 150 cm object distance were constant for all tests. A grid of reference marks of known spacing, photographed while in the flare location, was used to establish a linear scale for measuring the flame size recorded on the film. The total physical flame depth z' was taken to be the distance between equal film density regions at the flame edge perpendicular to the flame axis and through a point 5 cm from the flare surface. The same film density was used in examining all photographs.

Wavelength Calibration

To calibrate the spectrograph film for wavelength, an argon ion and helium-neon laser were exposed to the film providing lines at 476.5, 488.0, 496.5, 514.5 and 632.8 nm. In addition, Na D

lines at 588.99 and 589.59 nm, Na doublet at 568.3 and 568.8 nm, Na doublet at 615.4 and 616.1 nm, K lines at 578.2, 580.2, 581.2, and 583.2 nm, and the Ba line at 553.6 nm, appearing in the flare spectra, were used as calibration points. The Ba line appears in the flare spectra as an impurity originating from residue of the composition used to ignite the flare. The ignition composition was 10% boron and 90% barium chromate.

Radiant Power Determination

To determine the relative spectral radiant power of the flare, it is necessary to apply corrections which represent (a) the relationship between the irradiance working standard used during the experiment and an irradiance standard traceable to NBS, (b) the spectral characteristics of the window-mirror arrangement, and (c) the relative power of the irradiance working standard and the flare. These three corrections appear as time ratios in the expression for the relative spectral radiant power of the flare Φ_λ' at wavelength λ

$$\Phi_\lambda' = k\, E_\lambda^\circ (t_1/t_1^\circ)(t_2^\circ/t_2)(t_3^\circ/t_3) \ , \qquad (1)$$

where k is a proportionality constant and E_λ° is the working standard irradiance. Each of the time ratios is, in effect, a calibration factor. The two times in a given ratio are those required to expose the film to the same density for each of the two sources or source arrangements being compared. The ratios are

measured at film positions corresponding to each wavelength. In each case, t_x° represents the time for direct exposure of the spectrograph film to the working irradiance standard, where x=1,2, or 3.

The ratio (t_1/t_1°) compares system characteristics. The flare flux passes through window W_1 and subsequently is reflected by mirror M onto spectrograph slit S as shown in Fig. 1. The spectrograph film was exposed for time t_1 to the spectral irradiance working standard from position F with mirror M in place. This is called system exposure. The film was also exposed with the working standard in position L and with the mirror M retracted. This is called direct exposure. The optical path length was 254 cm in each case. The transmittance τ_λ of the window and reflectance ρ_λ of the mirror are taken into account by t_1. The comparison of t_1 to the time t_1° for direct exposure of the film to the working standard is in effect a correction for losses due to the window and mirror.

The ratio (t_2°/t_2) compares the working standard irradiance to that of the flare. In each case, the film was exposed to the flare for a known time period t_2 chosen to provide film transmittance between 0.2 and 0.8 in the vicinity of the sodium D lines. The ratio (t_3°/t_3) compares the working standard direct exposure to NBS irradiance standard direct exposures.

To obtain exposures at the various times needed to evaluate each of the three ratios, exposures were placed on each film in a similar pattern. Each film contained one exposure of the source or source arrangement to be evaluated, and multiple time exposures of a reference source. The reference exposure times were chosen to include the upper and lower limits of film density for the source exposure.

To determine the ratio (t_1/t_1°), the value of t_1° for a working standard direct exposure having the same film density as the working standard system exposure t_1 is interpolated from the various reference exposures of t_1°. To determine the ratio t_2°/t_2, the value of a working standard direct exposure time t_2° for a reference exposure having the same film density as the flame exposure t_2 is interpolated from the various reference exposures t_2°. To determine t_3°/t_3, the value of t_3 for an NBS standard direct exposure having the same film density as the working standard direct exposure t_3° is interpolated from the various exposures of t_3.

To perform the interpolations, the transmittance $\tau_{n\lambda}$ of each of n exposures on the film was measured with a scanning densitometer. Transmittance values of the n reference source exposures were used to construct a calibration curve for the film for each wavelength interval $\Delta\lambda(.1\mathring{A} \leq \Delta\lambda \leq 1\mathring{A})$. The interval was determined by the resolution required. The calibration curve, a plot of film transmittance $\tau_{n\lambda}$ against $\log_{10} t_{n\lambda}$, where $t_{n\lambda}$ is the exposure time for reference source n, is roughly linear over the useful range. By interpolation,

a time ($t_1°$, $t_2°$ or t_3) is found where the film densities of the source and reference exposures are equal. That time corresponds to t_1, t_2 or $t_3°$ of the source exposure respectively. The times $t_1°$, $t_2°$, and t_3 found in this manner are used to evaluate Eq. (1).

Data Averaging

The film transmittance data from the densitometer fluctuated over a range of about 10% of the mean value due to film inhomogeneities such as graininess and emulsion blemishes. To minimize these fluctuations, the data were smoothed by averaging adjacent wavelength positions. In effect, the procedure was to record spectra at higher resolution than was actually needed, then apply to the resultant data a mathematical slit function which was wider than the physical slit width. In this running average method, the i-th value of the transmittance is

$$\tau(i) = \left[\sum_{j=i-k}^{j=i+k} \tau(j) \right] / (2k+1) \ , \qquad (2)$$

where $i = k+1, k+2, k+3, \ldots, n-k$ and n is the number of data points in the spectrum. The slit function parameter, $2k+1$, is the number of data points over which the average is taken. This is made as large as needed to achieve desired smoothing without distorting the spectrum.

Data averaging was kept to a minimum. Smoothing was performed on the spectral correction data resulting from the product of $E_\lambda°$, $(t_1/t_1°)$ and $(t_3°/t_3)$ using k=5. In this case the average value of a point was influenced only by data within ±5 Å. Individual transmittance curves used to determine the above ratios were not smoothed. Transmittance values of the multiple reference exposures of the working standard used to obtain $t_2°$ were averaged using k=4 causing only data within ±4 Å to influence the averaged value. No data averaging was applied to any of the flare exposures.

Results

Relative radiant power spectra P_λ' of typical flares for each pressure-formula combination are plotted in Figs. 2 and 3. Relative power spectra of all the flares tested during the present research are plotted in Appendix A. The solid curves in Figs. 2 and 3 are the experimental data. These spectra were normalized so that the peak value is unity for convenience in the first step of the theoretical comparison. Spectra were not obtained for formula groups 2 and 3 at 6 torr because the flares did not sustain combustion at this pressure. Group 1 flares at 6 torr barely burned. Combustion difficulty was visually observable for all flares tested at 75 torr or less. The lengthening of the flare burning time (decreasing burning rate) with pressure reduction is shown in Table II.

The relative radiant power Φ' of each flare was obtained by numerical integration of the flare relative radiant power spectrum Φ_λ' (before normalization) over the wavelength interval of interest. Because the radiant intensity of these flames fluctuates considerably even under normal conditions, flare radiant power values are most difficult to pin down, particularly at low pressures where combustion is especially irregular. Nevertheless, flare radiant power values, relative over the whole family of flares, are plotted in Fig. 4 for comparison with theoretically predicted power values.

Parameter $\Delta W_R'$, the difference between the sodium D_2 resonance wavelength λ_R and the wavelength of maximum spectral flux density at shorter wavelength than λ_R, was obtained directly from the flare radiant power spectrum Φ_λ'. Values of $\Delta W_R'$ for each pressure-formula combination are plotted in Fig. 5 where they are compared with values obtained theoretically.

The flare spectrum half-width $\Delta W_{\frac{1}{2}}'$, measured directly from the flare power spectrum Φ_λ', is plotted in Fig. 6 for each pressure-formula combination. The flare spectrum half-width, like the radiant power Φ', fluctuates considerably during normal flare burning. For this reason, representative half-width values are difficult to obtain. Furthermore, an ambiguity in the definition of $\Delta W_{\frac{1}{2}}'$ arises at pressures low enough for each of the reversed components of the Na doublet to be resolved. The nature of the ambiguity is resolved in the discussion.

The physical flame depth z' of each flare was measured from the photographic negative of the flare flame. Values of z' range from 6 cm for formula group 1, 760 torr to 2.5 cm for formula group 3, 30 torr, a rather narrow range considering the large range of experimental conditions.

DETERMINATION OF THERMODYNAMIC PARAMETERS

To solve the equation of radiative transfer, it is necessary to know the flame optical thickness and flame particle velocities which govern broadening half-widths. These can be calculated knowing values for gaseous sodium atom number density in the flame N_0 and adiabatic flame temperature T_0. As far as the radiative transfer model is concerned, knowing T_0 and N_0 are therefore necessary and sufficient conditions for solution of the transfer equation for the model to be described.

Values for these parameters could be obtained relatively unambiguously. The equilibrium composition of the combustion species (mole fractions) and the adiabatic temperature were computed using the computer program developed by Gordon and McBride.[4] The program uses a free-energy minimization technique to determine the dynamic equilibrium flame properties. The calculation recognizes condensed as well as gaseous species. Thermodynamic functions such as specific heat, enthalpy, and entropy are calculated as functions of temperature for the reactants and combustion species, for solid, liquid, and gas phases. These are incorporated in the program in the form of least squares coefficients, having been derived mainly from data taken from JANAF Thermochemical Tables.[5]

Using ambient pressure, flame formula, and enthalpy values of the reactants as input parameters,[4] the adiabatic temperature T_0 and the equilibrium composition were computed for each pressure-

formula combination. It is estimated that 30% of the heat of combustion of the material in the observation region is lost through radiative, convective, and conductive processes. This loss bears a reasonable relation to the 25% reported[7] for flares of larger size.

The ratio of gaseous atomic sodium mole fraction to mole fraction of all gaseous species is β, the atomic sodium partial pressure being the product of β with ambient pressure P. The number density of gaseous sodium atoms N_0 in the flame was computed by the ideal gas equation

$$N_0 = (P\beta)/RT_0 , \qquad (3)$$

where R is the ideal gas constant. Values of T_0 and N_0 are provided in Table II for each ambient pressure-formula combination.

THEORETICAL

The Radiative Transfer Equation

Diffusion of radiation through a gaseous atmosphere produces behavior that is qualitatively similar to that of the observed resonance-line continuum. When the gases of the flame are transparent only in the extreme wings of the line scattering profile, maxima develop on either side of the line and a minimum develops at the resonance position, where the optical depth is greatest.[7] However, the broadening observed in pyrotechnic flare flames can be extraordinary in comparison with that which is normally treated by radiative transfer theory.

A radiative-transfer mechanism was tested by numerical integration of the transfer equation[8] using parameters in the range of those expected in flares of widely different formulas burning at ambient pressures ranging from 760 to 6 torr. The total radiant intensity $I_{\nu\mu}(\tau)$ at frequency ν in a direction described by $\mu = \cos\theta$ and issuing from a volume element at optical depth τ is given by the radiative-transfer equation

$$\mu dI_{\nu\mu}(\tau)/d\tau = \phi_{\nu\alpha}[I_{\nu\mu}(\tau) - S_{\nu}(\tau)] , \qquad (4)$$

where $\mu = \cos\theta$ is the cosine of the angle of observation with respect to the outward normal to the flame surface. A detailed derivation and formal integration of the transfer equation is given in Appendix B. The optical depth τ is related to the

physical depth z by $\tau_\nu = \int k_\nu dz$, where k_ν is the absorptivity of the flame. The normalized spectral profile of the absorption coefficient $\phi_{\nu a}$ is a function which takes account of the flame line broadening mechanisms. Parameter a will be defined later. The line-source function $S_\nu(\tau)$ accounts for increments or decrements in the radiant intensity from a volume element at optical depth τ due to emitters and absorbers within that volume element. It is defined at a given frequency by $S_\nu = \epsilon_\nu / k_\nu$, where ϵ_ν is the monochromatic volume emission coefficient.

Formal integration of the transfer equation yields the expression

$$I_{\nu 1} = I_{\nu 2} \exp[-(\tau_2 - \tau_1)\, \phi_{\nu a}/\mu] + \int_{\tau=\tau_1}^{\tau=\tau_2} [S_\nu(\tau)\phi_{\nu a}/\mu] \exp[-(\tau - \tau_1)\phi_{\nu a}/\mu] d\tau \ , \quad (5)$$

where τ_1 and τ_2 are the optical depth integration limits from front to the rear of the atmosphere respectively, and $I_{\nu 1}$ and $I_{\nu 2}$ are the spectral intensity at optical depths τ_1 and τ_2 respectively. In order to solve the transfer equation, for the observed radiant intensity, the flame is represented by the following model.

(1) The flame is a homogeneous gaseous atmosphere with plane-parallel stratification.

( ) The gas consists of inert molecules plus sodium atoms which can be excited to the $^2P_{\frac{1}{2}}$ or $^2P_{\frac{3}{2}}$ level.

(3) There is local thermodynamic equilibrium LTE governed by the local temperature.

(4) Energy exchange by radiation leads to radiative equilibrium.

(5) The refractive index of the medium is unity.

(6) The radiation is unpolarized when emitted and remains unpolarized in its interactions with flame species.

(7) The temperature gradient can be represented by a parabola whose vertex is at the center of the flame.

(8) The absorption profile $\phi_{\nu a}$ and number density of sodium atoms N_0 have average values, inside the flame that are independent of τ.

The form of Eq. (5) has been simplified for the present case. (a) The observed flux is that emerging normal to the surface ($\mu=1$). (b) No flux is incident on the rear surface of the atmosphere ($I_{\nu 2}=0$). (c) $S_\nu(\tau) = B_\nu(T')$ for the LTE case. The Planck function is

$$B_\nu(T') = (2h\nu^3/c^2)[\exp(h\nu/kT')-1]^{-1} , \qquad (6)$$

where h is the Planck constant, c is the velocity of light, k is the Boltzmann constant, and T' is the flame temperature at flame optical depth τ. Under these conditions, integrating from the front surface, where z and τ_1 are 0, to the rear surface where $\tau_2 = \tau$, the total optical thickness, the monochromatic emergent intensity is

$$I_\nu^\circ = \phi_{\nu a}\int_{\tau=0}^{\tau=\tau} B_\nu(T') \exp(-\tau\phi_{\nu a})d\tau . \qquad (7)$$

Theoretical relative spectral radiant power Φ_ν, proportional to spectral emergent intensity I_ν° for a particular model, was found by numerical integration of Eq. (7) on a CDC 6600 digital computer using Simpson's rule of 2m intervals[7] described by

$$\int_a^b f(x)dx = \frac{h}{3}\left[f(a)+f(b)+2\sum_{i=1}^{m-1} f(x_{2i})+4\sum_{i=1}^{m} f(x_{2i-1})\right] - \frac{mh^5}{90} f^{(4)}(u), \quad (8)$$

where $m>0$ is an integer, $h = (b-a)/2m$ and $x_i = a+ih$ for $i=0,1, ---, 2m$. The Fortran program is listed in Appendix C.

Each computed spectrum Φ_λ, normalized so its power maximum is unity, was plotted for comparison with the corresponding experimentally determined flare spectrum Φ_λ' as shown in Figs. 2 and 3. The total radiant power Φ of the theoretical flare spectrum, plotted in Fig. 4 for each formula-pressure combination, was obtained by integration of Φ_ν over the spectral frequency region of interest, the latter having been multiplied by $B_{\nu_0}(T_0)$ where ν_0 is the line center frequency. Parameter ΔW_R, the separation between the wavelength of maximum flux density and the sodium D_2 line wavelength, and the spectrum half-width $\Delta W_{\frac{1}{2}}$ were each measured directly from the theoretical power spectrum Φ_λ. Parameters ΔW_R and $\Delta W_{\frac{1}{2}}$ are plotted in Figs. 5 and 6 respectively for comparison with the corresponding experimental parameters $\Delta W_R'$ and $\Delta W_{\frac{1}{2}}'$.

Parameters of the theory that must be supplied from properties of the flame are (a) optical thickness $\tau(z)$ as a function of position in the flame, (b) a flame temperature gradient $T'(z)$ as a function of position in the flame, and (c) the scattering profile a parameter in $\phi_{\nu a}$. Relative radiant power spectra were computed and compared with experimental spectra. It remains to show that combining these values with the model are, in fact, consistent with properties of the flame.

Justification for LTE Assumption

A source function which does not assume LTE can be expressed in terms of the radiation field as

$$S_\nu(\tau) = [(1-\gamma)\int_0^\infty J(\nu';\nu,\tau)\,\phi_a(\nu')\,d\nu'] + \gamma\, B_\nu(\tau)$$

where the mean intensity $J_{\nu\tau}$ is the simple average of intensity over all solid angles, ν is the frequency parameter out of the ν' frequency set, and the probability per collision of collisional deexcitation of sodium,

$$\gamma = C_{21}/\{C_{21} + A_{21}[1 - \exp(-h\nu_0/kT_0)]^{-1}\}\ , \qquad (70)$$

relates the rate of collisional deactivation C_{21} to the Einstein coefficient for stimulated emission A_{21}. For the sodium D lines[8] $A_{21} = 0.65\times10^8\ s^{-1}$ Hummer[6] observes that when γ

has its maximum value of unity, the source function $S_\nu(\tau)$ becomes the Planck function $B_\nu(T')$, i.e., LTE is valid. The determination of C_{21} will be described later. In the following, it will be shown that a value of γ large enough (nearly unity) to justify an LTE assumption exists at both experimental extremes of ambient pressure and sodium atom number density.

In the case where the ambient pressure P = 760 torr, the adiabatic temperature T_0 = 2939°K, and the sodium atom number density is $N_0 = 1\times10^{13}$ cm^{-3}, γ is about 0.35 when nitrogen, a major flame species with relatively low quenching cross section, is the only quenching species considered. An even larger value of γ is obtained when other flame species with larger quenching cross sections than that of nitrogen are considered. Under conditions of high temperature, ambient pressure, and sodium atom number density, the value of γ is sufficiently close to unity to justify the LTE assumption.

At the experimental limit of low pressure, temperature, and sodium atom number density where P = 30 torr, T_0 = 2500°K, $N_0 = 4.6\times10^{14}$, and N_2 as the effective quencher, γ is about 0.43. A more realistic flame species mixture, predominantly of N_2, CO, and CO_2, has an effective quenching cross section of 40×10^{-16} cm^2. For this mixture, the value of γ is about 0.61. In order for the LTE assumption to be valid in this range of values of γ, it is necessary for the terms of Eq. (9) to balance in such a way

that the resulting source function $S_\nu(\tau)$ equals the Planck function $B_\nu(T')$. Values of $S_\nu(\tau)$ were compared with $B_\nu(T')$ by the Hummer-Rybicki formalism.[8] Some typical values of the source function $S_\nu(\tau)$ at various optical thicknesses for $\gamma = 0.5$ and $\alpha = 0.01$ are listed in Table III. Except near the flame surface where the optical thickness is very small, the source function S_ν is approximately equal to the Planck value making the LTE assumption acceptable in this experimental limit as well.

In order to determine the value of γ by Eq. (10), the rate of collisional deactivation C_{21} is needed. C_{21} can be equated to the number of quenching collisions per second $Q_{21}(T)$ given by Hooymayers[9] as

$$C_{21}(T) = Q_{21}(T) = n_j \, \bar{v}_j \, \sigma_j \tag{11}$$

where n_j is the density of the quenching flame species, $\bar{v}_j$ is average relative velocity of approach of the colliding species, and σ_j is the specific quenching cross section. When the sodium atoms undergo quenching collisions in a mixture of flame molecules of different species, the quenching frequency is given by[9]

$$C_{21}(T) = Q_{21}(T) = \sum_{j=1}^{m} n_j \, \bar{v}_j \, \sigma_j \tag{12}$$

where j represents various species of flame molecules. The relationship[10] which describes $\bar{v}_j$ is

$$\bar{v}_j = [(\bar{v}_{NA}')^2 + (\bar{v}_j')^2]^{\frac{1}{2}} . \tag{13}$$

The mean speed $\bar{v}_{NA}'$, of the sodium particle and the mean speed $\bar{v}_j'$, of a particular species j of quenching particle is

$$\bar{v}_{NA}' = \bar{v}_j' = (8kTN_A/\pi M_j)^{\frac{1}{2}} , \tag{14}$$

where N_A is Avagadro's number and M_j is the molecular weight of sodium or species j as appropriate.

The ideal gas law was used to estimate the number density of quenching flame species n_j . Values of the specific quenching cross section σ_j between Na and quenching species N_2, O_2, H_2, CO, CO_2 and H_2O are 8, 34, 21, 41, 50, and 2.2×10^{-16} cm^2 respectively.[11] The dependence of σ_j on temperature has been reported[11] to be not much stronger than $\sigma_j \simeq T^{-1}$.

Construction of 2-line Voigt Function

Under conditions of low pressure and low sodium atom density, it is necessary to solve the transfer equation simultaneously for both of the sodium D lines in order to describe spectral distributions. One alternative for doing this is to replace their individual dispersion profile $\phi_{\nu a}$ in Eq. (7) with a 2-line function $V_a''(\nu)$. This approximation is valid because the D lines are strongly coupled,[12] thereby maintaining their relative strengths. A 2-line Voigt function profile is therefore applicable to the entire pressure and sodium density range encountered in the present research.

The 2-line Voigt function, $V_a''(\nu)$, was constructed numerically by generating the function for each line separately using the procedure described by Hummer,[13] then summing them.

$$V_a''(\nu) = \sum_{j=1}^{j=2} V_{aj}(\nu)[f_j/(f_1 + f_2)] , \qquad (15)$$

where $V_{a1}(\nu)$ and $V_{a2}(\nu)$ are single line Voigt functions, both with the same value of a, centered on the Na D_1 and D_2 line center frequency respectively. Oscillator strengths f_1 and f_2 of the Na D_1 and D_2 lines are 0.312 and 0.624 respectively.[14] Function normalization and relative line strength were maintained by multiplying $V_{aj}(\nu)$ by oscillator strengths whose weighted sum equals unity.

Superposition of Broadening Mechanisms

When the line is broadened by several independent effects, the distributions found for the individual kinds of broadening must be superimposed. The mathematics of this superposition is complicated by the fact that the functions which represent broadening fall into two classes, dispersive and non-dispersive. A superposition of dispersion functions results in a new dispersion function having a half-width equal to the sum of the half-widths. However, if heterogeneous functions are superimposed, each point on one interacts with every point on the other. Such superposition, referred to as convolution or folding, of a Lorentz with a Gaussian distribution results in a single line Voigt function

$$V_a(\nu) = \int_{-\infty}^{\infty} f_1(\nu-y)\, f_2(y)\, dy \ , \qquad (16)$$

where $f_1(\nu)$ is the Lorentz type profile and $f_2(\nu)$ is a Gaussian distribution.[14,15]

The normalized forms of the three functions are[5,16]

$f_1(\nu) = \pi^{-1}(1 + \nu^2)^{-1}$ Lorentz (dispersive)

$f_2(\nu) = \pi^{-1/2} \exp(-\nu^2)$ Doppler (Gaussian)

$$V_a(\nu) = \frac{a}{\pi^{\frac{3}{2}}} \int_{-\infty}^{\infty} \frac{\exp(-y^2)dy}{(\nu-y) + a^2} \qquad \text{Voigt (combined)} \quad (19)$$

where ν is the frequency measured from the line center in units of Doppler half-width and a is the dispersion parameter defined below.

Voigt Function a Parameter

The Voigt line profile that is used must take account of all of the factors which contribute to the line width in the absence of radiation transfer. Line broadening mechanisms which were considered in the present research are (a) natural broadening, a consequence of the Heisenberg uncertainty principle, (b) pressure broadening of both Holtsmark and van der Waals types, the result of collisions with like and unlike neutral species respectively, (c) broadening due to quenching collisions, and (d) Doppler broadening due to the relative motion of the radiating systems and the observer.[9,14,17] Pressure broadening caused by charged perturbers (Stark broadening) was neglected, the degree of sodium ionization in the flame being small as shown by computation of Na^+ concentration using the thermodynamic computer program developed by Gordon and McBride[4] as described earlier. The collective effect of these broadening mechanisms is accounted for by the Voigt function a parameter obtained from the relation

$$a = [(\Delta\lambda_N + \Delta\lambda_L + \Delta\lambda_R + \Delta\lambda_Q)/\Delta\lambda_D](\ln 2)^{\frac{1}{2}} , \qquad (20)$$

where $\Delta\lambda_N$, $\Delta\lambda_L$, $\Delta\lambda_R$, $\Delta\lambda_Q$, and $\Delta\lambda_D$ are the natural, Lorentz (unlike particle), resonance (like particle), quenching, and Doppler line broadening half-widths respectively, each to be evaluated separately below. The value of a evaluated by Eq. 20 for each of the three illuminating flare formulas is 6.8, 1.3, and 0.65 for Groups 1, 2, and 3 respectively at 760 torr and at conditions of the flame center. The values selected as the average value of a in the flame are 1.2, 0.4, and 0.3, which are in about the same ratio as the values at the flame center.

Values of a for other ambient pressures P were obtained by $a_P = P/760$, since the dominant broadening half-widths $\Delta\lambda_L$ and $\Delta\lambda_R$ are linear with the ambient gas pressure.[18]

The equation for Na D line natural broadening half-width is

$$\Delta\lambda_N(\mathring{A}) = 10^8 \lambda_0^2/2\pi\tau c = 10^8 \lambda_0^2 A_{21}/2\pi c \qquad (21)$$

where τ is the state lifetime and λ_0 is the line center wavelength (cm). $\Delta\lambda_N$ is 1.2×10^{-4} Å for the Na D_2 line.

The Doppler broadening half-width for the Na D_2 line is given by

$$\Delta\lambda_D = 2\times10^8[(2 R \ln 2)^{\frac{1}{2}}/c]\lambda_0(T_0/M)^{\frac{1}{2}} , \qquad (22)$$

where M is the sodium molecular weight (g). $\Delta\lambda_D$ = 0.0477 and 0.0474 Å at T_0 = 2939 and 2905°K respectively.

The collisional broadening half-width due to unlike species is given by

$$\Delta\lambda_L(\mathring{A}) = 10^8(2\lambda_0^2/\pi c)\sigma_L n_2 \{2\pi kT_0[(N_A/m)+(N_A/M)]\}^{\frac{1}{2}}, \qquad (23)$$

where σ_L is the optical cross section (cm^2), n_2 is the number density of perturbing species (cm^{-3}), and M and m are the molecular weights (g) of the emitting and perturbing species respectively. Rearrangement of Eq. 23 leads to

$$\Delta\lambda_L(\mathring{A}) = 10^8(\lambda_0^2/c)\sigma_L n_2(8kT_0N_A/\pi\mu)^{\frac{1}{2}}, \qquad (24)$$

where $\mu = [(mM)/(m+M)]$, the reduced mass. If the mean relative velocity of colliding species ($cm\ s^{-1}$) is

$$\bar{v}_j = (8kT_0N_A/\pi\mu)^{\frac{1}{2}}, \qquad (25)$$

where j is the species index, Eq. 24 can be written

$$\Delta\lambda_L(\mathring{A}) = 10^8(\lambda_0^2/c)\sigma_L n_2\bar{v}_j. \qquad (26)$$

If all non-sodium gaseous species are taken to be perturbing species, an upper limit is $n_2 = N_3 - N_0$, where $N_3(cm^{-3})$ is the total number density of the gaseous species in the flame computed from the ideal gas law at T_0. At 760 torr and using $\sigma_L = 60\times10^{-16}\ cm^2$ (reported by Hofmann and Kohn[19]), $\Delta\lambda_L = 0.0230$, 0.0371, and 0.0386 Å for formula groups 1, 2, and 3 respectively.

The resonance broadening half-width, resulting from interaction between like particles at high gas densities is[20]

$$\Delta\lambda_R(\mathring{A}) = [(3\times10^8)e^2 f N_o \lambda_o^3]/(4\pi^2 c^2 m_e) , \qquad (27)$$

where e is the elementary charge ($cm^{\frac{3}{2}} g^{\frac{1}{2}} s^{-1}$) and m_e is the electron rest mass (g). Broadening due to resonance interaction of like particles is dependent on the inverse cube of molecular separation whereas the broadening by two unlike particles under the same interaction force has an inverse sixth power dependence on the molecular separation.[19] Resonance broadening per atom is therefore very large. At 760 torr and f =1.0 for the Na doublet, calculated values of $\Delta\lambda_R$ are 0.442, 0.0481, and 0.00486 Å at $N_o = 1.01\times10^{18}$, 1.10×10^{17} , and 1.11×10^{16} cm^{-3} for formula groups 1, 2, and 3 respectively.

Hooymayers[9] describes the quenching process as a shortening of the radiative lifetime. The equation for quenching line half-width is

$$\Delta\lambda_Q(\mathring{A}) = 10^8 \lambda_o^2 [A_{21} + C_{21}(T)]/2\pi c . \qquad (28)$$

Calculated values of $\Delta\lambda_Q$ are 0.0014, 0.0022, and 0.0027 Å at 760 torr for formula groups 1, 2, and 3 respectively.

Optical Thickness

To evaluate Eq. 7, the optical thickness at physical depth z of the sodium resonance line is

$$\tau(z) = (h\nu_0/(4\pi\ \Delta\nu_D))(N_1 B_{12} - N_2 B_{21})z\ , \tag{29}$$

where B_{12} and B_{21}, the Einstein absorption and induced emission coefficients, are equal. The number density N_1 and N_2 of sodium atoms in the lower (^2S) state and upper (^2P) state, respectively, have average values inside the flame independent of flame depth z(cm). The Doppler half-width $\Delta\nu_D$ is in units of frequency. N_1 and N_2 are related to N_0 by the Boltzmann factor, $\exp(-h\nu/kT_0)$ where $N_0 \approx N_1$ and N_2 is negligible in comparison to N_1. Total optical thickness τ is obtained from Eq. 29 when z equals the total physical flame depth z', i.e. $\tau = \tau(z')$.

Radial Temperature Profile in Flame

The mass flow of a flare flame is characteristically along the flame axis. The optical path of interest in this research is along the flame radius, perpendicular to the mass flow. The radial temperature gradient $T'(z)$, along the optical path, is needed for evaluation of the radiative transfer equation where $T'(z)$ appears as a parameter of the Planck function.

There are two types of flame boundaries of interest here. The physical boundary is defined as the location of the interface between the ambient air and the flame medium containing sodium atoms. The optical boundary is defined as the location in the flame medium where luminescence ceases. These boundaries are not far apart physically. The temperature of the physical boundary must be below that of the optical boundary.

The radiative transfer calculation is sensitive to the temperature profile and physical boundary temperature. Parabolic temperature profiles have been reported[21] for high temperature media whose composition can be likened to the flare flame. Lewis and von Elbe[22] reported that sodium D line emission disappears below 1775°K, providing a temperature estimate for the optical boundary. Lowke[23] assigned a temperature of 1200°K to the physical (outer) boundary of a discharge in sodium vapor. Based on the above information, an approximately parabolic temperature gradient $T'(z)$ was constructed numerically to simulate the radial temperature gradient in the flare flame. A 1200°K physical boundary temperature was used. The temperature at the vertex of the parabola, coincident with the flame center ($z'/2$), was assigned equal to T_c, the adiabatic temperature.

DISCUSSION

Theoretical Φ_λ and experimental Φ_λ' relative radiant power spectra are plotted in Figs. 2 and 3 for the three formula groups at 8 levels of ambient pressure. Visual comparison of Φ_λ with Φ_λ' for each pressure-formula combination shows that the distribution computed from theory agrees quite well with the experimental distribution. A more detailed comparison can be made by considering relative values of three parameters which serve to characterize the spectrum. These are ΔW_R and $\Delta W_R'$ the distance from the sodium D_2 line wavelength to the wavelength of maximum flux density, $\Delta W_{\frac{1}{2}}$ and $\Delta W_{\frac{1}{2}}'$ the spectrum half-width, and Φ and Φ' the relative radiant power of the sodium D line emission, the superscript prime denoting the experimental parameter.

Some additional features appear in the experimental spectra shown in Figs. 2 and 3. These are (a) MgI $3p^3P$ - $4s^3S$ transitions at 516.7, 517.3 and 518.4 nm, (b) NaI $3p^2P$ - $4d^2D$ and $3p^2P$ - $5s^2S$ transitions at 568.3, 568.8, 615.4 and 616.1 nm. (c) KI $4p^2P$ - $7s^2S$ and $4p^2P$ - $5d^2D$ transitions at 578.2, 580.2, 581.2 and 583.2 nm, (d) a diffuse band, about 5nm wide, with maximum near 574 nm tentatively assigned[24] as being due to K_2 emission between an upper level bound state to a lower level repulsive state, and (e) a BaI $6s^1S$ - $6p^1P$ transition at 553.6 nm, barium being an impurity remaining from the boron-barium chromate composition used

to ignite the flares. No attempt was made to predict these features theoretically. Only sodium D line emission was treated in the radiative transfer model.

Careful visual examination of the radiant power spectra in Figs. 2 and 3 reveals that at line center and in the region between the two sodium D lines, theory predicts less radiant power than that observed experimentally, particularly when N_o is greater than 10^{17}. This difference is expected because the model uses average N_o for all flame regions and does not take account of substantial depletion of N_o (hence N_1) near the flame boundary as sodium atoms react with air to form Na_2O and Na_2O_2. In the line wings, the experimental power tends to be greater than that theoretically predicted in several cases particularly at higher N_o because of continuum radiation from condensed flame species such as solid magnesium oxide (smoke).

Parameters ΔW_R for the theoretical and $\Delta W_R'$ for the experimental spectra are plotted in Fig. 5. Except for the group 1 formula at 6 torr, where flare combustion was quite irregular making the experimental value doubtful, there is good agreement between the two values.

The theoretical $\Delta W_{\frac{1}{2}}$ and experimentally measured $\Delta W_{\frac{1}{2}}'$ half-widths of the radiant power spectra are plotted in Fig. 6 for comparison. Each of the continuous solid lines represents the theoretically determined half-width of sodium resonance lines

taken as a doublet. At these pressures and for these formula groups, the individual sodium D lines overlap to such a large degree that a half-width of the single line cannot be determined from the spectra. The dashed line and the individual points in Fig. 6 correspond to spectra in which half-width values of less than 10 angstroms are observed. In this region, overlap between the sodium D lines is small enough to require determination of the single line half-width. Although parameter $\Delta W_{\frac{1}{2}}'$ fluctuates considerably while the flare is burning making a representative value difficult to obtain, there is good agreement in all cases between the theoretical and experimental values plotted in Fig. 6.

The theoretical Φ and experimental Φ' total radiant power emitted in the region of the sodium D lines are plotted in Fig. 4 as a function of ambient pressure. Φ and Φ' both decrease with pressure, but the difference between the Φ and Φ' increases as the pressure decreases. Additionally, substantial dispersion of the experimental data is evident. Three factors contribute to the observed differences. First, combustion irregularity and fluctuating emissive flux were visually observable for all flares tested at 75 torr or less. These difficulties became more apparent as the pressure was reduced. Secondly, during the low pressure experiments, the intense radiative zone of the flame was visibly displaced outside the region viewed by the spectrograph, resulting in low power values for Φ'. Finally, as discussed earlier, the LTE

approximation is least acceptable at the lower pressures. The increasing deviation from LTE as the pressure is reduced makes assignment of the Planck value to the peak power increasingly unreliable, leading to overestimates of power values for Φ. Even in the presence of large flare output fluctuations and increasing differences between Φ and Φ' at the low pressures, the agreement between experimental and theoretical data is acceptable.

In summary, it has been shown that the spectral radiant power distribution of a pyrotechnic illuminating flare flame can be predicted by a two-line radiative transfer model which has been described. This can be done without introducing assumptions which require *ad hoc* modifications of the model to describe different flares. Known system variables such as flare formula, flare size, and ambient pressure are the necessary and sufficient input needed for the theoretical prediction.

REFERENCES

1. B. E. Douda, R. M. Blunt, and E. J. Bair, J. Opt. Soc. Am. 60, 1116 (1970).

2. B. E. Douda and E. J. Bair, J Opt. Soc. Am. 60, 1257 (1970).

3. D. G. Hummer and G. Rybicki, *Computational Methods for non-LTE Line-Transfer Problems* in *Methods in Computational Physics* (Academic Press, New York, 1967), Vol. 7, pp. 53-128.

4. S. Gordon and B. J. McBride, *Computer Program for Calculation of Complex Chemical Equilibrium Compositions, Rocket Performance, Incident and Reflected Shocks, and Chapman-Jouguet Detonations*, NASA SP-273, Lewis Research Center (1971). Available from National Technical Information Service, 5285 Port Royal Road, Springfield, Virginia 22151. #N71 37775.

5. D. R. Stull and H. Prophet, *JANAF Thermochemical Tables*, Second Edition, Nat. Stand. Ref. Data Ser , NSRDS-NBS 37 (Superintendent of Documents, U. S. Government Printing Office, Washington, D. C., June 1971).

6. D. G. Hummer, J. Quant. Spectrosc. Radiat. Transfer 8, 193 (1968).

7. D. G. Moursund and C. S. Duris, *Elementary Theory and Application of Numerical Analysis* (McGraw-Hill Book Company, New York, 1967), p. 191.

8. C. H. Corliss and W. R. Bozman, *Experimental Transition Probabilities for Spectral Lines of Seventy Elements*, NBS Monograph 53 (Superintendent of Documents, U. S. Government Printing Office, Washington, D. C., July 1962), p. 402.

9. H. P. Hooymayers and C. Th. J. Alkemade, J. Quant. Spectrosc. Radiat. Transfer 6, 501 (1966).

10. H. P. Hooymayers and C. Th. J. Alkemade, J. Quant. Spectrosc. Radiat. Transfer 6, 847 (1966).

11. H. P. Hooymayers and P. I Lijnse, J. Quant. Spectrosc. Radiat. Transfer 9, 995 (1969).

12. J. T. Jeffries, *Spectral Line Formation* (Blaisdell Publishing Company, Waltham, Massachusetts, 1968), pp. 17 and 191.

13. D. G. Hummer, Mem. R. Astr. Soc. 70, 1 (1965).

14. H. R. Griem, *Plasma Spectroscopy* (McGraw-Hill Book Company, New York, 1964), pp. 101 and 102.

15. J. Heberlein, *Nuclear Research - Spectroscopic Investigations of Alkali Lines Using Flame Temperatures*, (West German) Federal Ministry of Scientific Research Report K 67-19 (March 1967).

16. D. Mihalas, *Stellar Atmospheres* (W. H. Freeman and Company, San Francisco, 1970), pp. 251, 295 and 356.

17. W. Behmenburg and H. Kohn, J. Quant. Spectrosc. Radiat. Transfer 4, 163 (1964).

18. A. C. G. Mitchell and M. W. Zemansky, *Resonance Radiation and Excited Atoms* (Cambridge University Press, New York, 1971), p. 170.

19. F. W. Hofmann and H. Kohn, J. Opt. Soc. Am. 51, 512 (1961).

20. R. G. Breene, Jr., *The Shift and Shape of Spectral Lines* (Pergamon Press, New York, 1961), p. 226.

21. N. Ozaki, J. Quant. Spectrosc. Radiat. Transfer 11, 1111 (1971).

22. B. Lewis and G. von Elbe, *Combustion, Flames and Explosions of Gases* (Academic Press, New York, 1961), p. 281.

23. J. J. Lowke, J. Quant. Spectrosc. Radiat. Transfer 9, 839 (1969).

24. M. M. Rebbeck and J. M. Vaughan, J. Phys. B: Atom. Molec. Phys. 4, 258 (1971).

TABLE I. Flare Formulations

Ingredients	Formula Groups 1	2	3
Magnesium	44.0[a]	40.4	40.04
Sodium nitrate	51.5	5.15	0.515
Potassium nitrate	--	49.95	54.945
Epoxy binder mix	4.5	4.5	4 5

[a]Percent by weight

Table II . Flare mean burning time, computed number density of sodium atoms in flame, and computed adiabatic flame temperature of 3 flare formulas at 8 ambient pressures.

Pressure	Quantity	Flare Formula Groups 1	2	3
760 torr	$\overline{\Delta t}$ sec	28	28	26
	N_o cm^{-3}	1.01×10^{18}	1.10×10^{17}	1.11×10^{16}
	T_o Kelvin	2939	2905	2904
630 torr	$\overline{\Delta t}$	31	30	33
	N_o	8.46×10^{17}	9.20×10^{16}	9.26×10^{15}
	T_o	2920	2887	2886
300 torr	$\overline{\Delta t}$	30	35	37
	N_o	4.08×10^{17}	4.44×10^{16}	4.47×10^{15}
	T_o	2842	2816	2815
225 torr	$\overline{\Delta t}$	--	38	39
	N_o	3.08×10^{17}	3.34×10^{16}	3.37×10^{15}
	T_o	2812	2788	2787
150 torr	$\overline{\Delta t}$	35	41	44
	N_o	2.07×10^{17}	2.24×10^{16}	2.26×10^{15}
	T_o	2770	2748	2747
75 torr	$\overline{\Delta t}$	37	45	47
	N_o	1.05×10^{17}	1.14×10^{16}	1.15×10^{15}
	T_o	2698	2680	2679
30 torr	$\overline{\Delta t}$	52	59	66
	N_o	4.29×10^{16}	4.65×10^{15}	4.65×10^{14}
	T_o	2606	2592	2591
6 torr	$\overline{\Delta t}$	75	--	--
	N_o	8.90×10^{15}	9.63×10^{14}	9.70×10^{13}
	T_o	2453	2443	2442

TABLE III. Values of the source function $S(\tau)$ as a function of depth τ when $\gamma = 0.5$ and $\alpha = 0.01$.

$S(\tau)$	τ	
0.7070	0.0	front of flame
0.7288	0.1	
0.7919	0.5	
0.8398	1.0	
0.9540	5.0	
0.9803	1.0×10^{1}	
0.9961	5.0×10^{1}	
0.9973	1.0×10^{2}	
0.9987	5.0×10^{2}	
0.9990	1.0×10^{3}	
0.9994	5.0×10^{3}	
0.9996	1.0×10^{4}	
0.9997	5.0×10^{4}	flame center
0.7070	1.0×10^{5}	rear of flame

Fig. 1. A schematic of the experimental set up.

Legend: G - glass plate, W_1, W_2 - windows, F - flare, A - Aperture, L - irradiance standard, M - retractable mirror, and S - slit and shutter.

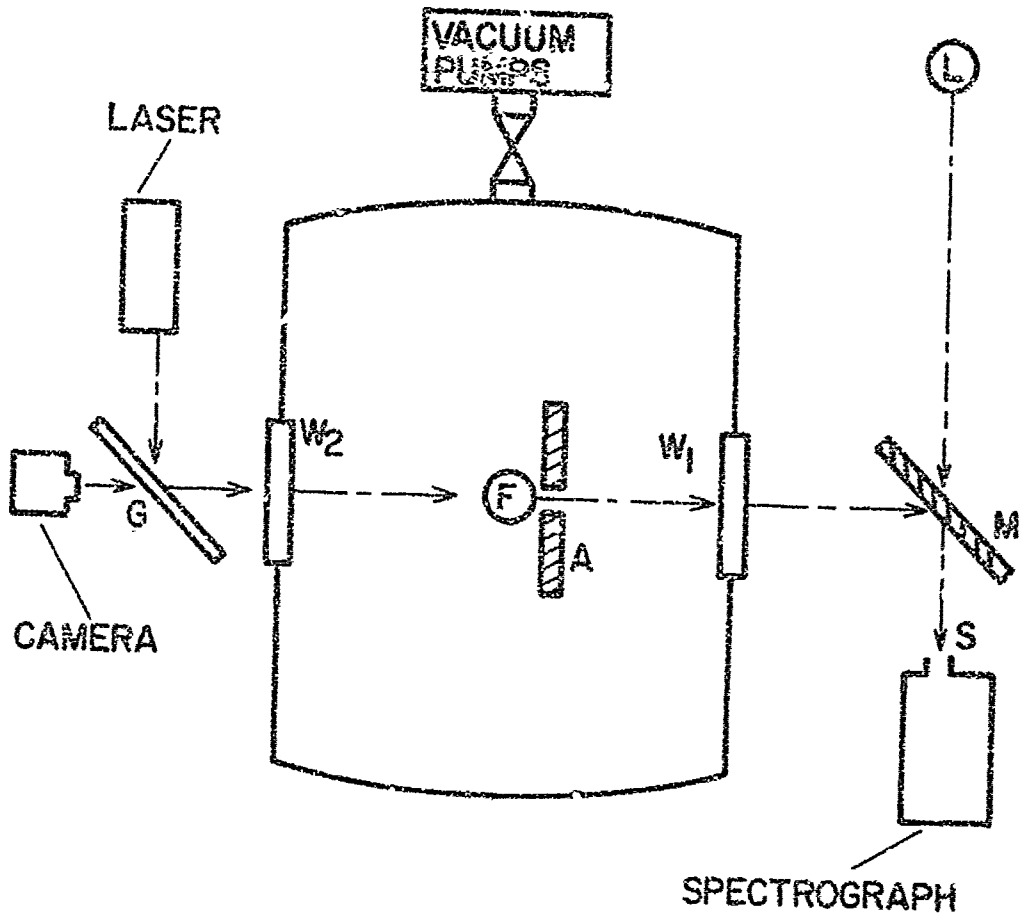
VACUUM PUMPS
LASER
L
W2
W1
F
A
G
M
CAMERA
S
SPECTROGRAPH

Fig. 2. Illuminating Flare Flame Spectra for formula groups 1, 2, and 3 at 4 levels of ambient pressure. Theoretical relative radiant power values ϕ_λ are indicated by boxes (▭). Experimentally determined relative radiant power values ϕ_λ' are shown by the solid line.

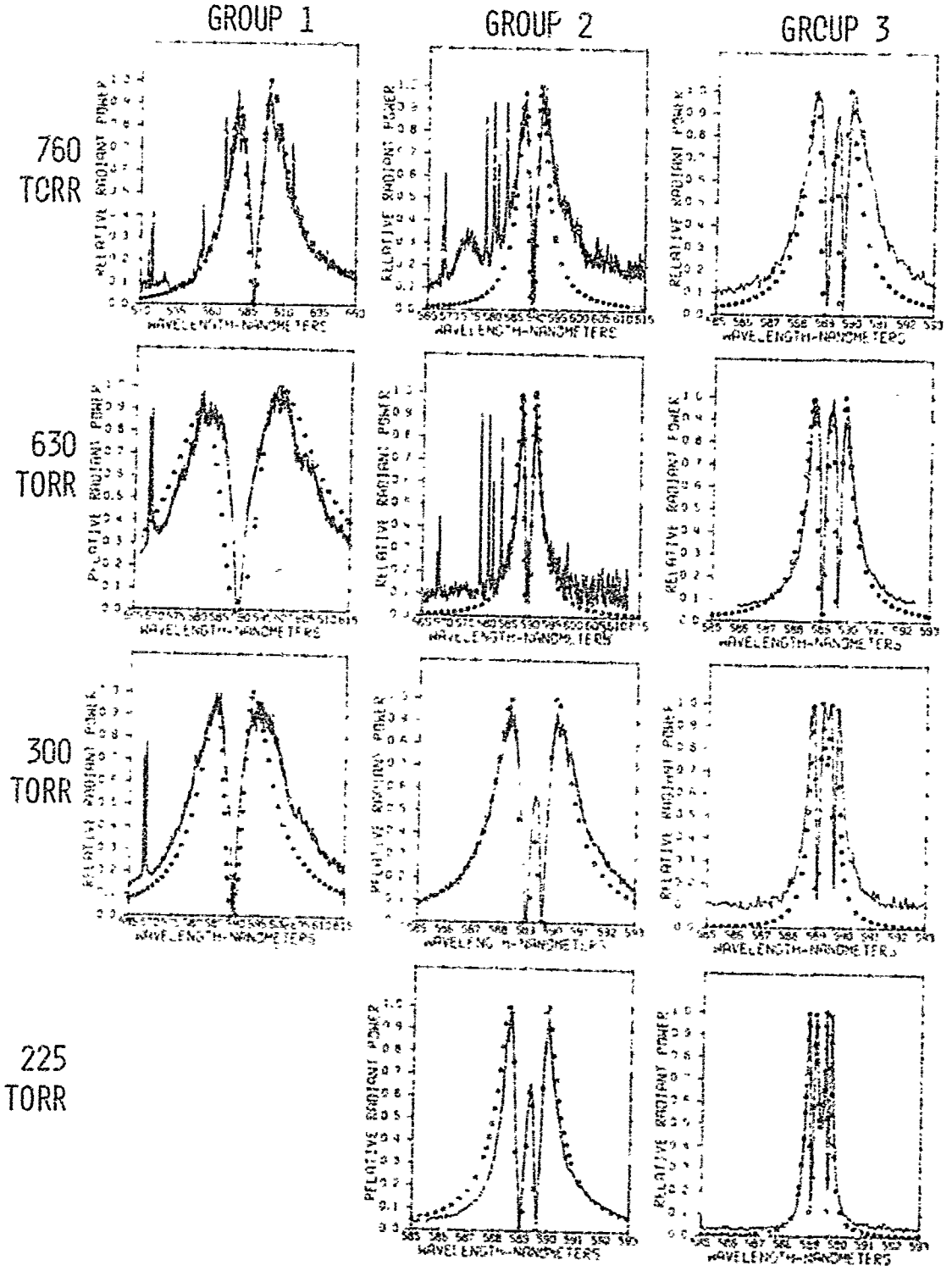
GROUP 1
GROUP 2
GROUP 3
760 TORR
630 TORR
300 TORR
225 TORR
RELATIVE RADIANT POWER
WAVELENGTH-NANOMETERS

Fig. 3. Illuminating Flare Flame Spectra for formula groups 1, 2, and 3 at 4 levels of ambient pressure. Theoretical relative radiant power values Φ_λ are indicated by boxes (▫). Experimentally determined relative radiant power values Φ_λ' are shown by the solid line.

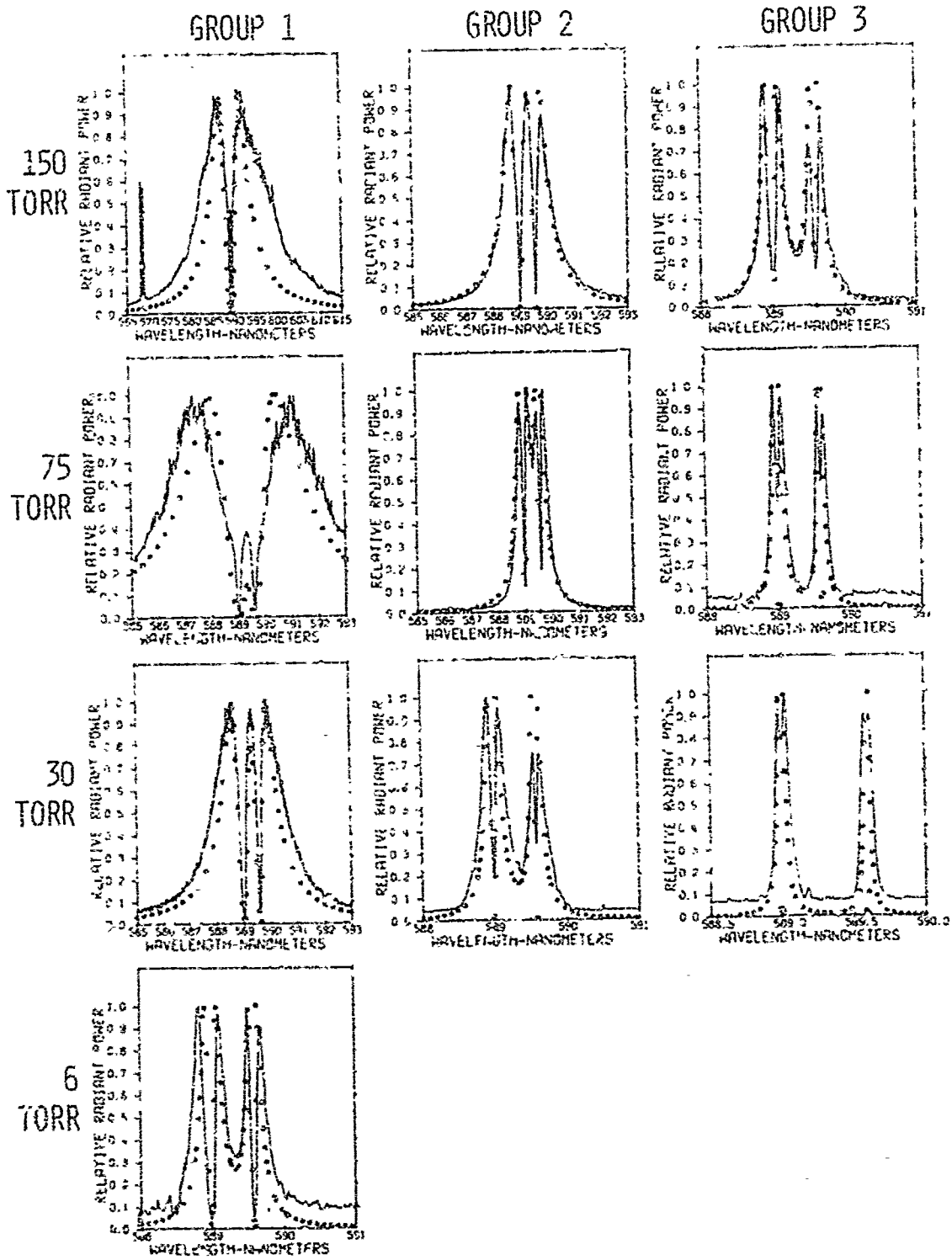
GROUP 1
GROUP 2
GROUP 3
150 TORR
75 TORR
30 TORR
6 TORR
RELATIVE RADIANT POWER
WAVELENGTH-NANOMETERS

Fig. 4. Theoretical Φ and experimentally measured Φ' flare relative radiant power as a function of pressure. Φ values are shown for formula groups 1, 2, and 3 by the solid lines and Φ' values are indicated by O, Δ, and X for formula groups 1, 2, and 3 respectively.

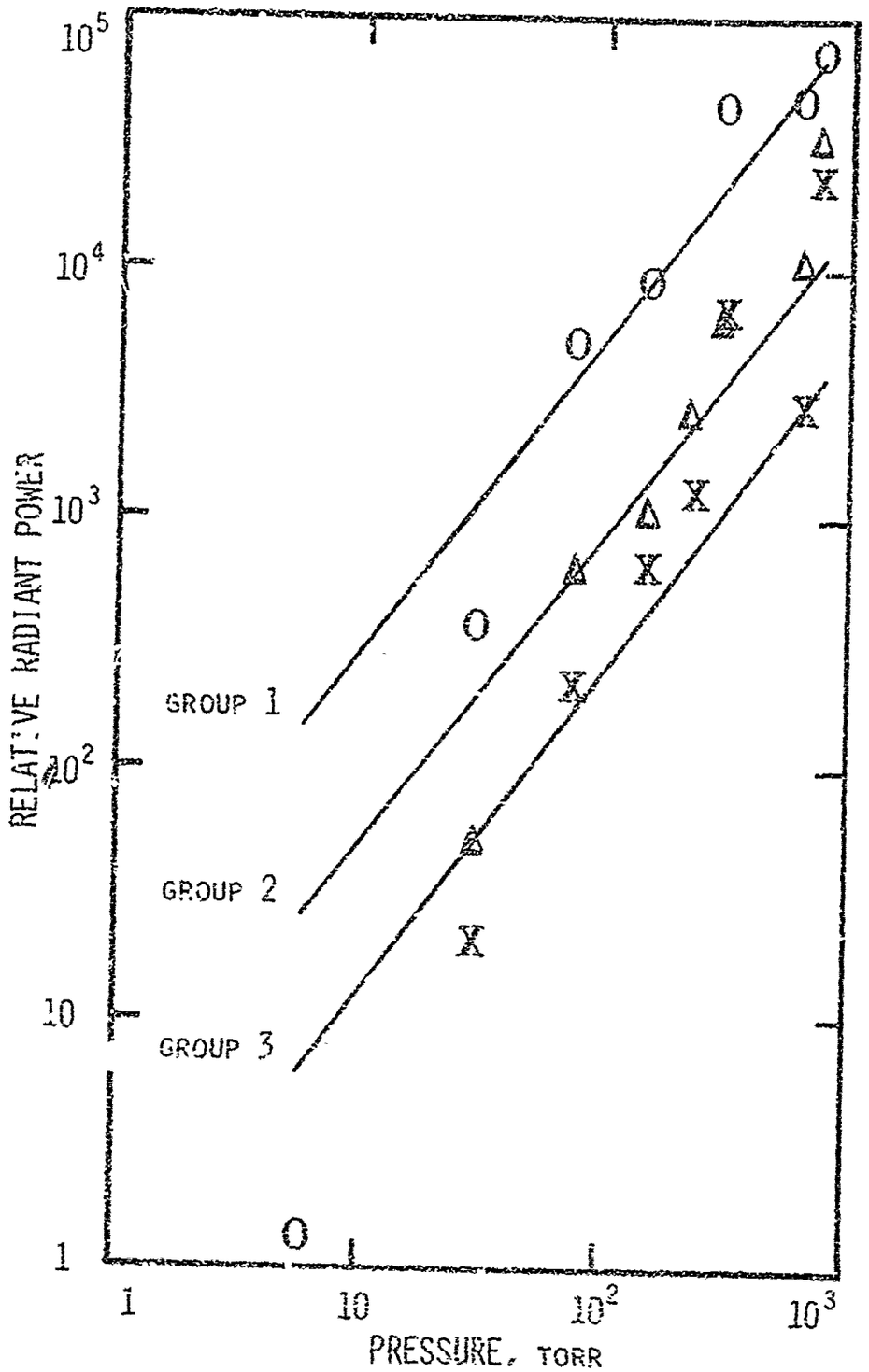
RELATIVE RADIANT POWER
PRESSURE, TORR
GROUP 1
GROUP 2
GROUP 3
10^5
10^4
10^3
10^2
10
1
1
10
10^2
10^3

Fig. 5. Theoretical ΔW_R and experimentally measured $\Delta W_R'$ widths between sodium D_2 resonance line center and wavelength of maximum spectral flux density as a function of pressure. ΔW_R values are shown for formula groups 1, 2, and 3 by the solid lines and ΔW_R values are indicated by O, Δ, and X for formula groups 1, 2, and 3 respectively.

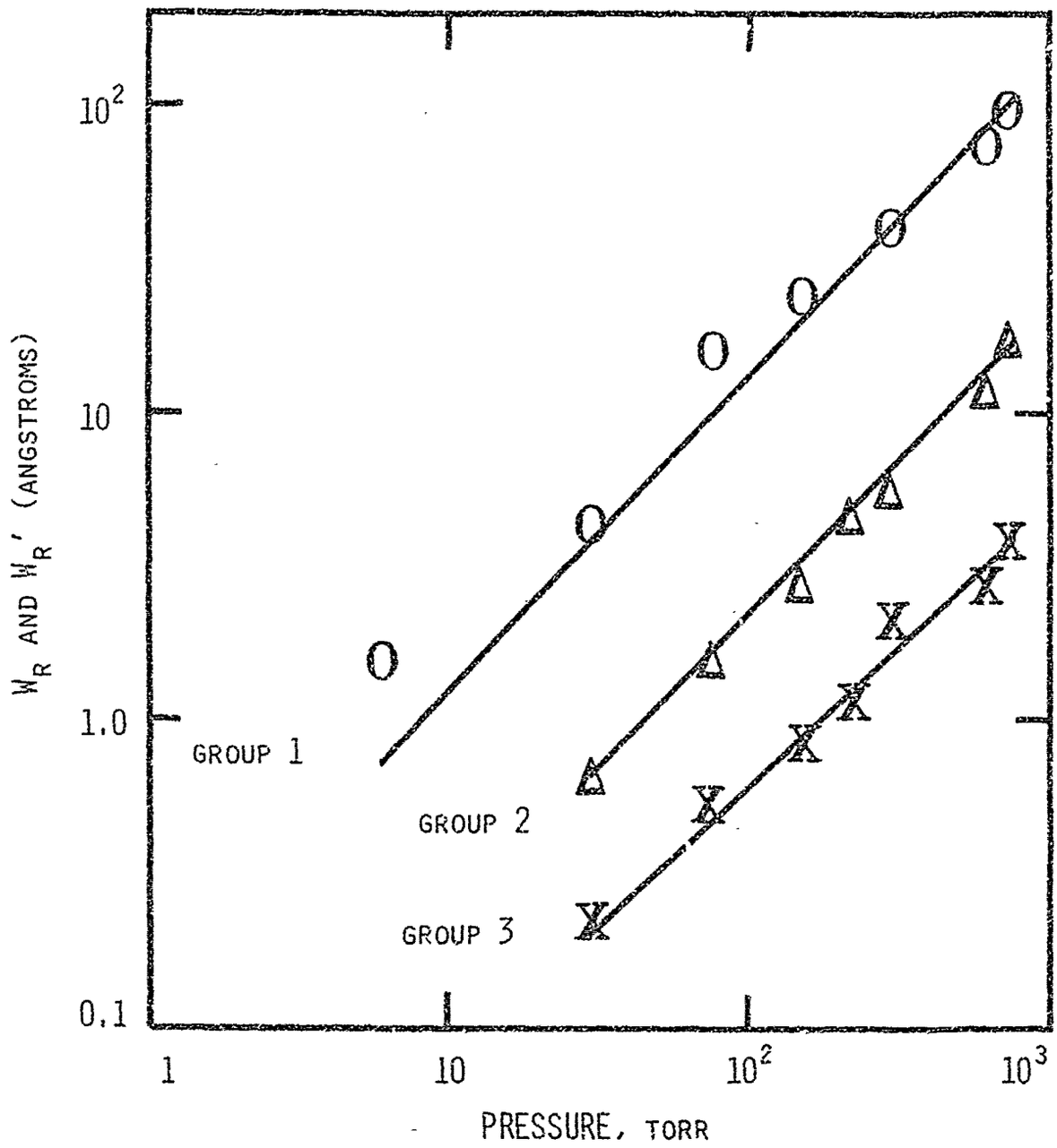
10^2
10
1.0
0.1
W_R AND W_R' (ANGSTROMS)
GROUP 1
GROUP 2
GROUP 3
1
10
10^2
10^3
PRESSURE, TORR

Fig. 6. Theoretical $\Delta W_{\frac{1}{2}}$ and experimentally measured $\Delta W_{\frac{1}{2}}'$ half-widths of the radiant power spectra as a function of pressure. $\Delta W_{\frac{1}{2}}$ values are shown for formula groups 1, 2, and 3 by the continuous solid line, the single points, and the dashed line. $\Delta W_{\frac{1}{2}}'$ values are shown by $\bigcirc$, $\triangle$, and X for formula groups 1, 2, and 3 respectively.

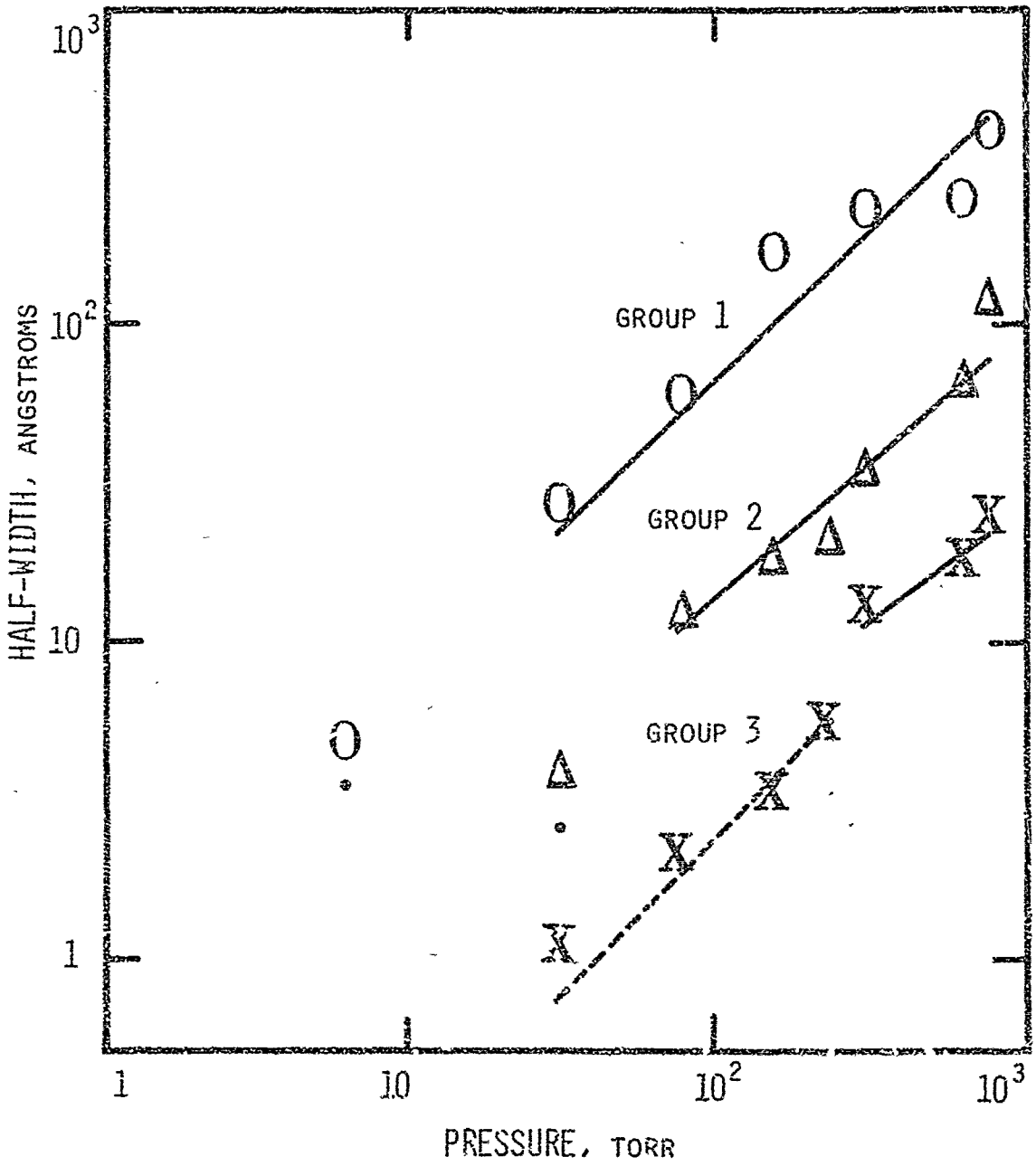
10^3
10^2
10
1
HALF-WIDTH, ANGSTROMS
GROUP 1
GROUP 2
GROUP 3
1
10
10^2
10^3
PRESSURE, TORR

APPENDICES

APPENDIX A

RELATIVE POWER SPECTRA OF ALL FLARES TESTED

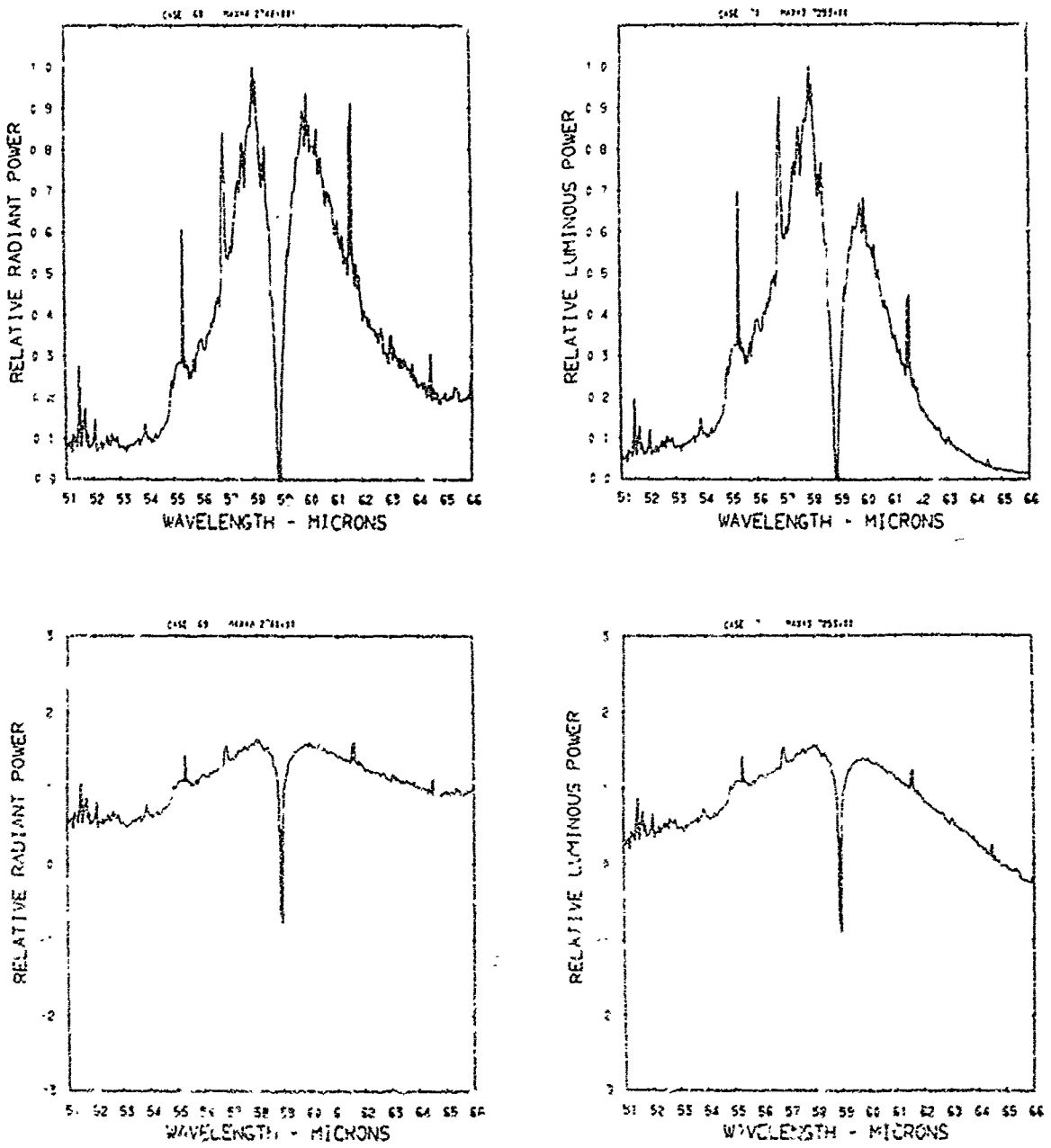

Figure A1 . Relative power spectra of test flare 72 , formula group 1, burned at 760 torr ambient pressure. The top two spectra are normalized with the peak value equal to unity. The $\log_{10}$ of the spectral power is plotted in the bottom spectra. Flare formula group 1 contains 44.0% magnesium, 51.5% sodium nitrate, and 4.5% binder.

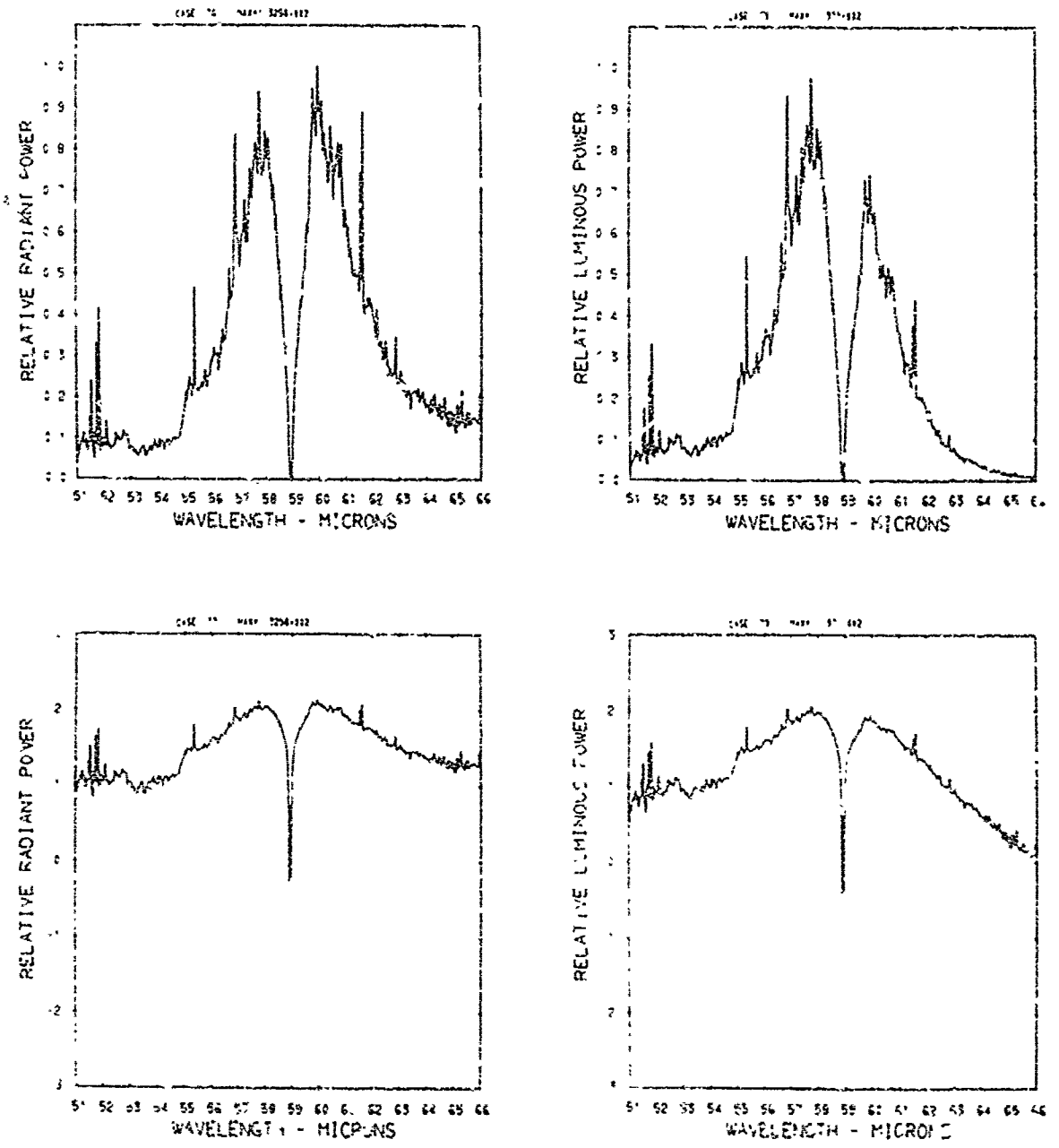

Figure A2 . Relative power spectra of test flare 75 , formula group 1, burned at 760 torr ambient pressure. The top two spectra are normalized with the peak value equal to unity. The $\log_{10}$ of the spectral power is plotted in the bottom spectra. Flare formula group 1 contains 44.0% magnesium, 51.5% sodium nitrate, and 4.5% binder.

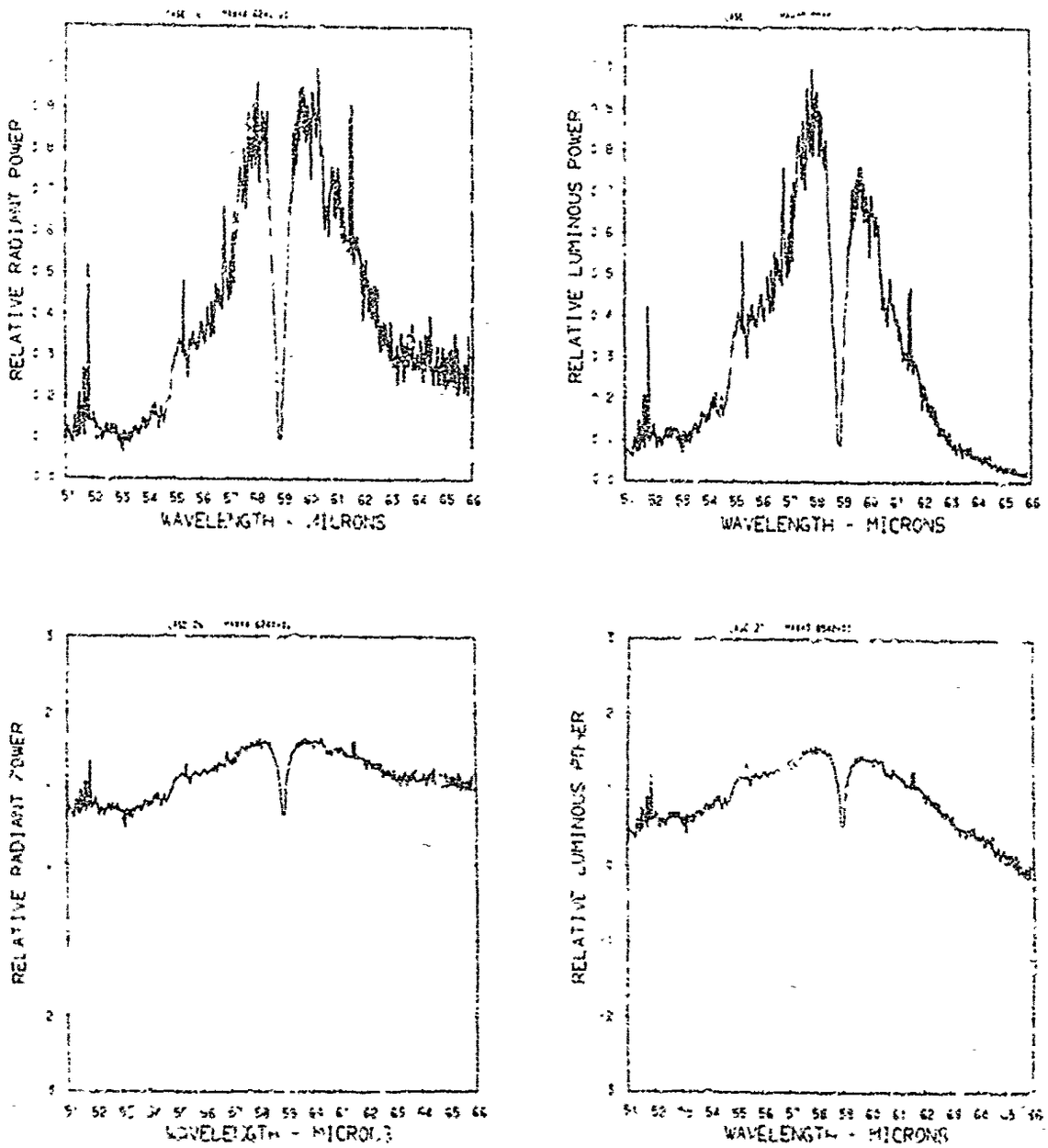

Figure A3 . Relative power spectra of test flare 145 , formula group 1, burned at 760 torr ambient pressure. The top two spectra are normalized with the peak value equal to unity. The log$_{10}$ of the spectral power is plotted in the bottom spectra. Flare formula group 1 contains 44.0% magnesium, 51.5% sodium nitrate, and 4.5% binder.

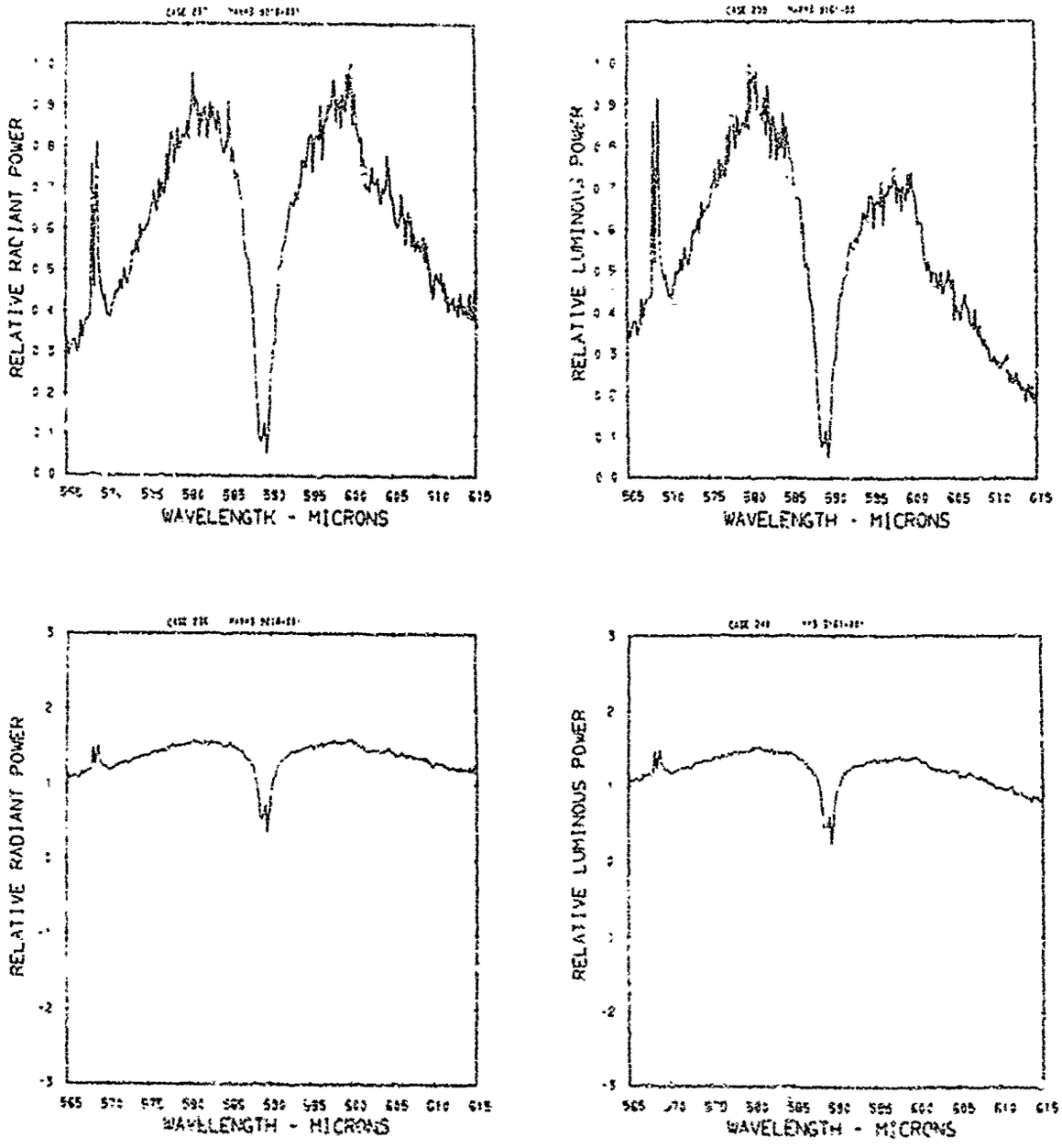

Figure A4 . Relative power spectra of test flare 20A , formula group 1, burned at 630 torr ambient pressure. The top two spectra are normalized with the peak value equal to unity. The $\log_{10}$ of the spectral power is plotted in the bottom spectra. Flare formula group 1 contains 44.0% magnesium, 51.5% sodium nitrate, and 4.5% binder.

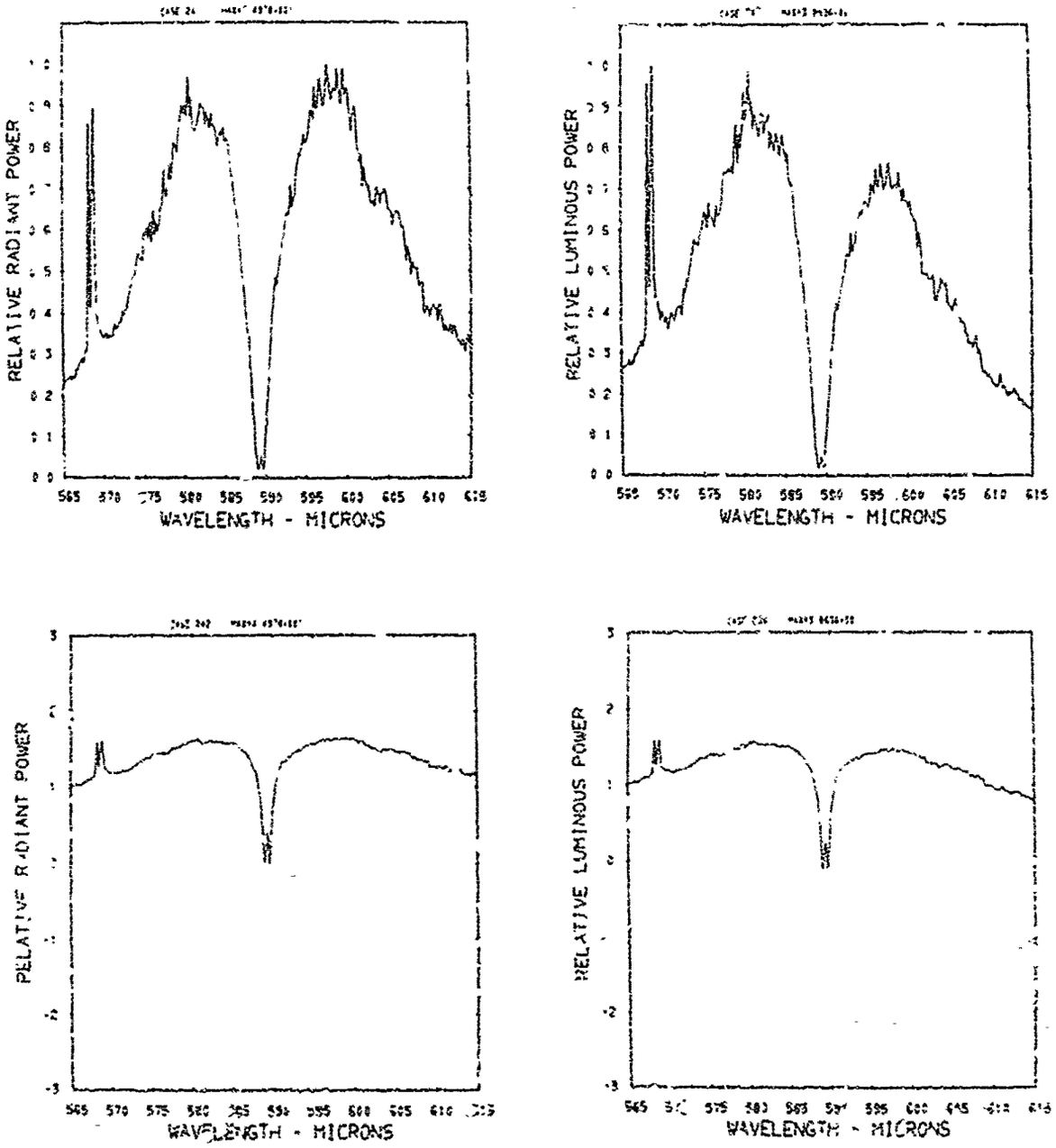

Figure A5 . Relative power spectra of test flare 208 , formula group 1, burned at 630 torr ambient pressure. The top two spectra are normalized with the peak value equal to unity. The $\log_{10}$ of the spectral power is plotted in the bottom spectra. Flare formula group 1 contains 44.0% magnesium, 51.5% sodium nitrate, and 4.5% binder.

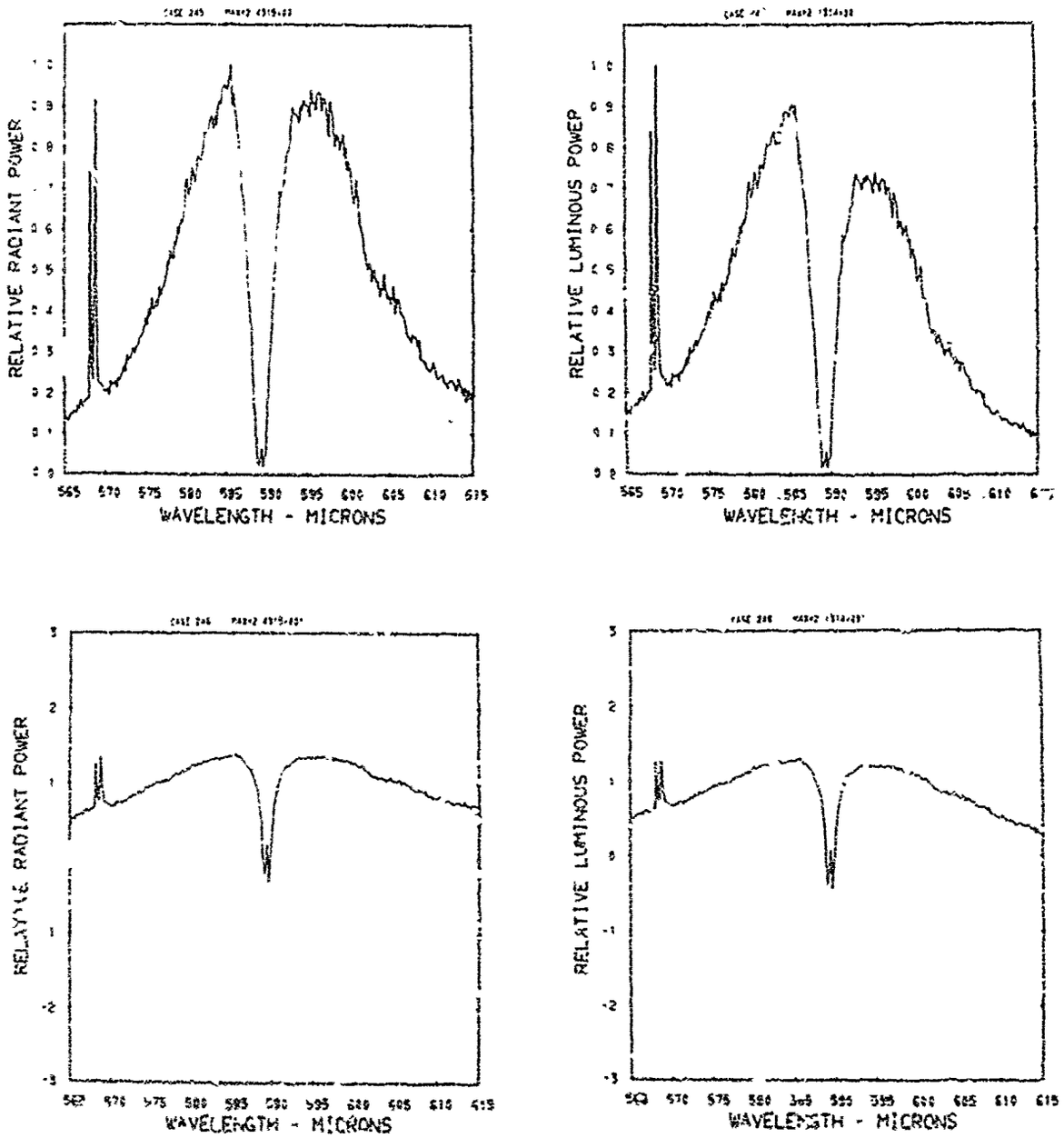

Figure A6 . Relative power spectra of test flare 20C , formula group 1, burned at 630 torr ambient pressure. The top two spectra are normalized with the peak value equal to unity. The $\log_{10}$ of the spectral power is plotted in the bottom spectra. Flare formula group 1 contains 44.0% magnesium, 51.5% sodium nitrate, and 4.5% binder.

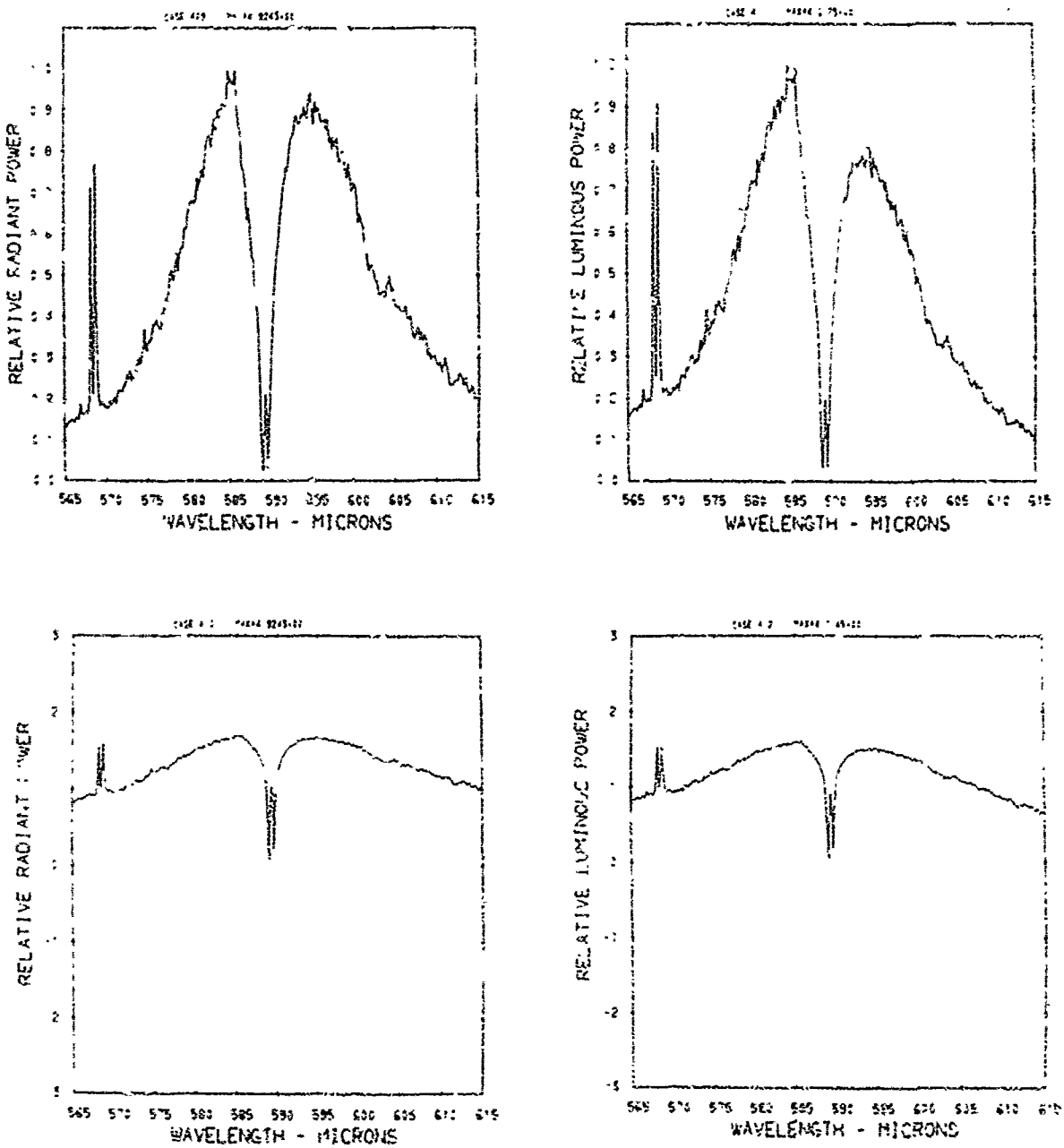

Figure A7 . Relative power spectra of test flare 115 , formula group 1, burned at 300 torr ambient pressure. The top two spectra are normalized with the peak value equal to unity. The $\log_{10}$ of the spectral power is plotted in the bottom spectra. Flare formula group 1 contains 44.0% magnesium, 51.5% sodium nitrate, and 4.5% binder.

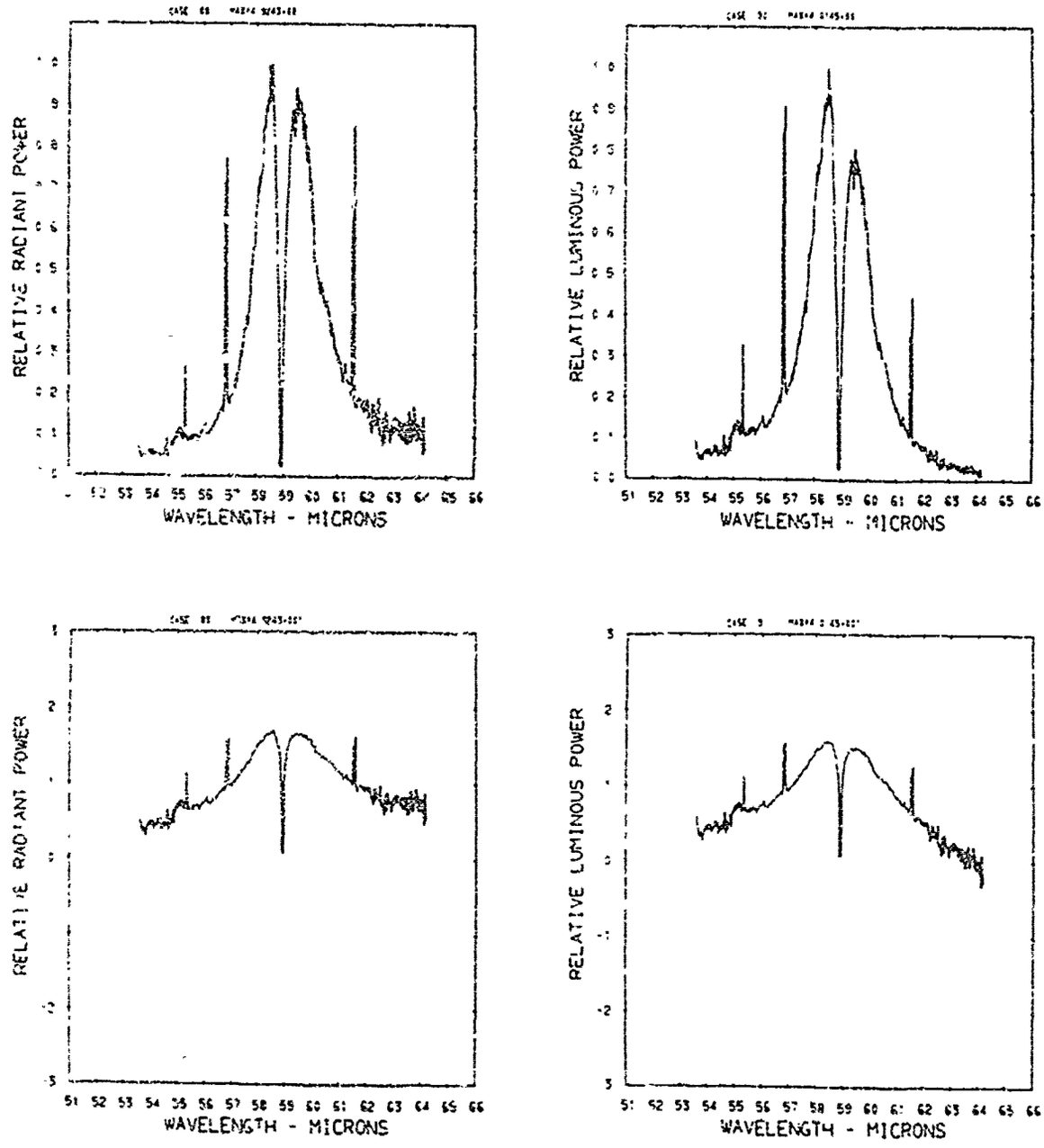

Figure A8 . Relative power spectra of test flare 115 , formula group 1, burned at 300 torr ambient pressure. The top two spectra are normalized with the peak value equal to unity. The $\log_{10}$ of the spectral power is plotted in the bottom spectra. Flare formula group 1 contains 44.0% magnesium, 51.5% sodium nitrate, and 4.5% binder.

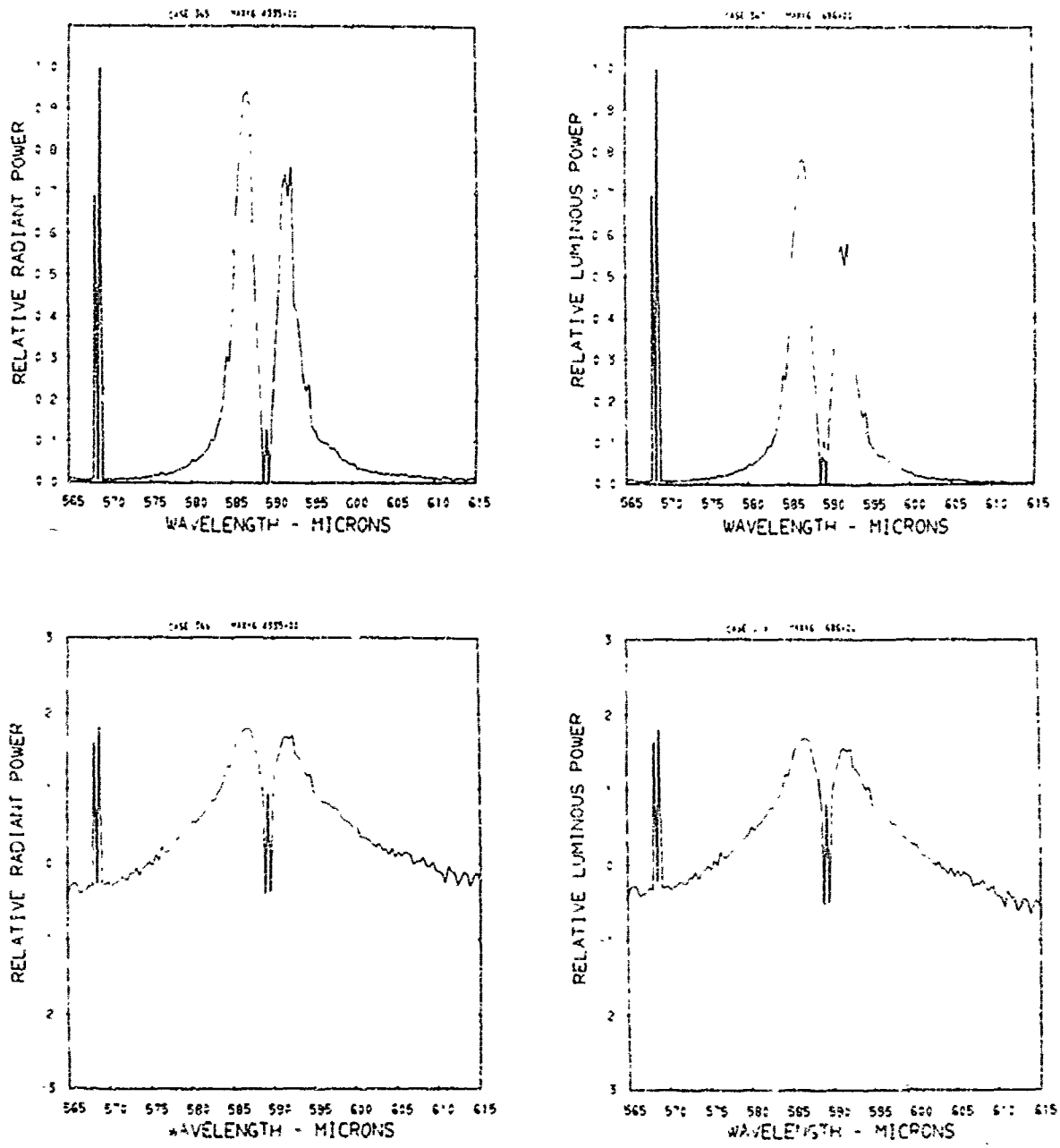

Figure A9 . Relative power spectra of test flare 46 , formula group 1, burned at 150 torr ambient pressure. The top two spectra are normalized with the peak value equal to unity. The $\log_{10}$ of the spectral power is plotted in the bottom spectra. Flare formula group 1 contains 44.0% magnesium, 51.5% sodium nitrate, and 4.5% binder.

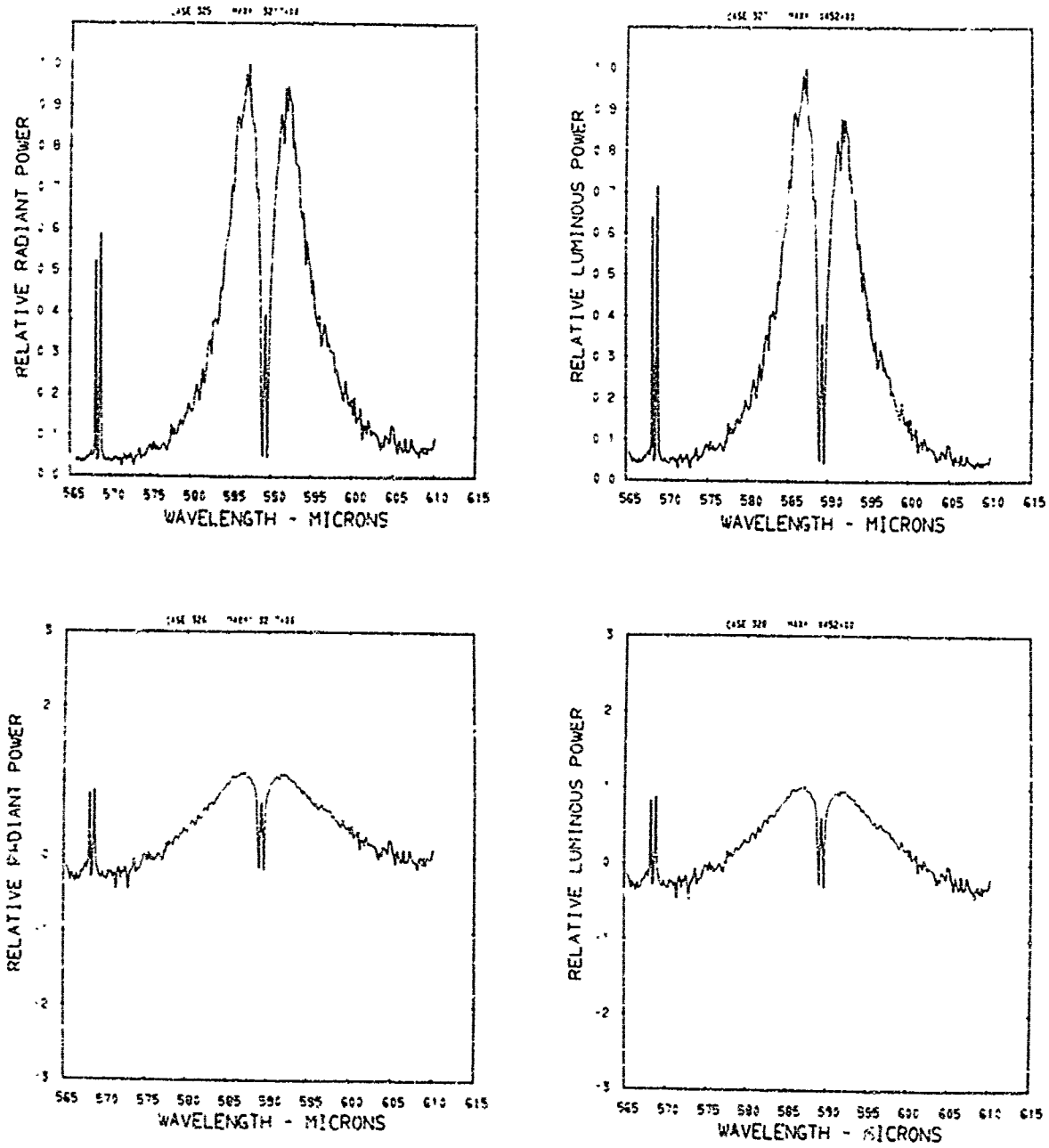

Figure A10. Relative power spectra of test flare 50 , formula group 1, burned at 150 torr ambient pressure. The top two spectra are normalized with the peak value equal to unity. The $\log_{10}$ of the spectral power is plotted in the bottom spectra. Flare formula group 1 contains 44.0% magnesium, 51.5% sodium nitrate, and 4.5% binder.

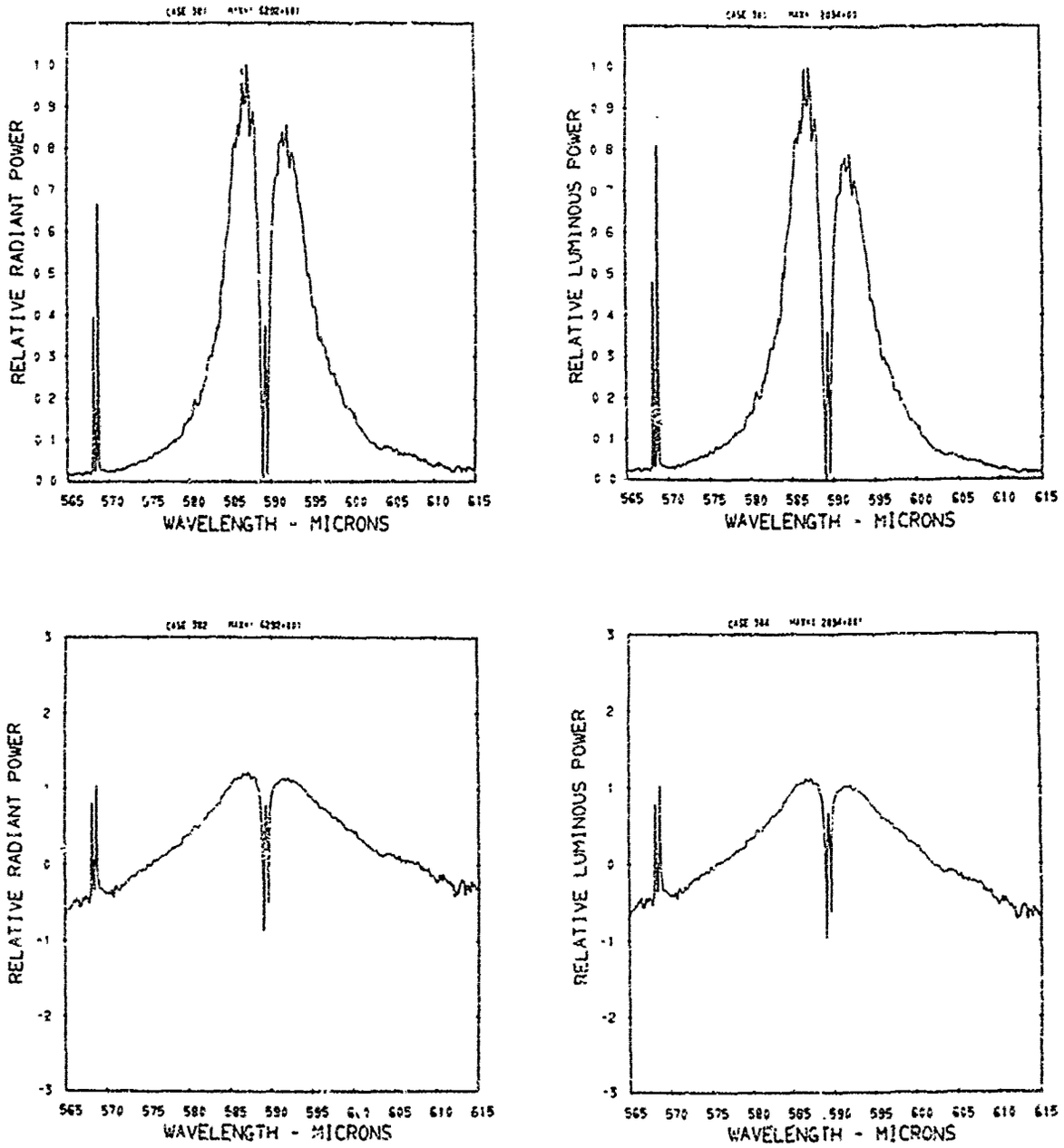

Figure A11. Relative power spectra of test flare 54 , formula group 1, burned at 150 torr ambient pressure. The top two spectra are normalized with the peak value equal to unity. The $\log_{10}$ of the spectral power is plotted in the bottom spectra. Flare formula group 1 contains 44.0% magnesium, 51.5% sodium nitrate, and 4.5% binder.

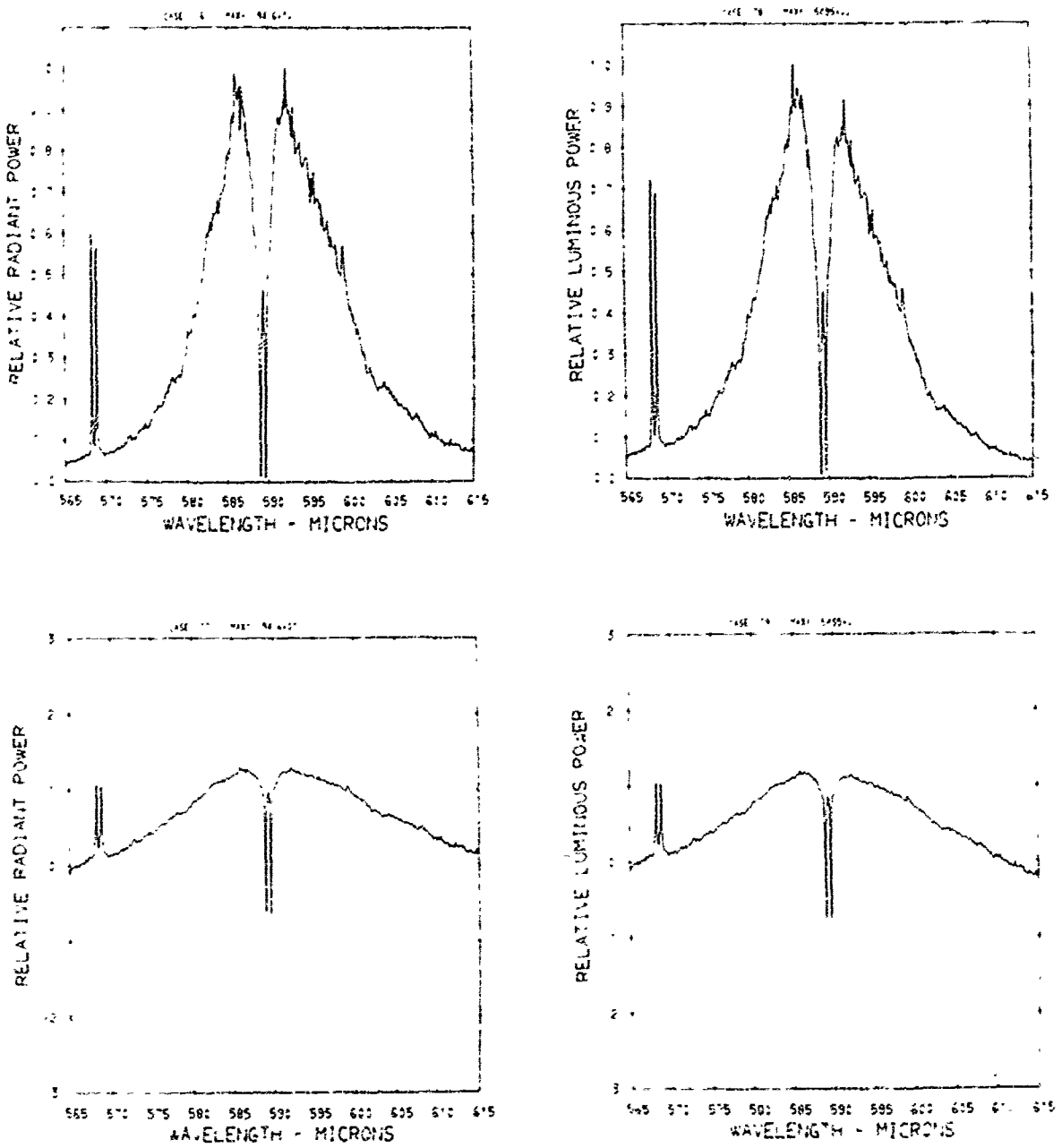

Figure A12. Relative power spectra of test flare 113 , formula group 1, burned at 150 torr ambient pressure. The top two spectra are normalized with the peak value equal to unity. The $\log_{10}$ of the spectral power is plotted in the bottom spectra. Flare formula group 1 contains 44.0% magnesium, 51.5% sodium nitrate, and 4.5% binder.

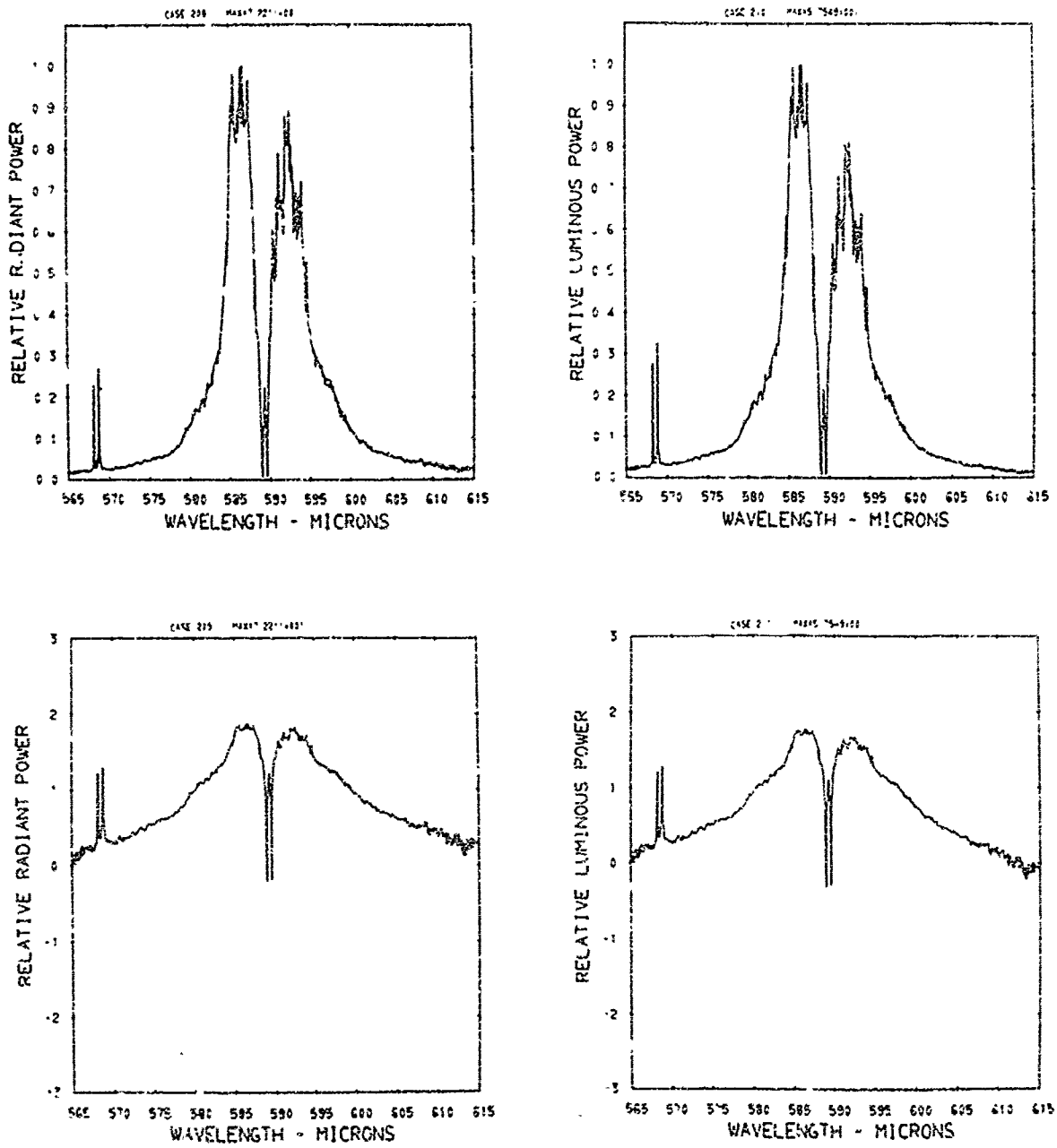

Figure A13. Relative power spectra of test flare 128 , formula group 1, burned at 150 torr ambient pressure. The top two spectra are normalized with the peak value equal to unity. The $\log_{10}$ of the spectral power is plotted in the bottom spectra. Flare formula group 1 contains 44.0% magnesium, 51.5% sodium nitrate, and 4.5% binder.

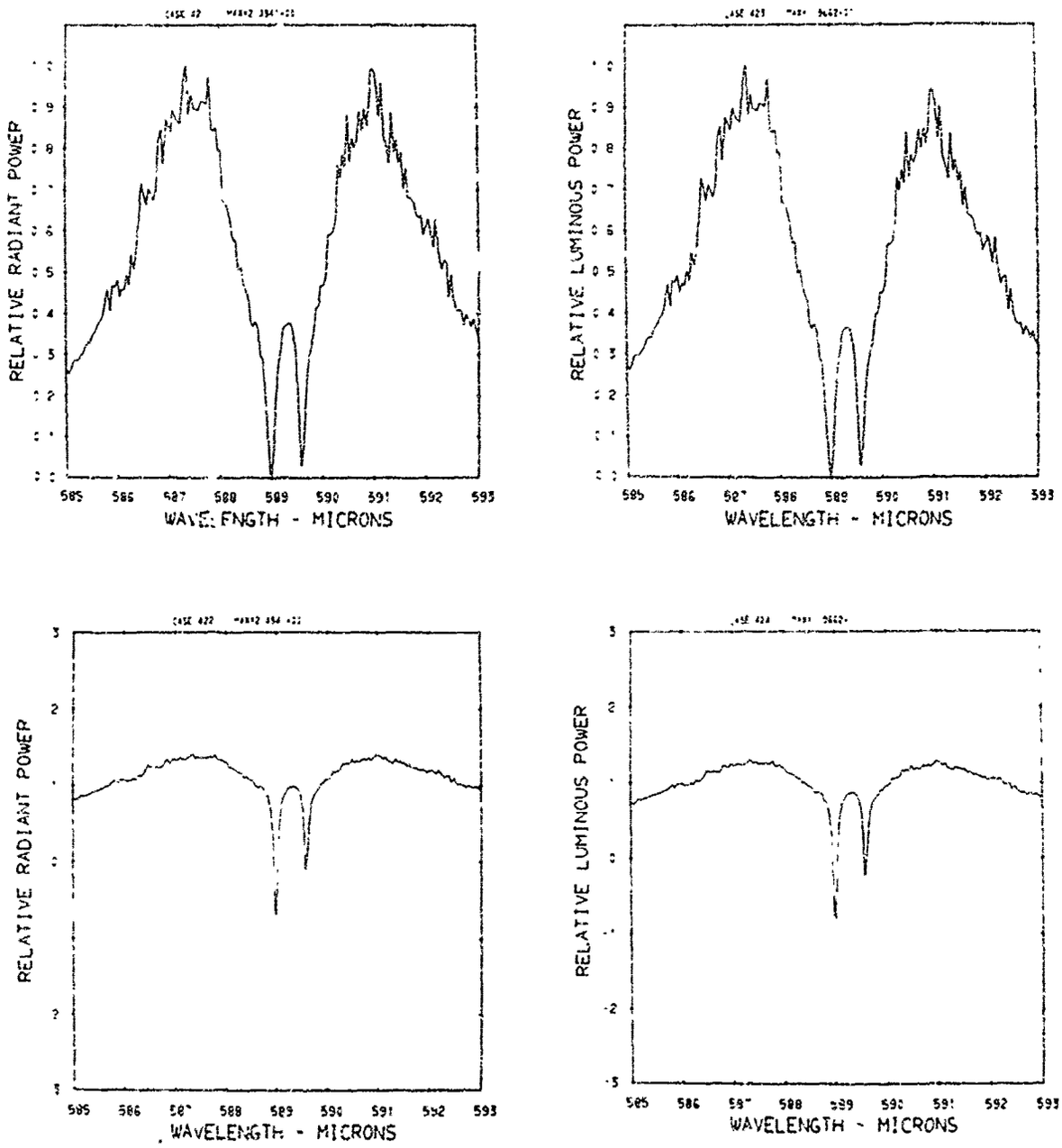

Figure A14. Relative power spectra of test flare 123 , formula group 1, burned at 75 torr ambient pressure. The top two spectra are normalized with the peak value equal to unity. The $\log_{10}$ of the spectral power is plotted in the bottom spectra. Flare formula group 1 contains 44.0% magnesium, 51.5% sodium nitrate, and 4.5% binder.

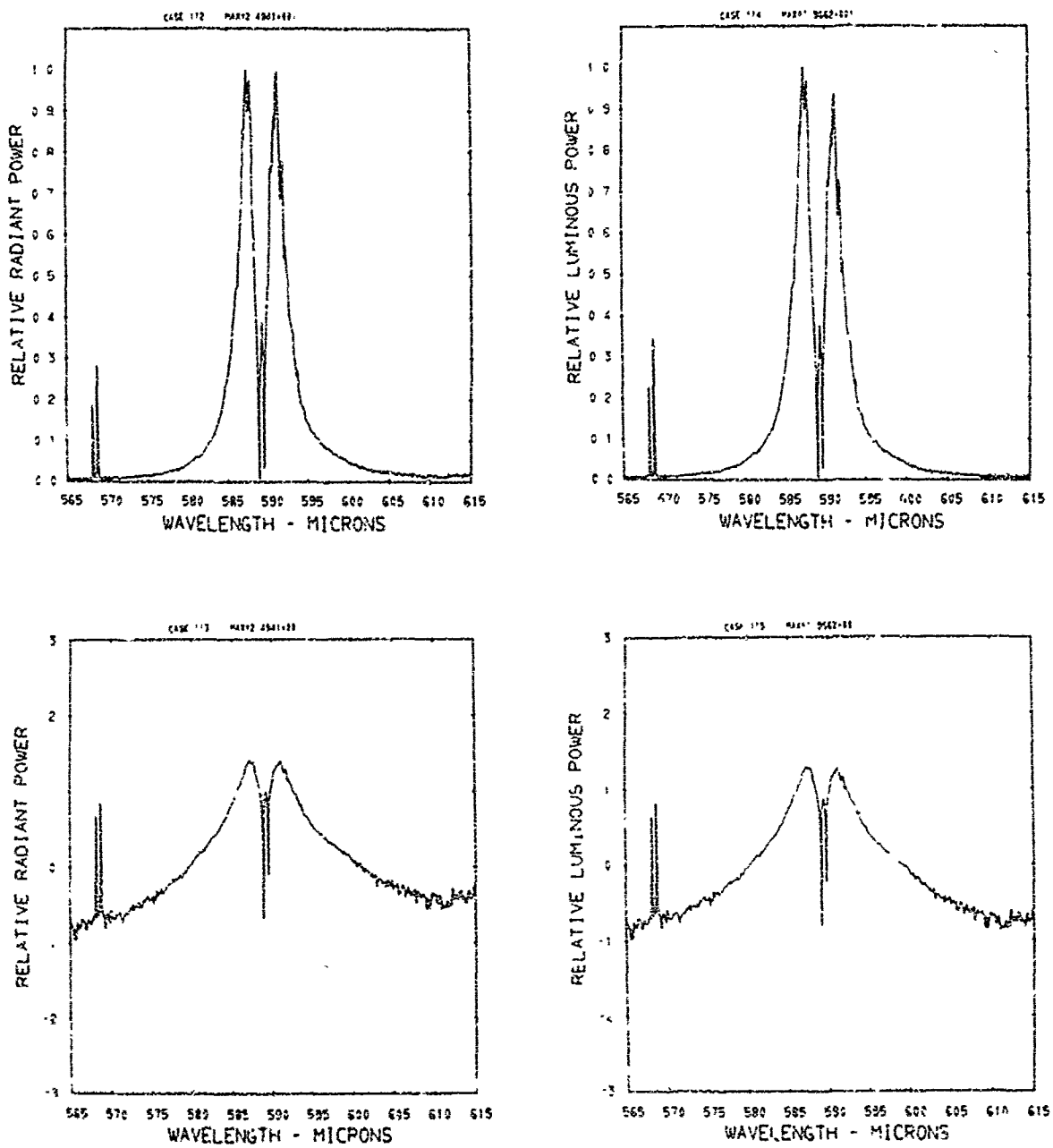

Figure A15. Relative power spectra of test flare 123 , formula group 1, burned at 75 torr ambient pressure. The top two spectra are normalized with the peak value equal to unity. The $\log_{10}$ of the spectral power is plotted in the bottom spectra. Flare formula group 1 contains 44.0% magnesium, 51.5% sodium nitrate, and 4.5% binder.

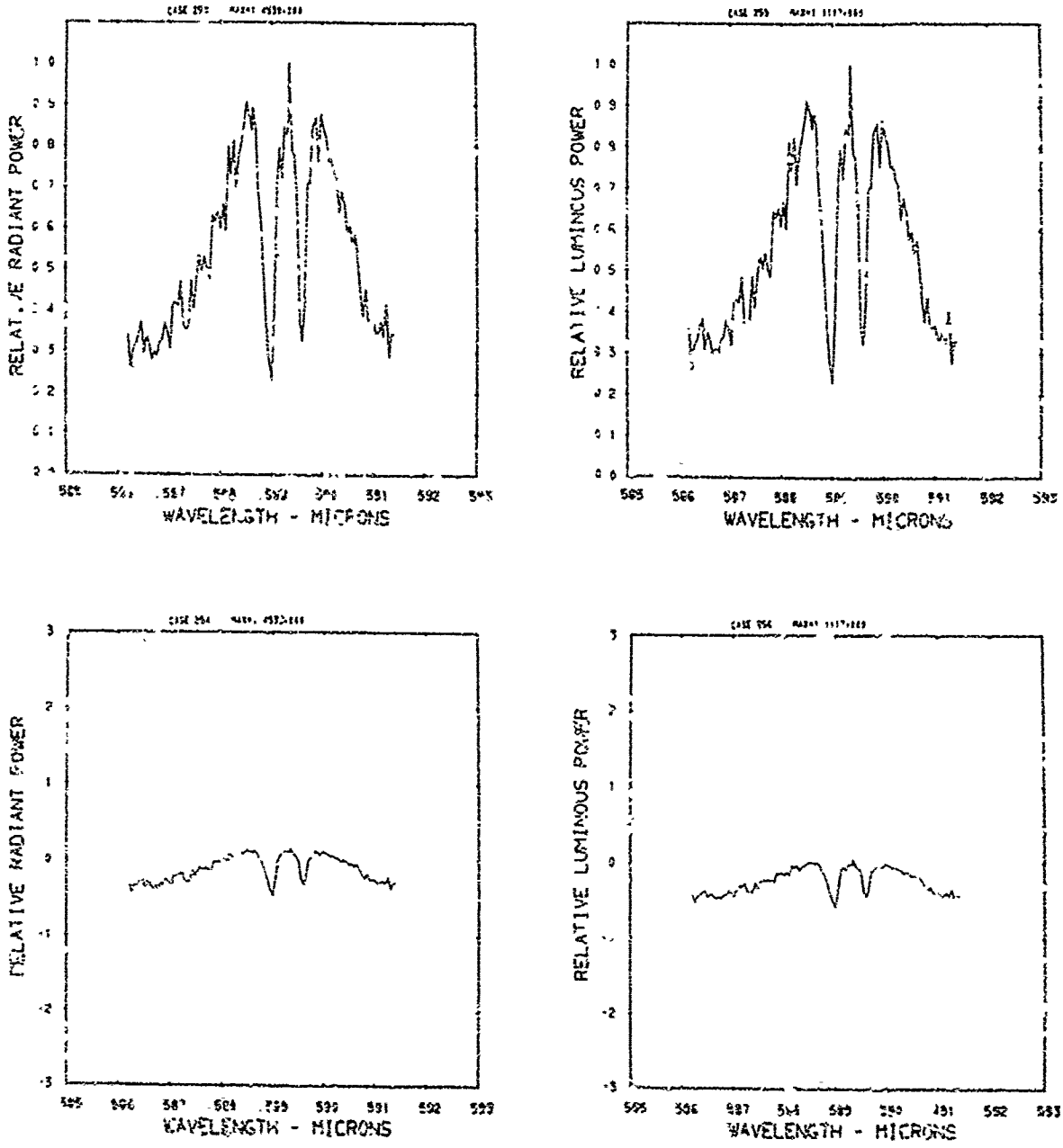

Figure A16. Relative power spectra of test flare 22A , formula group I, burned at 30 torr ambient pressure. The top two spectra are normalized with the peak value equal to unity. The $\log_{10}$ of the spectral power is plotted in the bottom spectra. Flare formula group I contains 44.0% magnesium, 51.5% sodium nitrate, and 4.5% binder.

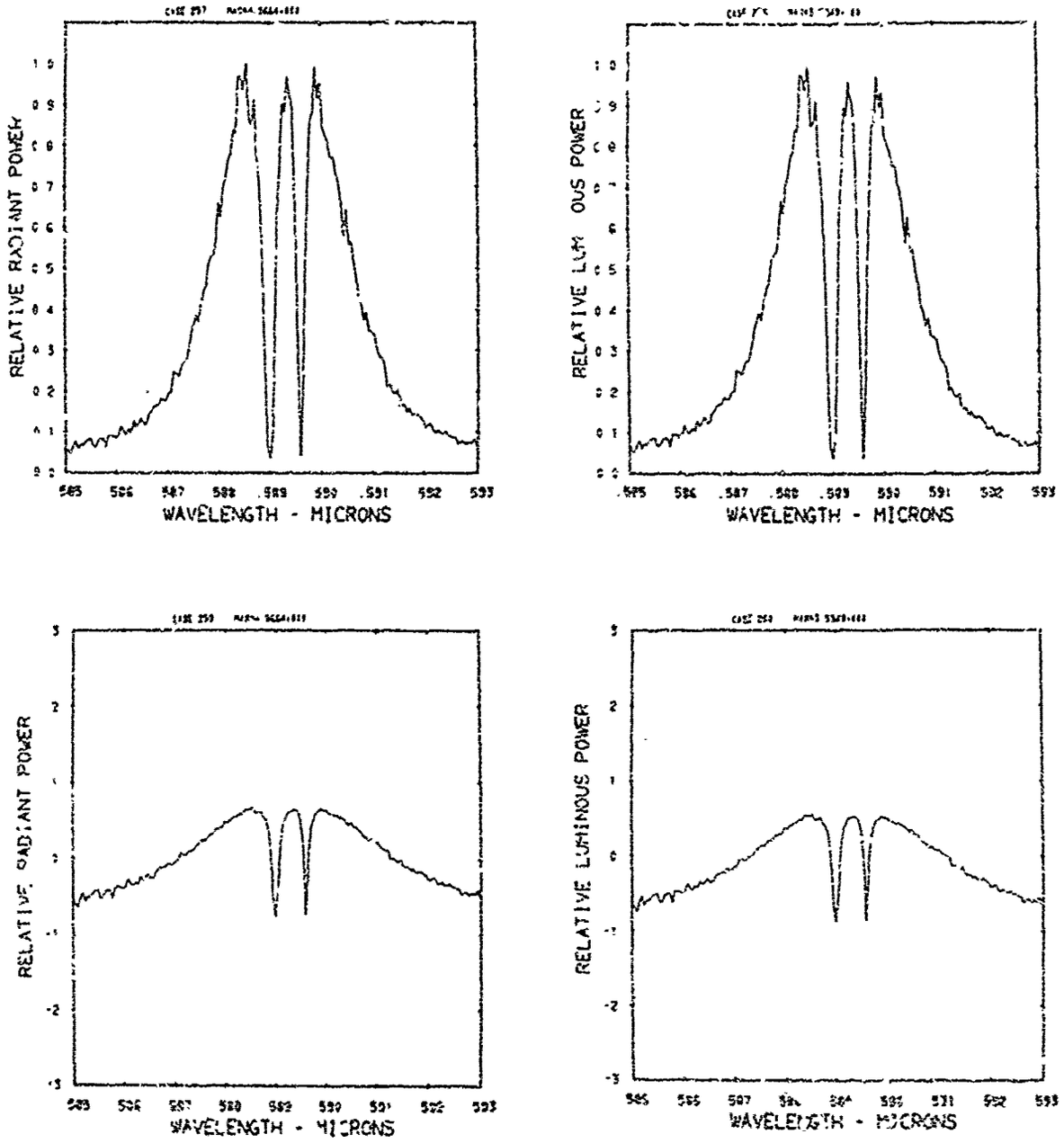

Figure A17. Relative power spectra of test flare 22B , formula group 1, burned at 30 torr ambient pressure. The top two spectra are normalized with the peak value equal to unity. The $\log_{10}$ of the spectral power is plotted in the bottom spectra. Flare formula group 1 contains 44.0% magnesium, 51.5% sodium nitrate, and 4.5% binder.

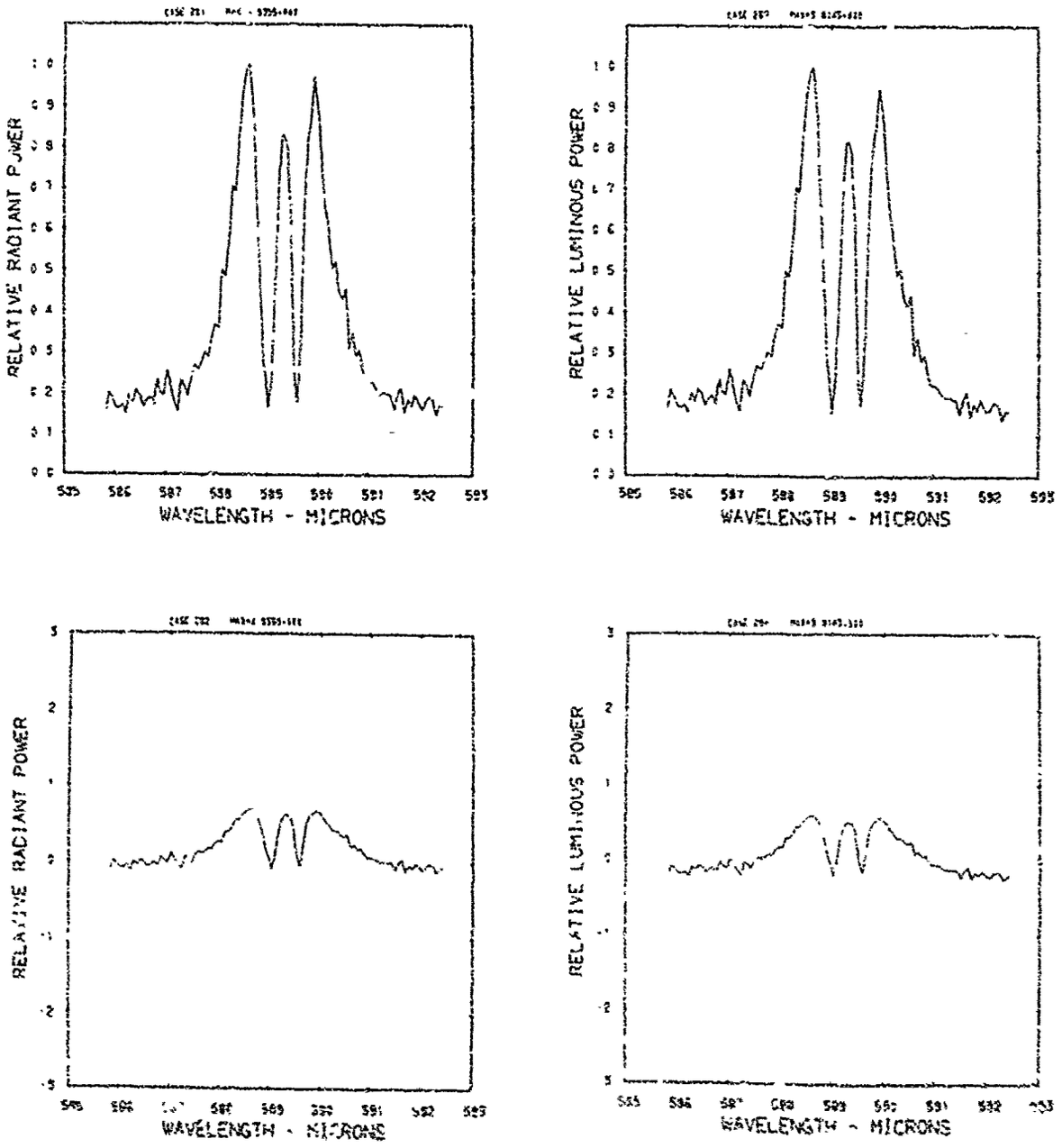

Figure A.8. Relative power spectra of test flare 34 , formula group 1, burned at 30 torr ambient pressure. The top two spectra are normalized with the peak value equal to unity. The $\log_{10}$ of the spectral power is plotted in the bottom spectra. Flare formula group 1 contains 44.0% magnesium, 51.5% sodium nitrate, and 4.5% binder.

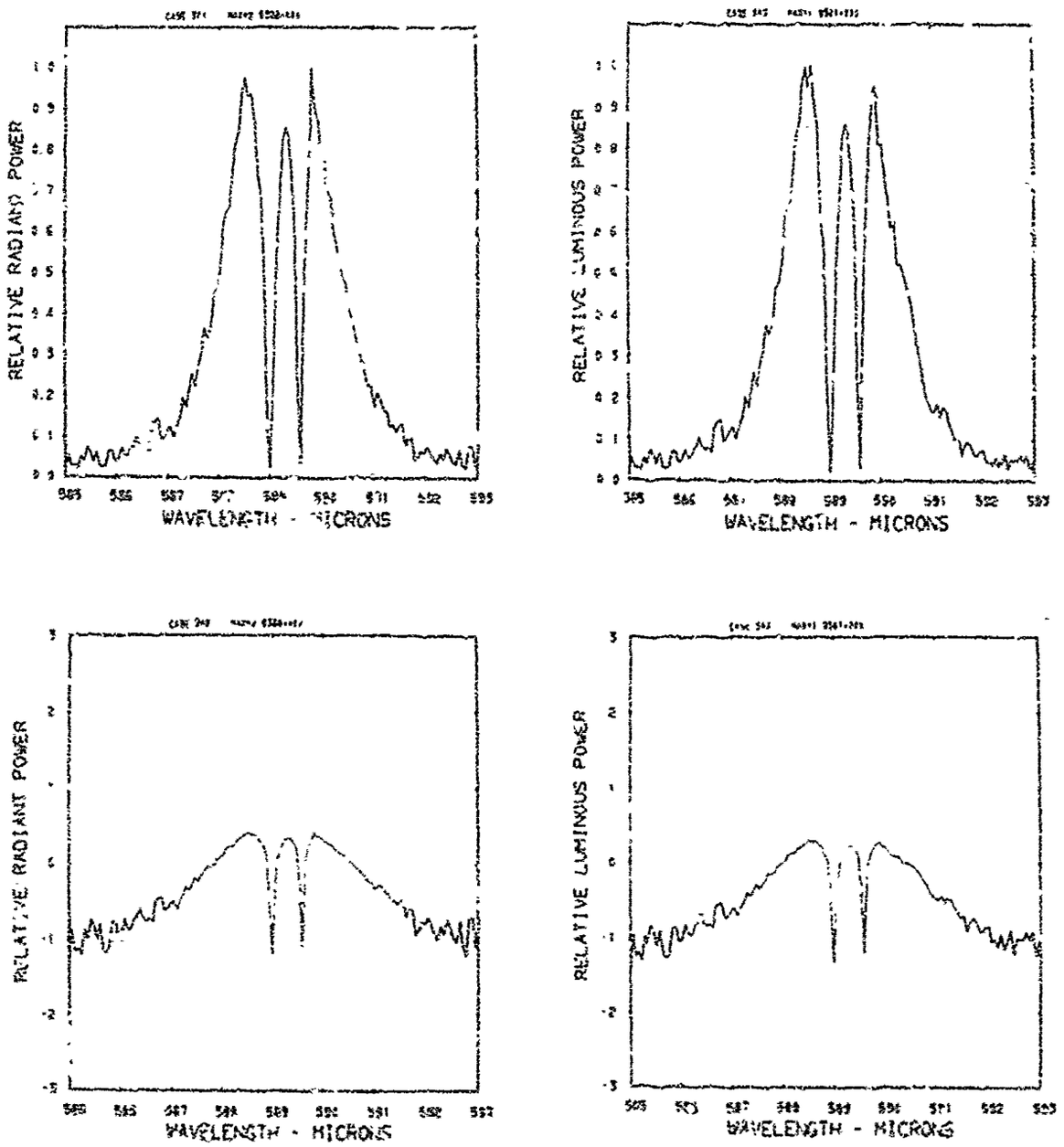

Figure A19. Relative power spectra of test flare 40 , formula group 1, burned at 30 torr ambient pressure. The top two spectra are normalized with the peak value equal to unity. The log. of the spectral power is plotted in the bottom spectra. Flare formula group 1 contains 44.0% magnesium, 51.5% sodium nitrate, and 4.5% binder.

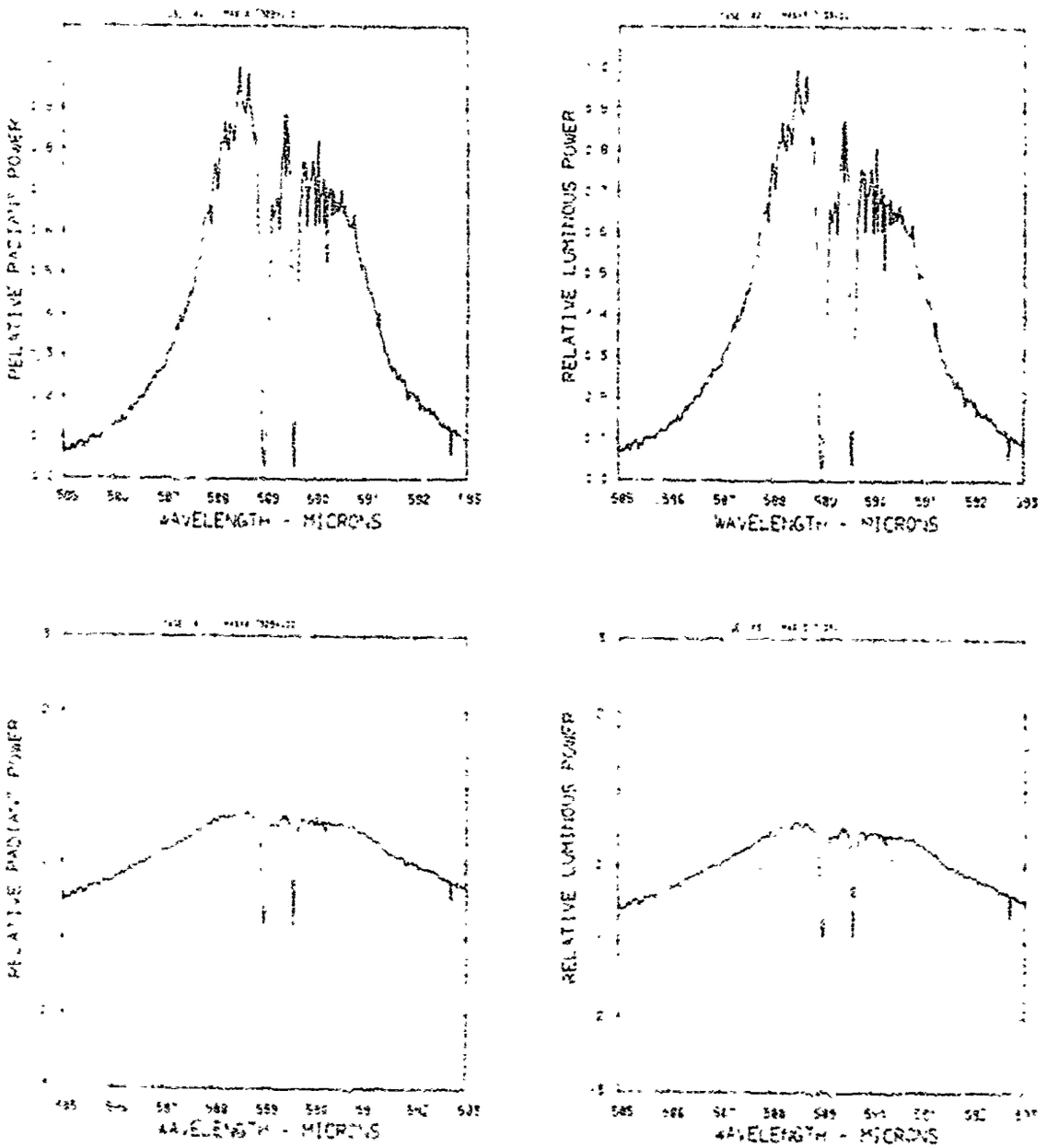

Figure A20. Relative power spectra of test flare 95 , formula group 1, burned at 30 torr ambient pressure. The top two spectra are normalized with the peak value equal to unity. The $\log_{10}$ of the spectral power is plotted in the bottom spectra. Flare formula group 1 contains 44.0% magnesium, 51.5% sodium nitrate, and 4.5% binder.

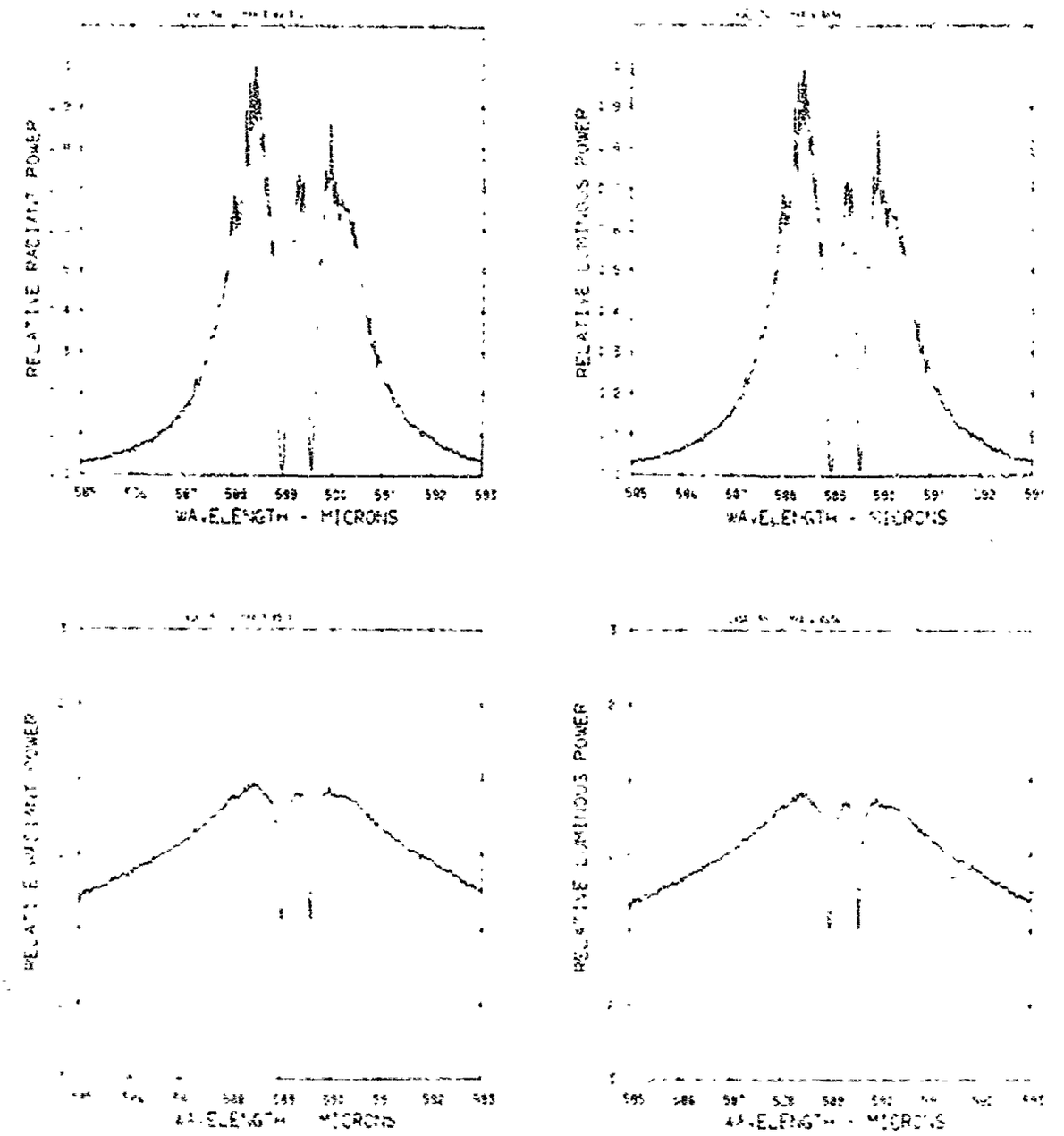

Figure A21. Relative power spectra of test flare 1-3 , formula group 1, burned at 30 torr ambient pressure. The top two spectra are normalized with the peak value equal to unity. The log. of the spectral power is plotted in the bottom spectra. Flare formula group 1 contains 44.0% magnesium, 51.5% sodium nitrate, and 4% binder.

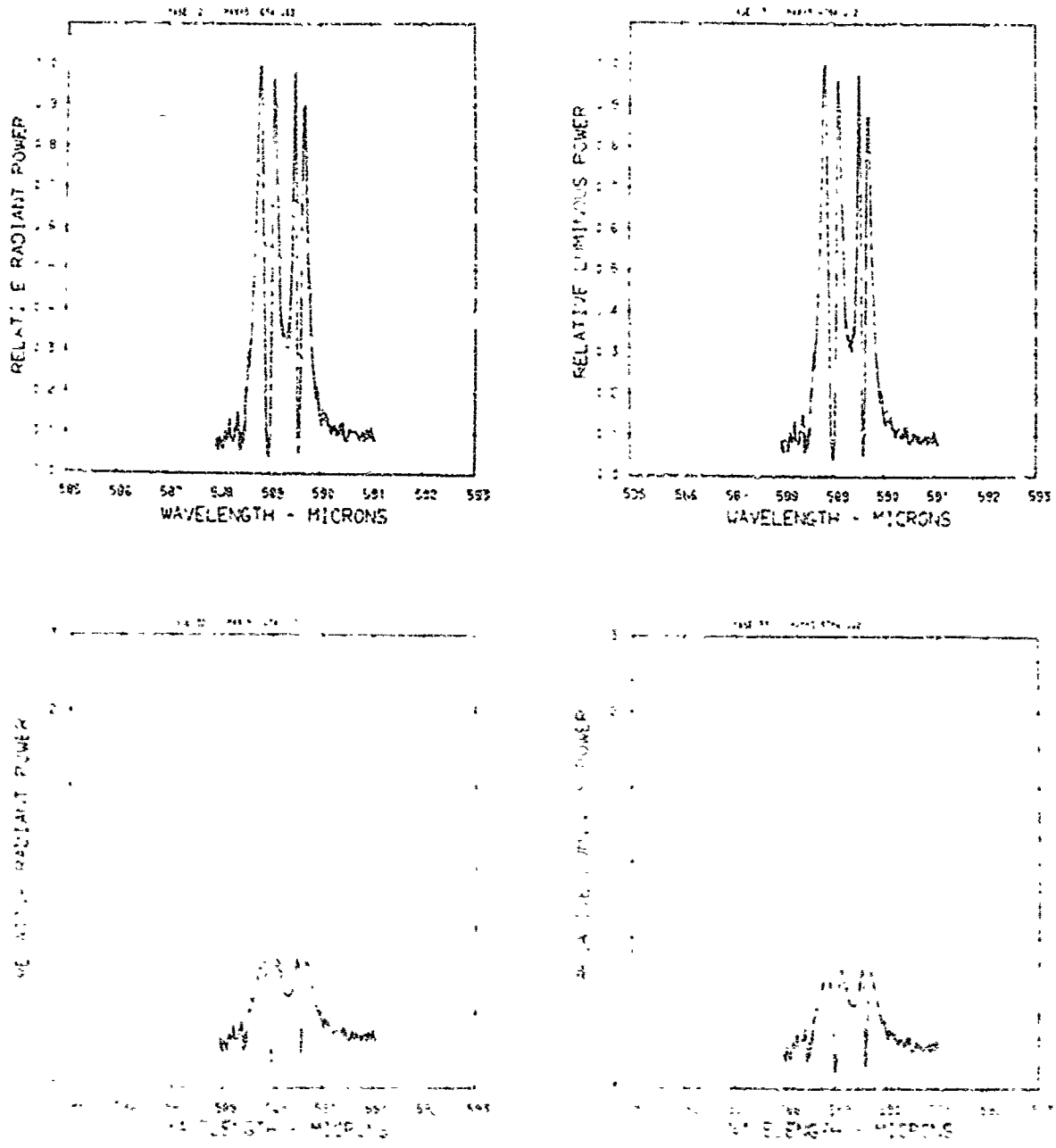

Figure A2C. Relative power spectra of test flare 87 , formula group 1, burned at 6 torr ambient pressure The top two spectra are normalized with the peak value equal to unity. The $\log_{10}$ of the spectral power is plotted in the bottom spectra. Flare formula group 1 contains 41.0% magnesium, 53.5% sodium nitrate, and 4.5% binder.

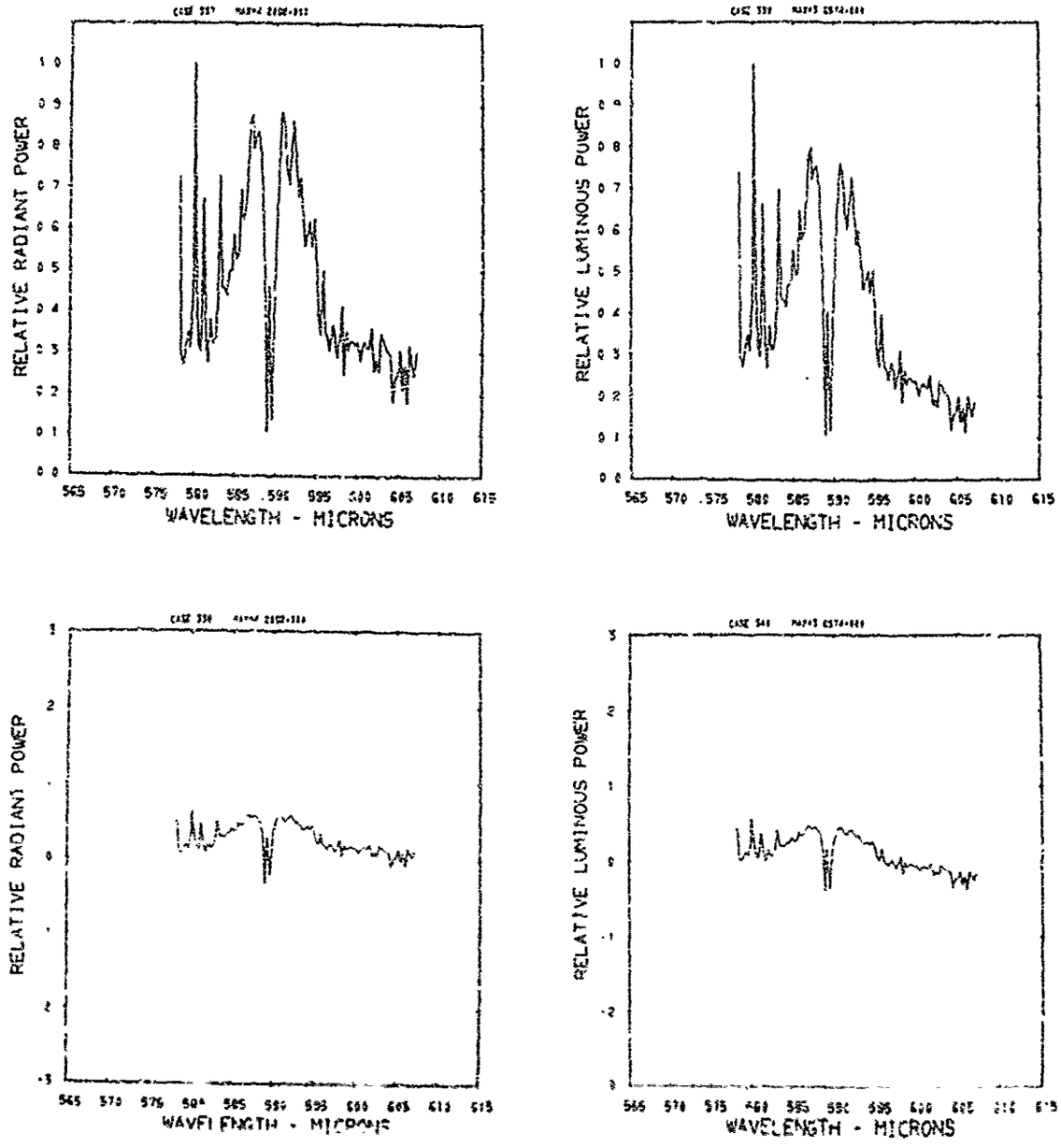

Figure A23. Relative power spectra of test flare 6[illegible], formula group 2, burned at 760 torr ambient pressure. The top two spectra are normalized with the peak value equal to unity. The $\log_{10}$ of the spectral power is plotted in the bottom spectra. Flare formula group 2 contains 40.4% magnesium, 5.15% sodium nitrate, 49.95% potassium nitrate, and 4.5% binder.

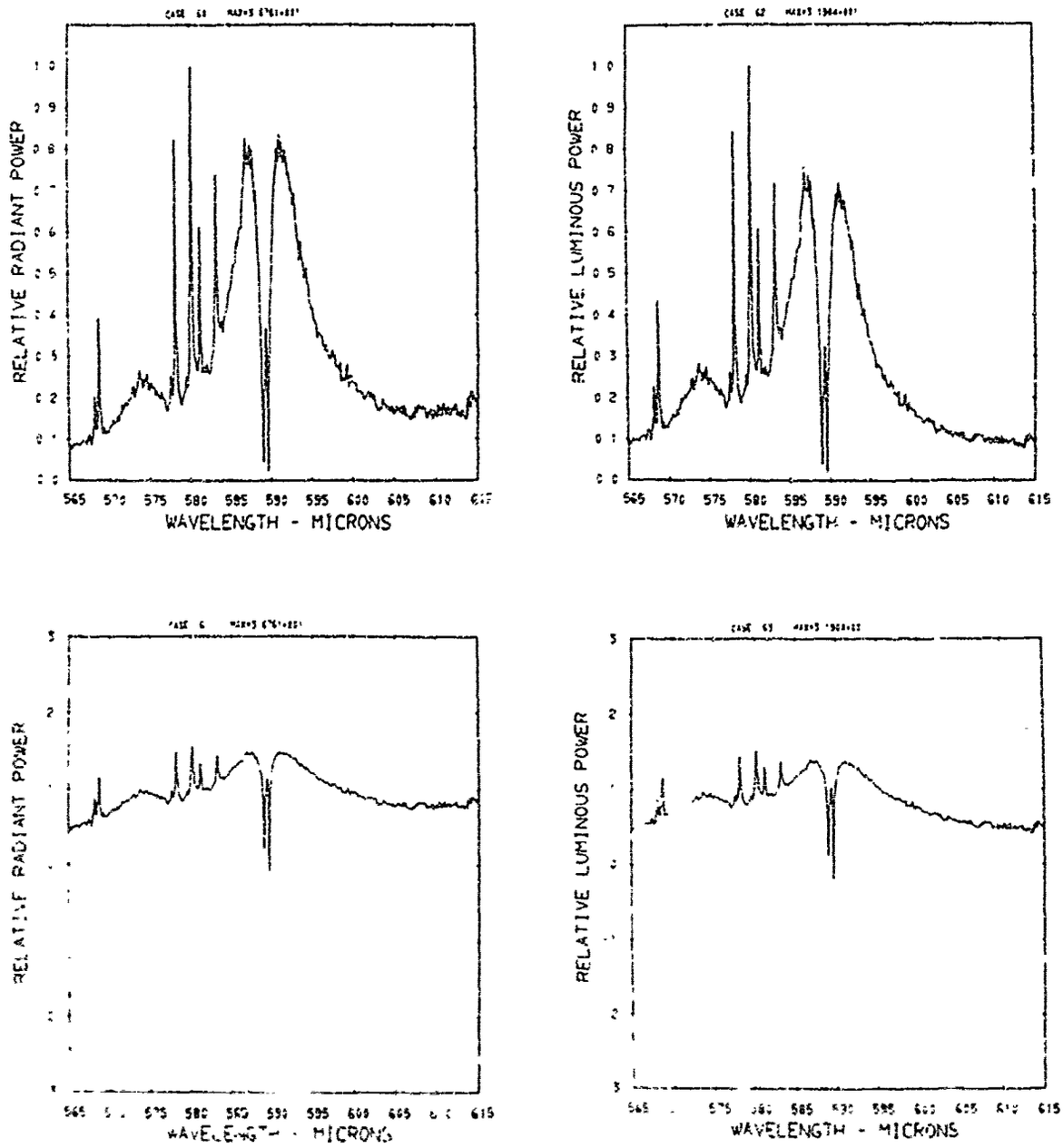

Figure A24. Relative power spectra of test flare [illegible], formula group 2, burned at 760 torr ambient pressure. The top two spectra are normalized with the peak value equal to unity. The $\log_{10}$ of the spectral power is plotted in the bottom spectra. Flare formula group 2 contains 40.4% magnesium, 5.15% sodium nitrate, 49.95% potassium nitrate, and 4.5% binder.

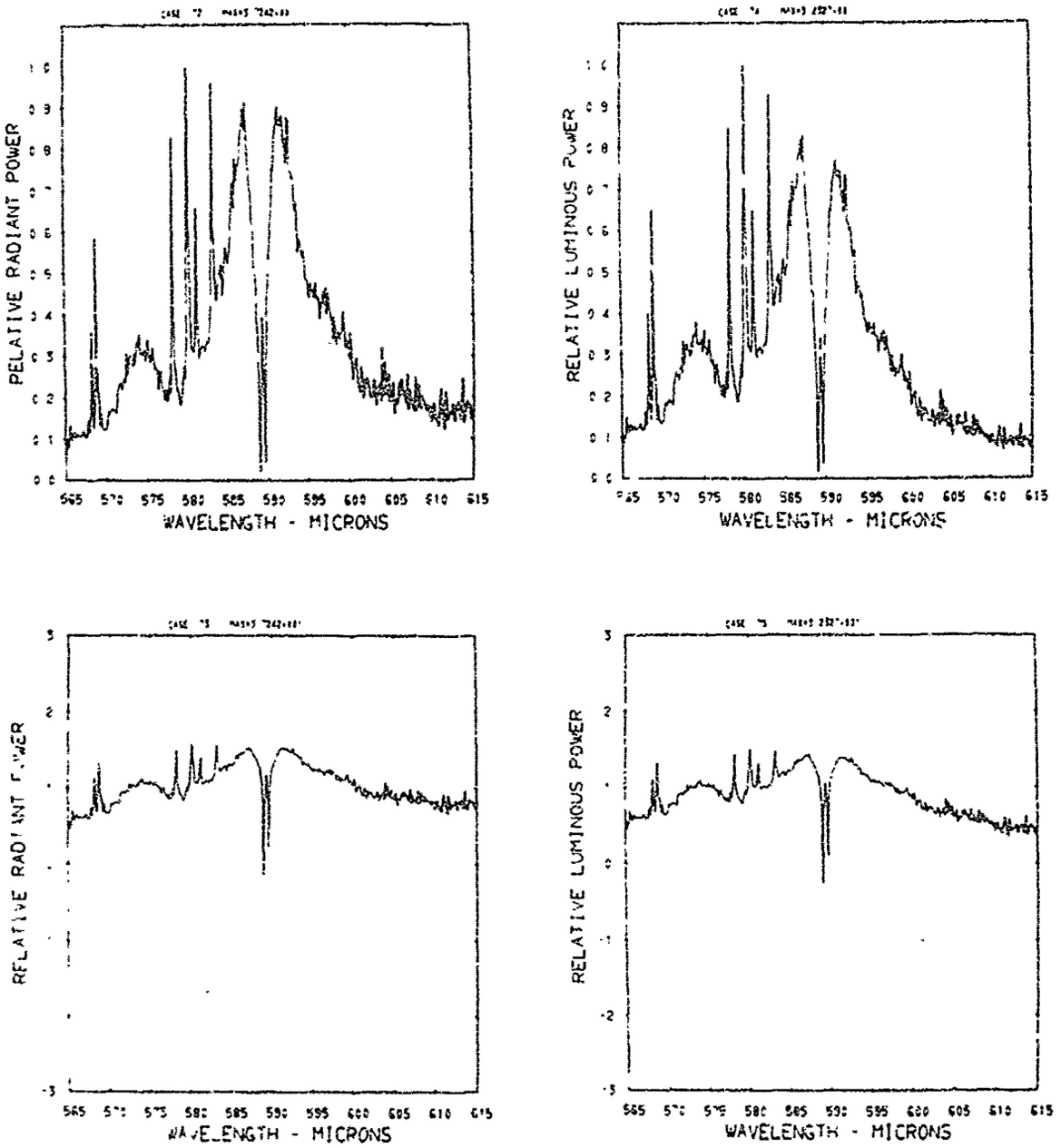

Figure A25. Relative power spectra of test flare 74 , formula group 2, burned at 760 torr ambient pressure. The top two spectra are normalized with the peak value equal to unity. The $\log_{10}$ of the spectral power is plotted in the bottom spectra. Flare formula group 2 contains 40.4% magnesium, 5.15% sodium nitrate, 49.95% potassium nitrate, and 4.5% binder.

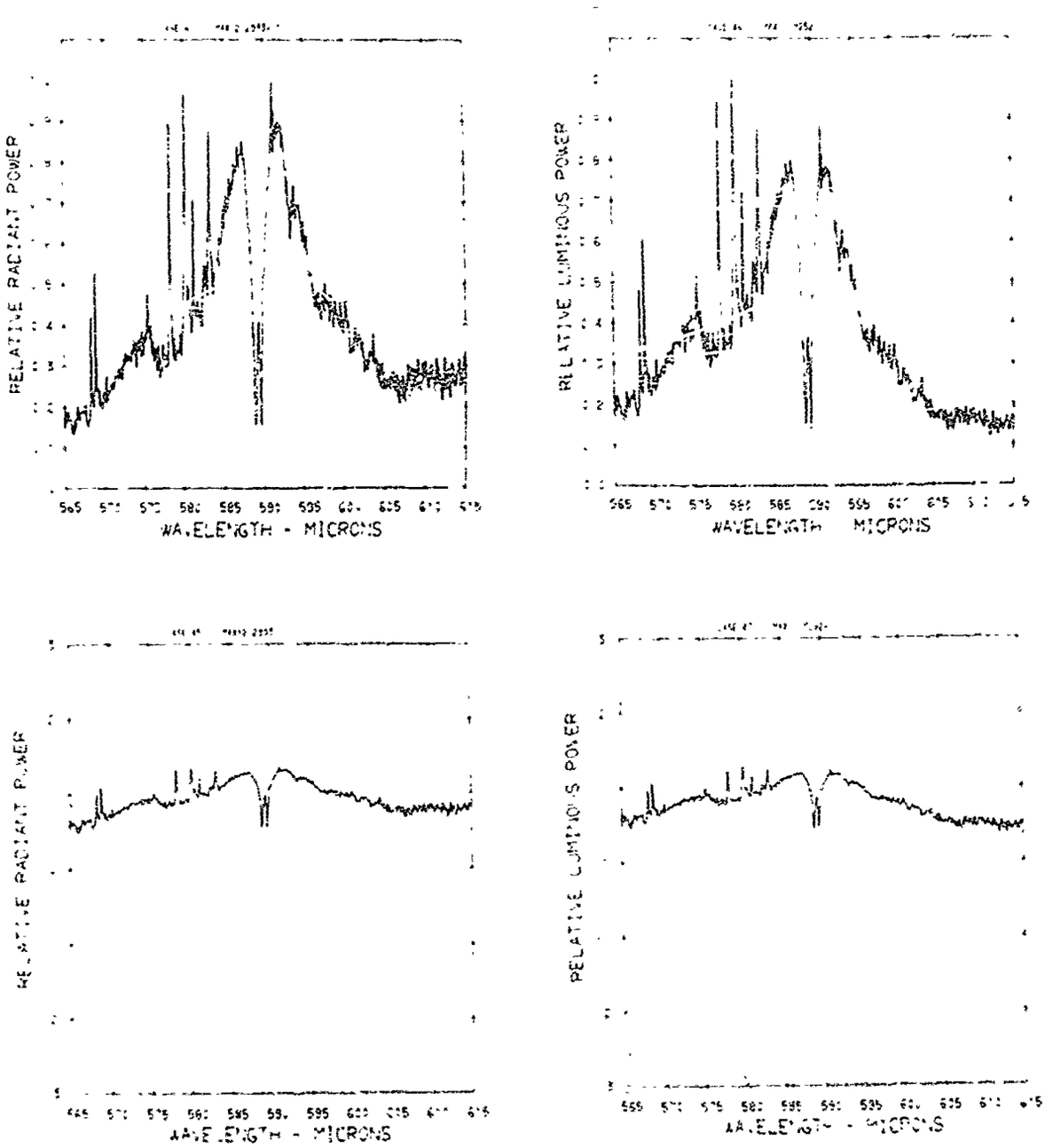

Figure A26. Relative power spectra of test flare 144 , formula group 2, burned at 760 torr ambient pressure. The top two spectra are normalized with the peak value equal to unity. The $\log_{10}$ of the spectral power is plotted in the bottom spectra. Flare formula group 2 contains 40.4 magnesium, 5.15% sodium nitrate, 49.95% potassium nitrate, and 4.5% binder.

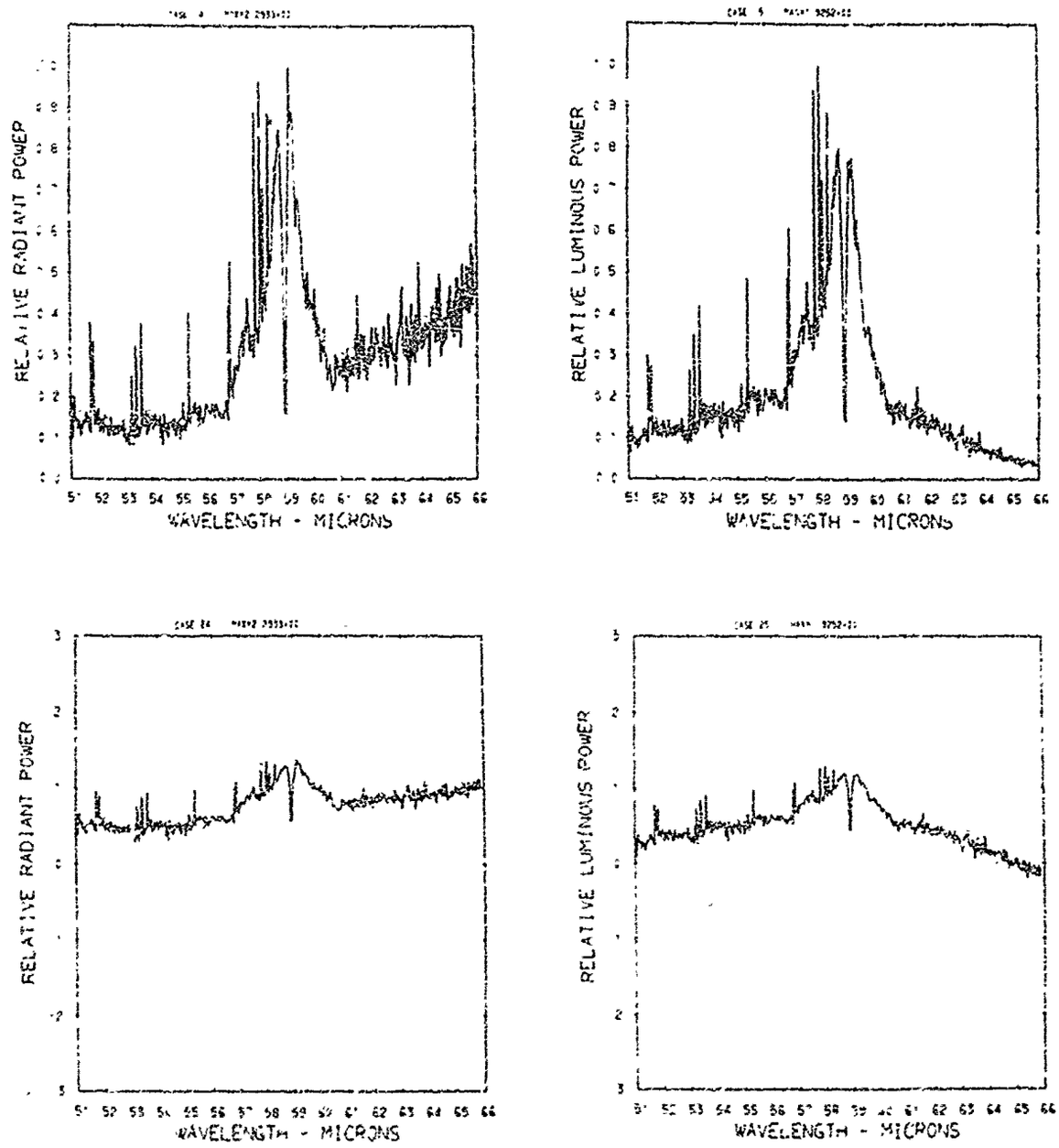

Figure A27. Relative power spectra of test flare 144 , formula group 2, burned at 760 torr ambient pressure. The top two spectra are normalized with the peak value equal to unity. The $\log_{10}$ of the spectral power is plotted in the bottom spectra. Flare formula group 2 contains 40.4% magnesium, 5.15% sodium nitrate, 49.95% potassium nitrate, and 4.5% binder.

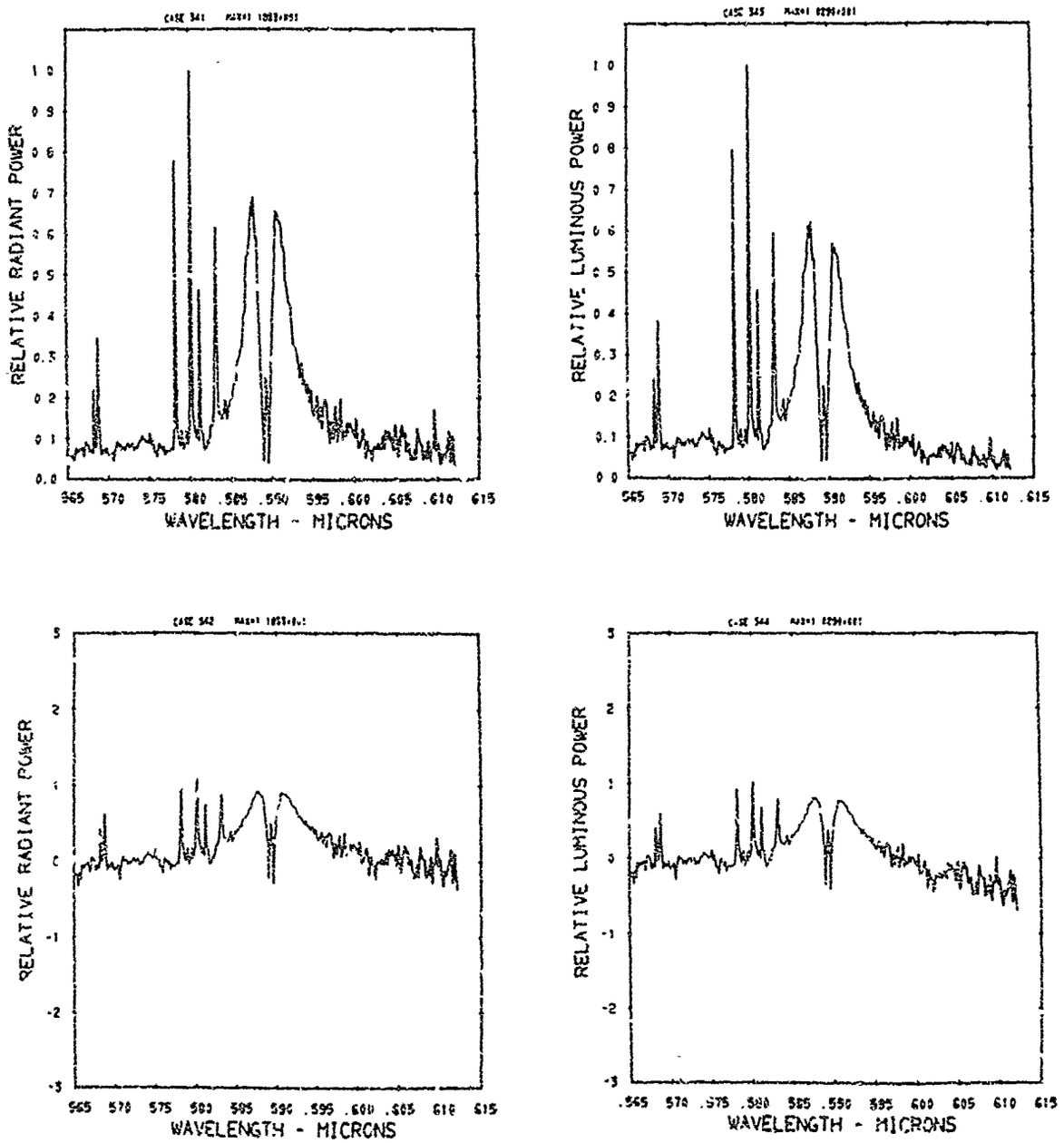

Figure A28. Relative power spectra of test flare 261A, formula group 2, burned at 630 torr ambient pressure. The top two spectra are normalized with the peak value equal to unity. The $\log_{10}$ of the spectral power is plotted in the bottom spectra. Flare formula group 2 contains 40.4% magnesium, 5.15% sodium nitrate, 49.95% potassium nitrate, and 4.5% binder.

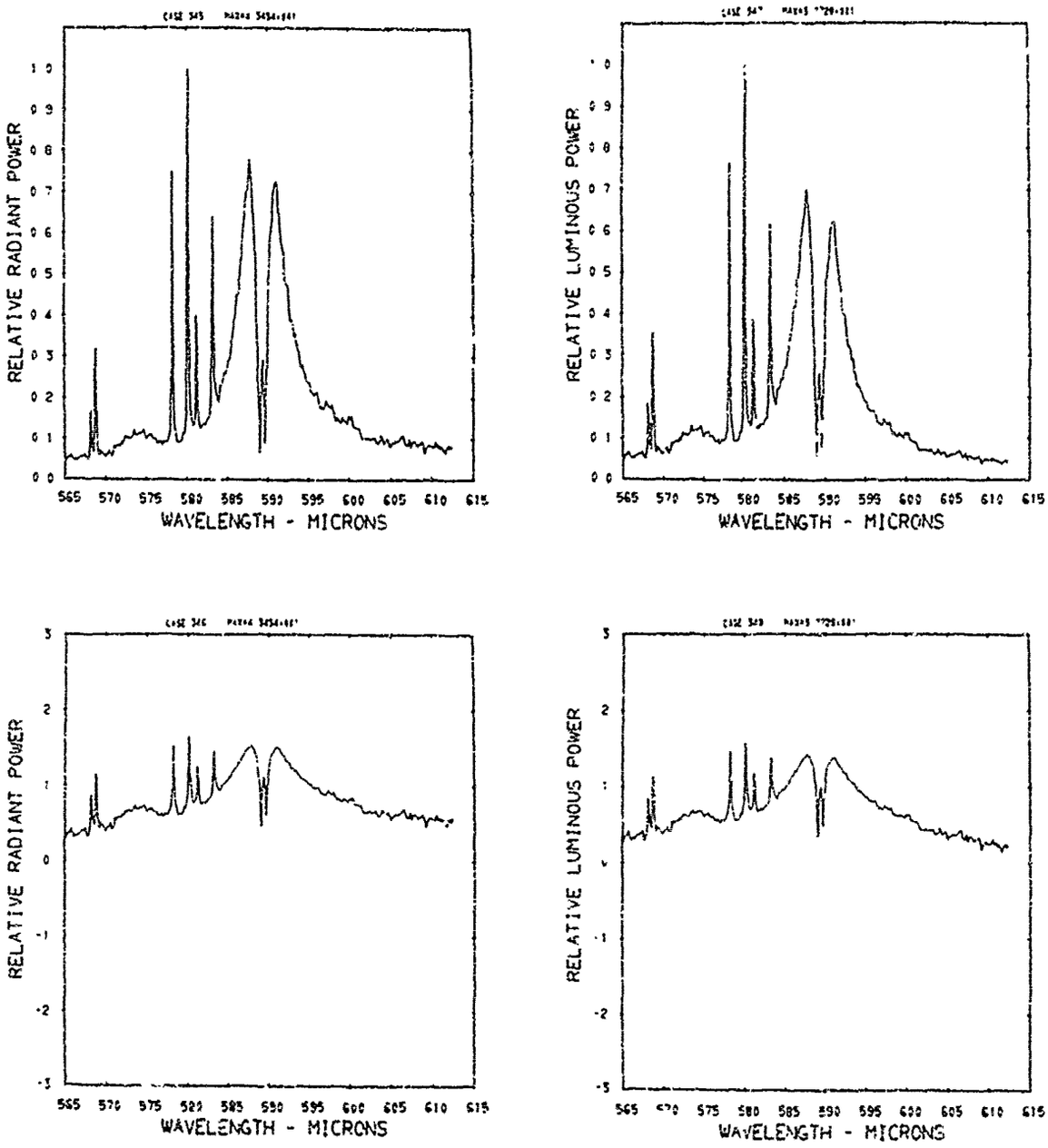

Figure A29. Relative power spectra of test flare 261B, formula group 2, burned at 630 torr ambient pressure. The top two spectra are normalized with the peak value equal to unity. The log[illegible] of the spectral power is plotted in the bottom spectra. Flare formula group 2 contains 40.4% magnesium, 5.15% sodium nitrate, 4[illegible].95% potassium nitrate, and 4.5% binder.

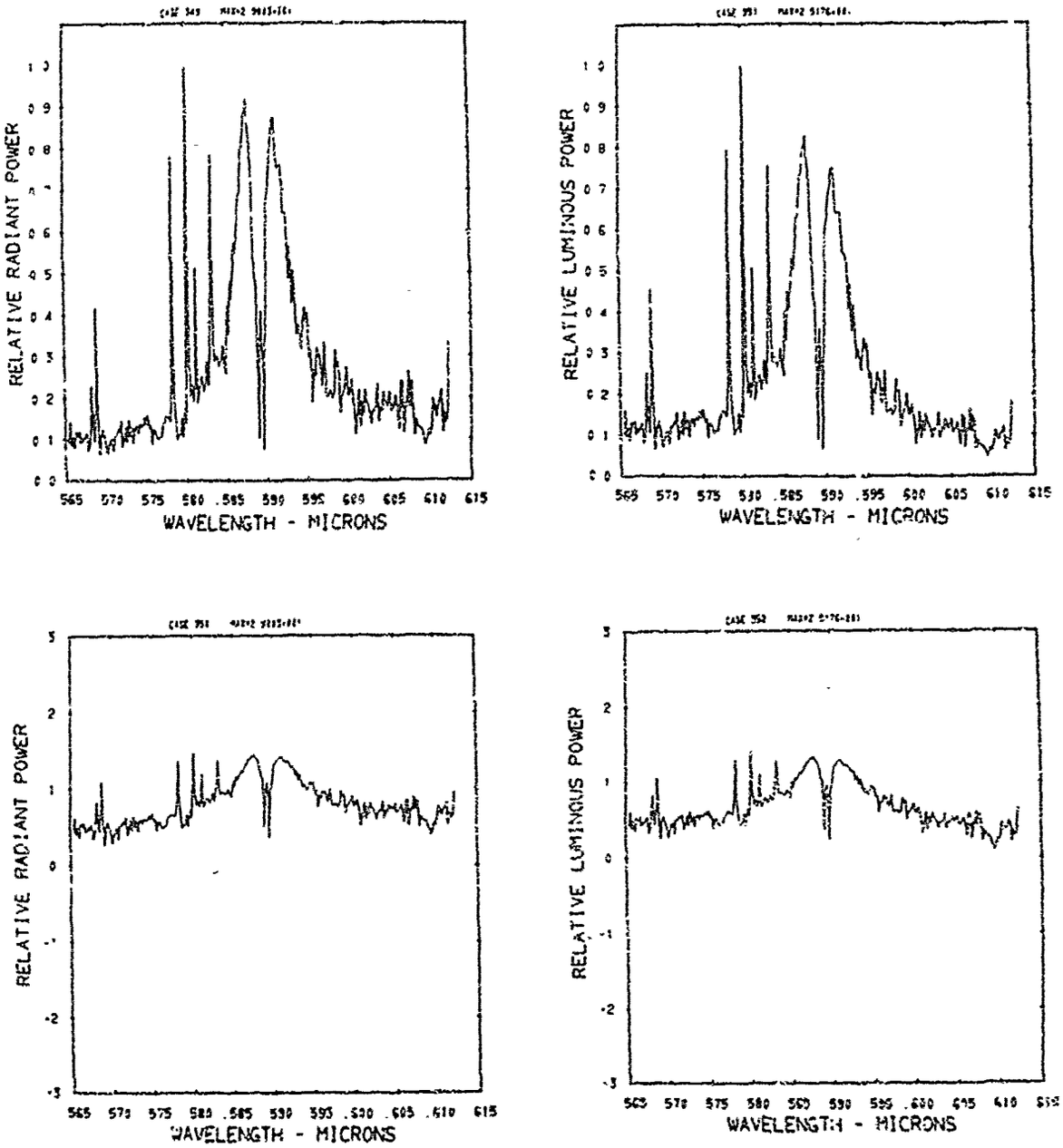

Figure A30. Relative power spectra of test flare 262A, formula group 2, burned at 630 torr ambient pressure. The top two spectra are normalized with the peak value equal to unity. The $\log_{10}$ of the spectral power is plotted in the bottom spectra. Flare formula group 2 contains 40.4% magnesium, 5.15% sodium nitrate, 49.95% potassium nitrate, and 4.5% binder.

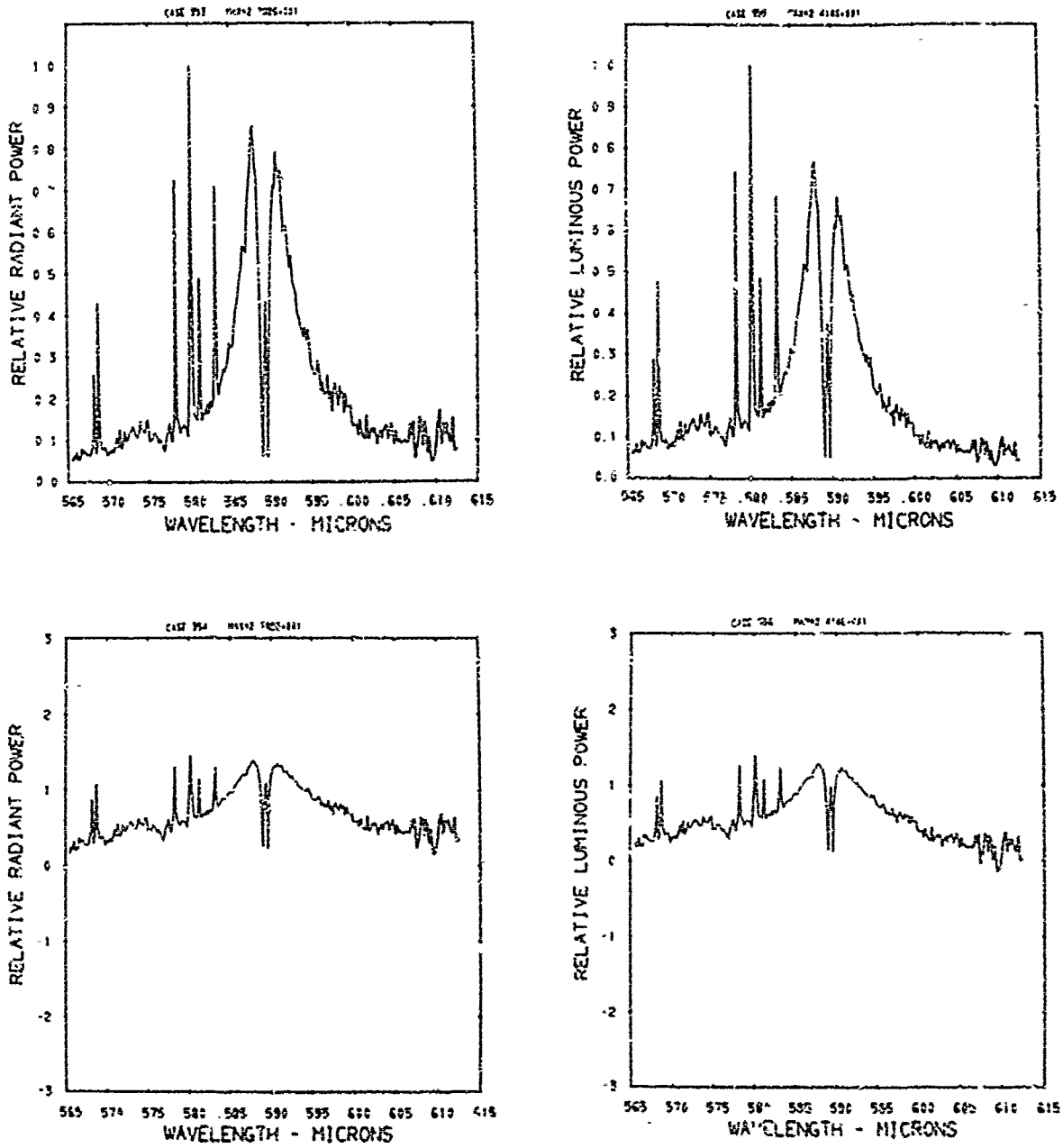

Figure A31. Relative power spectra of test flare 262B, formula group 2, burned at 630 torr ambient pressure. The top two spectra are normalized with the peak value equal to unity. The $\log_{10}$ of the spectral power is plotted in the bottom spectra. Flare formula group 2 contains 40.4% magnesium, 5.15% sodium nitrate, 49.95% potassium nitrate, and 4.5% binder.

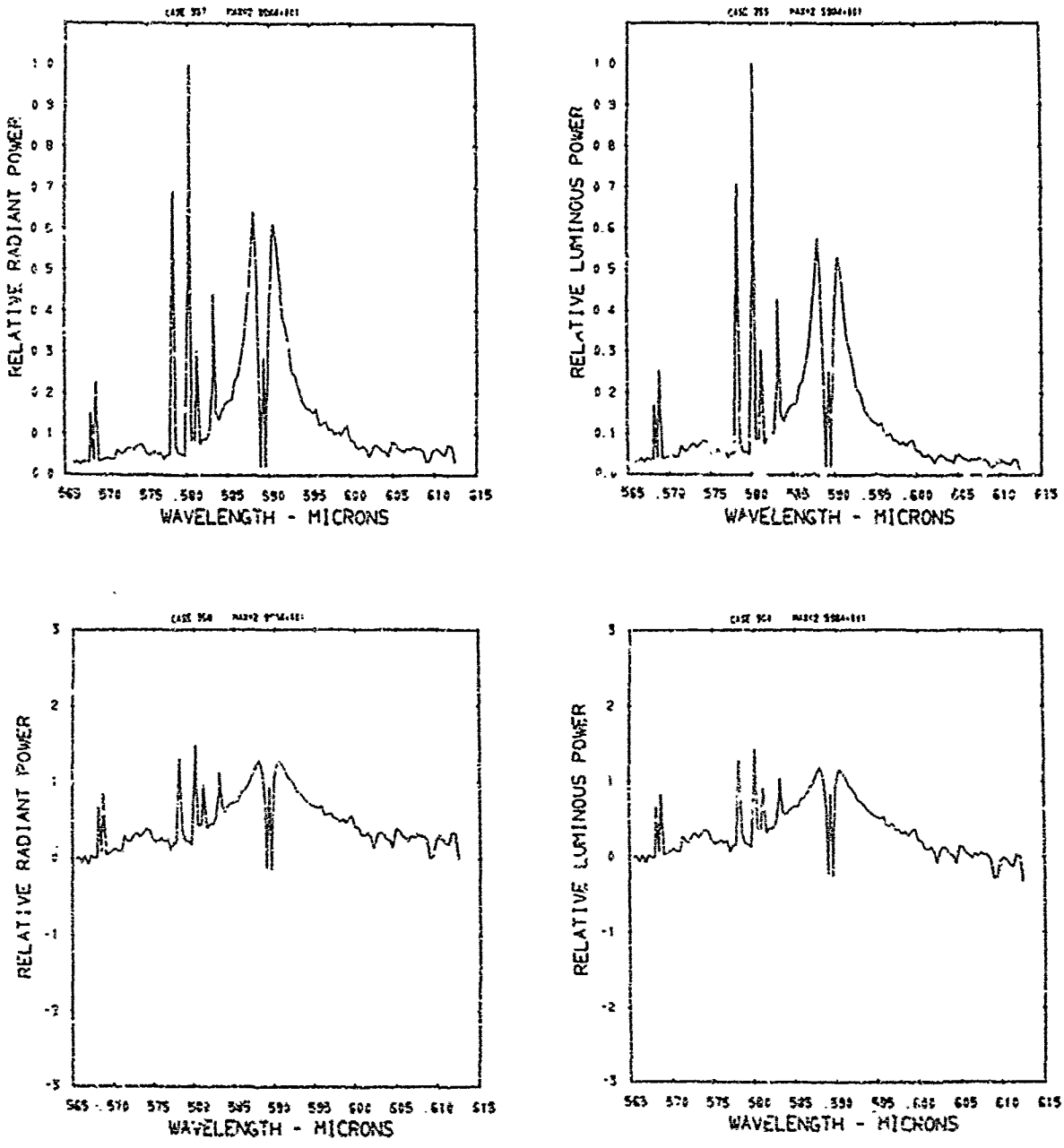

Figure A32. Relative power spectra of test flare 262C, formula group 2, burned at 630 torr ambient pressure. The top two spectra are normalized with the peak value equal to unity. The $\log_{10}$ of the spectral power is plotted in the bottom spectra. Flare formula group 2 contains 40.4% magnesium, 5.15% sodium nitrate, 49.95% potassium nitrate, and 4.5% binder.

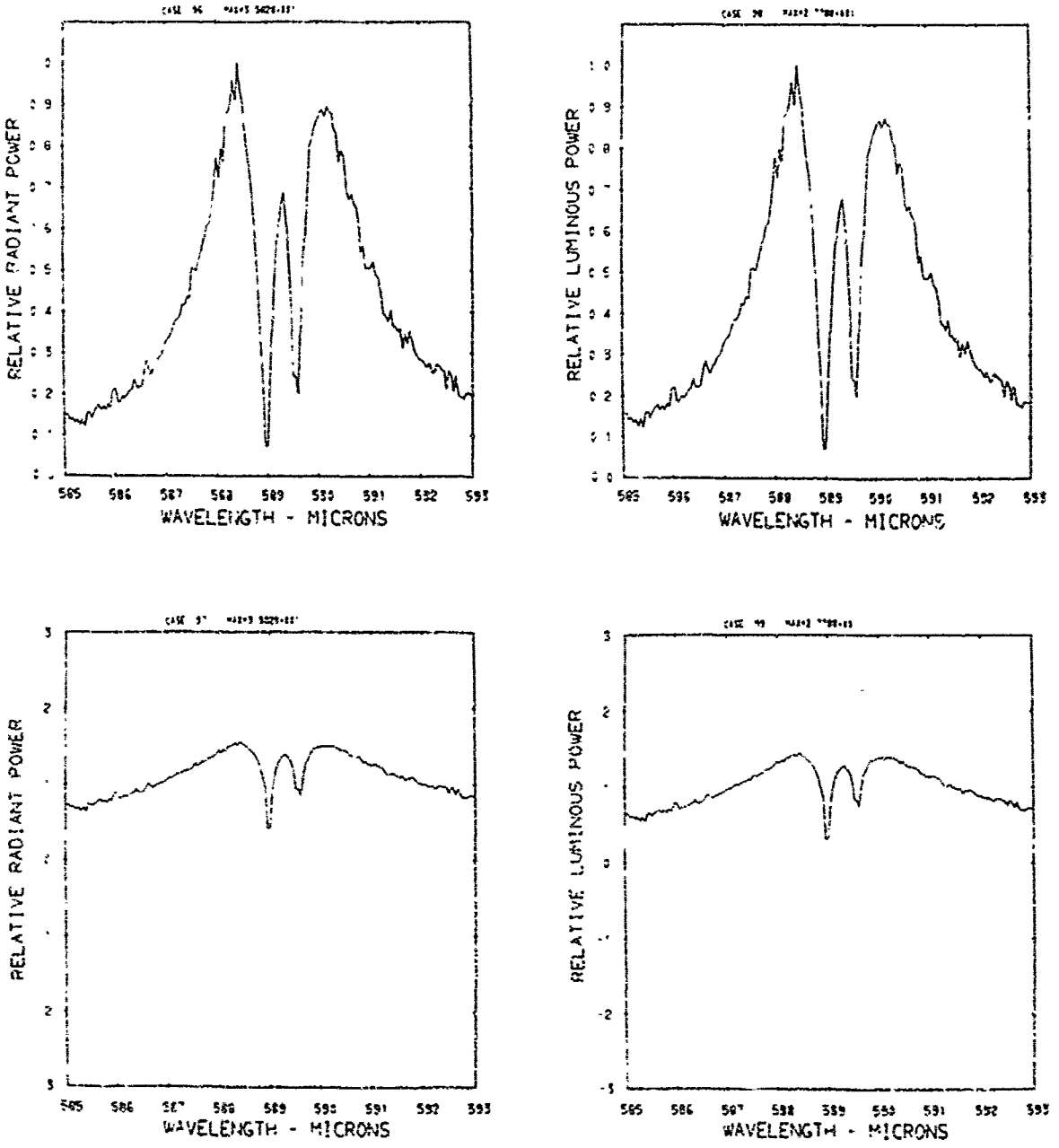

Figure A33. Relative power spectra of test flare 117 , formula group 2, burned at 300 torr ambient pressure. The top two spectra are normalized with the peak value equal to unity. The $\log_{10}$ of the spectral power is plotted in the bottom spectra. Flare formula group 2 contains 40.4% magnesium, 5.15% sodium nitrate, 49.95% potassium nitrate, and 4.5% binder.

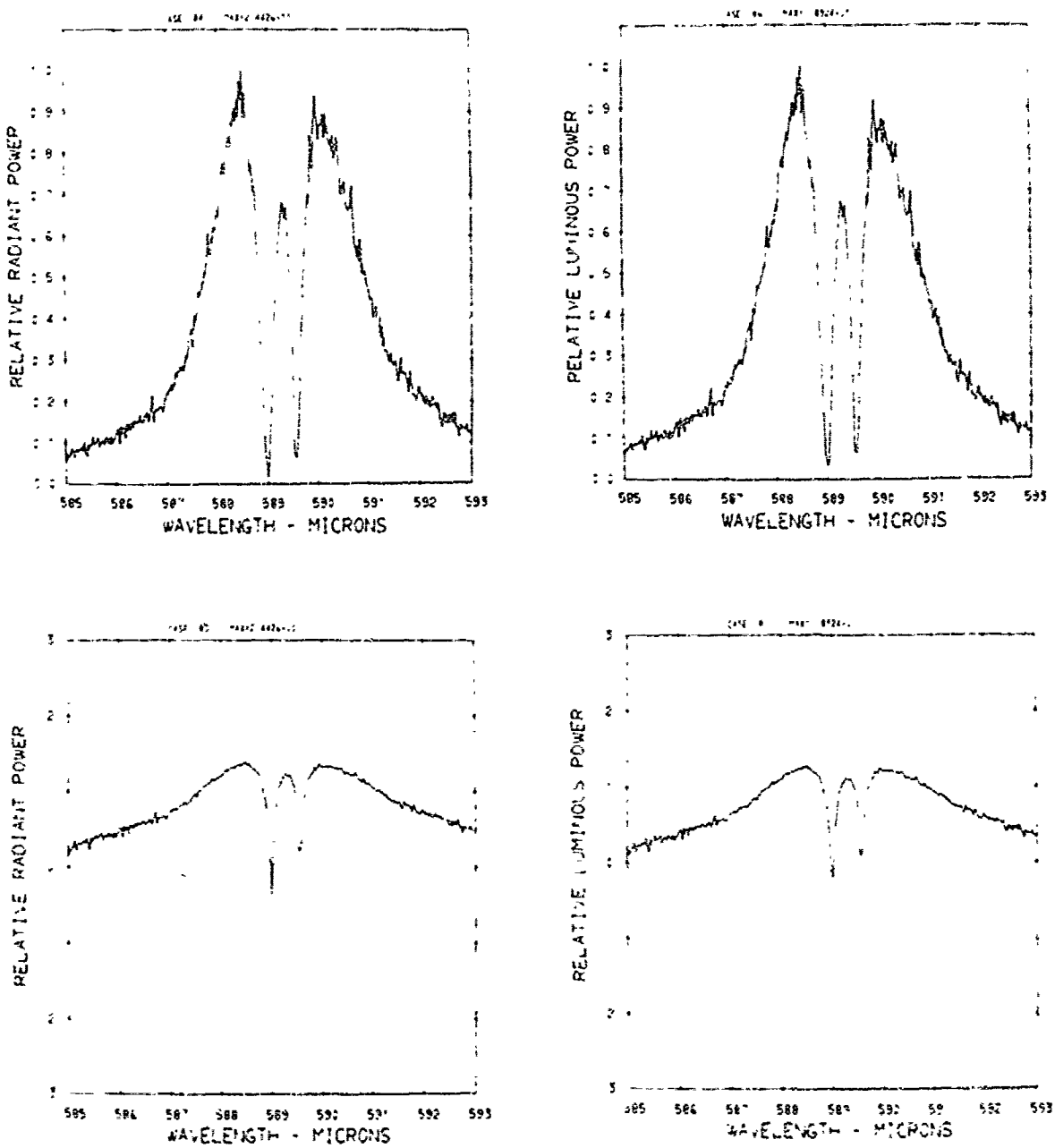

Figure A34. Relative power spectra of test flare 119B, formula group 2, burned at 300 torr ambient pressure. The top two spectra are normalized with the peak value equal to unity. The $\log_e$ of the spectral power is plotted in the bottom spectra. Flare formula group 2 contains 40.4% magnesium, 5.15% sodium nitrate, 49.95% potassium nitrate, and 4.5% binder.

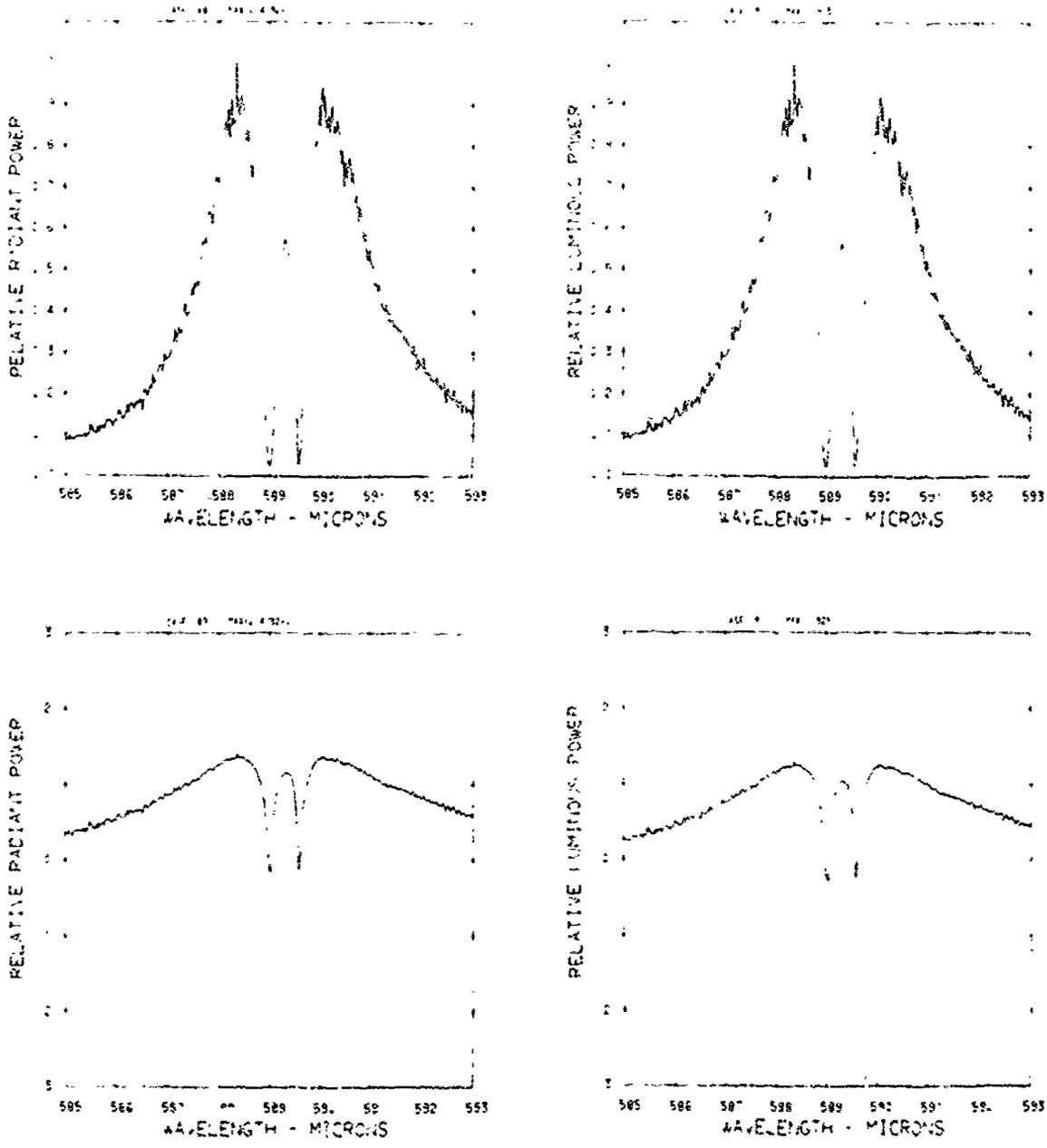

Figure A35. Relative power spectra of test flare 119C, formula group 2, burned at 300 torr ambient pressure. The top two spectra are normalized with the peak value equal to unity. The $\log_{10}$ of the spectral power is plotted in the bottom spectra. Flare formula group 2 contains 40.4% magnesium, 5.15% sodium nitrate, 49.95% potassium nitrate, and 4.5% binder.

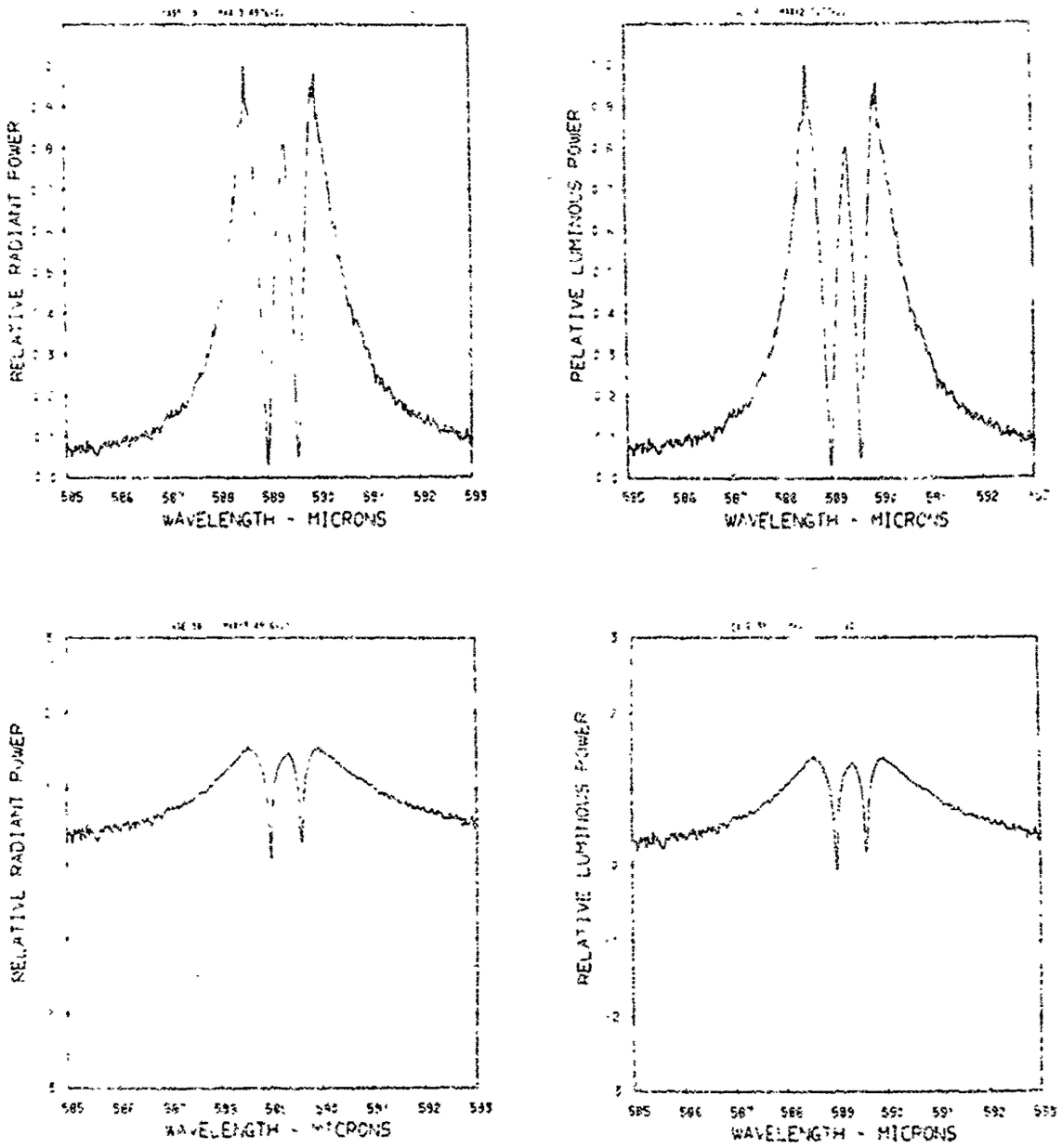

Figure A36. Relative power spectra of test flare 149A, formula group 2, burned at 2.5 torr ambient pressure. The top two spectra are normalized with the peak value equal to unity. The $\log_{10}$ of the spectral power is plotted in the bottom spectra. Flare formula group 2 contains 40.4% magnesium, 5.15% sodium nitrate, 49.95% potassium nitrate, and 4.5% binder.

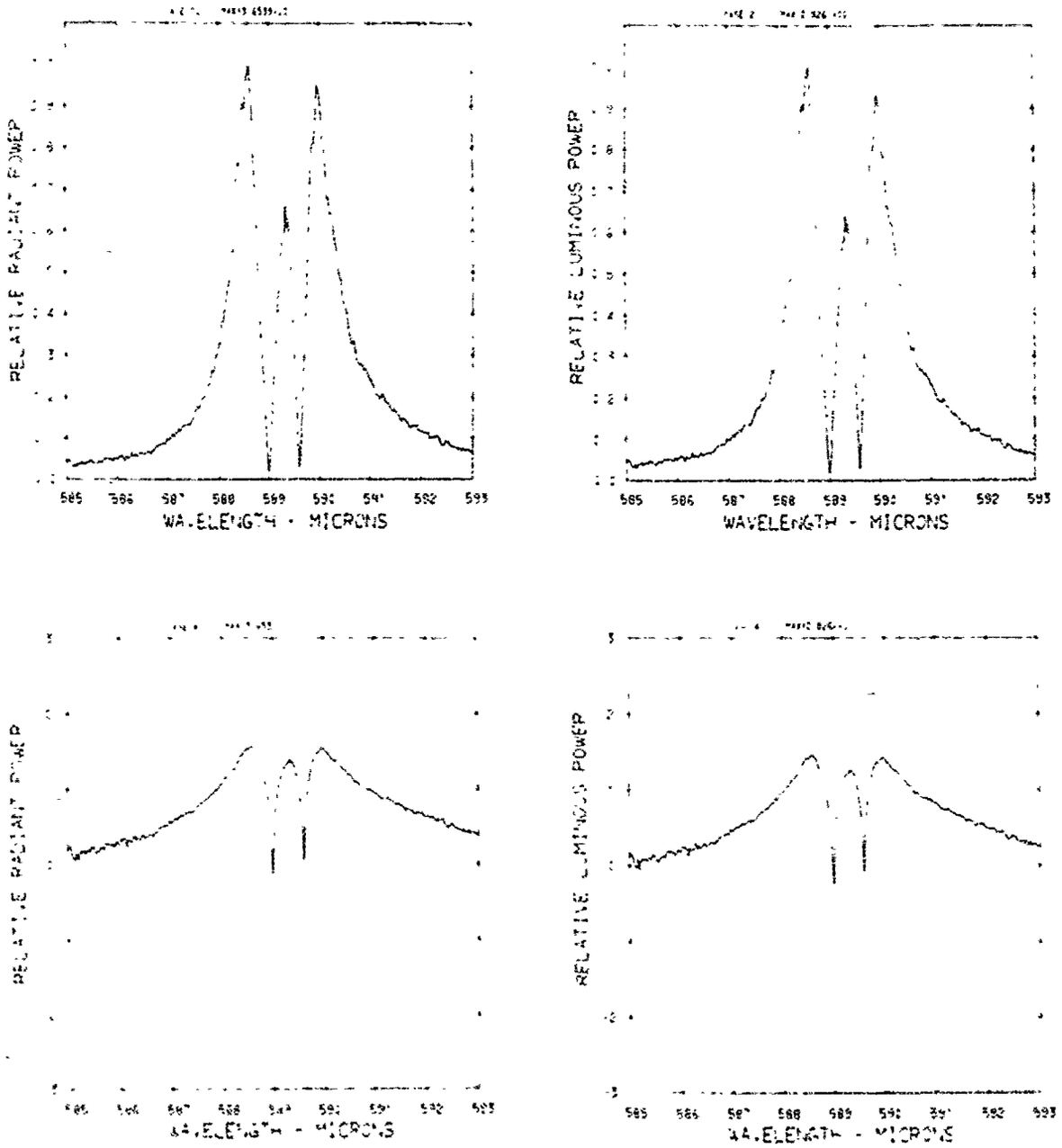

Figure A37. Relative power spectra of test flare 149B, formula group 2, burned at 225 torr ambient pressure. The top two spectra are normalized with the peak value equal to unity. The $\log_{10}$ of the spectral power is plotted in the bottom spectra. Flare formula group 2 contains 40.4% magnesium, 5.15% sodium nitrate, 49.95% potassium nitrate, and 4.5% binder.

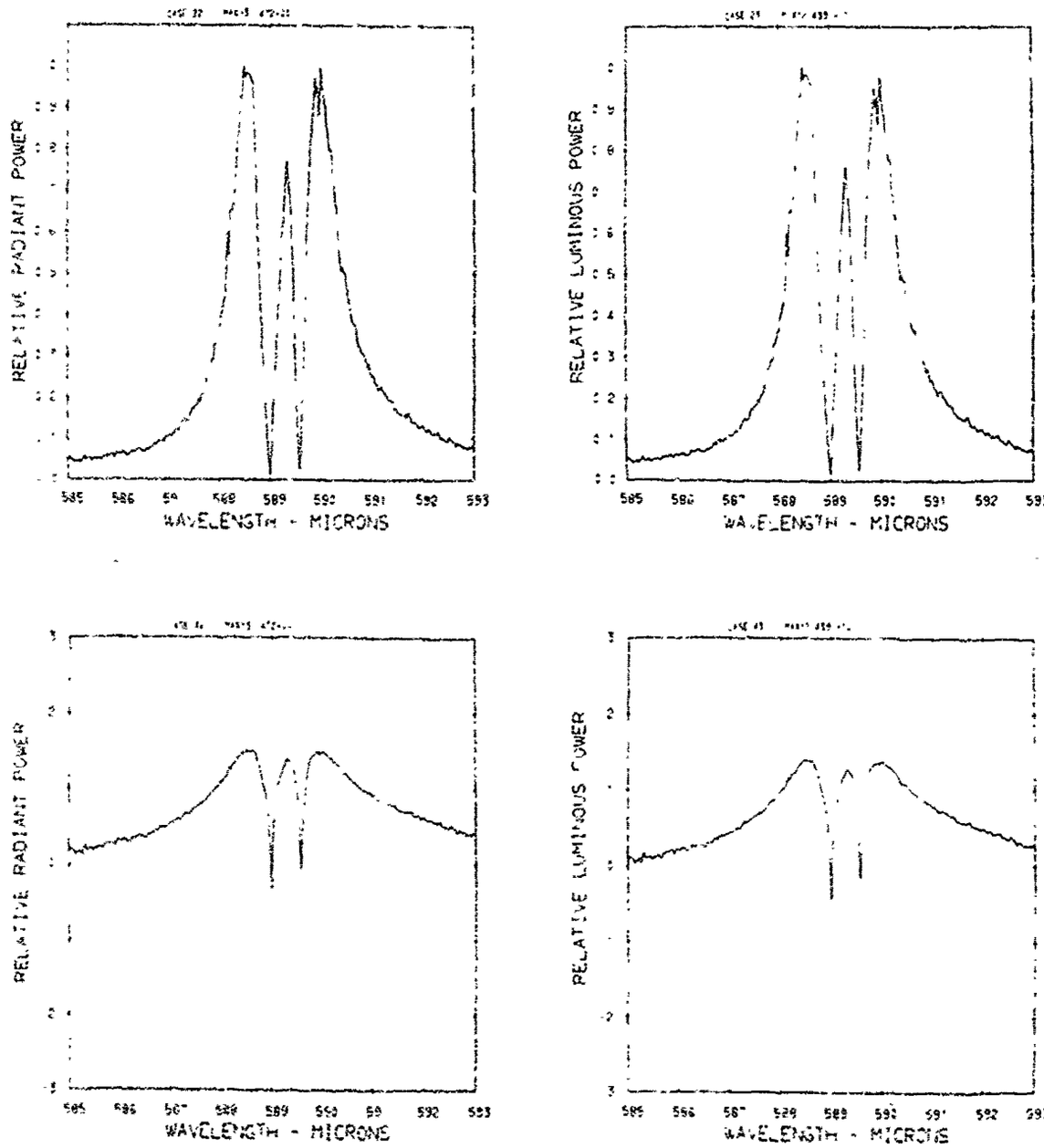

Figure A38. Relative power spectra of test flare 149C, formula group 2, burned at 225 torr ambient pressure. The top two spectra are normalized with the peak value equal to unity. The $\log_{10}$ of the spectral power is plotted in the bottom spectra. Flare formula group 2 contains 40.4% magnesium, 5.15% sodium nitrate, 49.95% potassium nitrate, and 4.5% binder.

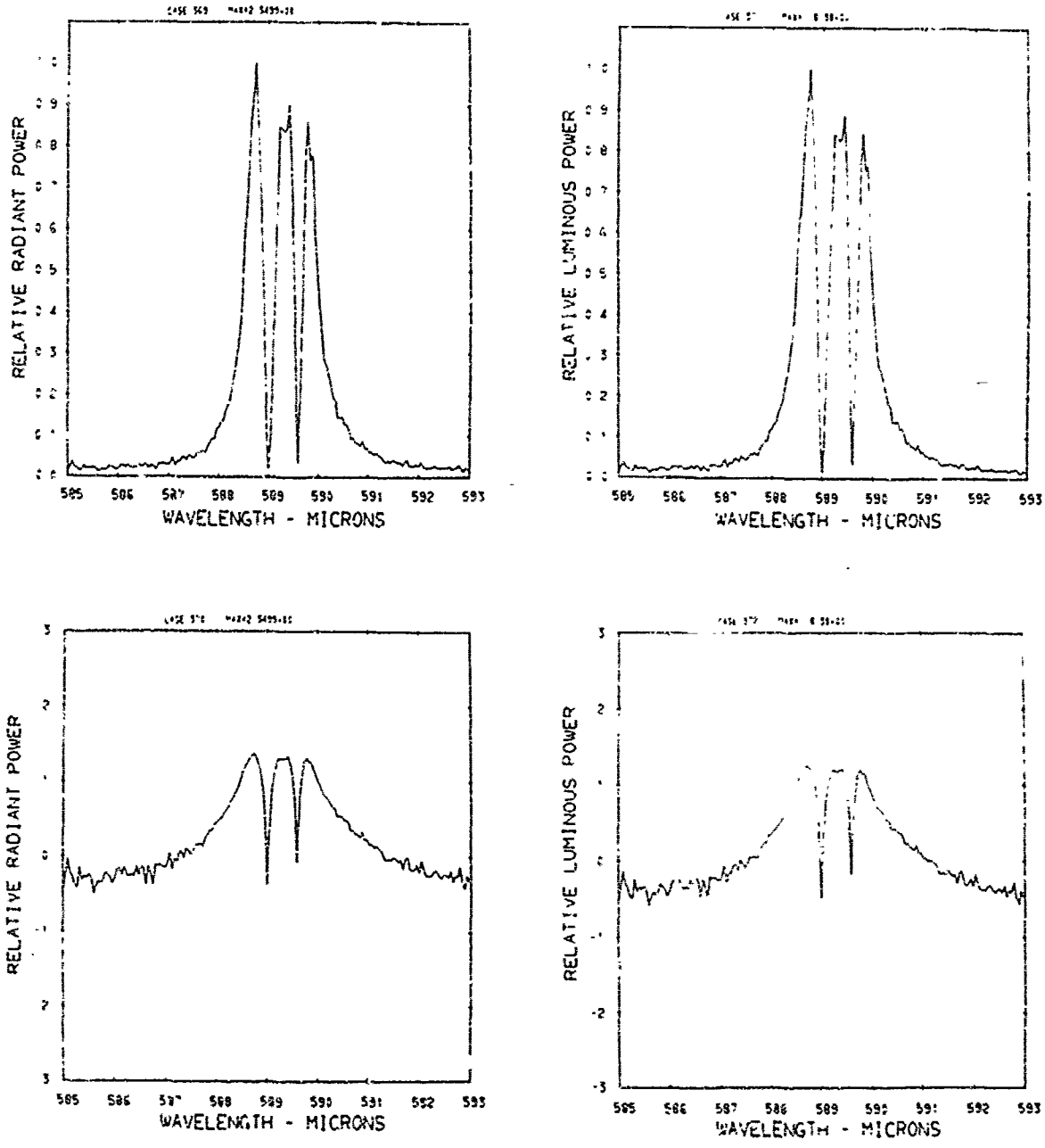

Figure A39. Relative power spectra of test flare 47 , formula group 2, burned at 150 torr ambient pressure. The top two spectra are normalized with the peak value equal to unity. The $\log_{10}$ of the spectral power is plotted in the bottom spectra. Flare formula group 2 contains 40.4% magnesium, 5.15% sodium nitrate, 49.95% potassium nitrate, and 4.5% binder.

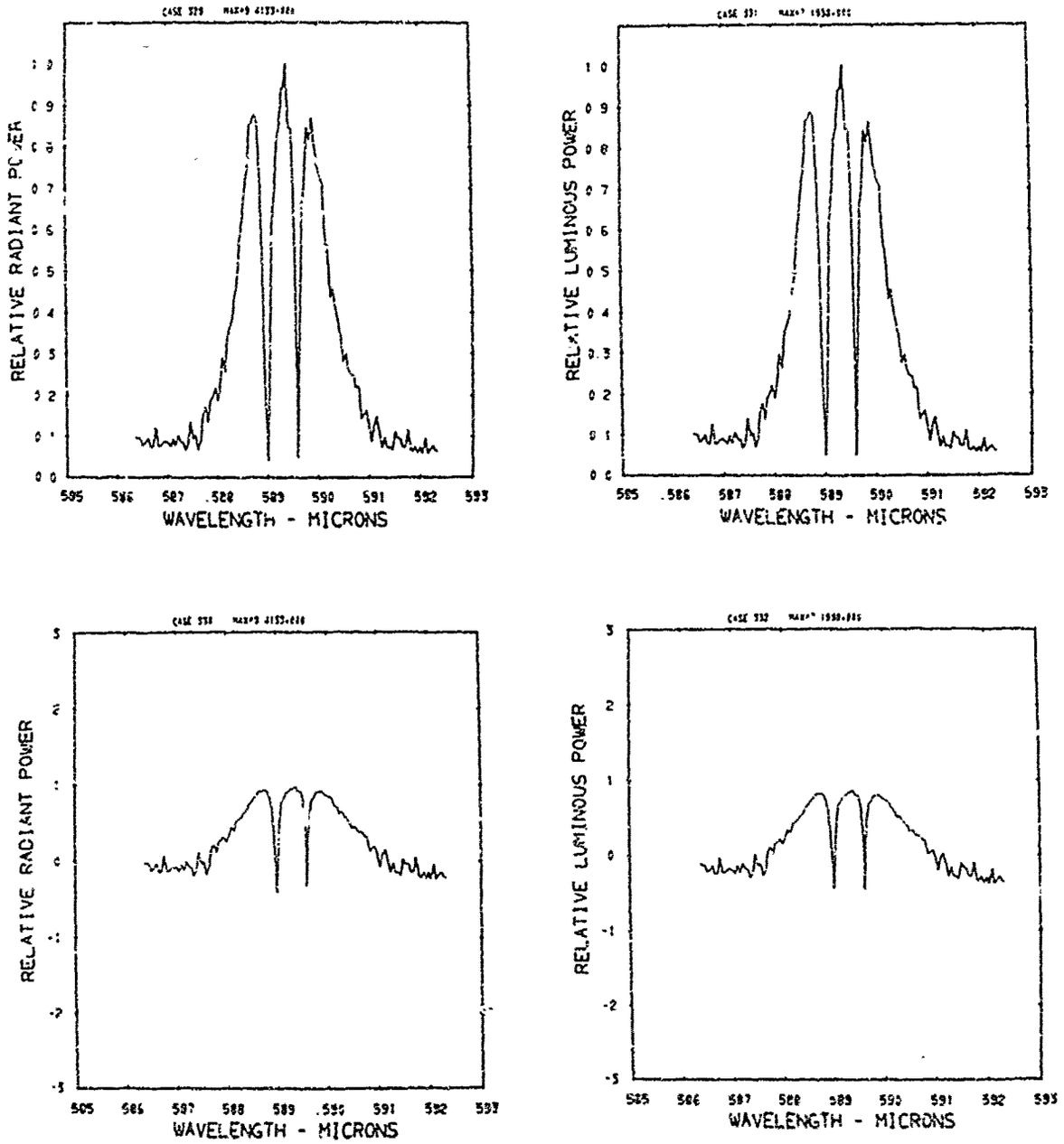

Figure A40. Relative power spectra of test flare 51 , formula group 2, burned at 150 torr ambient pressure. The top two spectra are normalized with the peak value equal to unity. The $\log_{10}$ of the spectral power is plotted in the bottom spectra. Flare formula group 2 contains 40.4% magnesium, 5.15% sodium nitrate, 49.95% potassium nitrate, and 4.5% binder.

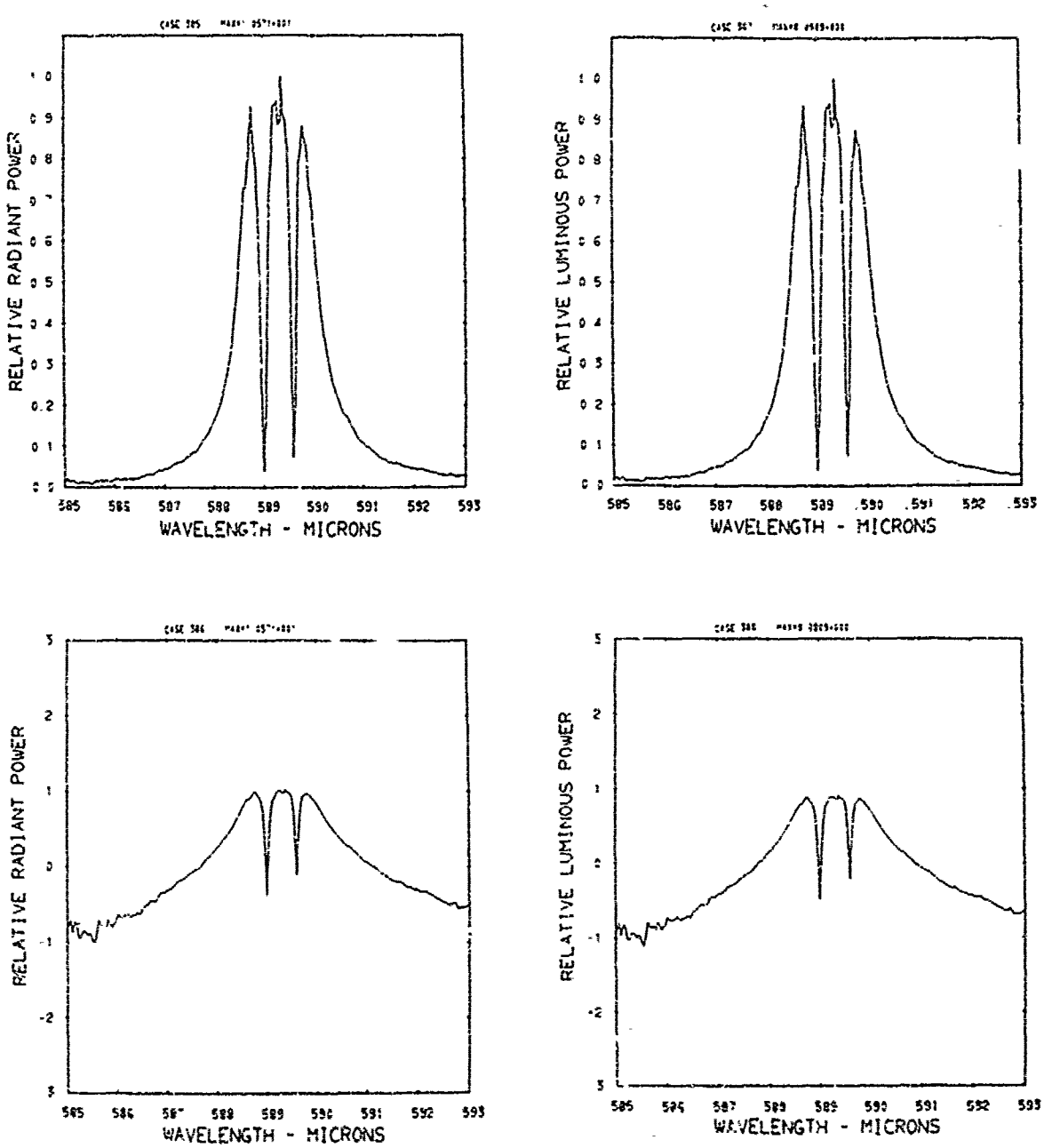

Figure A41. Relative power spectra of test flare 55 , formula group 2, burned at 150 torr ambient pressure. The top two spectra are normalized with the peak value equal to unity. The $\log_{10}$ of the spectral power is plotted in the bottom spectra. Flare formula group 2 contains 40.4% magnesium, 5.15% sodium nitrate, 49.95% potassium nitrate, and 4.5% binder.

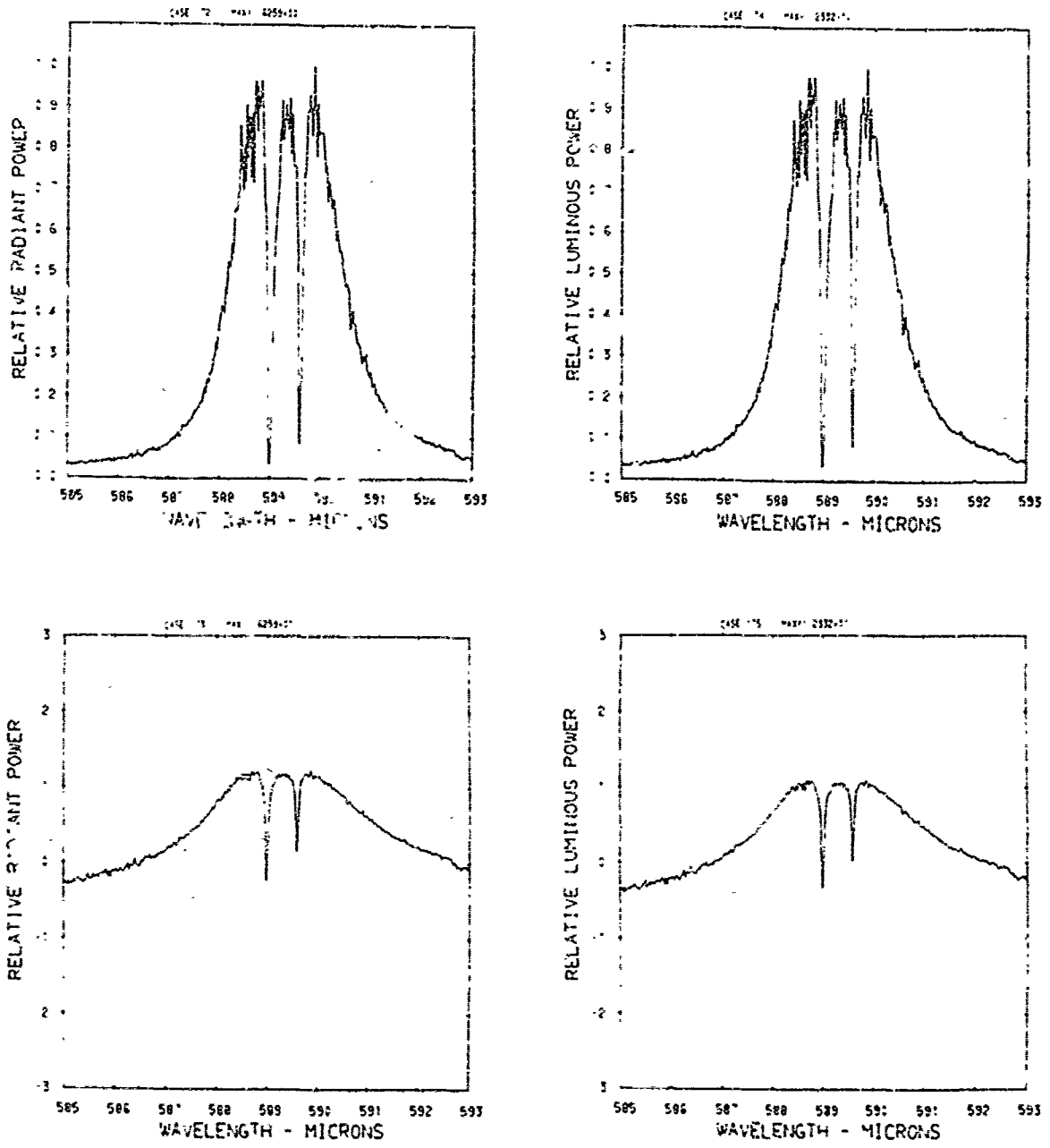

Figure A42. Relative power spectra of test flare 112 , formula group 2, burned at 150 torr ambient pressure. The top two spectra are normalized with the peak value equal to unity. The $\log_{10}$ of the spectral power is plotted in the bottom spectra. Flare formula group 2 contains 40.4% magnesium, 5.15% sodium nitrate, 49.95% potassium nitrate, and 4.5% binder.

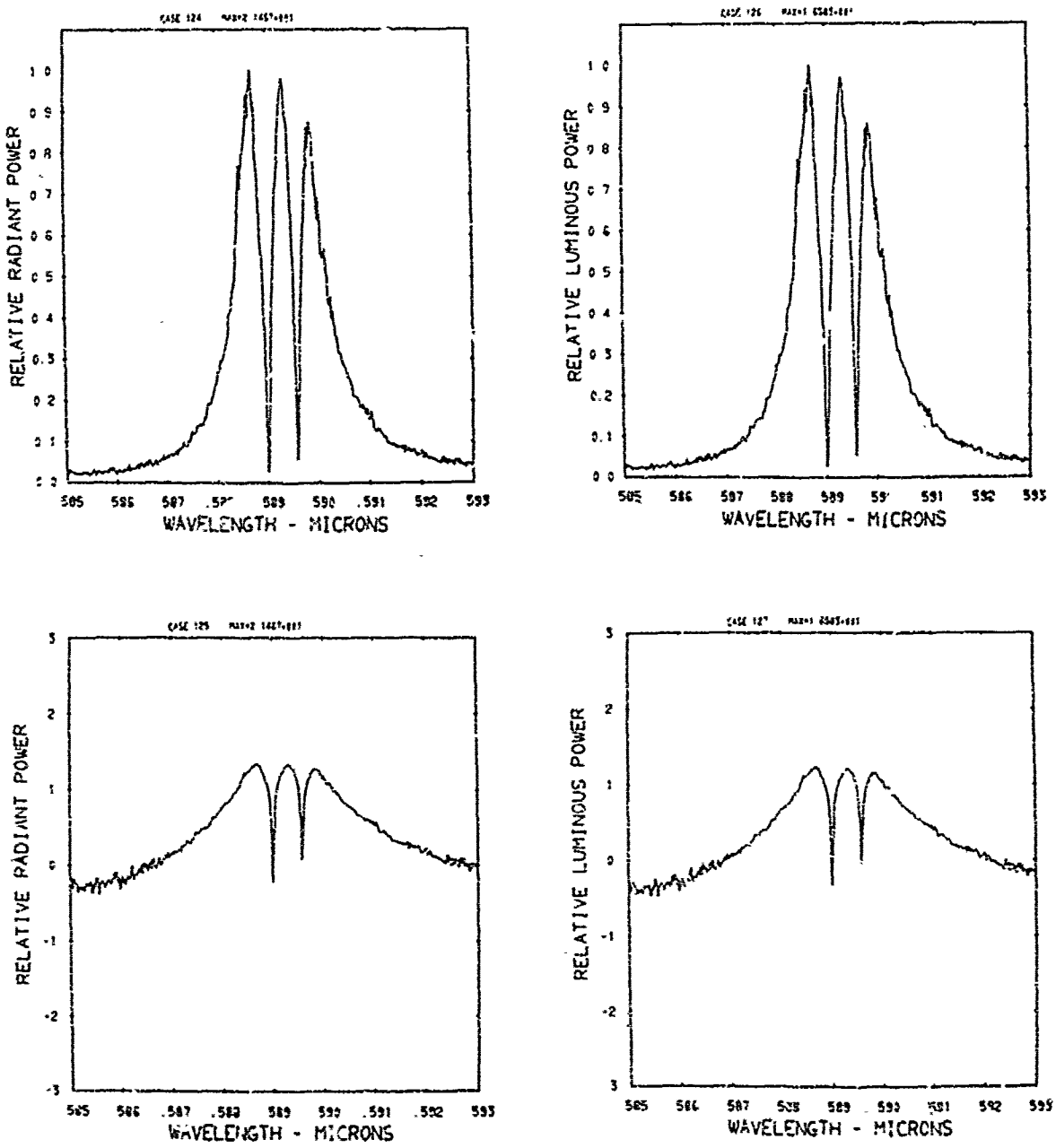

Figure A43. Relative power spectra of test flare 125 , formula group 2, burned at 150 torr ambient pressure. The top two spectra are normalized with the peak value equal to unity. The $\log_{10}$ of the spectral power is plotted in the bottom spectra. Flare formula group 2 contains 40.4% magnesium, 5.15% sodium nitrate, 49.95% potassium nitrate, and 4.5% binder.

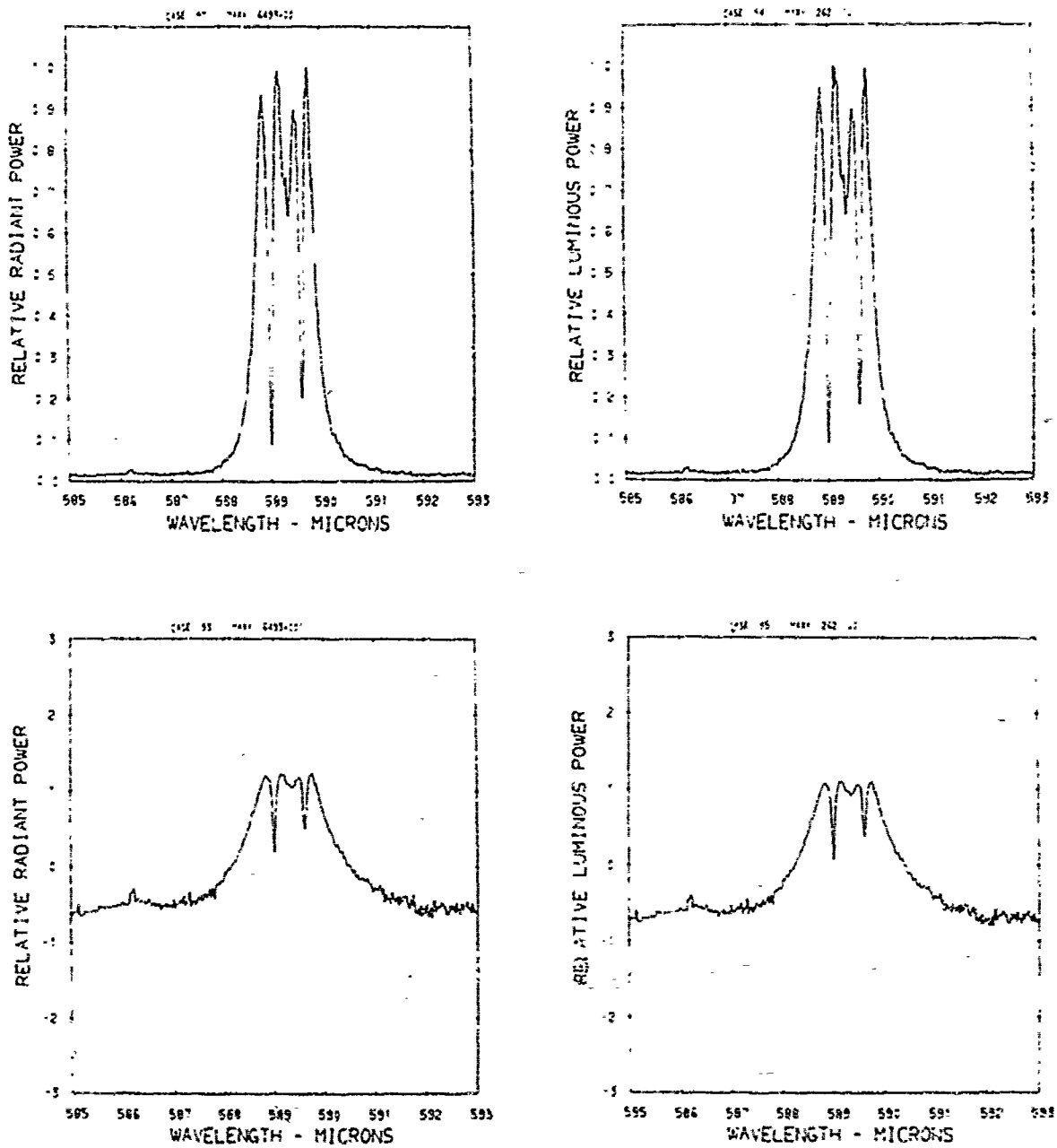

Figure A44. Relative power spectra of test flare 120 , formula group 2, burned at 75 torr ambient pressure. The top two spectra are normalized with the peak value equal to unity. The $\log_{10}$ of the spectral power is plotted in the bottom spectra. Flare formula group 2 contains 40.4% magnesium, 5.15% sodium nitrate, 49.95% potassium nitrate, and 4.5% binder.

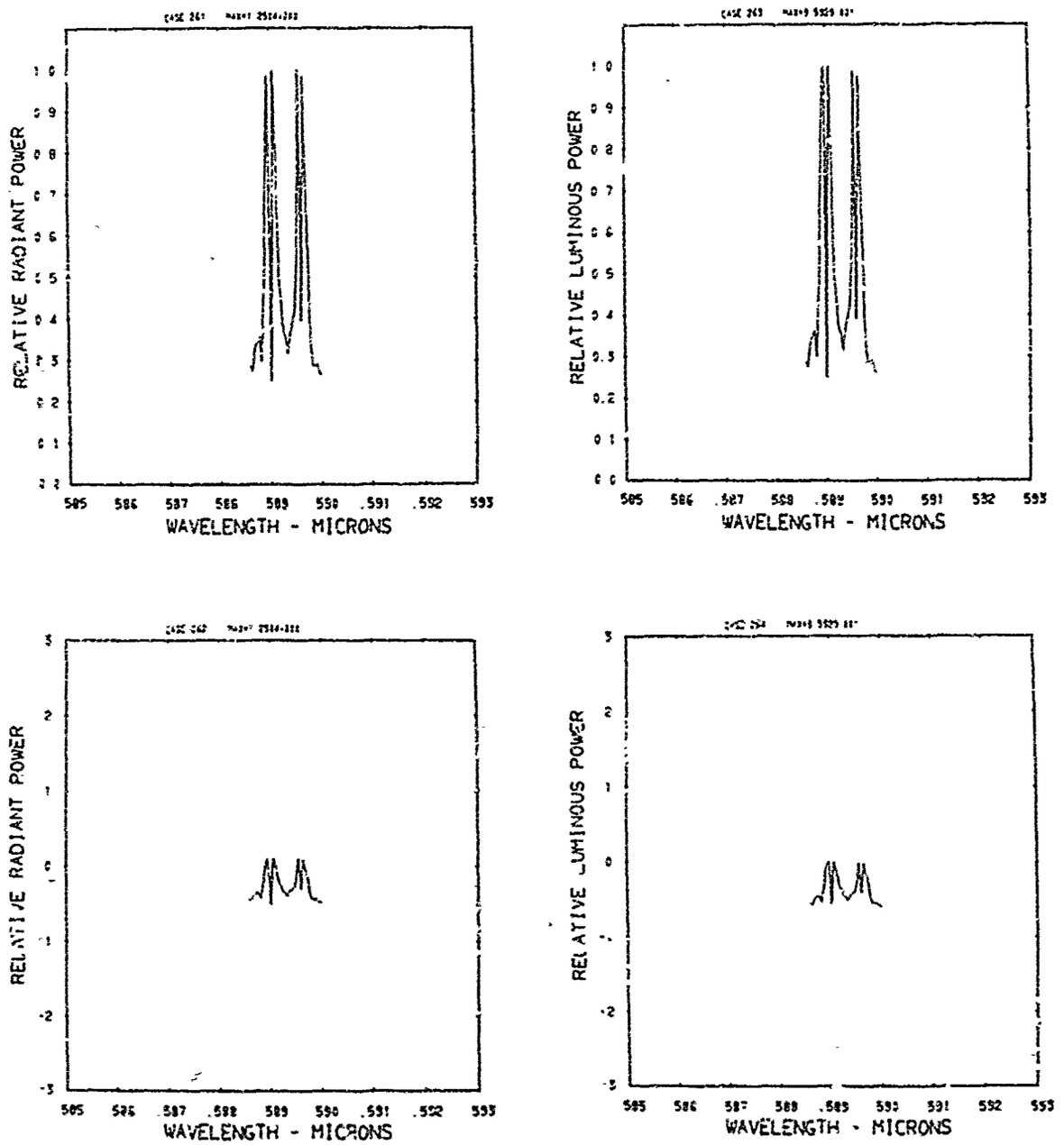

Figure A45. Relative power spectra of test flare 23A , formula group 2, burned at 30 torr ambient pressure. The top two spectra are normalized with the peak value equal to unity. The $\log_{10}$ of the spectral power is plotted in the bottom spectra. Flare formula group 2 contains 40.4% magnesium, 5.15% sodium nitrate, 49.95% potassium nitrate, and 4.5% binder.

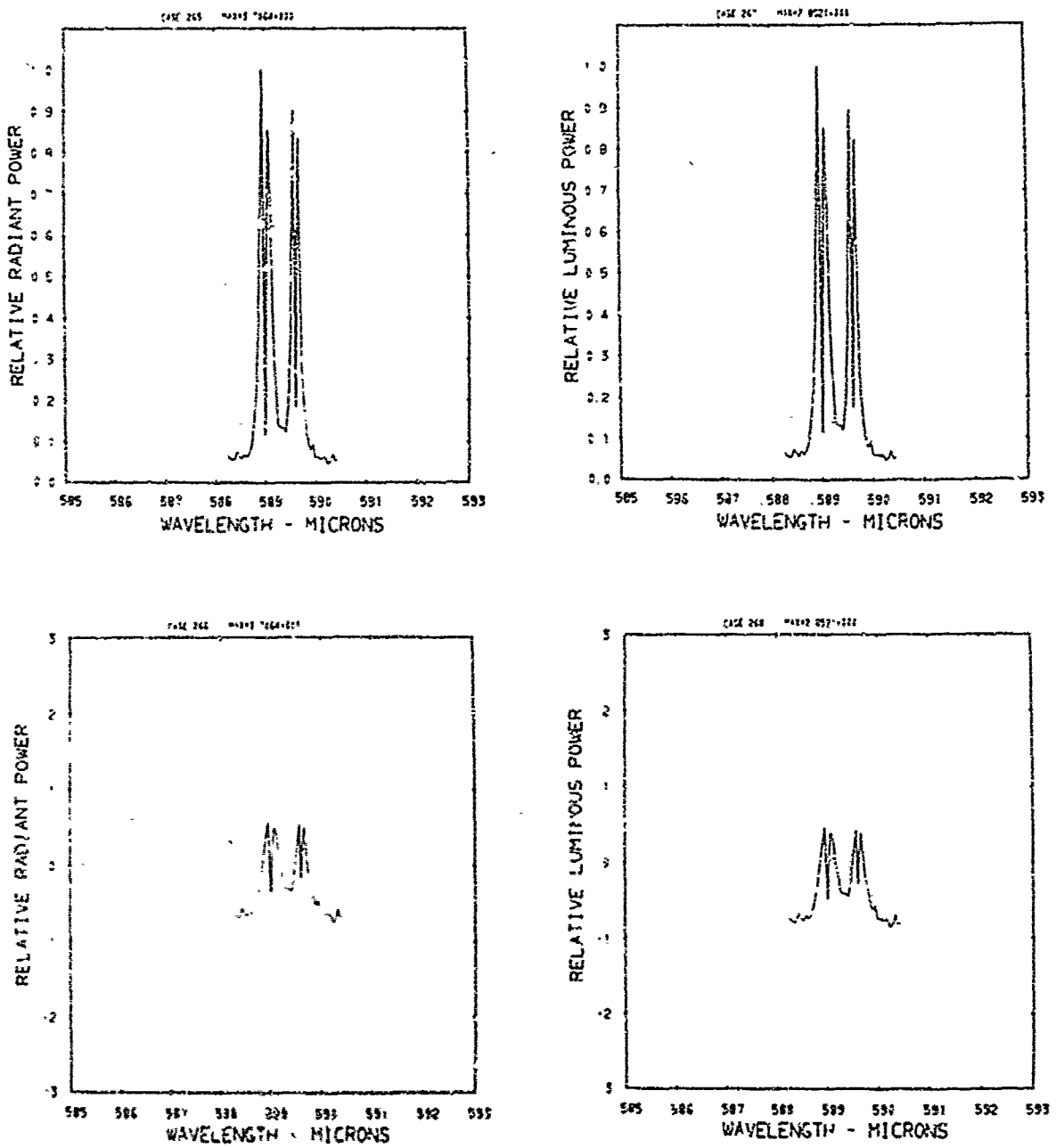

Figure A46. Relative power spectra of test flare 23B , formula group 2, burned at 30 torr ambient pressure. The top two spectra are normalized with the peak value equal to unity. The $\log_{10}$ of the spectral power is plotted in the bottom spectra. Flare formula group 2 contains 40.4% magnesium, 5.15% sodium nitrate, 49.95% potassium nitrate, and 4.5% binder.

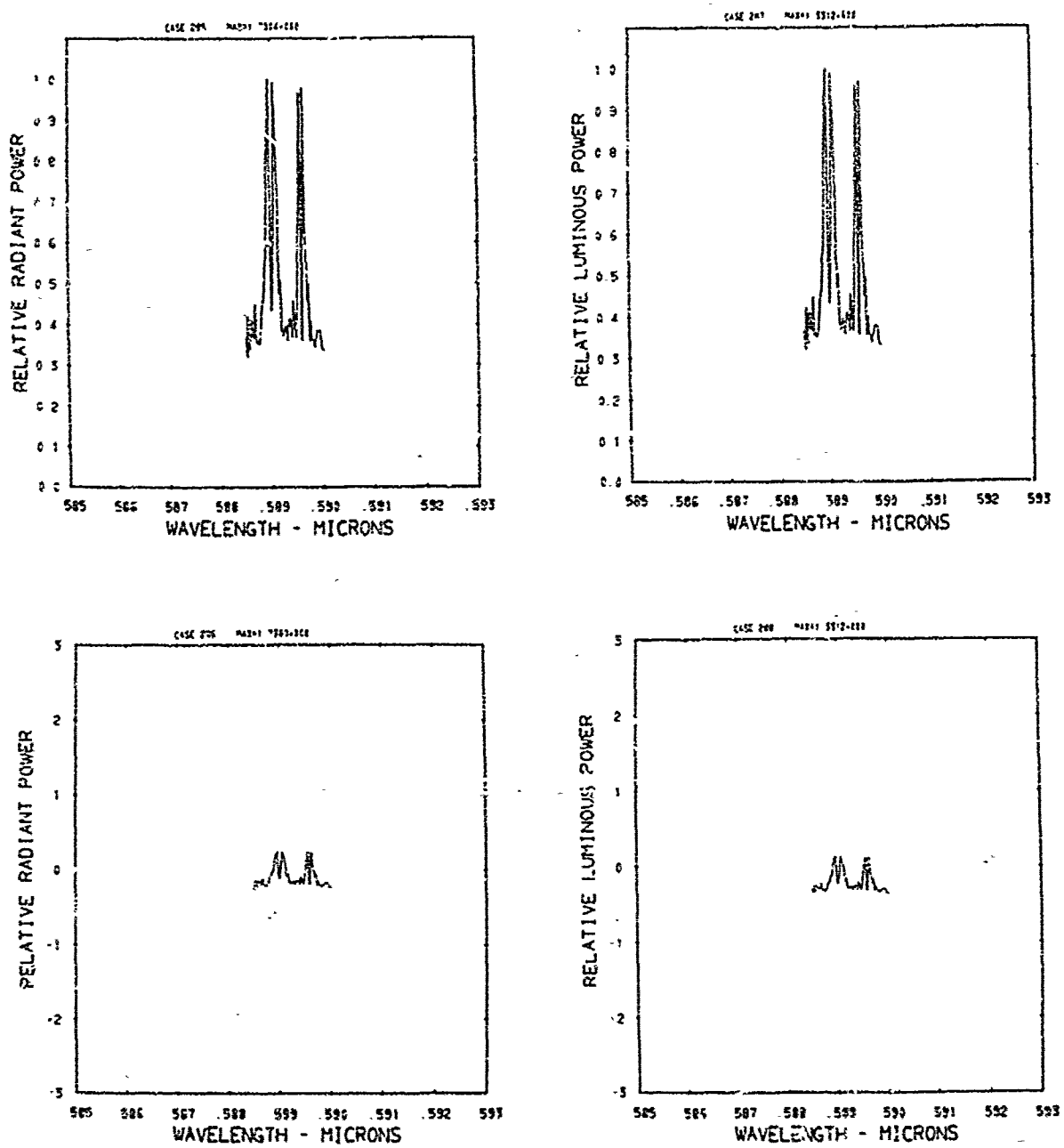

Figure A47. Relative power spectra of test flare 35 , formula group 2, burned at 30 torr ambient pressure. The top two spectra are normalized with the peak value equal to unity. The $\log_{10}$ of the spectral power is plotted in the bottom spectra. Flare formula group 2 contains 40.4% magnesium, 5.15% sodium nitrate, 49.95% potassium nitrate, and 4.5% binder.

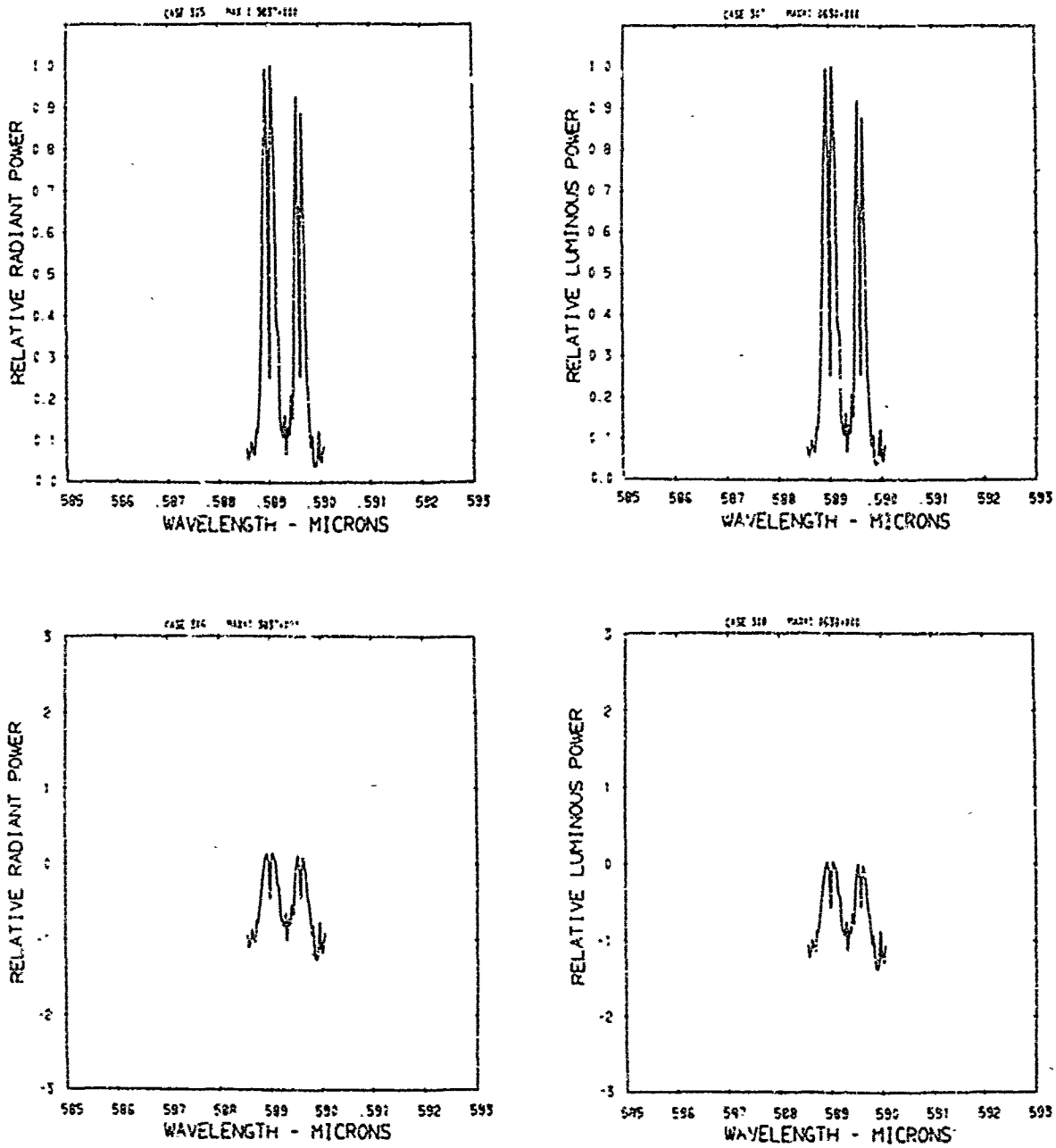

Figure A48. Relative power spectra of test flare 41 , formula group 2, burned at 30 torr ambient pressure. The top two spectra are normalized with the peak value equal to unity. The $\log_{10}$ of the spectral power is plotted in the bottom spectra. Flare formula group 2 contains 40.4% magnesium, 5.15% sodium nitrate, 49.95% potassium nitrate, and 4.5% binder.

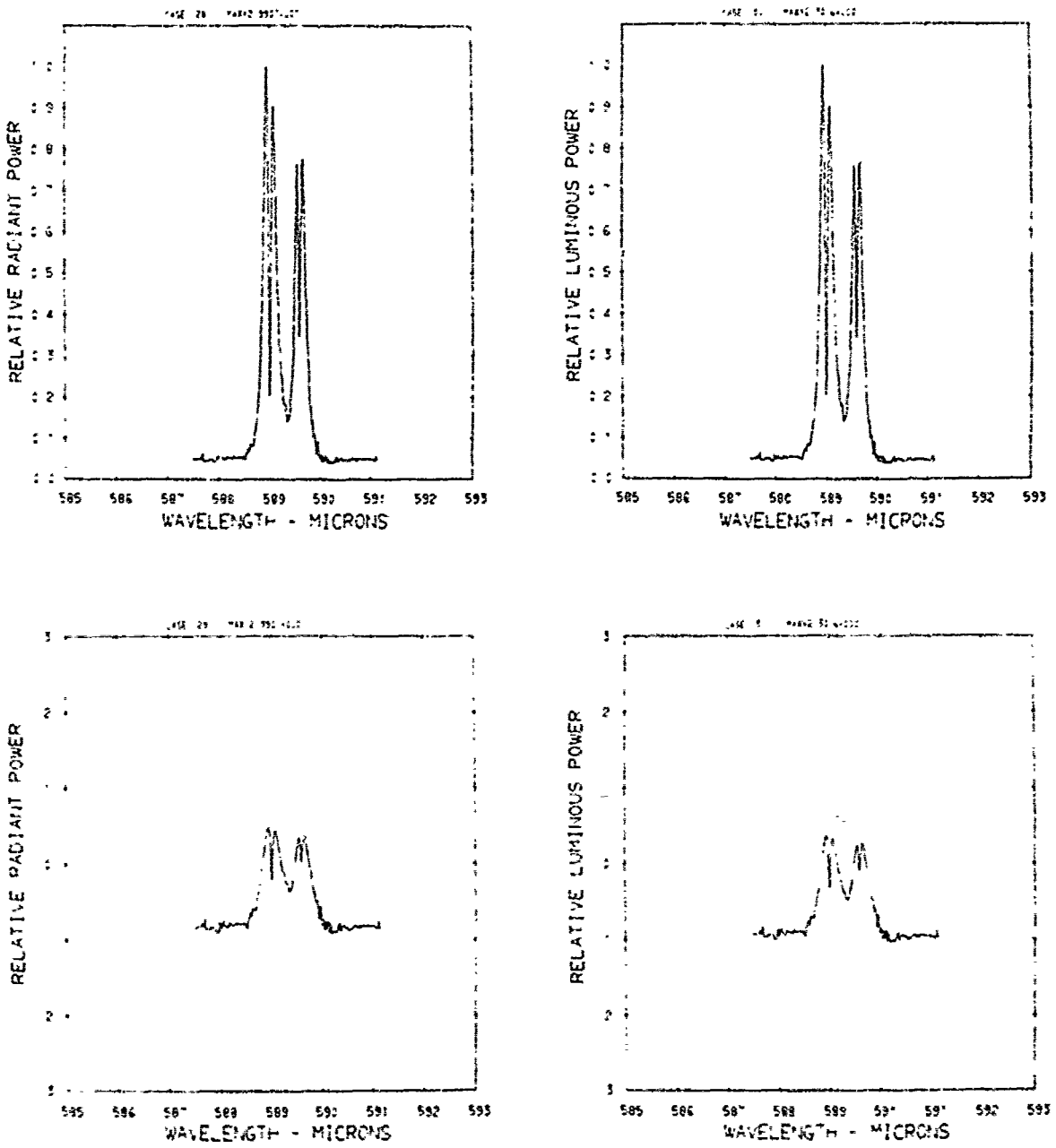

Figure A49. Relative power spectra of test flare 96 , formula group 2, burned at 30 torr ambient pressure. The top two spectra are normalized with the peak value equal to unity. The $\log_{10}$ of the spectral power is plotted in the bottom spectra. Flare formula group 2 contains 40.4% magnesium, 5.15% sodium nitrate, 49.95% potassium nitrate, and 4.5% binder.

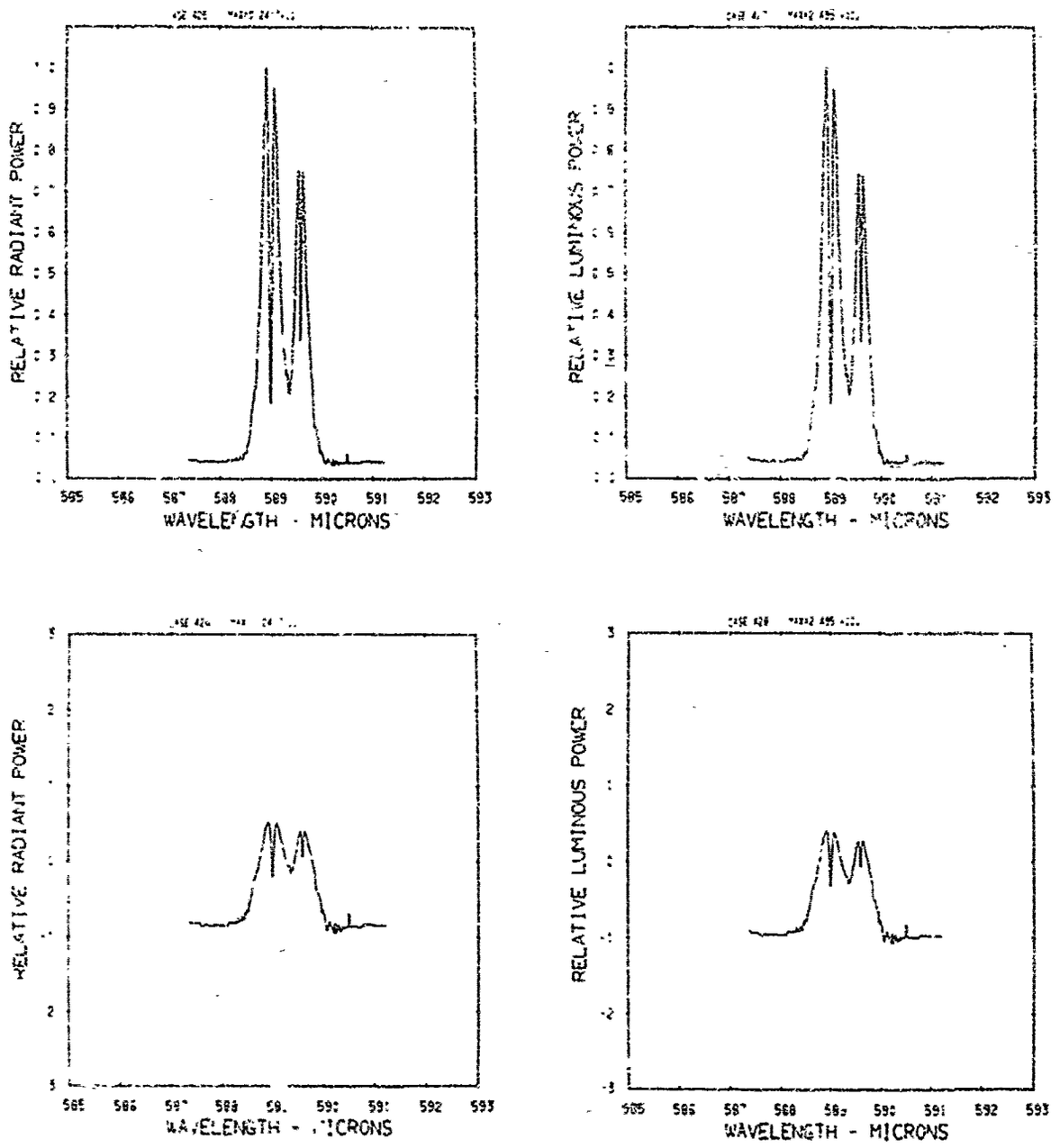

Figure A50. Relative power spectra of test flare 100 , formula group 2, burned at 30 torr ambient pressure. The top two spectra are normalized with the peak value equal to unity. The $\log_{10}$ of the spectral power is plotted in the bottom spectra. Flare formula group 2 contains 40.4% magnesium, 5.15% sodium nitrate, 49.95% potassium nitrate, and 4.5% binder.

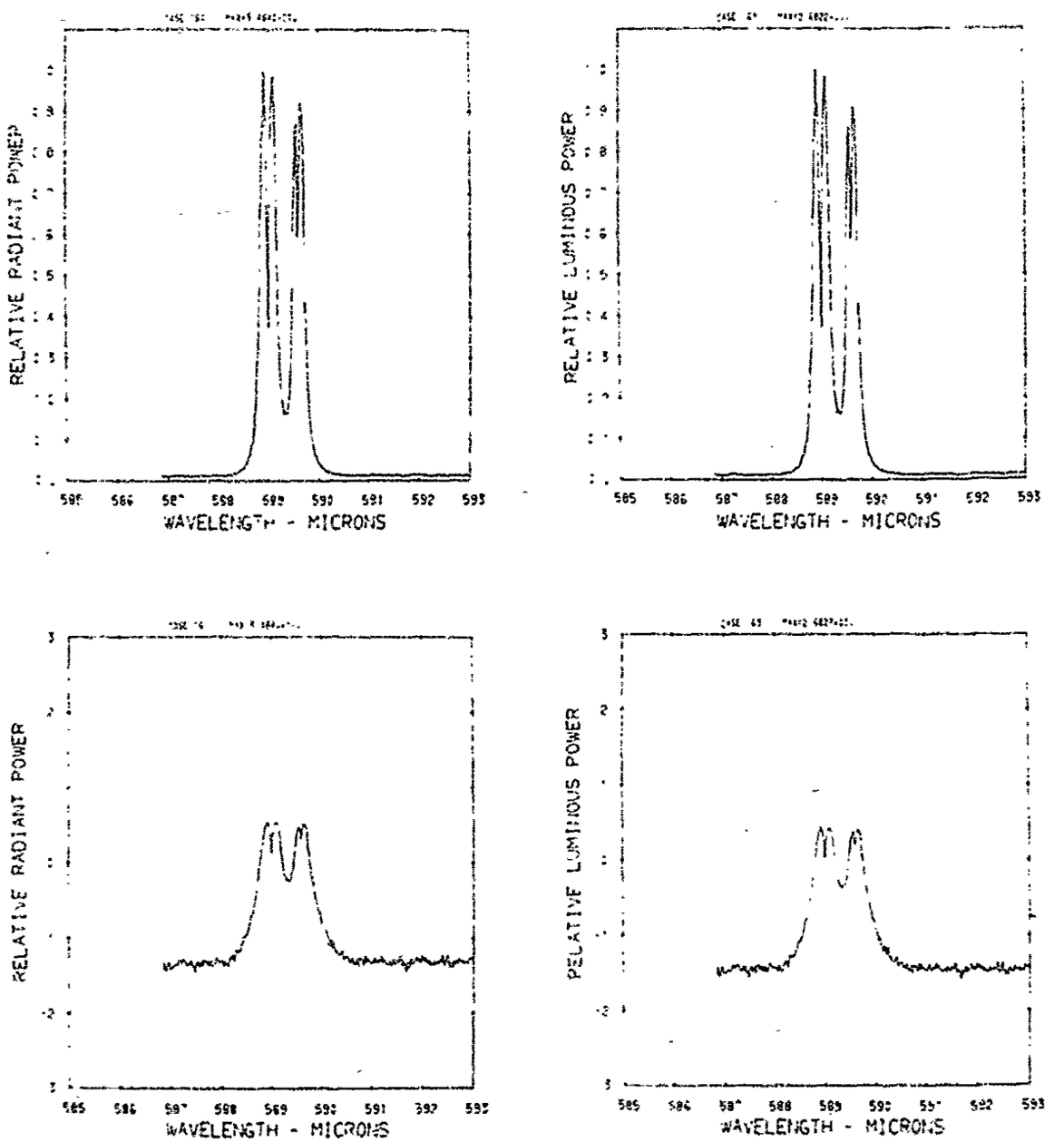

Figure A51. Relative power spectra of test flare 104-6, formula group 2, burned at 30 torr ambient pressure. The top two spectra are normalized with the peak value equal to unity. The $\log_{10}$ of the spectral power is plotted in the bottom spectra. Flare formula group 2 contains 40.4% magnesium, 5.15% sodium nitrate, 49.95% potassium nitrate, and 4.5% binder.

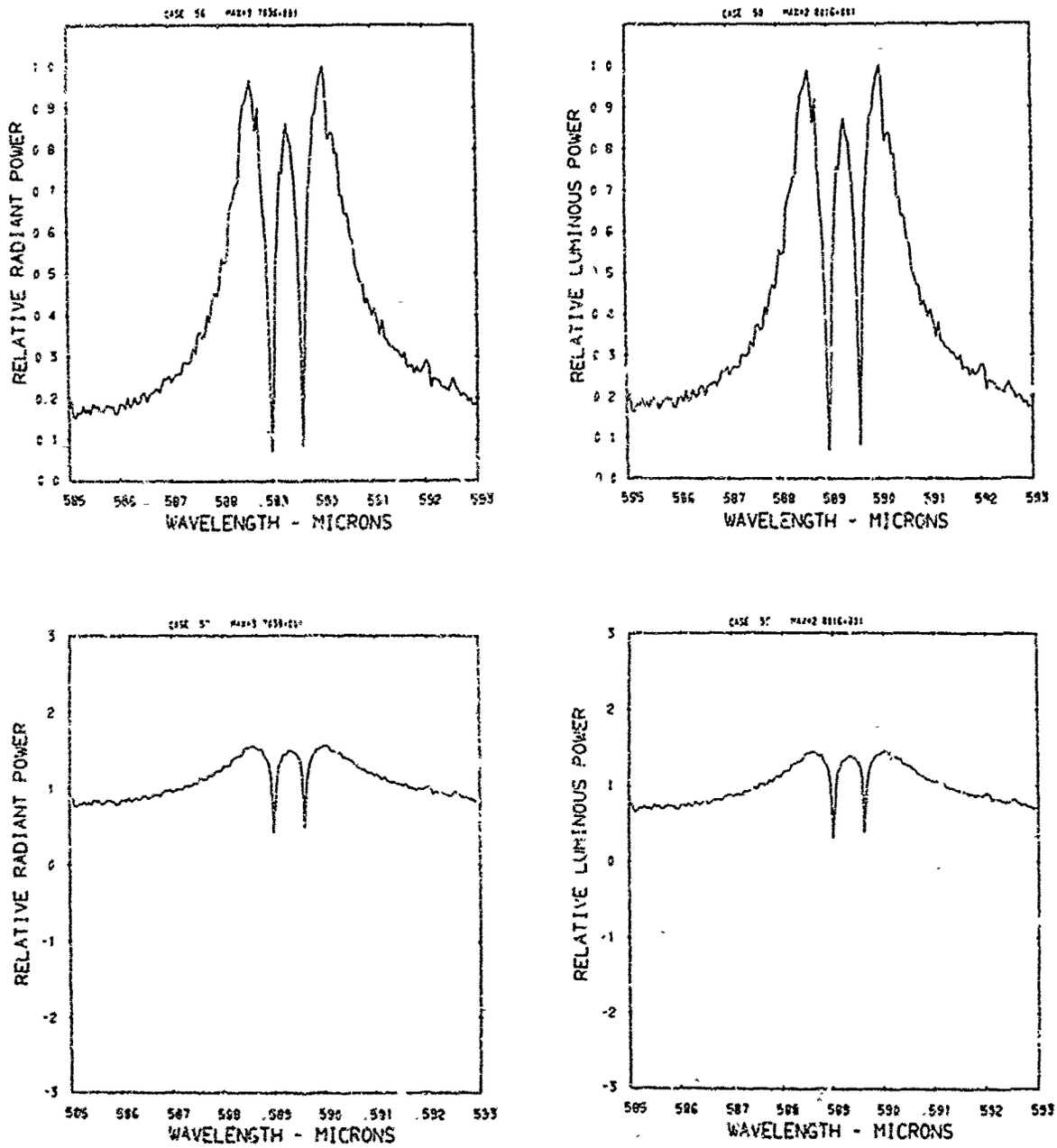

Figure A52. Relative power spectra of test flare 68 , formula group 3, burned at 760 torr ambient pressure. The top two spectra are normalized with the peak value equal to unity. The $\log_{10}$ of the spectral power is plotted in the bottom spectra. Flare formula group 3 contains 40.04% magnesium, 0.515% sodium nitrate, 54.945% potassium nitrate, and 4.5% binder.

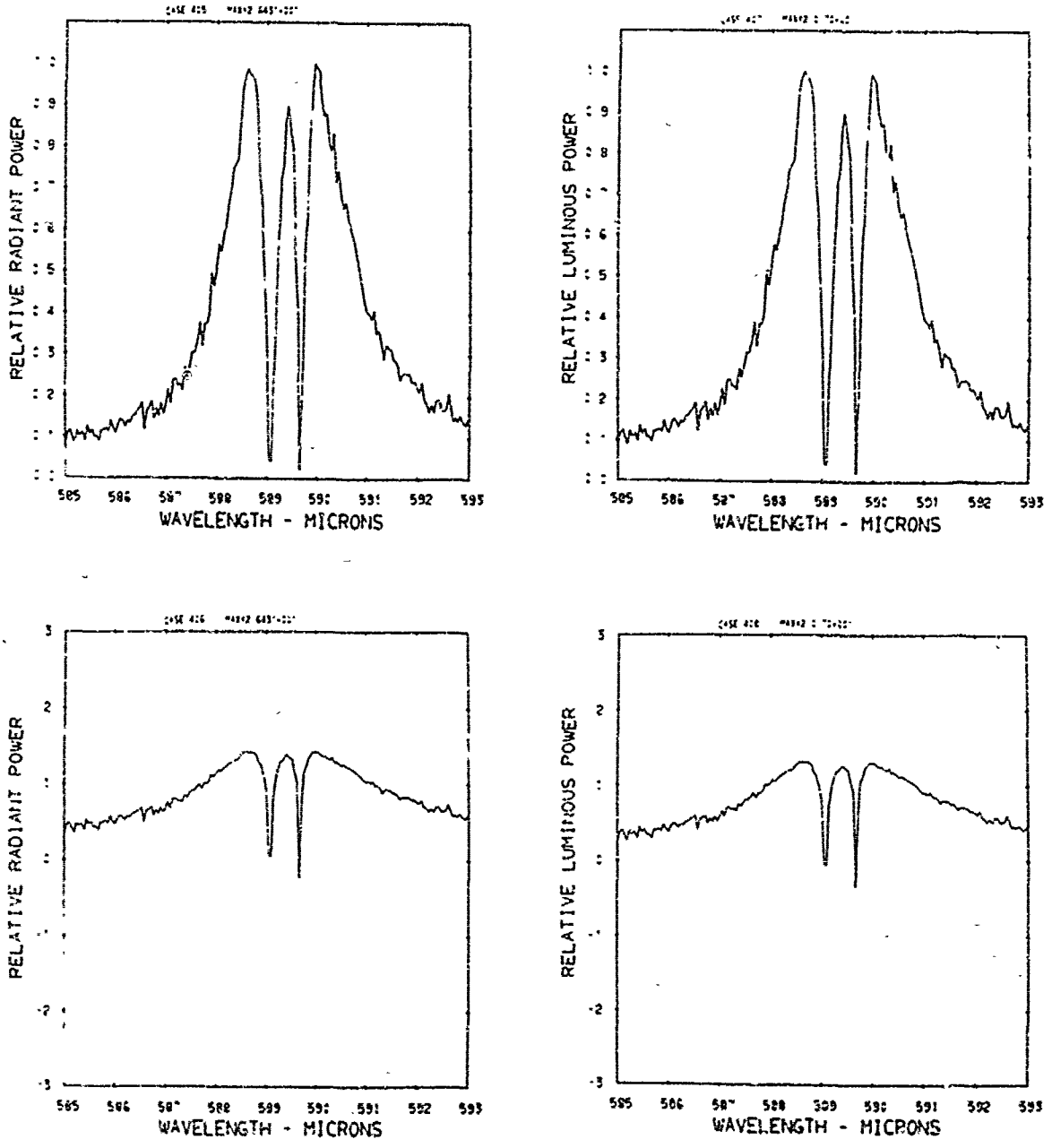

Figure A53. Relative power spectra of test flare 77 , formula group 3, burned at 760 torr ambient pressure. The top two spectra are normalized with the peak value equal to unity. The $\log_{10}$ of the spectral power is plotted in the bottom spectra. Flare formula group 3 contains 40.04% magnesium, 0.515% sodium nitrate, 54.945% potassium nitrate, and 4.5% binder.

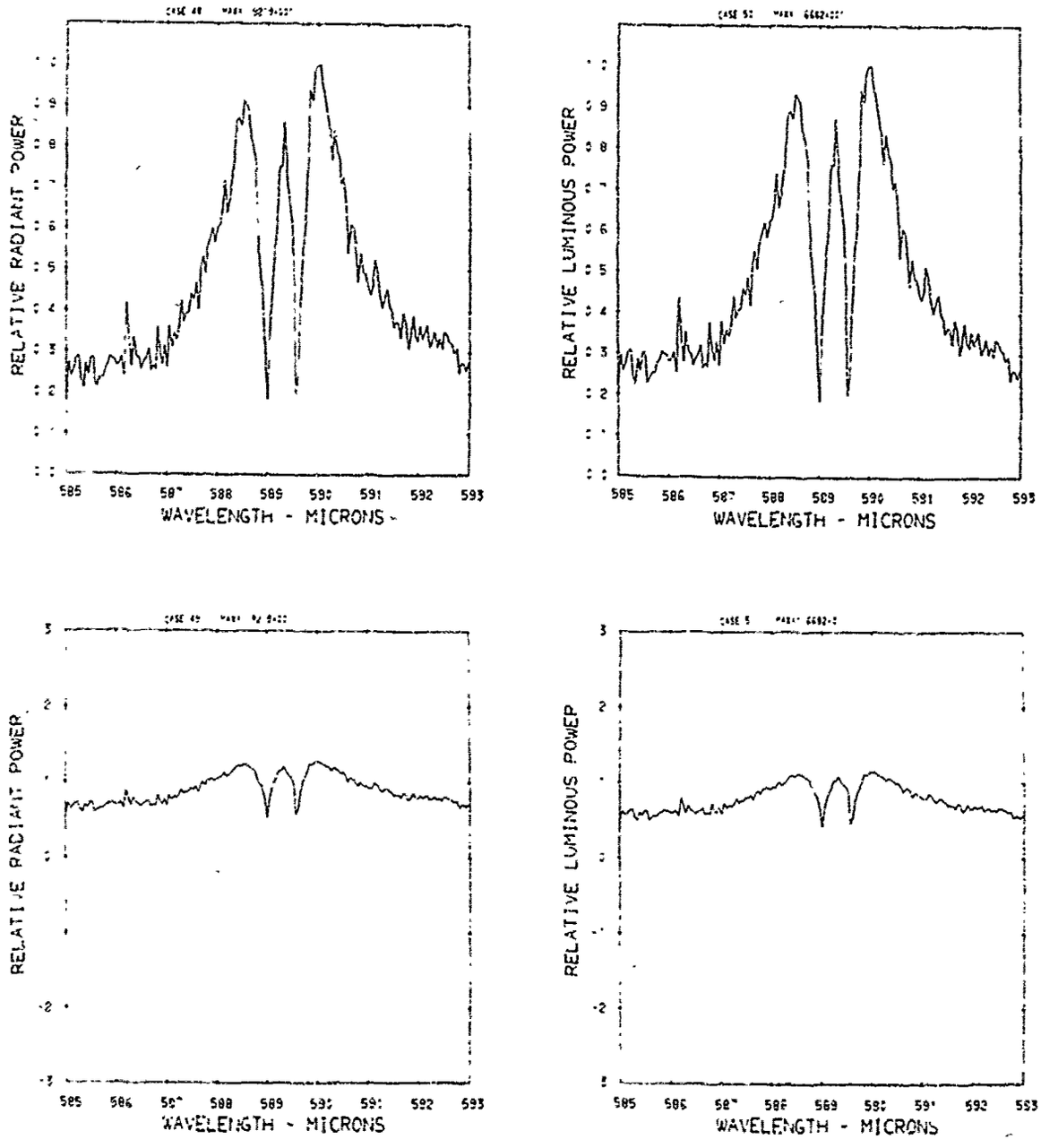

Figure A54. Relative power spectra of test flare 147 , formula group 3, burned at 760 torr ambient pressure. The top two spectra are normalized with the peak value equal to unity. The $\log_{10}$ of the spectral power is plotted in the bottom spectra. Flare formula group 3 contains 40.04% magnesium, 0.515% sodium nitrate, 54.945% potassium nitrate, and 4.5% binder.

Flare 147 Group 26 Torr 760

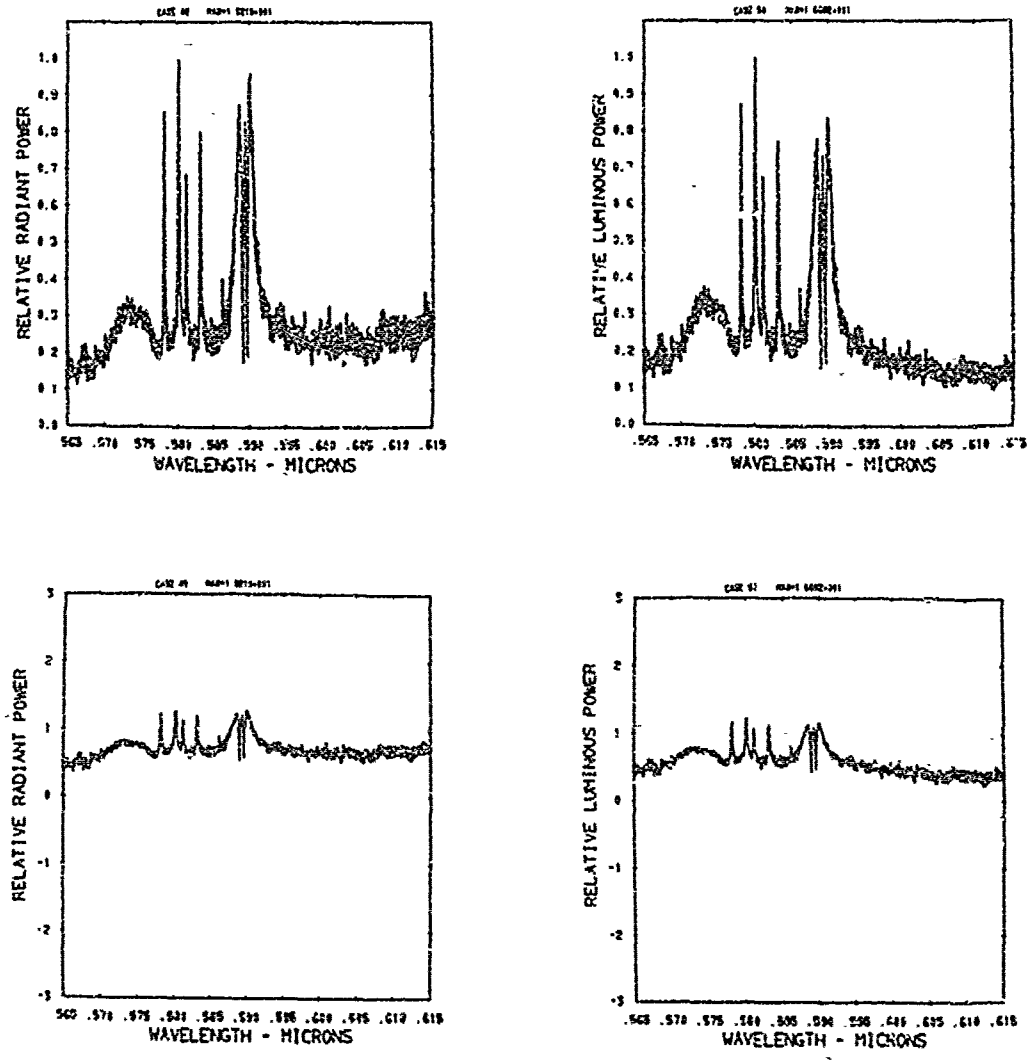

Figure A55. Relative power spectra of test flare 147 , formula group 3, burned at 760 torr ambient pressure. The top two spectra are normalized with the peak value equal to unity. The $\log_{10}$ of the spectral power is plotted in the bottom spectra. Flare formula group 3 contains 40.04% magnesium, 0.515% sodium nitrate, 54.945% potassium nitrate, and 4.5% binder.

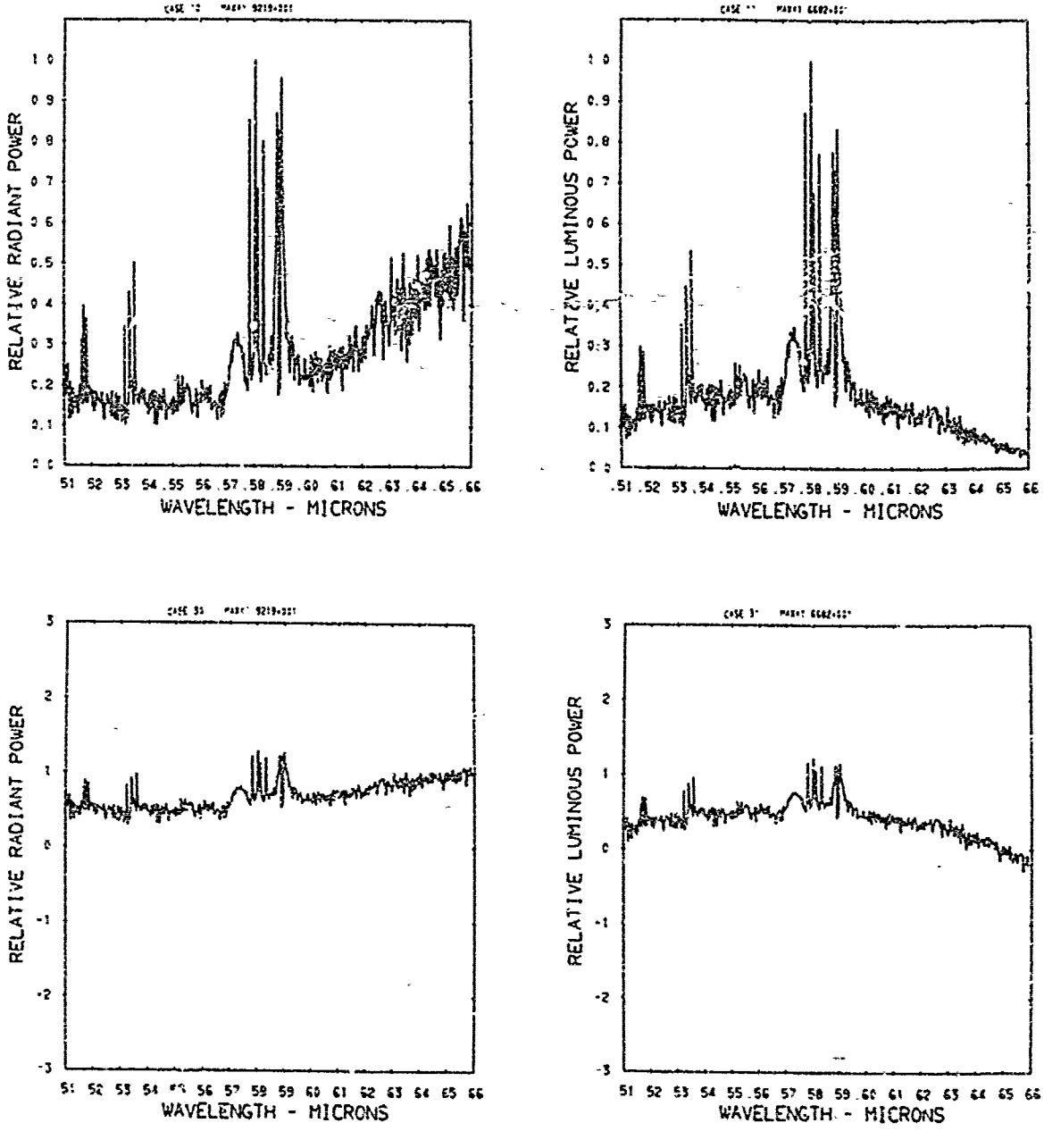

Figure A56. Relative power spectra of test flare 147 , formula group 3, burned at 760 torr ambient pressure. The top two spectra are normalized with the peak value equal to unity. The $\log_{10}$ of the spectral power is plotted in the bottom spectra. Flare formula group 3 contains 40.04% magnesium, 0.515% sodium nitrate, 54.945% potassium nitrate, and 4.5% binder.

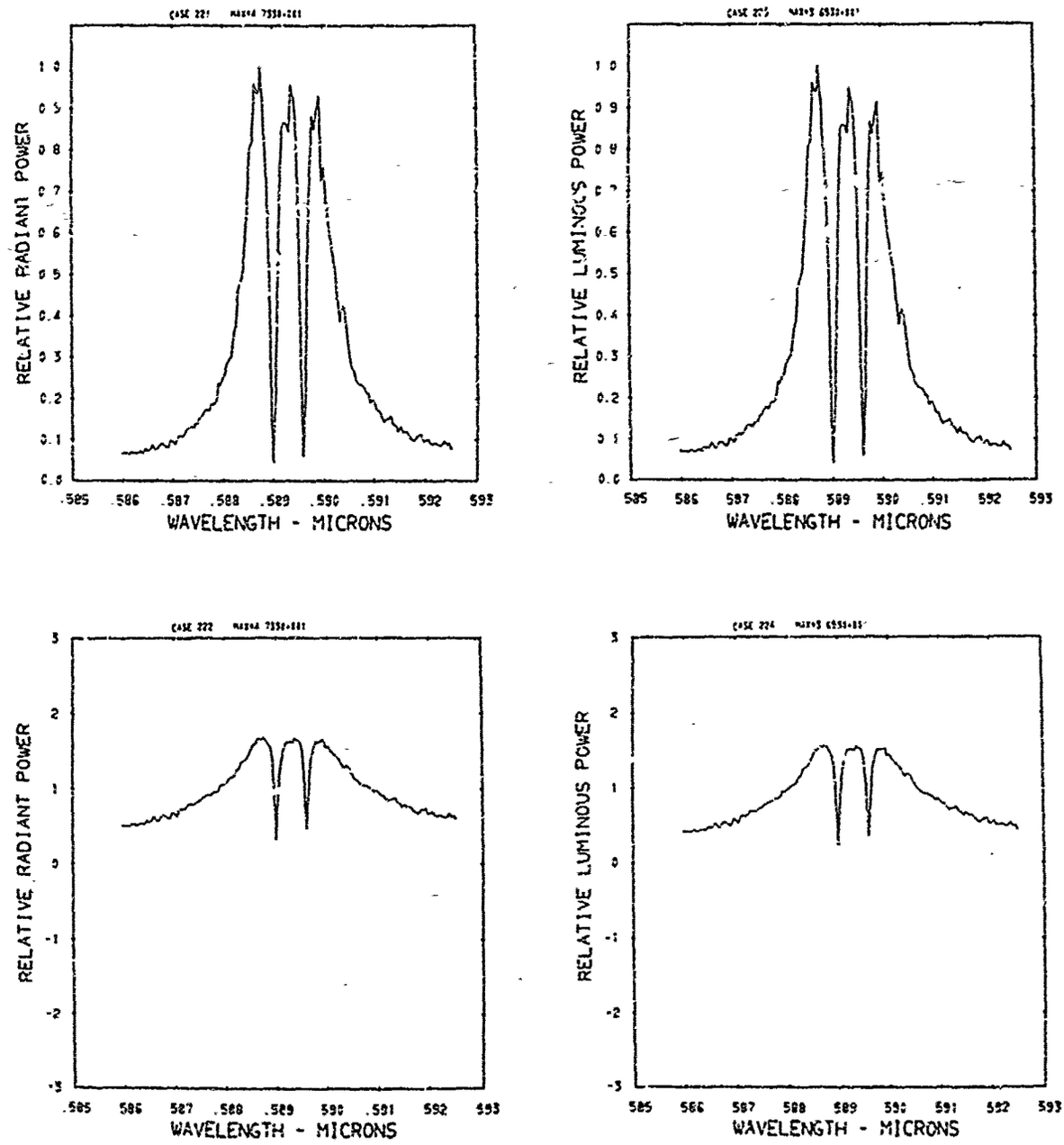

Figure A57. Relative power spectra of test flare 4A , formula group 3, burned at 630 torr ambient pressure. The top two spectra are normalized with the peak value equal to unity. The $\log_{10}$ of the spectral power is plotted in the bottom spectra. Flare formula group 3 contains 40.04% magnesium, 0.515% sodium nitrate, 54.945% potassium nitrate, and 4.5% binder.

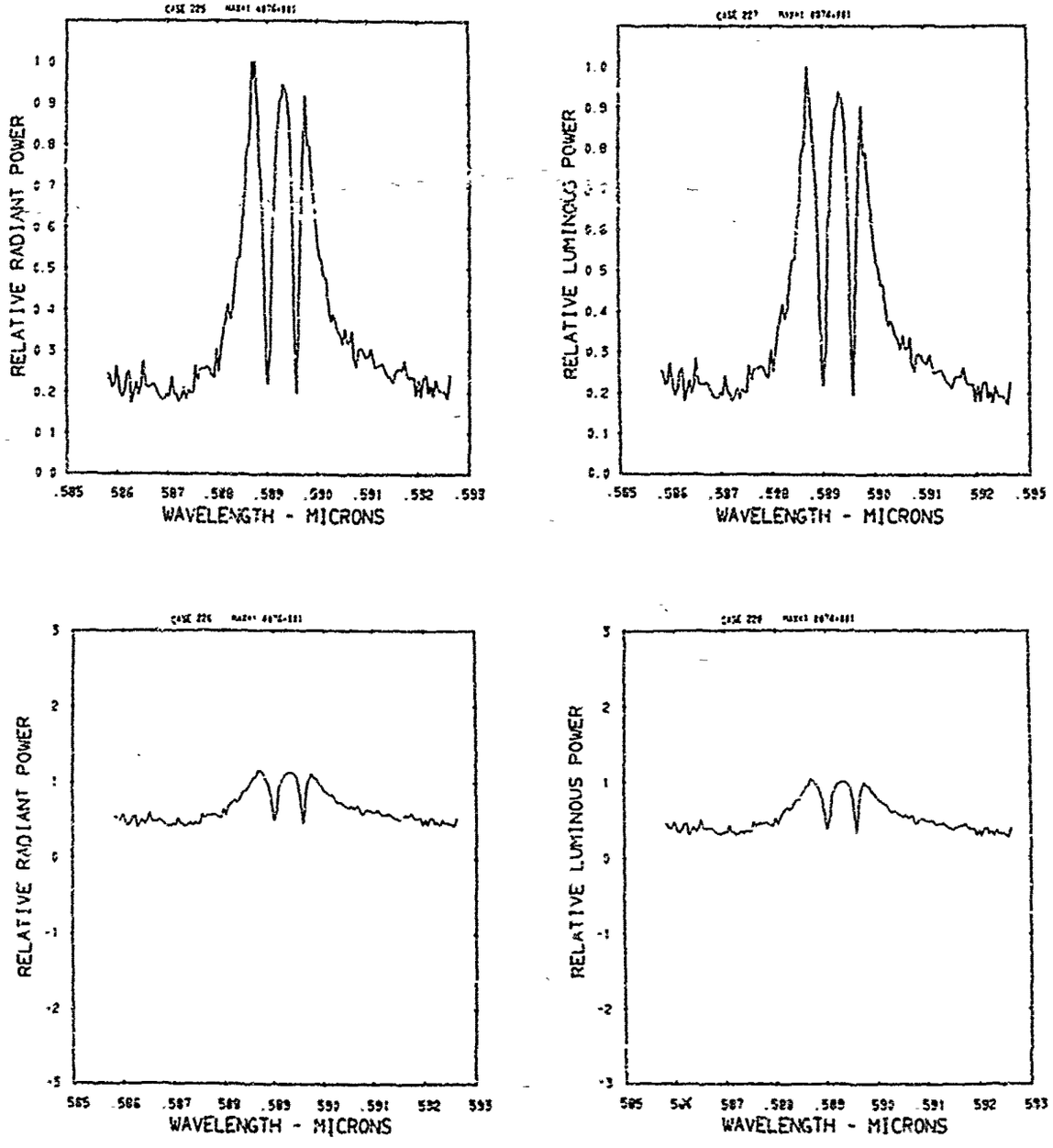

Figure A58. Relative power spectra of test flare 4B , formula group 3, burned at 630 torr ambient pressure. The top two spectra are normalized with the peak value equal to unity. The $\log_{10}$ of the spectral power is plotted in the bottom spectra. Flare formula group 3 contains 40.04% magnesium, 0.515% sodium nitrate, 54.945% potassium nitrate, and 4.5% binder.

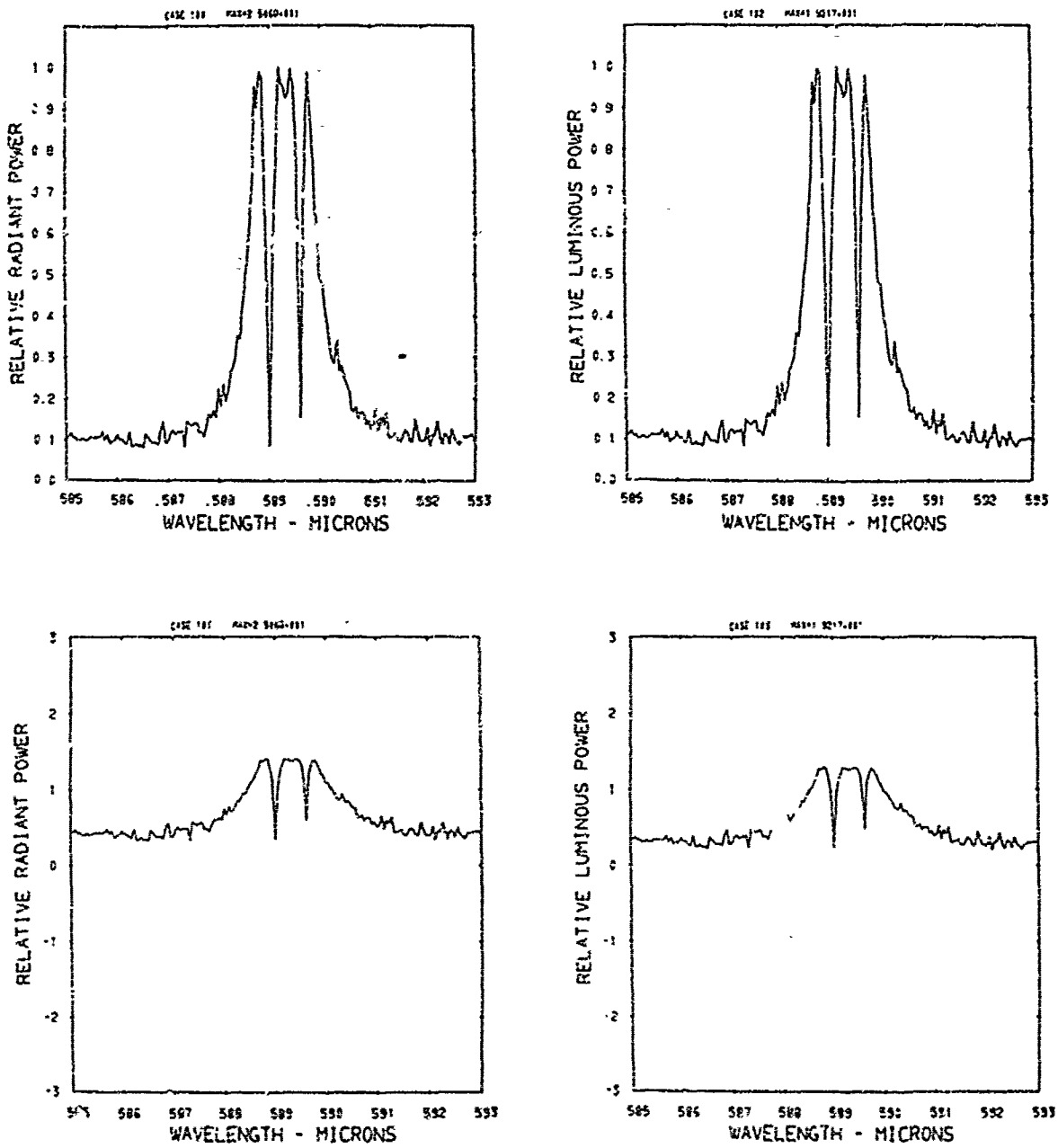

Figure A59. Relative power spectra of test flare 118A, formula group 3, burned at 300 torr ambient pressure. The top two spectra are normalized with the peak value equal to unity. The $\log_{10}$ of the spectral power is plotted in the bottom spectra. Flare formula group 3 contains 40.04% magnesium, 0.515% sodium nitrate, 54.945% potassium nitrate, and 4.5% binder.

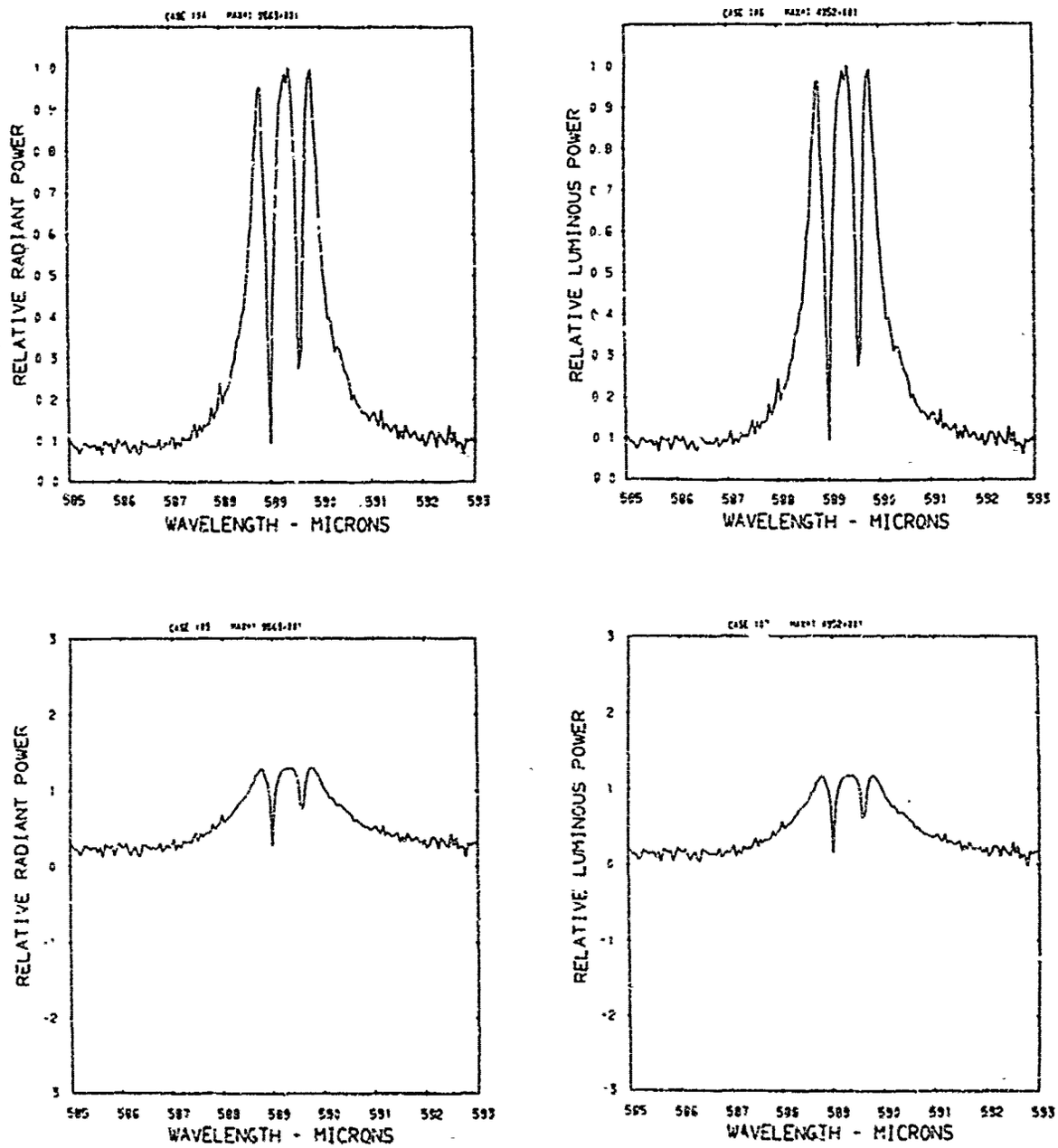

Figure A60. Relative power spectra of test flare 118B, formula group 3, burned at 300 torr ambient pressure. The top two spectra are normalized with the peak value equal to unity. The $\log_{10}$ of the spectral power is plotted in the bottom spectra. Flare formula group 3 contains 40.04% magnesium, 0.515% sodium nitrate, 54.945% potassium nitrate, and 4.5% binder.

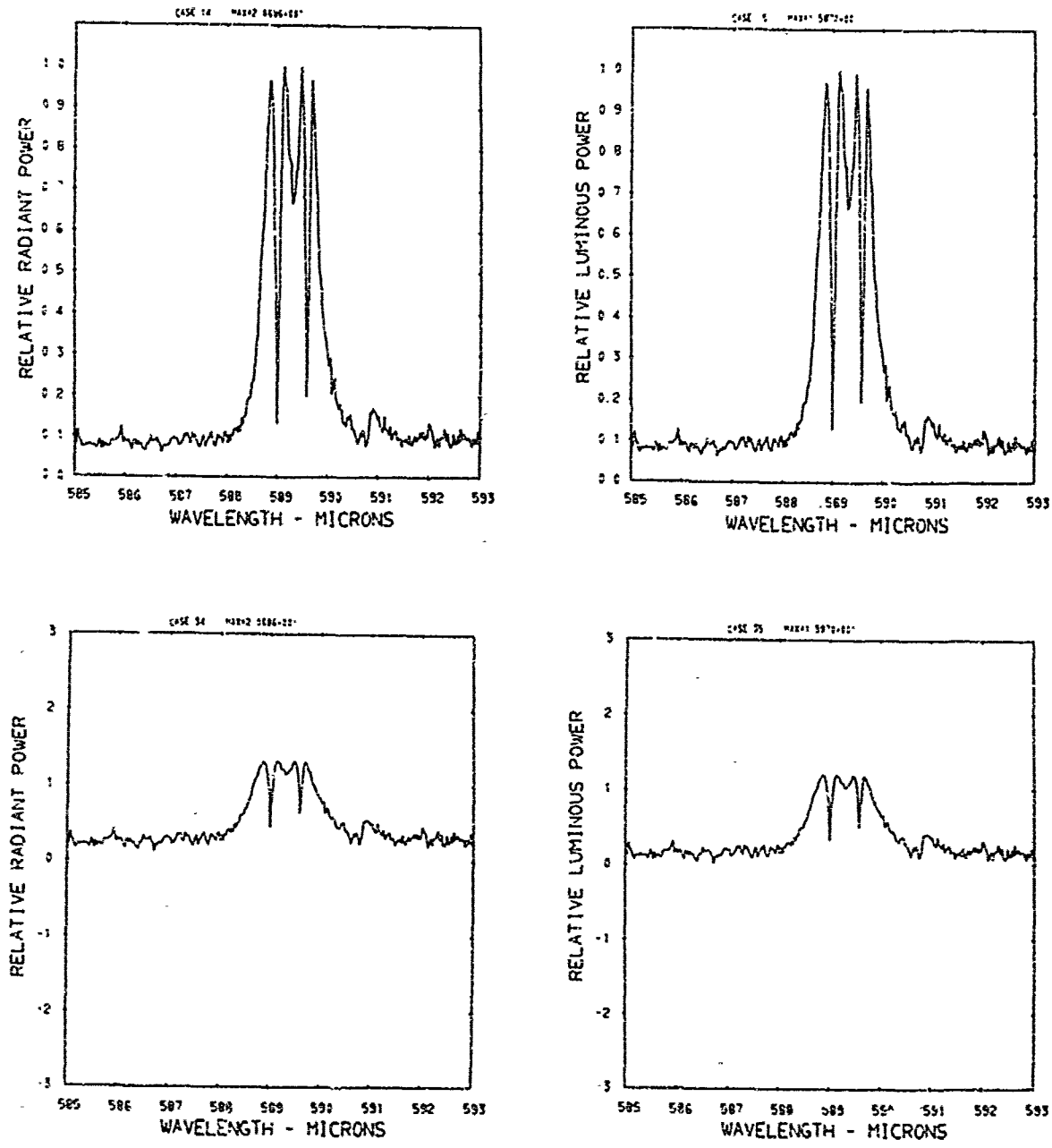

Figure A61. Relative power spectra of test flare 148A, formula group 3, burned at 225 torr ambient pressure. The top two spectra are normalized with the peak value equal to unity. The $\log_{10}$ of the spectral power is plotted in the bottom spectra. Flare formula group 3 contains 40.04% magnesium, 0.515% sodium nitrate, 54.945% potassium nitrate, and 4.5% binder.

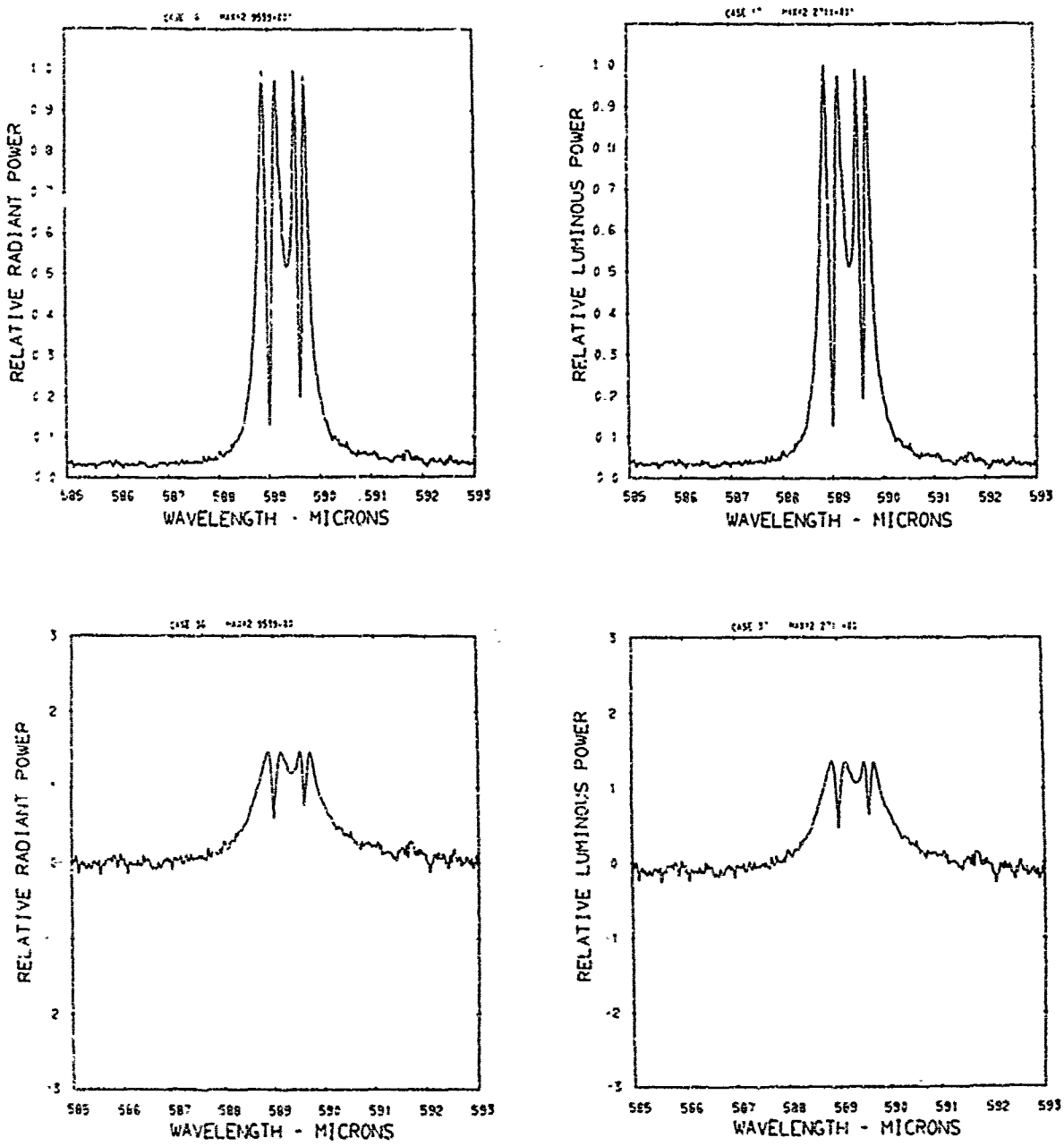

Figure A62. Relative power spectra of test flare 148B, formula group 3, burned at 225 torr ambient pressure. The top two spectra are normalized with the peak value equal to unity. The $\log_{10}$ of the spectral power is plotted in the bottom spectra. Flare formula group 3 contains 40.04% magnesium, 0.515% sodium nitrate, 54.945% potassium nitrate, and 4.5% binder.

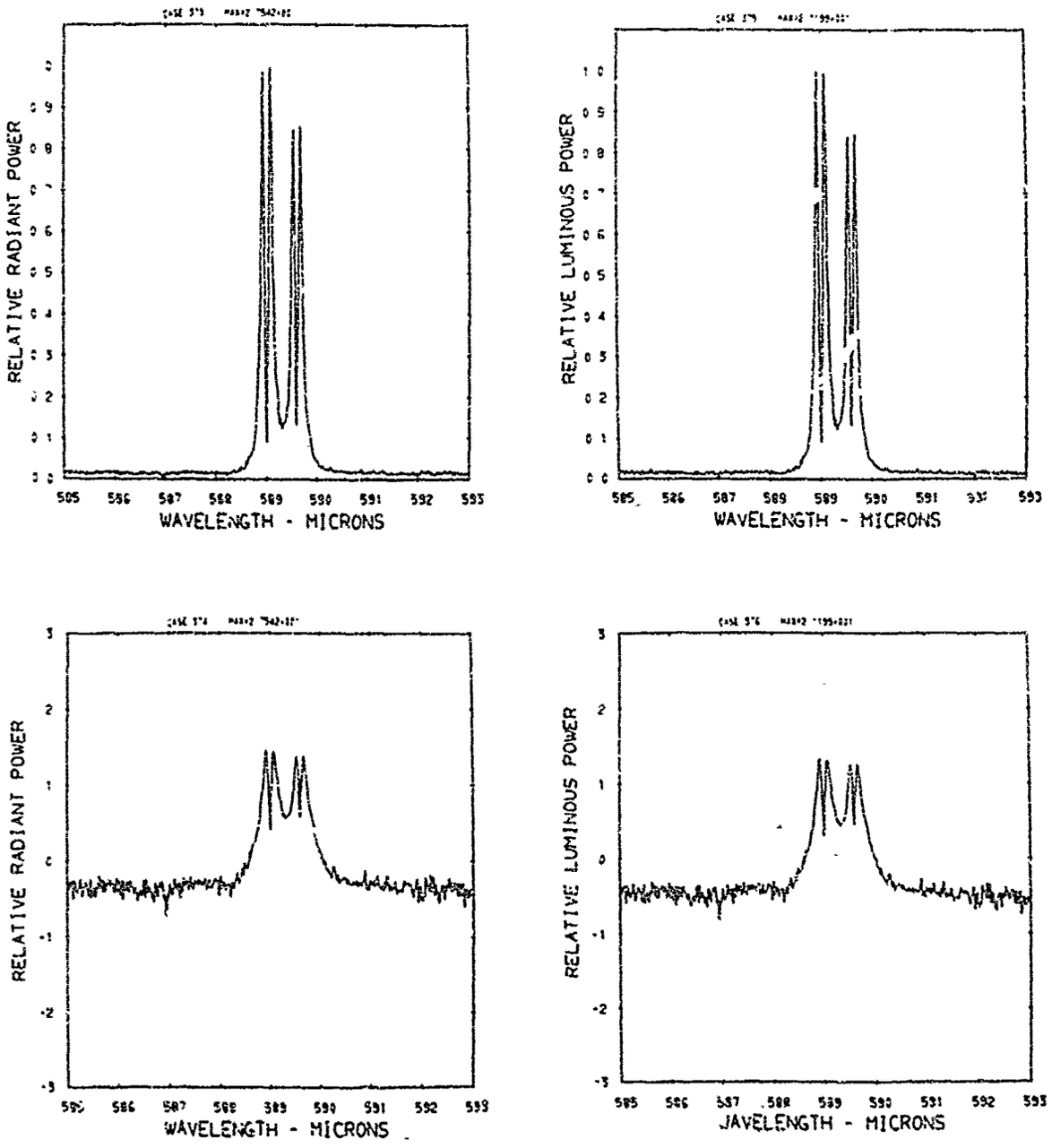

Figure A63. Relative power spectra of test flare 48 , formula group 3, burned at 150 torr ambient pressure. The top two spectra are normalized with the peak value equal to unity. The $\log_{10}$ of the spectral power is plotted in the bottom spectra. Flare formula group 3 contains 40.04% magnesium, 0.515% sodium nitrate, 54.945% potassium nitrate, and 4.5% binder.

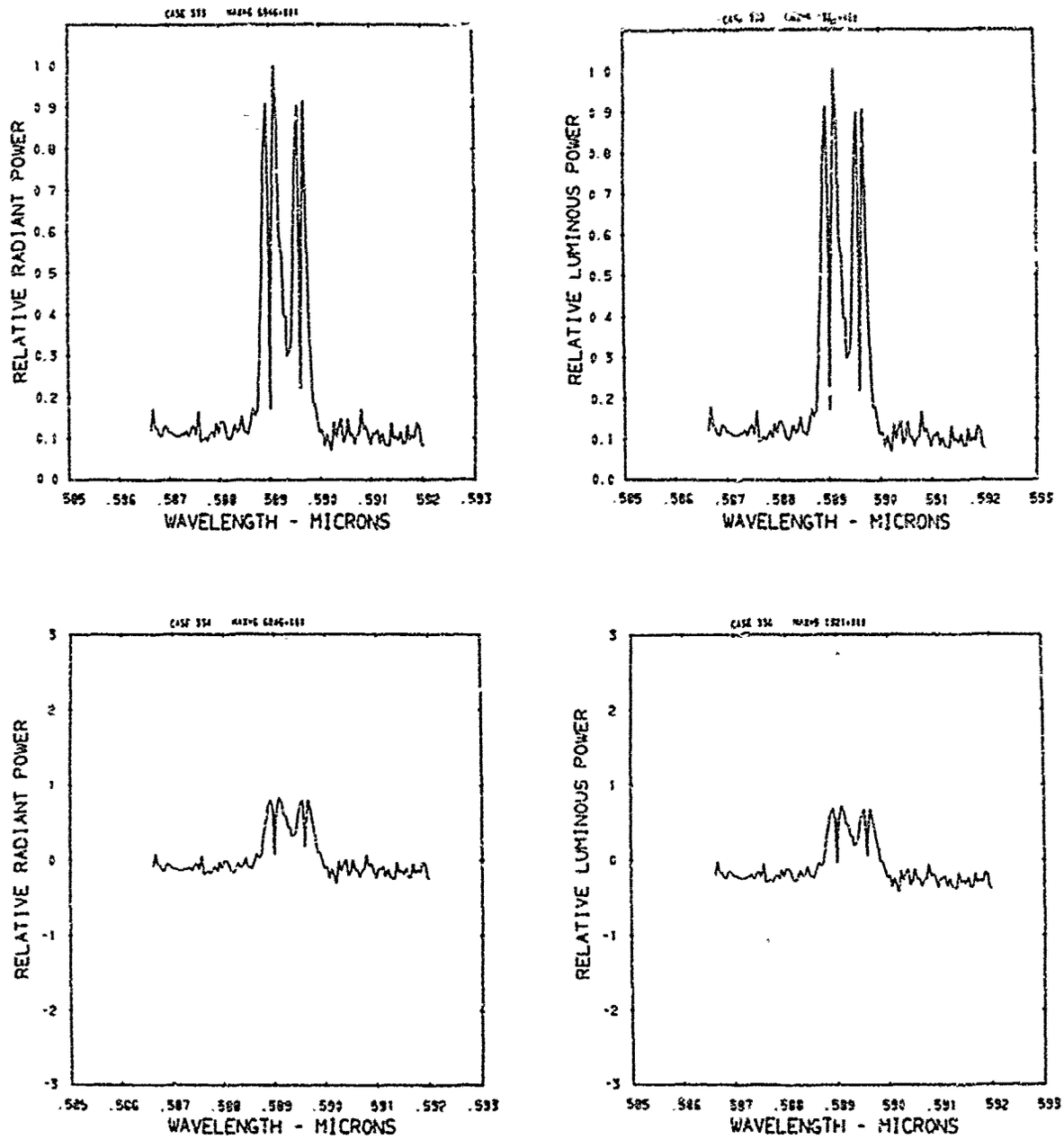

Figure A64. Relative power spectra of test flare 52 , formula group 3, burned at 150 torr ambient pressure. The top two spectra are normalized with the peak value equal to unity. The $\log_{10}$ of the spectral power is plotted in the bottom spectra. Flare formula group 3 contains 40.04% magnesium, 0.515% sodium nitrate, 54.945% potassium nitrate, and 4.5% binder.

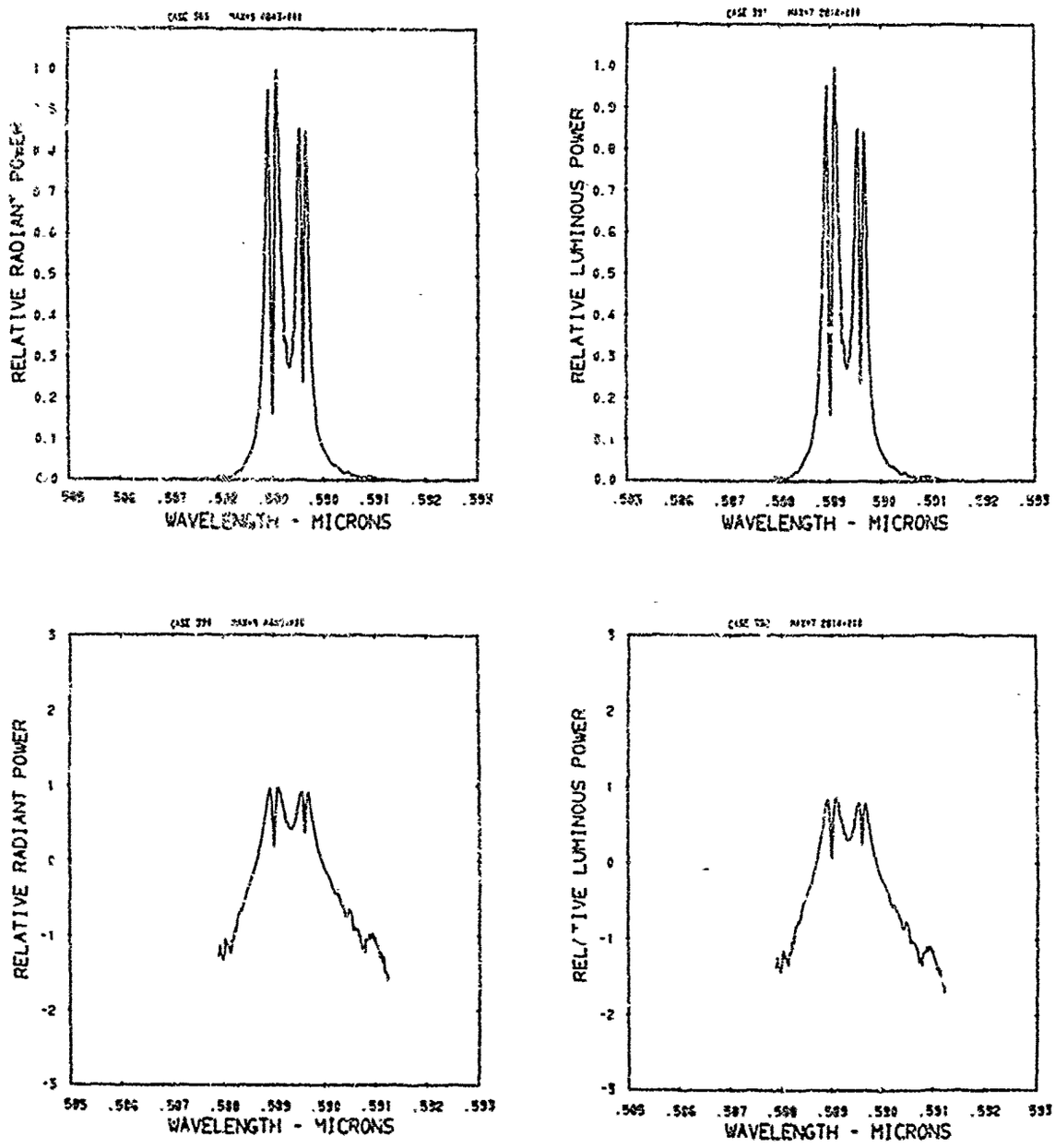

Figure A65. Relative power spectra of test flare 56 , formula group 3, burned at 150 torr ambient pressure. The top two spectra are normalized with the peak value equal to unity. The $\log_{10}$ of the spectral power is plotted in the bottom spectra. Flare formula group 3 contains 40.04% magnesium, 0.515% sodium nitrate, 54.945% potassium nitrate, and 4.5% binder.

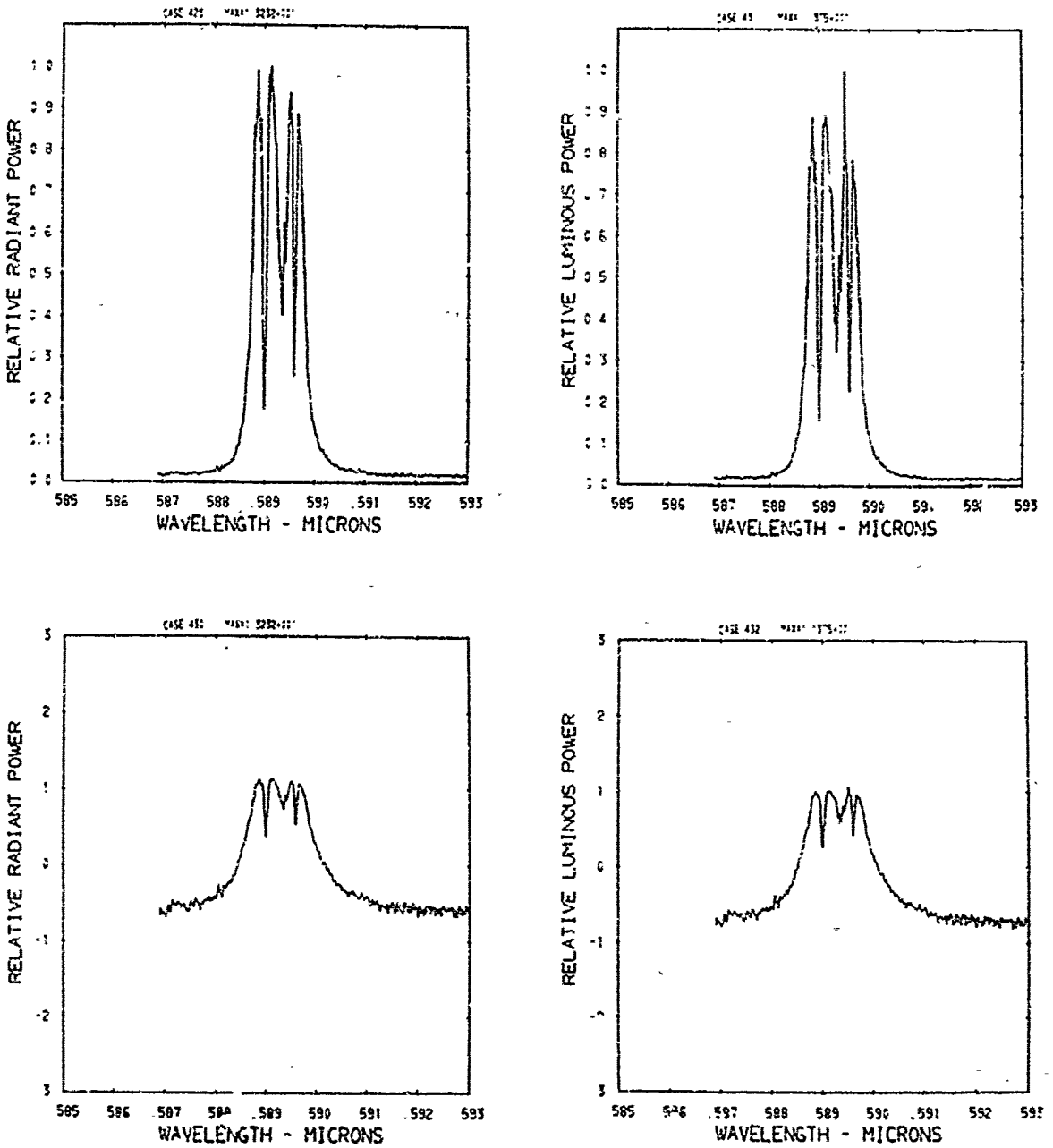

Figure A66. Relative power spectra of test flare 111 , formula group 3, burned at 150 torr ambient pressure. The top two spectra are normalized with the peak value equal to unity. The $\log_{10}$ of the spectral power is plotted in the bottom spectra. Flare formula group 3 contains 40.04% magnesium, 0.515% sodium nitrate, 54.945% potassium nitrate, and 4.5% binder.

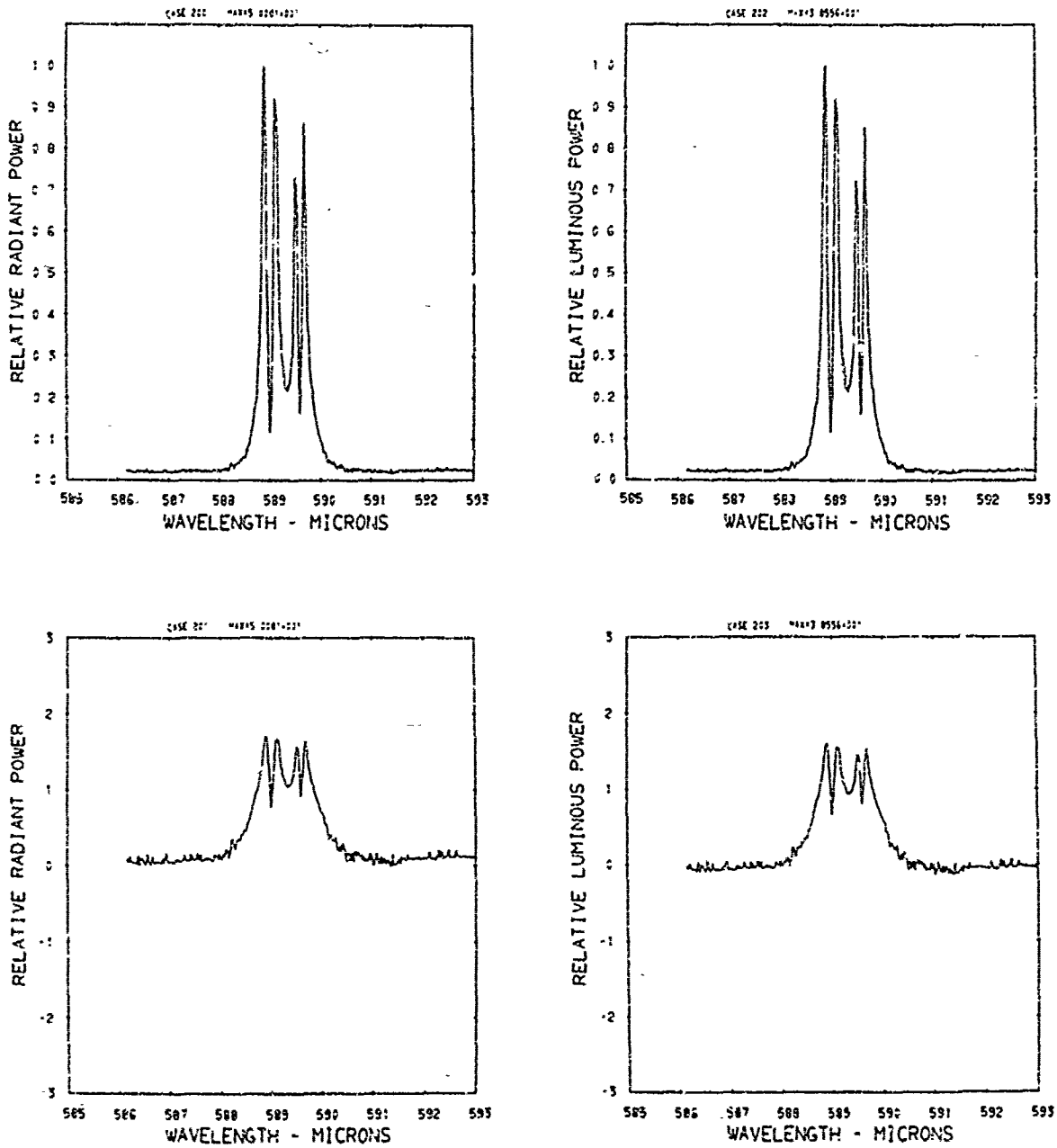

Figure A67. Relative power spectra of test flare 126 , formula group 3, burned at 150 torr ambient pressure. The top two spectra are normalized with the peak value equal to unity. The $\log_{10}$ of the spectral power is plotted in the bottom spectra. Flare formula group 3 contains 40.04% magnesium, 0.515% sodium nitrate, 54.945% potassium nitrate, and 4.5% binder.

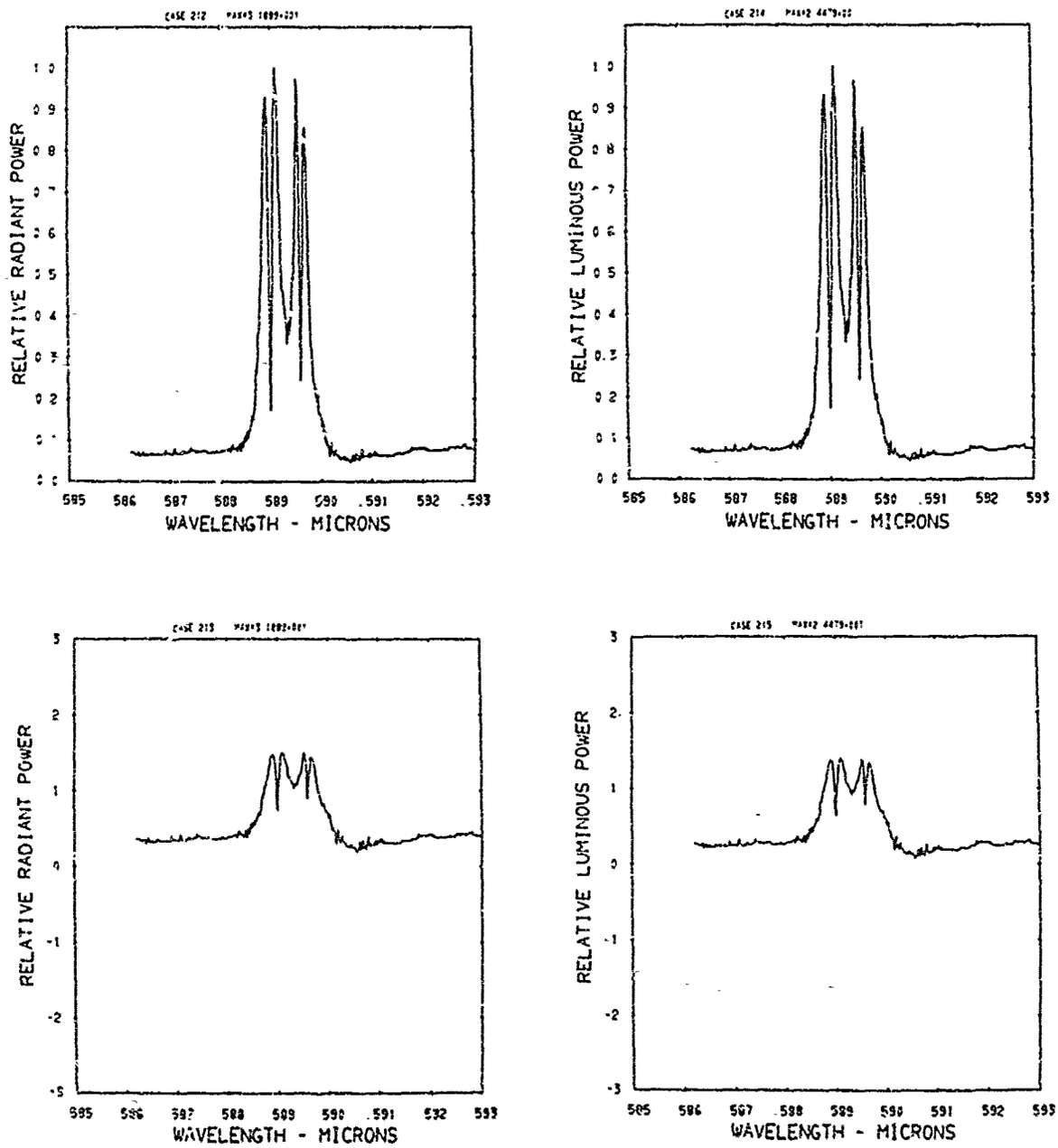

Figure A68. Relative power spectra of test flare 129A, formula group 3, burned at 150 torr ambient pressure. The top two spectra are normalized with the peak value equal to unity. The $\log_{10}$ of the spectral power is plotted in the bottom spectra. Flare formula group 3 contains 40.04% magnesium, 0.515% sodium nitrate, 54.945% potassium nitrate, and 4.5% binder.

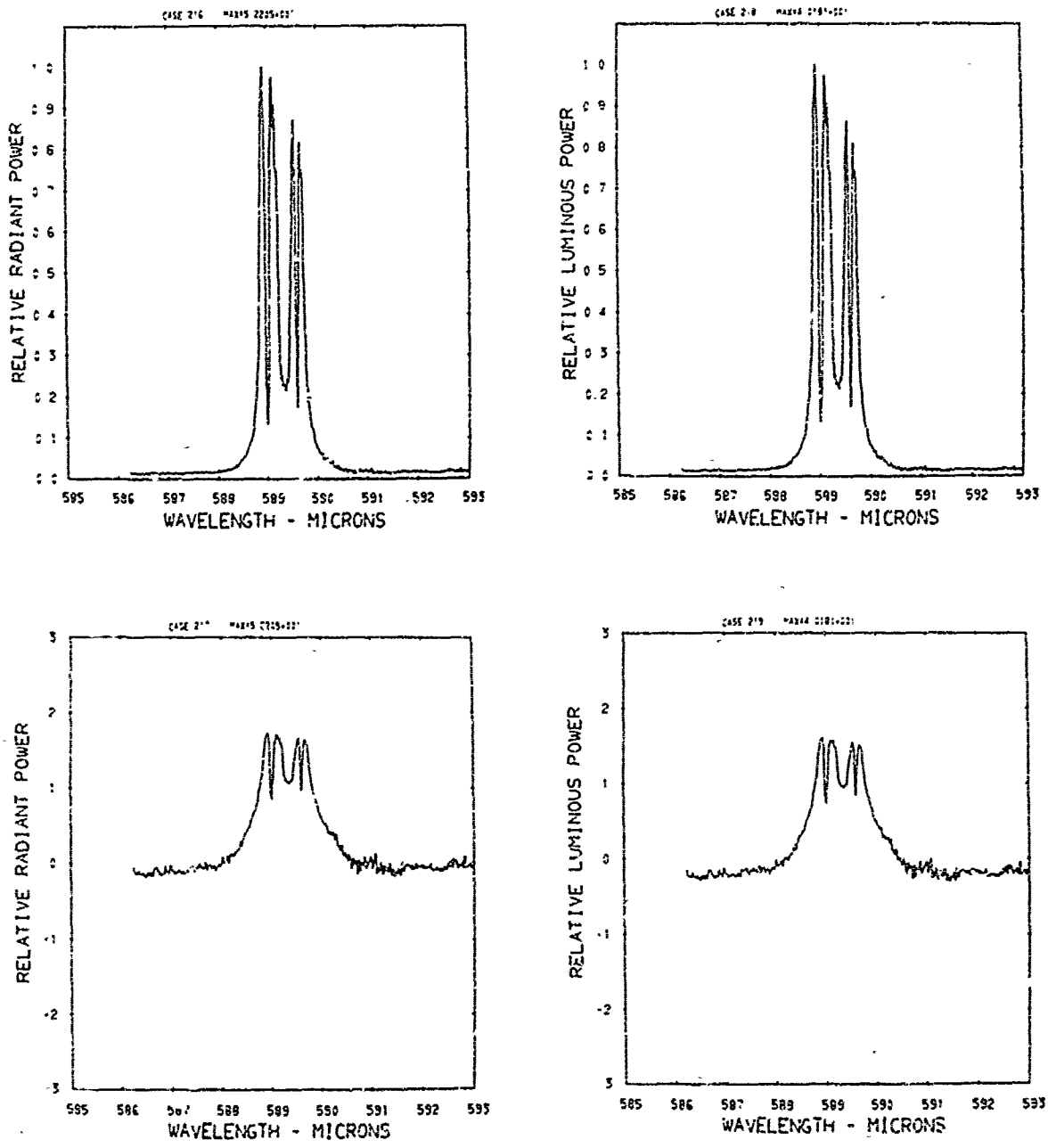

Figure A69. Relative power spectra of test flare 129B, formula group 3, burned at 150 torr ambient pressure. The top two spectra are normalized with the peak value equal to unity. The $\log_{10}$ of the spectral power is plotted in the bottom spectra Flare formula group 3 contains 40.04% magnesium, 0.515% sodium nitrate, 54.945% potassium nitrate, and 4.5% binder.

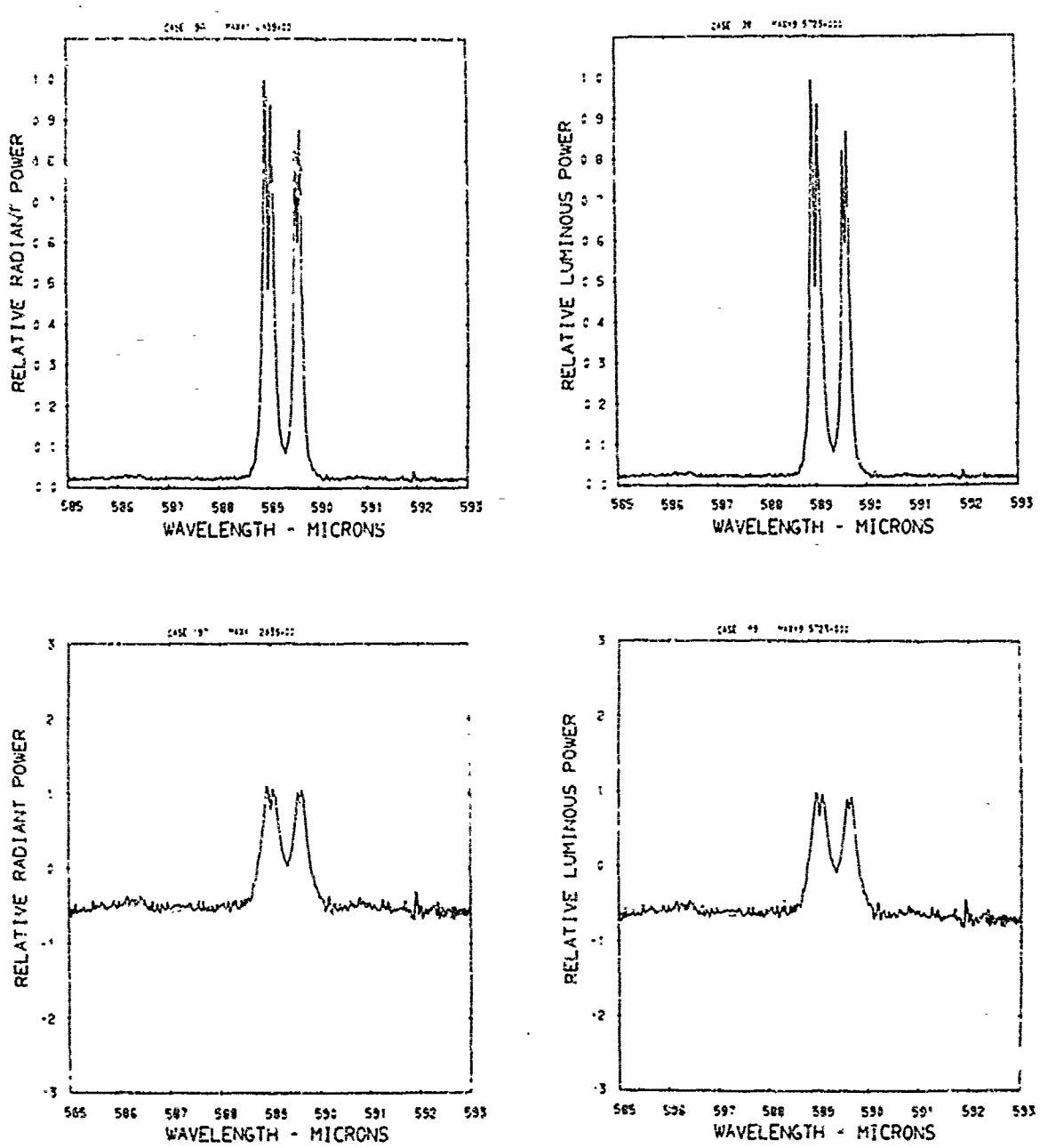

Figure A70. Relative power spectra of test flare 121 , formula group 3, burned at 75 torr ambient pressure. The top two spectra are normalized with the peak value equal to unity. The $\log_{10}$ of the spectral power is plotted in the bottom spectra. Flare formula group 3 contains 40.04% magnesium, 0.515% sodium nitrate, 54.945% potassium nitrate, and 4.5% binder.

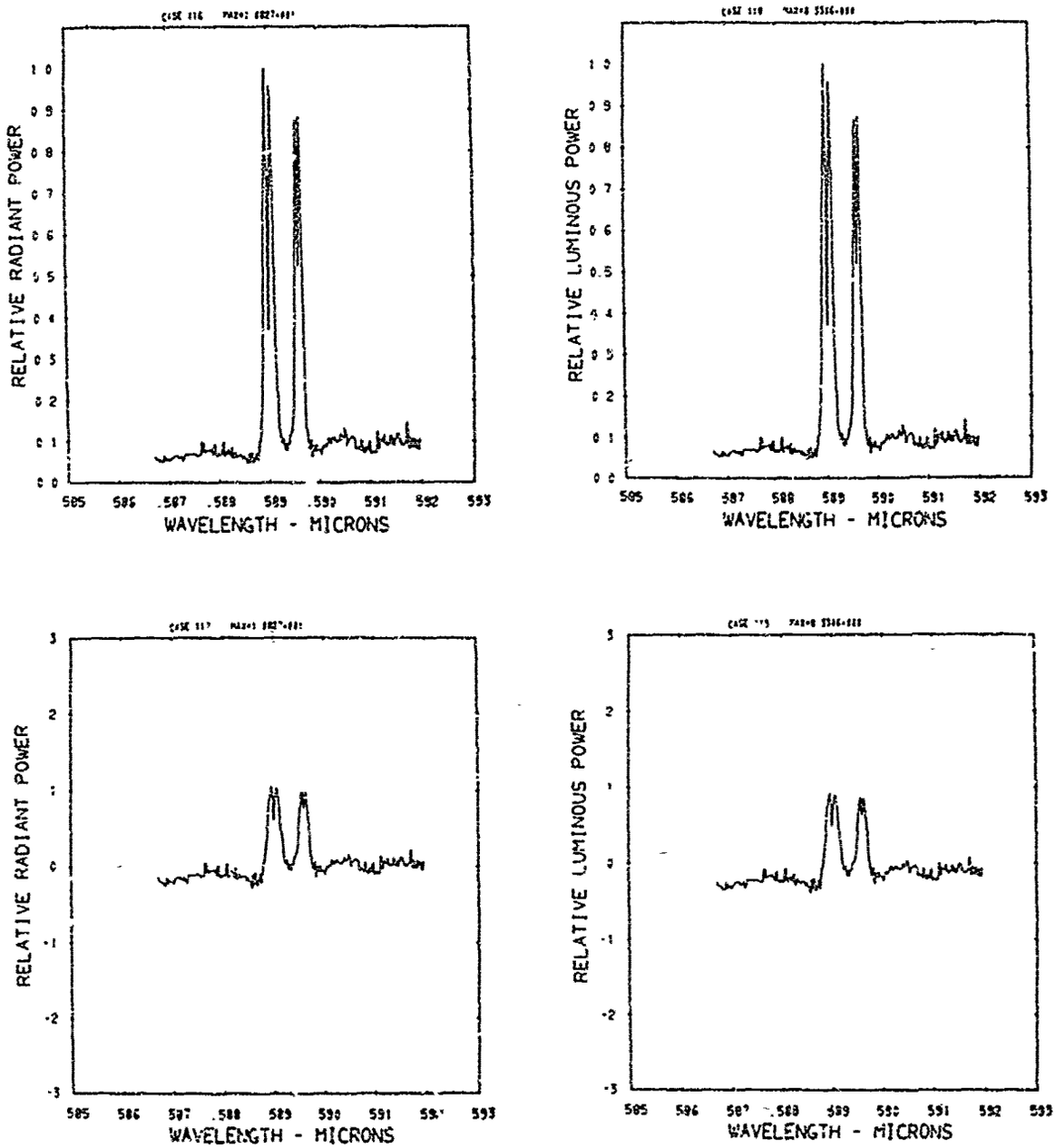

Figure A71. Relative power spectra of test flare 124A, formula group 3, burned at 75 torr ambient pressure. The top two spectra are normalized with the peak value equal to unity. The $\log_{10}$ of the spectral power is plotted in the bottom spectra. Flare formula group 3 contains 40.04% magnesium, 0.515% sodium nitrate, 54.945% potassium nitrate, and 4.5% binder.

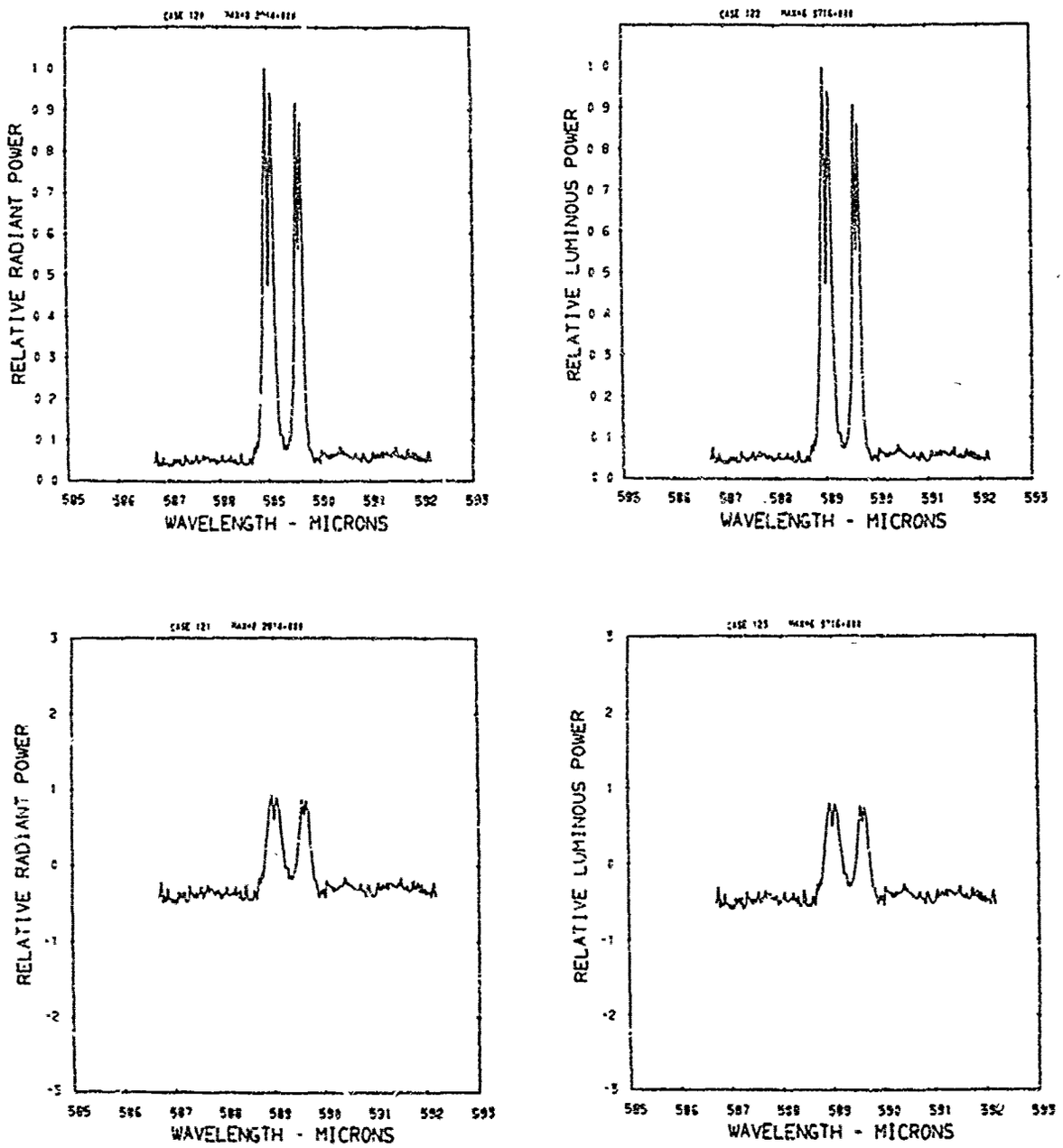

Figure A72. Relative power spectra of test flare 124B, formula group 3, burned at 75 torr ambient pressure. The top two spectra are normalized with the peak value equal to unity. The $\log_{10}$ of the spectral power is plotted in the bottom spectra. Flare formula group 3 contains 40.04% magnesium, 0.515% sodium nitrate, 54.945% potassium nitrate, and 4.5% binder.

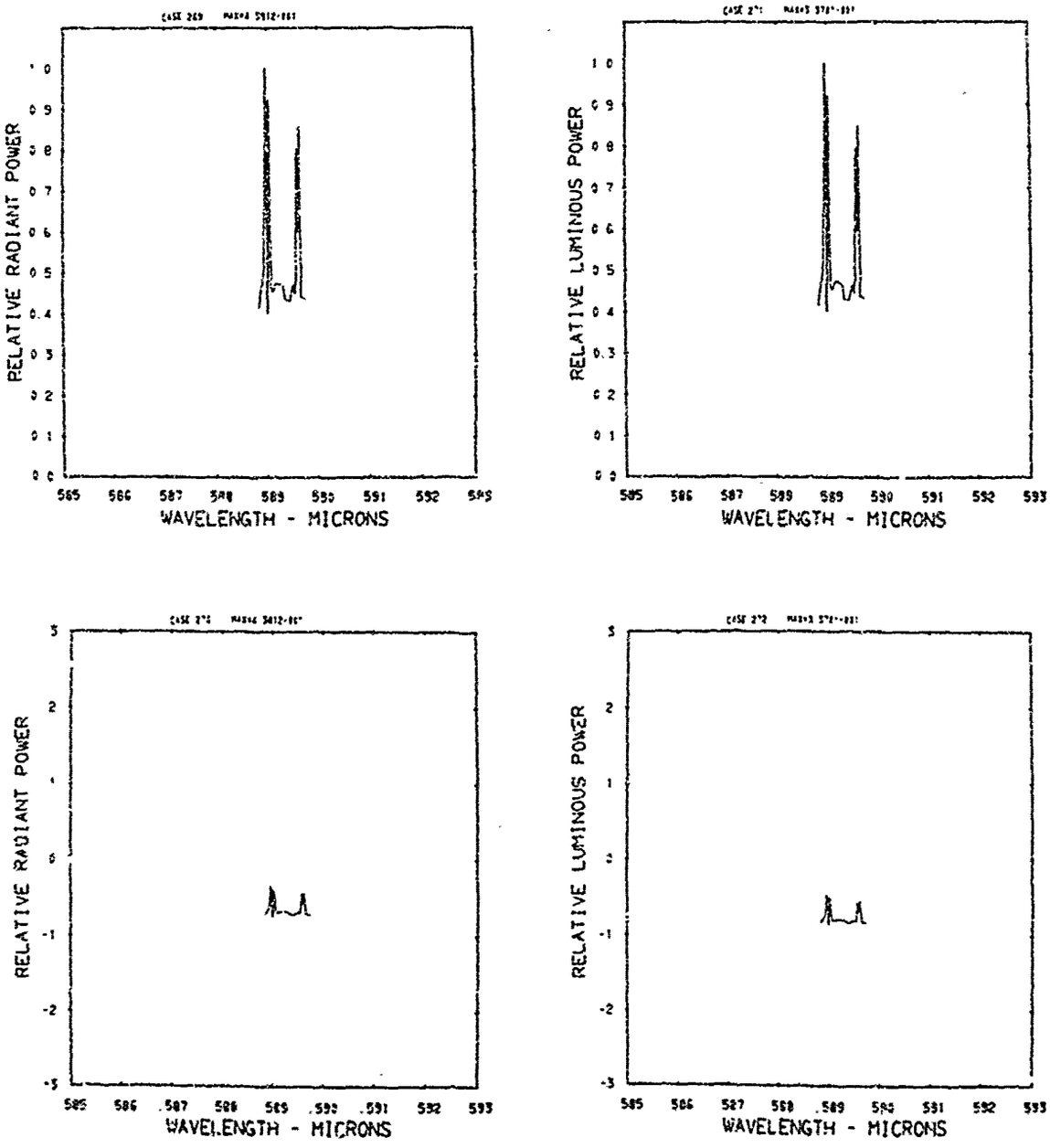

Figure A73. Relative power spectra of test flare 24A , formula group 3, burned at 30 torr ambient pressure. The top two spectra are normalized with the peak value equal to unity. The $\log_{10}$ of the spectral power is plotted in the bottom spectra. Flare formula group 3 contains 40.04% magnesium, 0.515% sodium nitrate, 54.945% potassium nitrate, and 4.5% binder.

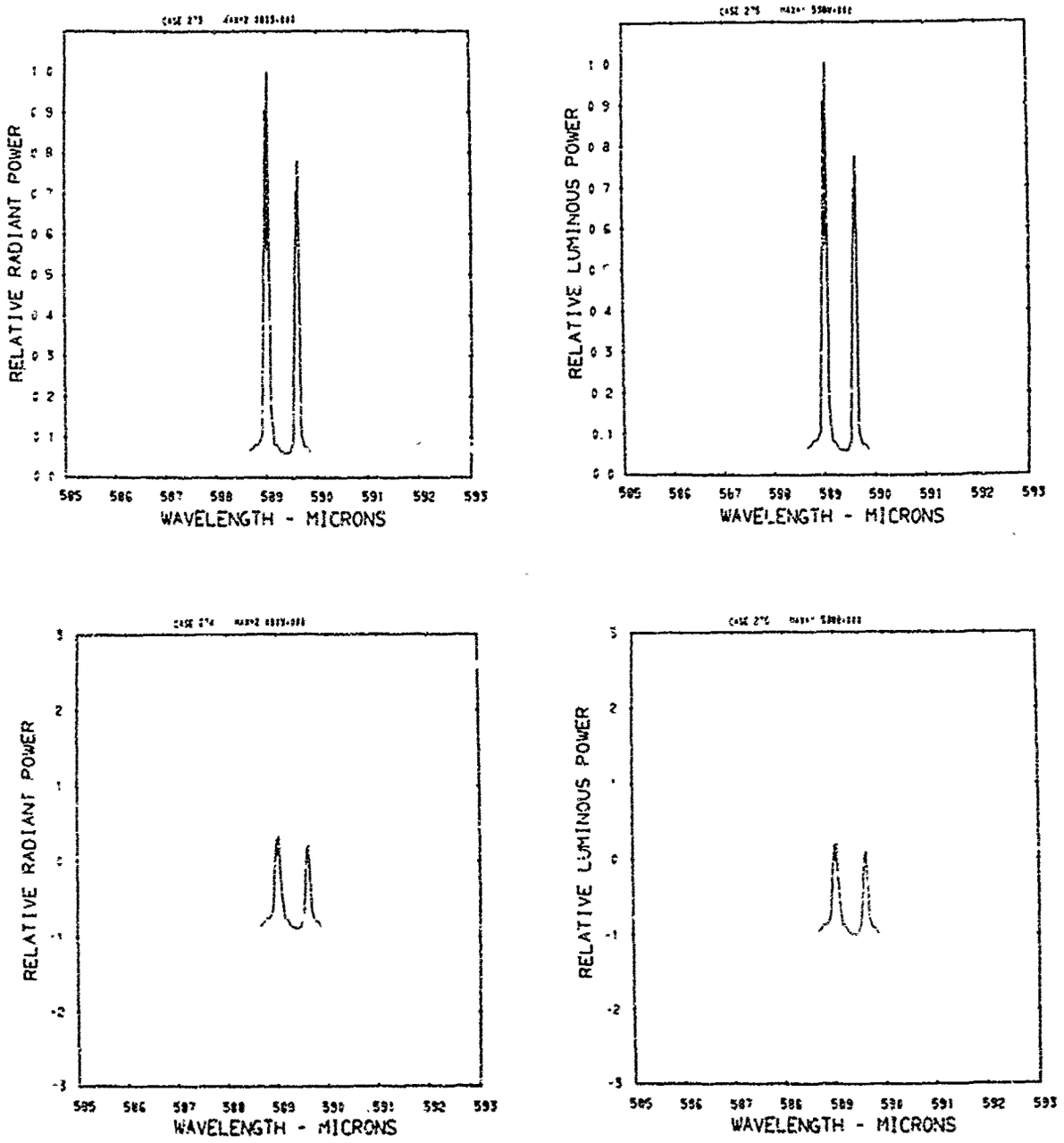

Figure A74. Relative power spectra of test flare 24B , formula group 3, burned at 30 torr ambient pressure. The top two spectra are normalized with the peak value equal to unity. The $\log_{10}$ of the spectral power is plotted in the bottom spectra. Flare formula group 3 contains 40.04% magnesium, 0.515% sodium nitrate, 54.945% potassium nitrate, and 4.5% binder.

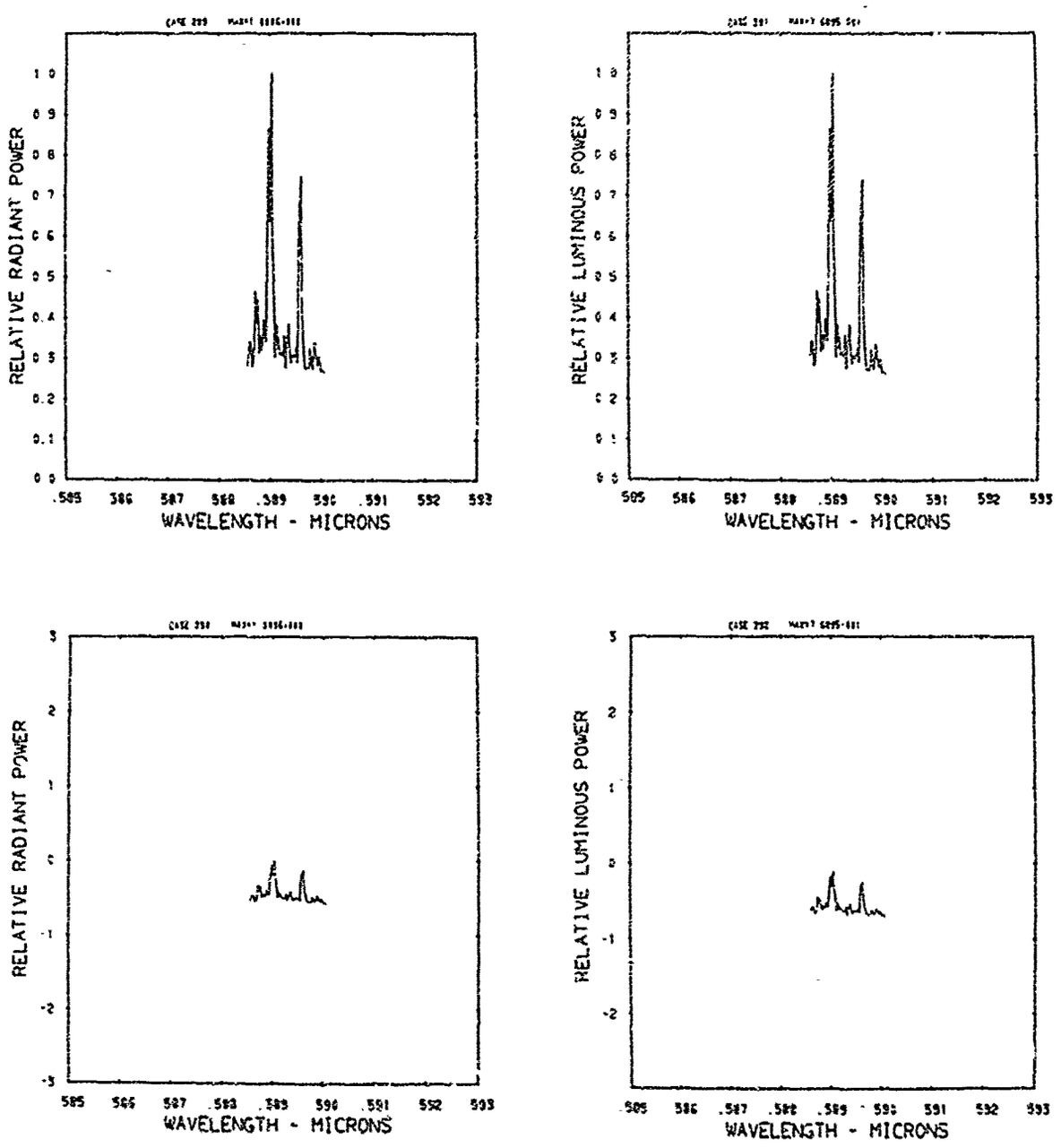

Figure A75. Relative power spectra of test flare 36 , formula group 3, burned at 30 torr ambient pressure. The top two spectra are normalized with the peak value equal to unity. The $\log_{10}$ of the spectral power is plotted in the bottom spectra. Flare formula group 3 contains 40.04% magnesium, 0.515% sodium nitrate, 54.945% potassium nitrate, and 4.5% binder.

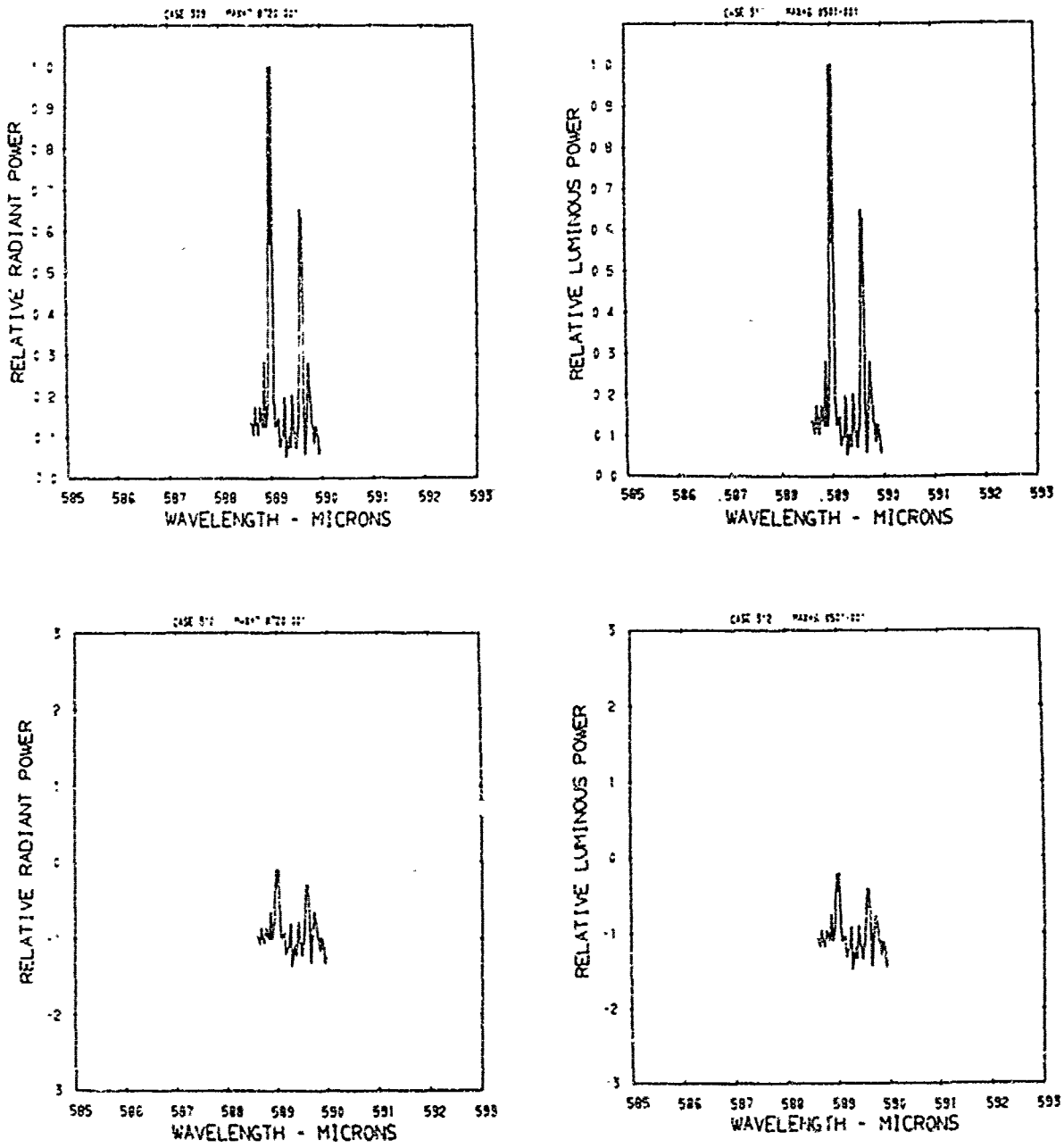

Figure A76. Relative power spectra of test flare 42 , formula group 3, burned at 30 torr ambient pressure. The top two spectra are normalized with the peak value equal to unity. The $\log_{10}$ of the spectral power is plotted in the bottom spectra. Flare formula group 3 contains 40.04% magnesium, 0.515% sodium nitrate, 54.945% potassium nitrate, and 4.5% binder.

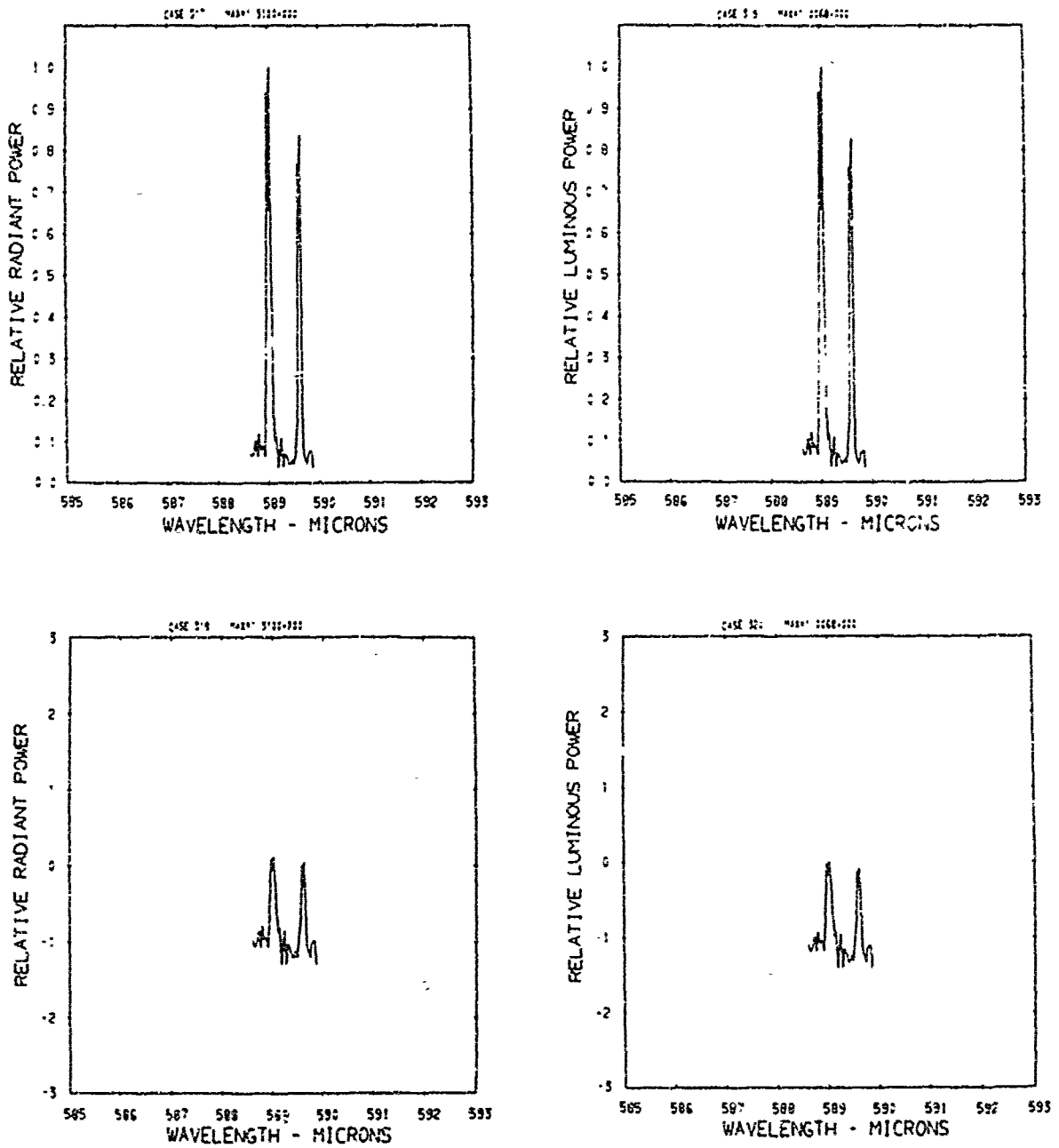

Figure A77. Relative power spectra of test flare 44 , formula group 3, burned at 30 torr ambient pressure. The top two spectra are normalized with the peak value equal to unity. The $\log_{10}$ of the spectral power is plotted in the bottom spectra. Flare formula group 3 contains 40.04% magnesium, 0.515% sodium nitrate, 54.945% potassium nitrate, and 4.5% binder.

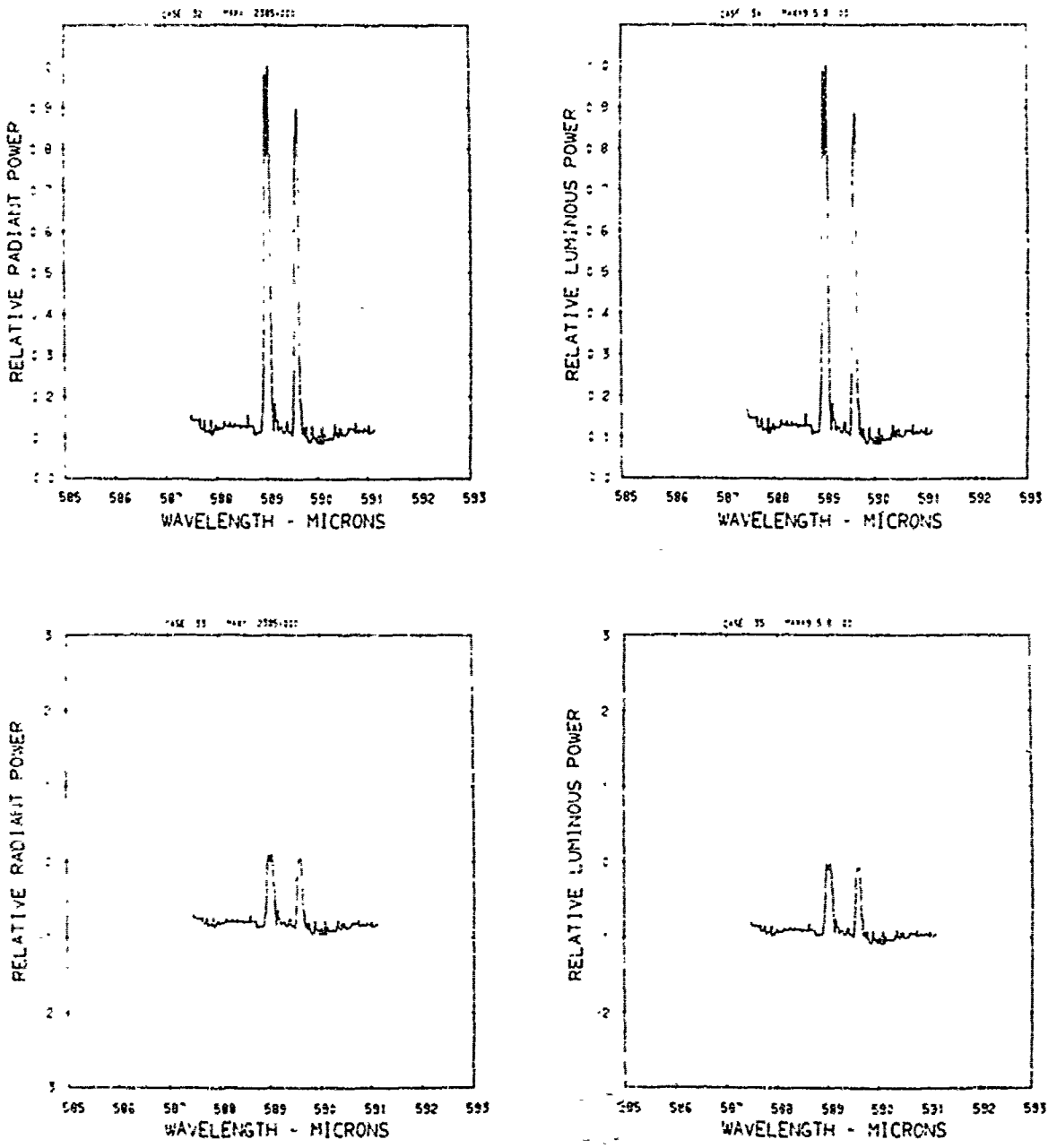

Figure A78. Relative power spectra of test flare 97 , formula group 3, burned at 30 torr ambient pressure. The top two spectra are normalized with the peak value equal to unity. The $\log_{10}$ of the spectral power is plotted in the bottom spectra. Flare formula group 3 contains 40.04% magnesium, 0.515% sodium nitrate, 54.945% potassium nitrate, and 4.5% binder.

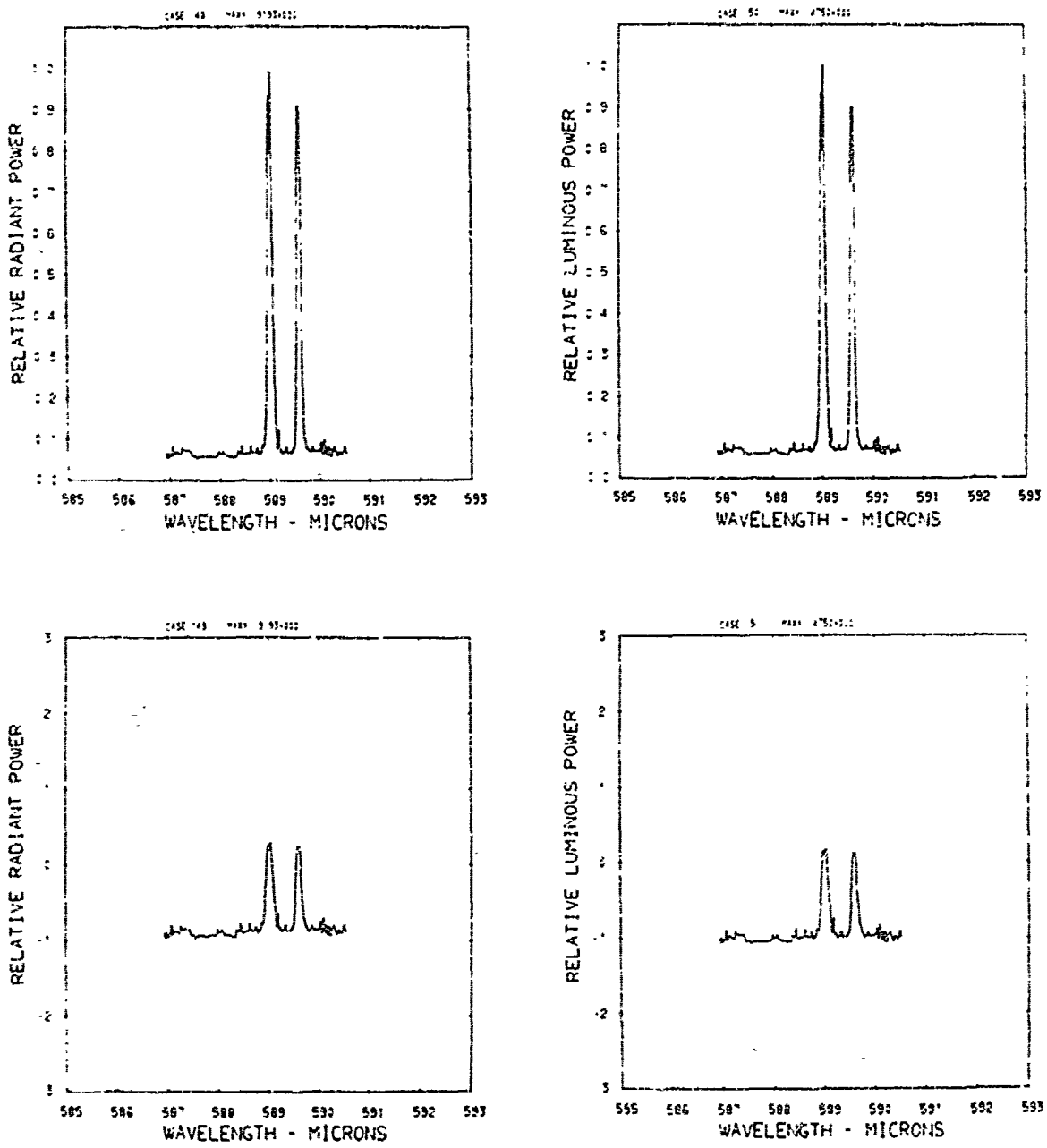

Figure A79. Relative power spectra of test flare 101 , formula group 3, burned at 30 torr ambient pressure. The top two spectra are normalized with the peak value equal to unity. The $\log_{10}$ of the spectral power is plotted in the bottom spectra. Flare formula group 3 contains 40.04% magnesium, 0.515% sodium nitrate, 54.945% potassium nitrate, and 4.5% binder.

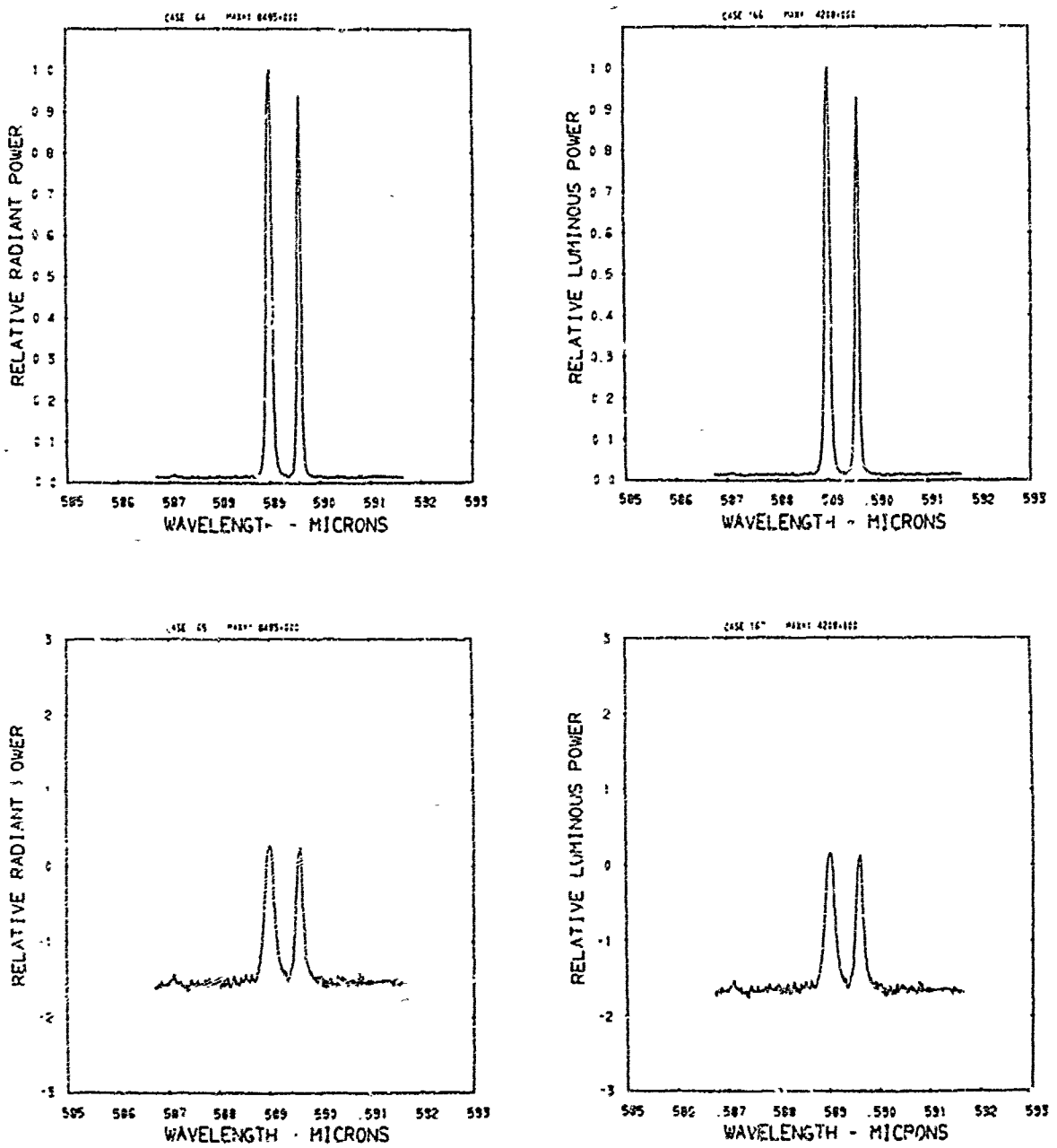

Figure A80. Relative power spectra of test flare 107-10, formula group 3, burned at 30 torr ambient pressure. The top two spectra are normalized with the peak value equal to unity. The $\log_{10}$ of the spectral power is plotted in the bottom spectra. Flare formula group 3 contains 40.04% magnesium, 0.515% sodium nitrate, 54.945% potassium nitrate, and 4.5% binder.

APPENDIX B

DERIVATION AND INTEGRATION OF RADIATIVE TRANSFER EQUATION

DERIVATION AND INTEGRATION OF RADIATIVE TRANSFER EQUATION

Derivation

The contribution by any differential volume element $dz \cdot d\sigma$ to the intensity of a flame, taken to be a slab of plane parallel stratification, is determined by the balance of emission and absorption of energy within the volume element where dz and $d\sigma$ are element thickness and cross-sectional area respectively. By convention, the z axis is taken to be normal N to the slab and measured from $z = 0$ at some point outside the slab toward the center of the slab. On the other hand, the direction of flux flow s is taken to be positive in the direction of the observer outside the flame with θ being the angle between s and N. Therefore,

$$s = -z \sec\theta \quad \text{and} \quad ds = -dz \sec\theta \tag{B1}$$

as shown in Fig. B1.

The increment of intensity lost by absorption is

$$-dI_\nu^a = k_\nu I_\nu ds \tag{B2}$$

where k_ν is the linear coefficient of absorption and I_ν is the specific intensity of light of frequency ν incident on the rear of the volume element along path ds. The energy emitted within this same volume element is

$$dE_\nu^e = \varepsilon_\nu \, d\nu \, d\omega \, dt \, ds \cos\theta \, d\sigma \tag{B3}$$

where ε_ν is the monochromatic volume emission coefficient through solid angle $d\omega$ and time interval dt. Alternatively, in terms of its specific intensity, this energy is

$$dE_\nu^e = dI_\nu^e \, d\nu \, d\omega \, dt \cos\theta \, d\sigma \; . \tag{B4}$$

It follows from Eqs. (B3) and (B4) that

$$dI_\nu^e/ds = \varepsilon_\nu \tag{B5}$$

and from Eq. (B2) that

$$dI_\nu^a/ds = -k_\nu I_\nu \; . \tag{B6}$$

Combining Eqs. (B5) and (B6), the emission and absorption contributions to the intensity, leads to

$$dI_\nu/ds = -k_\nu I_\nu + \varepsilon_\nu \; . \tag{B7}$$

Substituting Eq. (B1) into (B7) gives the following equivalent expressions

$$dI_\nu/(-dz \sec\theta) = -k_\nu I_\nu + \varepsilon_\nu \; , \tag{B8a}$$

$$-\cos\theta(dI_\nu/dz) = -k_\nu I_\nu + \varepsilon_\nu \; , \text{ and} \tag{B8b}$$

$$\mu(dI_\nu/dz) = k_\nu I_\nu - \varepsilon_\nu \tag{B8c}$$

where $\mu = \cos\theta$.

It is now convenient, mathematically, to combine the emission and absorption coefficient to define a source function

$$S_\nu \equiv \epsilon_\nu / k_\nu \tag{B9}$$

and to define the differential element of monochromatic optical depth

$$d\tau_\nu \equiv k_\nu dz \ . \tag{B10}$$

Dividing Eq. (B8c) by k_ν and substituting Eqs. (B9) and (B10), the differential equation of radiative transfer becomes

$$\mu(dI_\nu / d\tau_\nu) = I_\nu - S_\nu \ . \tag{B11}$$

Introducing the normalized profile of the absorption coefficient ϕ_ν defined as

$$\phi_\nu \equiv k_\nu / \int_0^\infty k_\nu d\nu \ , \tag{B12}$$

the monochromatic optical depth differential element is described by

$$d\tau_\nu = \phi_\nu \, d\tau \ . \tag{B13}$$

Substituting Eq. (B13) into (B11) leads to another form of the radiative transfer equation,

$$\mu(dI_\nu / d\tau) = \phi_\nu (I_\nu - S_\nu) \ . \tag{B14}$$

Integration

Formal integration of the radiative transfer equation can be completed as follows. Divide Eq. (B14) by μ and rearrange to get

$$(dI_\nu/d\tau) - (I_\nu\phi_\nu/\mu) = -S_\nu\phi_\nu/\mu \ . \tag{B15}$$

Multiply through by $\exp(-\tau\phi_\nu/\mu)$ to get

$$[(dI_\nu/d\tau)\exp(-\tau\phi_\nu/\mu)] - [(I_\nu\phi_\nu/\mu)\exp(-\tau\phi_\nu/\mu)] = -[(S_\nu\phi_\nu/\mu)\exp(-\tau\phi_\nu/\mu)]. \tag{B16}$$

Since the left side of Eq. (B16) equals $d[I_\nu \exp(-\tau\phi_\nu/\mu)]/d\tau$, substitution leads to

$$d[I_\nu \exp(-\tau\phi_\nu/\mu)]/d\tau = -[(S_\nu\phi_\nu/\mu)\exp(-\tau\phi_\nu/\mu)] \ . \tag{B17}$$

The integral form, with τ_1 the limit toward the front of the atmosphere and τ_2 the li toward the rear, is

$$\int_{\tau=\tau_2}^{\tau=\tau_1} d[I_\nu \exp(-\tau\phi_\nu/\mu)] = -\int_{\tau=\tau_2}^{\tau=\tau_1} [(S_\nu\phi_\nu/\mu)\exp(-\tau\phi_\nu/\mu)]d\tau \ . \tag{B18}$$

Integrating Eq. (B18) gives

$$[I_{\nu 1}\exp(-\tau_1\phi_\nu/\mu)] - [I_{\nu 2}\exp(-\tau_2\phi_\nu/\mu)] = -\int_{\tau=\tau_2}^{\tau=\tau_1} [(S_\nu\phi_\nu/\mu)\exp(-\tau\phi_\nu/\mu)]d\tau \tag{B19}$$

where $I_{\nu 1}$ is intensity at τ_1 and $I_{\nu 2}$ is intensity at τ_2. Next, by multiplying through by $\exp(\tau_1\phi_\nu/\mu)$, and using the identity

$$[\exp(-\tau_1\phi_\nu/\mu)][\exp(+\tau_1\phi_\nu/\mu)] = \exp(0) = \text{unity} \ , \tag{B20}$$

we obtain

$$I_{\nu 1} = I_{\nu 2} \exp[-(\tau_2-\tau_1)\phi_\nu/\mu] - \int_{\tau=\tau_2}^{\tau=\tau_1} (S_\nu\phi_\nu/\mu) \exp(-\tau\varphi_\nu/\mu) \exp(\tau_1\phi_\nu/\mu)d\tau \ . \tag{B21}$$

By combining terms under the integral, changing the limits and thus the sign, Eq. (B21) becomes

$$I_{\nu 1} = I_{\nu 2} \exp[-(\tau_2-\tau_1)\phi_\nu/\mu] + \int_{\tau=\tau_1}^{\tau=\tau_2} (S_\nu\phi_\nu/\mu) \exp[-(\tau-\tau_1)\phi_\nu/\mu]d\tau \ . \tag{B22}$$

Eq. (B22) shows that at a given ν and μ, the intensity $I_{\nu 1}$ emerging from the atmosphere at any τ_1 is equal to the intensity $I_{\nu 2}$ incident at τ_2 attenuated by the atmosphere between τ_2 and τ_1 plus the integral of the source function incrementally attenuated by the atmosphere between τ_2 and τ_1.

The form of Eq. (B22) is simplified for the present case by considering (a) only flux emerging normal to the surface $(\mu=1)$ and (b) no flux is incident on the rear surface of the atmosphere $(I_{\nu 2}=0)$. Under these conditions, integrating from the front surface, where z and τ_1 are 0, to the rear surface where the total optical thickness $T = \tau_2$, the monochromatic emergent intensity is

$$I_\nu^\circ = \phi_\nu \int_{\tau=0}^{\tau=T} S_\nu \exp(-\tau\phi_\nu)d\tau \ . \tag{B23}$$

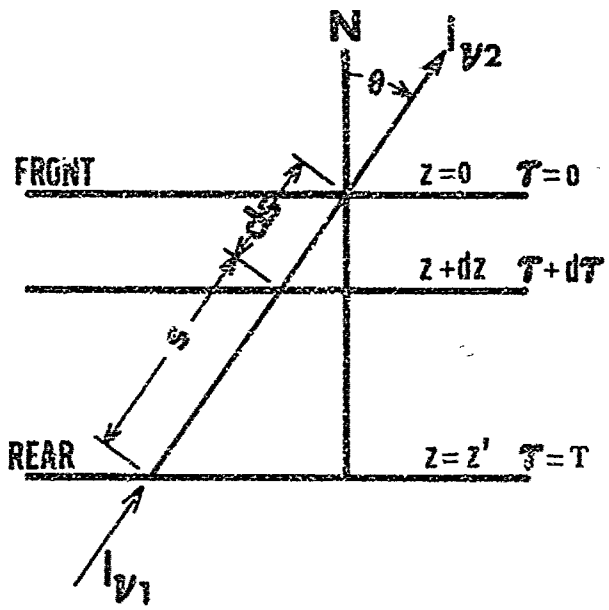
N
$I_{\nu 2}$
θ
FRONT
z=0 $\tau=0$
ds
z+dz $\tau+d\tau$
s
REAR
z=z' $\tau=T$
$I_{\nu 1}$

APPENDIX C

PROGRAM LTE4 TO SOLVE RADIATIVE TRANSFER EQUATION

PROGRAM LTE4 TO SOLVE RADIATIVE TRANSFER EQUATION

This is the main program used to solve the radiative transfer equation (Eqn. 7) as described in the THEORETICAL Section. It computes the relative radiative power spectrum of a pyrotechnic illuminating flame from known system variables such as flare formula, flare size, and ambient pressure. It considers only flux emerging normal to the flame surface and that no flux is incident on the rear surface of the flame. It solves the LTE case using the Planck function as the source function. A two-line Voigt profile as a function of frequency is constructed in the program for a specified value of the a parameter. The radial temperature profile in the flame along the optical axis is constructed in the program as specified by input parameters.

Only variables in the NAMELIST statement of the program are needed to operate the program. These are:

a. AA - Voigt parameter a.

b. NFREQ - number of frequency intervals in Voigt subroutine. The number of intervals and width of the interval define the frequency range over which computations are performed.

c. F - Doppler half-width in frequency units. When F = zero, F and DWN are computed. When F is provided as input, DWN must also be provided as input.

d. DWN - Doppler width in wavenumbers.

e. STEP - input option used as a scalar.

f. STEP * DWN - distance in wavenumbers between successive values of X in Voigt profile. This product controls the width of the wavelength interval between computations.

g. OS1 - oscillator strength of D1 line.

h. OS2 - oscillator strength of D2 line.

i. OS - oscillator strength sum of OS1 and OS2.

j. XLAM - wavelength of point halfway between the D line doublet. This parameter is used to compute DWN.

k. XLAM1 - wavelength of D1 line.

l. XLAM2 - wavelength of D2 line.

m. Z - total physical depth of flame in cm. Z must be provided in multiple of .062 cm.

n. TEMPL - temperature in kelvin used to compute F and DWN.

o. DENS - sodium atom number density in the flame.

p. M - integer in Simpson rule of 2M intervals used to perform integration.

q. TORR - ambient pressure in torr.

r. GROUP - formula identification. Only used for caption printing.

s. TEMPS - array of temperatures of the flame at various depths. A TEMPS value at the flame boundary (TEMPS(1)) and at the flame middle (TEMPS((Z*8)+1)) must be

provided as input. Between these points, TEMPS values at intervals of .062 cm are input as necessary to construct the profile desired.

t. PUNCH1 - logical variable. If true, non-normalized radiant power spectrum is punched on cards as well as printed.

u. PUNCH2 - logical variable. If true, the radiant power spectrum, normalized so that the maximum equals PLNK2, is punched on cards. PLNK2 is the Planck value at XLAM and TEMPS((Z*8)+1).

v. PUNCH3 - logical variable. If true, the luminous power spectrum, normalized so that the maximum is unity, is punched on cards.

w. NDUPS - integer variable which specifies number of duplicate sets of punch card output one gets when PUNCH1, PUNCH2 or PUNCH3 are true.

x. PLOT1 - logical variable. If true, the computed power spectra are plotted by the printer.

y. DBUG and DBUG2 - logical variables. If true, intermediate printing takes place.

A listing of PROGRAM LTE4 is given on the following pages.

```
      PROGRAM LTE4( INPUT, OUTPUT,TAPE5=INPUT,TAPE6=OUTPUT,PUNCH)
C                    STATEMENT NUMBERS USED
C      NEXT STATEMENT NUMBER IS
C      131
C                 **********  NOTE  **********
C      LTE3 CONVERTED TO LTE4 14 SEP 72 BY COMPUTING LUMINOUS POWER.
C      SUBROUTINES COREKT,EYEBAL AND BLOCK DATA EYEB ADDED.

C      UPDATED 12 SEP 72 TO PUNCH OUTPUT.

C      15 AUG 72 UPDATE TO NORMALIZE TO PLANCK VALUE AT XLAM
C       AND CENTER TEMPERATURE.  ALSO GETS INTEGRAL VALUE OF SPECTRUM.

C      UPDATED 31JULY72.  PUT IN OSCILLATOR STRENGTH VALUES FROM
C       HANS GRIEM BOOK PLASMA SPECTROSCOPY.

C      PROGRAM LTE2 IS A MODIFICATION OF LTE1 TO INCORPORATE A
C       2-LINE VOIGT PROFILE.
C      PROGRAM LTE1 DOES SINGLE LINE PROBLEM IN THERMAL EQUILIBRIUM.
C      IT USES ASSIGNED (INPUT) THERMAL GRADIENT (SYMMETRICAL) TABLE.
C      WE NEED INPUT DATA  AS LISTED IN NAMELIST INPT1
C      IT IS SET UP TO DO ONLY SODIUM PROBLEMS.
C      TO DO OTHER LINES, CHANGE XMASS IN SUBROUTINE DOPPLER.

      INTEGER 7HALF
      COMMON /B6/A2(392)
      DIMENSION EINT(2000)
      DIMENSION XV1(2000),XV2(2000),XV3(2000),PHI1(2000),PHI2(2000),
     *  PHI3(2000)
      DIMENSION TEMPS(201), XVV(2000)
      DIMENSION JL(101)
      INTEGER P,Q
      INTEGER ZHP1
      INTEGER GROUP
      LOGICAL PUNCH1,PUNCH2
      LOGICAL PUNCH3
      LOGICAL DBUG2
      INTEGER ZP1
      EQUIVALENCE (XVV,XV3),(EINT,XV2)
      DATA ZZ/1HZ/
      DATA P/5/, Q/6/
      LOGICAL DBUG
      LOGICAL PLOT1

      NAMELIST /INPT1/ TEMPS,H,Z,F,OS,DENS,AA,NFREQ,TEMPL,DWN,XLAM
     * ,DBUG,STEP
     * ,PLOT1
     *  ,OS1,OS2,XLAM1,XLAM2
     *  ,GROUP, TORR, DBUG2
     *  ,PUNCH1,PUNCH2,NDUPS
     *  ,PUNCH3

C      PUNCH1 AND PUNCH2 CONTROL OUTPUT PUNCH LOOPS NEAR END OF
```

```
C       MAIN PROGRAM.
C      NDUPS IS NUMBER OF DUPLICATE DECKS OF PUNCHED OUTPUT.
C      IF PLOT1 IS TRUE,EMERGENT INTENSITY IS PLOTTED
C                                PRINT CONTROL
C      DBUG2 CONTROLS PRINT OF PHI1, PHI2, AND PHI3.
C      DBUG CONTROLS SOME PRINT.
C      WHEN DBUG IS TRUE, WE GET A LOT OF PRINT OUTPUT,
C      WHEN DBUG IS FALSE, WE GET REDUCED PRINTING.
C      DBUG IS INSIDE THE FREQUENCY LOOP AND THUS PRINTS A LOT FOR EACH
C          FREQUENCY.
C      SETTING OF NFREQ TO A LOW NUMBER WHEN DBUG IS TRUE IS RECOMMENDED.

C      STEP*DWN = THE DISTANCE IN WAVENUMBERS BETWEEN SUCCESSIVE
C           VALUES OF X IN VOIGT.
C      NFREQ = NUMBER OF FREQUENCY STEPS OF X IN VOIGT NEEDED
C           TO COMPUTE EINT.
C     NFREQ CONTROLS DIMENSION OF EINT AND XVV.
C      NFREQ CONTROLS DIMENSION OF XV1,XV2,XV3,PHI1,PHI2, AND PHI3.
C      XVV IS EQUIVALENCED WITH XV3.
C      XVV IS AN ARRAY FOR ALL FREQUENCIES OF THE XV.
C      XV3 IS ARRAY OF WAVELENGTH OF THE 2-LINE VOIGT PROFILE.
C      XLAM = WAVELENGTH HALFWAY BETWEEN THE TWO LINES
C      XLAM  IS INPUT IN ANGSTROMS.
C      XLAM1 = WAVELENGTH OF D1 LINE.  LONGER WAVELENGTH OF THE TWO LINE
C      XLAM2 IS WAVELENGTH OF D2 LINE, THE SHORTER WAVELENGTH OF THE TWO
C           LINES.
C      XLAM1 AND XLAM2 ARE BOTH INPUT IN ANGSTROMS.
C      OS = OSCILLATOR STRENGTH SUM OF THE TWO LINES.
C      OS1 IS OSCILLATOR STRENGTH OF D1 LINE, LONGER WAVELENGTH OF THE
C          TWO LINES.
C      OS2 IS OSCILLATOR STRENGTH OF D2 LINE, THE SHORTER WAVELENGTH
C       OF THE TWO LINES.
C      TEMPL = TEMPERATURE IN DOPPLER USED TO  COMPUTE F AND DWN.
C      DENS = ATOM (SPECIES) DENSITY IN THE ATMOSPHERE, N12.
C      F = DOPPLER HALF WIDTH IN FREQUENCY UNITS.
C      WHEN WE INPUT VALUE FOR F, DOPPLER ROUTINE IS SKIPPED.
C      WHEN WE INPUT F, WE ALSO MUST PROVIDE INPUT VALUE FOR DWN.
C      DWN = DOPPLER WIDTH IN WAVENUMBERS
C      IF F=0., OR F IS OMITTED, F IS COMPUTED IN DOPPLER USING
C           TEMPERATURE VALUE PUT IN AS TEMPL.
C      M = INTEGER IN SIMPSON RULE FOR 2M INTERVALS.
C      INTEGRAL IS DONE WITH SIMPSON RULE FOR 2M INTERVALS
C      AA = VOIGT PARAMETER A

C      Z = TOTAL PHYSICAL DEPTH OF ATMOSPHERE IN CM.
C      Z IS INPUT IN STEPS OF .062CM.  IT IS EXPANDED INTERNALLY TO
C      END UP AS AN EVEN WHOLE NUMBER.   ( BY ZA )

C      TEMPS ARE THE TEMPERATURES OF THE ATMOSPHERE AT VARIOUS DEPTHS.
C      THE INDEX OF TEMPS IS THE INTEGER CORRESPONDING TO 16TIMES THE
C      NUMBER OF .062CM STEPS OF Z PLUS 1,
C      TEMPS INDEX = ( Z*16)+1
C      EXAMPLE.  WHEN DEPTH = ZERO CM, INDEX = 1.
C      WHEN DEPTH = 2.5 CM, INDEX = 41.
C      TO MULTIPLY BY 16ASSURES AN EVEN NUMBER CORRESPONDING TO THE
```

```
C       TOTAL PHYSICAL DEPTH.
C       THIS ALLOWS ONE TO INPUT A TEMPS AT INTERVALS OF .062 CM
C       TEMPS MIDDLE INDEX = (Z*8)+1.
C       WE MUST PROVIDE TEMPS VALUES FOR DEPTH = 0,DEPTH = MIDDLE (CM),
C       AND OTHER VALUES BETWEEN 0 AND MIDDLE.
C       TEMPS ARE INPUT IN DEGREES KELVIN.

    1   CONTINUE
C       RESET INPUT VARIABLES TO DEFAULT VALUE
        DO 2 J=1,201
        TEMPS(J)=0.
    2   CONTINUE
        DWN=0.
        Z=4.0
        F=0.
        DENS=0.
        AA=0.
        STEP=1.
        DBUG=.FALSE.
        DBUG2=.FALSE.
        IHR=0
        MIN=0
        ISEC=0
        M=0
        M=200
        M=100
        M=50
        OS1=0.312
        OS2=0.624
        OS=OS1+OS2
        NFREQ=0
        NFREQ=300
        TEMPL=0.
        TEMPL=3098.
        XLAM=0.
        XLAM=5892.935
        XLAM1=5895.92
        XLAM2=5889.75
        PLOT1=.FALSE.
        PLOT1=.TRUE.
        PUNCH1=.TRUE.
        PUNCH1=.FALSE.
        PUNCH2=.FALSE.
        PUNCH3=.FALSE.
        PUNCH2=.TRUE.
        PUNCH3=.TRUE.
        NDUPS=1

        READ(P,INPT1)

C       PROGRAM TERMINATES WHEN M=0.
        IF(M.EQ.0) CALL EXIT

        WRITE(Q,11)
   11   FORMAT(1H1)
```

```
      CALL DATE(DM,YE)
C     CALL CLOCK(IHR,MIN,ISEC)
      WRITE(Q,63) DM,YE,IHR,MIN,ISEC
     *  ,GROUP, TORR
   63 FORMAT(2X,A10,A2,4X,3I3,
     *  50X,*GROUP*I3, F10.0, *TORR*)
      WRITE(Q,24)M,Z,F,OS,DENS,AA,NFREQ,TEMPL,DWN,XLAM,DBUG,STEP
     * ,PLOTI
   24 FORMAT(/*  M IN THE SIMPSON RULE IS*  I6,/
     * *  Z THE DEPTH OF THE ATMOSPHERE IN CM IS* F6.1,/
     * * F THE DOPPLER HALF WIDTH OF THE LINE IN FREQUENCY UNITS IS*
     *  E12.5,/
     * *  OS IS THE OSCILLATOR STRENGTH SUM OF THE TWO LINES.  IT IS*
     *   F10.3,/
     * * DENS THE SPECIES DENSITY IN THE ATMOSPHERE IN PARTICLES/CC IS*
     * E12.5,/
     * * AA THE LITTLE A PARAMETER IN THE VOIGT PROFILE IS* F10.5,/
     * *  NFREQ IS THE NUMBER OF STEPS OF FREQUENCY IN EMERGENT INTENSIT
     *Y.  IT IS* I6,/
     * *  TEMPL THE TEMPERATURE IN THE DOPPLER COMPUTATION IS*F9.3,/
     * *  DWN IS DOPPLER WIDTH IN WAVENUMBERS.  DWN IS*F10.3,/
     * *  XLAM THE WAVELENGTH HALFWAY BETWEEN THE TWO LINES IN ANGSTROMS
     * IS*
     * F10.3,/ *  DBUG=*  L4,/
     * *  STEP TIMES DWN IS THE DISTANCE IN WAVENUMBERS BETWEEN SUCCESSI
     *VE VALUES OF X IN VOIGT.  STEP =*F7.3,/
     * *  PLOTI=*L4  )
      WRITE(Q,81)OS1,OS2,XLAM1,XLAM2
   81 FORMAT(
     * *  OS1 THE OSCILLATOR STRENGTH OF THE D1 LINE IS* F10.3,/
     * *  OS2 THE OSCILLATOR STRENGTH OF THE D2 LINE IS* F10.3,/
     * *  XLAM1 THE WAVELENGTH IN ANGSTROMS OF THE D1 LINE IS*F10.3,/
     * *  XLAM2 THE WAVELENGTH IN ANGSTROMS OF THE D2 LINE IS*F10.3,/
     *  )

C      INITIALIZE VOIGT FUNCTION ROUTINE.
      DUMMY1=COFVOI(DUMMY2,DUMMY3)

      ZA=16.
      Z4=Z*ZA
      062=0.062
      0125=0.125
      ZP1= IFIX(Z4)+1
      IF(.NOT.DBUG) GO TO 86
      WRITE(Q,10) 062,(TEMPS(J),J=1,ZP1)
   86 CONTINUE
   10 FORMAT(*  THE TEMPERATURES AT VARIOUS DEPTHS IN THE ATMOSPHERE*
     *  /* WHERE THE TEMPS INDEX CORRESPONDS TO THE PHYSICAL DEPTH AT IN
     *TERVALS OF* F6.3* CM. ARE*
     *       / (5X,10F8.0))
      WRITE(Q,93) 062,0125
   93 FORMAT(
     *  *  THE FOLLOWING RELATES TO TEMPS INDEX */
     *                    * INDEX=1 MAPS TO DEPTH=ZERO CM*/
     *  *  INDEX=2 MAPS TO DEPTH=* F6.3* CM,*/
```

```
     *  *  INDEX=3 MAPS TO DEPTH=* F6.3* CM,ETC.*
     *  /*  TEMPS MIDDLE INDEX=(Z TIMES 8)+1  *
     *  /)

C      NEXT COMPUTE F AND DWN WHEN NOT PROVIDED IN INPT1.
C      TEMPL = TEMPERATURE (INPUT) FOR DOPPLER SUBROUTINE.
C      IN DOPPLER WHEN 2ND ARGUMENT = 0, WE FIND F AND DWN (OUTPUT).
C      AHW = COMPUTED DOPPLER HALF WIDTH IN ANGSTROMS AT TEMPL.
C      F = DOPPLER HALFWIDTH IN FREQUENCY UNITS.
C      DOPPLER IS ENTERED WHEN NO VALUE FOR F IS GIVEN IN NAMELIST INPT1.
C      DOPPLER IS SKIPPED IF WE PROVIDE VALUE FOR F.
C      DWN = DOPPLER WIDTH IN WAVENUMBERS

      IF(F .NE. 0.) GO TO 21
      CALL DOPPLER(XLAM, 0, TEMPL, F, DWN ,AHW )
      WRITE(Q,22) F, DWN,AHW
   22 FORMAT(//*  THE COMPUTED DOPPLER HALF WIDTH IN FREQUENCY UNITS =*
     *  E12.5,/
     * *  THE COMPUTED DOPPLER WIDTH DWN IN WAVENUMBERS =*F10.3,/
     *  *  THE DOPPLER HALF WIDTH AHW IN ANGSTROMS IS* F10.5,/ )
   21 CONTINUE

C      COMPUTE PLNK1
C      PLNK1 = VALUE OF PLANCK FUNCTION AT FREQ XLAM AND 3098 K.
      CALL PLANCK( 3098., XLAM,  2 ,PLNK1 )
      WRITE(Q,23) XLAM,PLNK1
   23 FORMAT(//* VALUE OF PLANCK FUNCTION AT CENTER FREQUENCY* F10.3,
     *  *  ANGSTROMS IS* E12.5,/)

C      FOR CONVENIENCE, WE INPUT TEMPS ONLY FROM DEPTH=0 THRU DEPTH
C      = MIDDLE.
C      WE ASSUME THE TEMPERATURE GRADIENT IS SYMMETRICAL ABOUT THE
C      MIDDLE.  NEXT WE GENERATE THE TEMPS BETWEEN MIDDLE, ZHALF, AND
C      THE REAR BOUNDARY OF THE ATMOSPHERE, Z.

      ZHALF= IFIX(Z4)/2
      ZHP1=ZHALF+1
      DO 13 J=1,ZHALF
      TEMPS(J+ZHP1) = TEMPS(ZHP1-J)
   13 CONTINUE
      IF(.NOT.DBUG) GO TO 87
      WRITE(Q,10) O62,(TEMPS(J),J=1,ZP1)
   87 CONTINUE
C      AT THIS POINT, WE HAVE AVAILABLE A TEMPERATURE GRADIENT AT
C      SELECTED DEPTHS OVER THE ENTIRE ATMOSPHERE

      MP1=M+1
      M2=M*2
      M2P1=M2+1
      WRITE(Q,12) M,M2
   12 FORMAT(* M IS THE SIMPSON RULE MIDDLE INDEX CORRESPONDING TO THE
     *PHYSICAL DEPTH OF THE MIDDLE OF THE ATMOSPHERE. M=*I3,/
     * * THE SIMPSON RULE INDEX CORRESPONDING TO THE TOTAL DEPTH, 2M, OF
     * THE ATMOSPHERE =*I4,///)
      WRITE(Q,15)
```

```
   15 FORMAT(//* Z MAPS TO ZM AND ZHALF MAPS TO M */
     * * ZP1 MAPS TO M2P1 AND ZHP1 MAPS TO MP1*//)
C      FIND THE TEMPS FOR EACH OF THE MISSING DEPTH POINTS BETWEEN
C      DEPTH = ZERO AND DEPTH = MIDDLE (ZHALF)
C      TEST FOR ZERO TEMPS AND RECORD THEIR LOCATION
      K=0
      DO 16 J=2,ZHP1
      J1=J
      IF(TEMPS(J)) 50,50,16
   16 CONTINUE
      GO TO 17
   50 CONTINUE
      K=K+1
      JL(K)=J1
      GO TO 16
   17 CONTINUE
C      NOW ALL THE ZERO TEMPS INDEX NUMBERS ARE STORED IN JL
C     THERE ARE K OF THEM BETWEEN ZEPO CM AND ZHALF

C     NEXT WE INTERPOLATE BETWEEN THE TEMPS AND FIND A TEMPS FOR ALL
C      THE TERMS THAT WERE ORIGINALLY ZERO.
      IF ( K .EQ. 0)  GO TO 55
      L=0
      DO 51 J=2,K
      J1=J
      IF(JL(J) .EQ. (JL(J- 1) + 1))GO TO 53
      L=L+1
      LP1=L+1
      GO TO 52
   53 L=L+1
      LP1=L+2
   56 DUM=0.
   51 CONTINUE
   52 CONTINUE
      JA = JL(J1-L) - 1
      JB = JA + LP1
      IF(K .EQ. 1 ) JA=1
      IF(K .EQ. 1 ) JB=3
      JBM1 = JB-1
      JAP1=JA+1
      TDIFF = TEMPS(JB) - TEMPS(JA)
      TADD = TDIFF / LP1
      DO 54 I=JAP1,JBM1
      TEMPS(I) = TEMPS(I-1) + TADD
      L=0.
   54 CONTINUE
      IF(K .EQ. 1 ) GO TO 55
      IF(J1 .EQ. K) GO TO 55
      GO TO 56
   55 CONTINUE
      IF(.NOT.DBUG) GO TO 88
      WRITE(Q,10) (TEMPS(J),J=1,ZP1)
   88 CONTINUE
C     NOW WE HAVE TEMPS FOR ALL POINTS BETWEEN Z=0 AND ZHALF
```

```
C      NEXT FIND THE TEMPS BETWEEN ZHALF AND Z BY SYMMETRY
      DO 18 J=1,ZHALF
       TEMPS(J+ZHP1) = TEMPS(ZHP1-J)
   18 CONTINUE
      WRITE(Q,20) 062,(TEMPS(J ,J=1,ZP1)
C      NOW WE HAVE A TEMPS FOR EACH CM OF DEPTH FROM ZERO THRU Z.

C      WE INTEGRATE BY SIMPSON RULE FROM 0 TO 2M INTERVALS, THAT
C           IS FROM  INDEX 1 THRU M2P1.
C      WE NEED A SUBROUTINE WHICH COMPUTES A DEPTH,ZCM, AND A
C      TEMPERATURE TEMPP FOR EACH INDEX POINT IN THE INTEGRATION.
C      WE CALL IT DEPTMP.
C       IT IS CALLED BY
C      CALL DEPTMP(M8,TEMPS,M2,Z,TEMPP,ZCM)
C      M8 IS THE SIMPSON RULE INDEX FOR WHICH WE FIND A TEMPP AND ZCM.
C      TEMPP IS THE TEMPERATURE IN KELVIN AT M8 (OUTPUT)
C      ZCM IS THE DEPTH IN CM AT M8 (OUTPUT)
C      TEMPS IS THE TEMPERATURE INPUT ARRAY
C      M2 IS 2M INTERVALS OF SIMPSON RULE


C      B E DONDA 20 MARCH 72
C      DOES SIMPSONS RULE FOR 2M INTERVALS
C      SEE EQN 6-66 OF MOURSUND AND DURIS
C      ELEMENTARY THEORY AND APPLICATION OF NUMERICAL ANALYSIS
C       MCGRAW HILL 1967
C      LET M = INTEGER .GT. ZERO
C      LET H = (B-A)/2M
C       A = INTEGRAL LOWER LIMIT
C      B = INTEGRAL UPPER LIMIT
C       X(I)=A+I*H FOR I=0,1,....,2M
C      TERM3 = 2*SUM OF F(X(2I)) FOR I=1,2,.....M-1
C       TERM4 = 4*SUM OF F(X(2I-1)) FOR I=1,2,.....M
C       TERM1 = F(X(A)) = F(X(I=0))
C       TERM2 = F(X(B)) = F(X(I=2M))
C      INTEGRAL = (H/3)*(TERM1+TERM2 + TERM3 + TERM4 )
C      WE NEED TO SOLVE FOLLOWING EQN AT EACH FREQUENCY
C       EINT = PHI * INTEGRAL OF (PLANCK*EXP(-TT*PHI))
C       INTEGRAL LIMITS ARE A=0, B=M2
C       INTEGRAL INDEX GOES A=1, B=M2P1
C       EINT = EMERGENT INTENSITY
C       PHI = VOIGT PROFILE OR OTHER ABSORPTION PROFILE
C       PLANCK = PLANCK FUNCTION AT TEMPERATURE CORRESPONDING TO DEPTH
C          IN THE ATMOSPHERE MAPPED TO INTEGRAL INDEX
C       TT = TOTAL THICKNESS AT DEPTH CORRESPONDING TO INTEGRAL INDEX

C      START HERE TO GENERATE 2-LINE VOIGT PROFILE.
      VGT=VOIGT(0.,AA)
      VGT10=VOIGT(10.,AA)
      WRITE(Q,94) VGT,VGT10
   94 FORMAT(/,10X*  VOIGT AT CENTER FREQUENCY I5*E12.5,/,
     * *        VOIGT AT FREQUENCY X=10 I5* E12.5,/  )
```

```
      NFREQH=NFREQ/2
      XWAVENO=1.0/( XLAM1 * 1.E-8)
      DO 69 J=1,NFREQ
      X=(FLOAT(J-1-NFREQH)) * STEP
      PHI1(J)=(VOIGT(X,AA))*OS1/OS
      XV1(J)= 1.E+8 / (XWAVENO - (DWN*X))
   69 CONTINUE
      IF( .NOT. DBUG2)  GO TO 90
      WRITE(Q,32)
   82 FORMAT(//*  PHI1 FOR THE LONGER WAVELENGTH LINE*)
      WRITE(Q,47)(((XV1(J),PHI1(J)),J=1,NFREQ))
   90 CONTINUE
      XWAVENO=1.0 / (XLAM2 * 1.E-8)
      DO 70 J=1,NFREQ
      X=(FLOAT(J-1-NFREQH)) * STEP
      PHI2(J)=(VOIGT(X,AA)) * OS2 /OS
      XV2(J)=1.E+8 / (XWAVENO - (DWN*X))
   70 CONTINUE
      IF( .NOT. DBUG2)  GO TO 91
      WRITE(Q,83)
   83 FORMAT(//*  PHI2 FOR THE SHORTER WAVELENGTH LINE*)
      WRITE(Q,47)(((XV2(J),PHI2(J)),J=1,NFREQ))
   91 CONTINUE
      XWAVENO=1. / (XLAM * 1.E-8)
      DO 71 J=1,NFREQ
      X=(FLOAT(J-1-NFREQH)) * STEP
      XV3(J)=1.E+8 / (XWAVENO - (DWN*X))
   71 CONTINUE
C      NEXT AT EACH XV3 WE FIND THE INTERPOLATED PHI1 AND PHI2
C        AND ADD THEM TOGETHER TO GET PHI3.
      DO 72 J=1,NFREQ
      DO 73 K=1,NFREQ
      KS=K
      IF(XV2(KS) .GE. XV3(J)) GO TO 74
   73 CONTINUE
      GO TO 75
   74 FRAC =(ABS(XV3(J)-XV2(KS-1)))/(ABS(XV2(KS)-XV2(KS-1)))
      PHI2J=PHI2(KS-1) + (FRAC*(PHI2(KS)-PHI2(KS-1)))
      GO TO 76
   75 CONTINUE
      PHI2J=PHI2(NFREQ)
   76 CONTINUE
      IF(XV3(J) . LE. XV1(1) ) GO TO 77
      DO 78 K=1,NFREQ
      KS=K
      IF(XV3(J) .LT. XV1(KS))  GO TO 79
   78 CONTINUE
      GO TO 72
   79 KS=KS-1
      FRAC=(ABS(XV3(J)-XV1(KS)))/(ABS(XV1(KS)-XV1(KS+1)))
      PHI1J=PHI1(KS) + (FRAC*(PHI1(KS+1)-PHI1(KS)))
      GO TO 80
   77 PHI1J=PHI1(1)
   80 PHI3(J) = PHI1J + PHI2J
   72 CONTINUE
```

```
      IF( .NOT. DBUG2)  GO TO 92
      WRITE(Q,84)
   84 FORMAT(//*  PHI3 THE 2-LINE VOIGT PROFILE*)
      WRITE(Q  7)(((XV3(J),PHI3(J)),J=1,NFREQ))
   92 CONTINUE
C      NOW WE HAVE THE 2-LINE VOIGT PROFILE IN PHI3(J).
C      EACH IS WEIGHTED FOR OSCILLATOR STRENGTH AND IS SYMMETRICAL
C      ABOUT XLAM.

C      ALL THE FOLLOWING IS INSIDE MASTER DO LOOP OVER FREQUENCY, X

      DO 999 JJJ=1,NFREQ
C      FIRST WE FIND TERM1
C      TERM1 = FUNCTION AT ZERO CM DEPTH
C      TT=0. AT ZERO DEPTH


      CALL THICK(TT,F,OS,0.,DENS)
      PHI=PHI3(JJJ)
      EX = EXP(-TT*PHI)
C      TEMPERATURE = TEMPS(1) AT ZERO DEPTH
C      XV IS ARBITRARY FREQ X CONVERTED TO CORRESPONDING WAVELENGTH
C             IN ANGSTROM UNITS.
      XV=XV3(JJJ)

      TEM = TEMPS(1)
      CALL PLANCK( TEM ,XV, 2,PLNK)

      IF(.NOT. DBUG) GO TO 25
      WRITE(Q,26)TT,X,AA,PHI,EX,XV,XLAM,DWN,PLNK,PLNK1,XWAVENO
   26 FORMAT(//*  TT=*E12.5,/*  X=*E12.5/*  AA=*F10.3/*  PHI=*E12.5/
     * *  EX=*
     *  E12.5/*  XV=*F10.3/*  XLAM=*F10.3/  *  DWN=*F10.3/*  PLNK=*E12.5
     * /*  PLNK1=*E12.5 /*  XWAVENO =*F10.3  )
      WRITE(Q,30)
   30 FORMAT( *  Z= 0 CM*)
      WRITE(Q,27)TEMPS(1)
   27 FORMAT(*  TEMPS(1)=*F10.3)
   25 CONTINUE

C      NORMALIZE SO PLNK AT CENTER FREQUENCY AND 3098K = 1.
C      PLNK AT XLAM    AND 3098K = PLNK1
      PLNK=PLNK/PLNK1
C      PLNK1 IS COMPUTED EARLY IN THE PROGRAM.
      TERM1 = PLNK*EX

      IF(.NOT. DBUG) GO TO 29
      WRITE(Q,28) PLNK,TERM1
   28 FORMAT(*  PLNK NORMALIZED =*E12.5/
     *  30X,                                *  VALUE OF TERM1=*E12.5)
   29 CONTINUE


C      NEXT WE FIND TERM2
C      TERM2 = FUNCTION AT Z CM DEPTH
```

```
      Z7=Z
      CALL THICK(TT,F,OS,Z7,DENS)
C      SAVE TT IN DUM FOR  USE TO PRINT CAPTION IN PLOT
      DUM=TT
      EX=EXP(-TT*PHI)
C      TEMPERATURE = TEMPS(ZP1) AT DEPTH Z=DEPTH Z7
      TEM =   MPS(ZP1)
      CALL PLANCK( TEM,   XV,  2, PLNK)

      IF(.NOT. DBUG) GO TO 31
      WRITE(Q,26)TT,X,AA,PHI,EX,XV,XLAM,DWN,PLNK,PLNK1,XWAVENO
      WRITE(Q,32)TEMPS(ZP1),Z7
   32 FORMAT(/*  TEMPS(ZP1)=*F10.3/*  Z7 DEPTH AT Z=*F10.3)
   31 CONTINUE

C      NORMALIZE.  SEE COMMENTS IN TERM1 ABOVE
      PLNK=PLNK/PLNK1
      TERM2=PLNK*EX

      IF(.NOT. DBUG) GO TO 33
      WRITE(Q,34) PLNK,TERM2
   34 FORMAT(/*  PLNK NORMALIZED =*E12.5/
     *  40X,                                *  VALUE OF TERM2 =*E12.5)
   33 CONTINUE


C      NEXT FIND TERM3
C      TERM3 = 2*SUM OF FUNCTION(2I) FOR I=1,2,.....M-1
C      WHEN DEPTH INDEX GOES FROM ZERO TO 2M, M8 GOES 1 TO M2P1
C      THUS TERM3 = 2*SUM OF FUNCTION(2J+1) FOR J=1,2,.....M-1
      SUM=0.0
      EXX=0.0
      MM1=M-1
      DO 19 J=1,MM1
      KK=J
      M8=(2*J)+1
      IZTEMP= IFIX(Z4)
      CALL DEPTMP(M8,TEMPS,M2,IZTEMP,TEMPP,ZCM)
      ZCM=ZCM/ZA
      CALL THICK(TT,F,OS,ZCM,DENS)
      EX=EXP(-TT*PHI)
C      SAVE THE FIRST EX IN EXX FOR COMPARISON TO LATER VALUES
      CALL PLANCK(TEMPP, XV, 2, PLNK)

      IF(.NOT. DBUG) GO TO 35
      WRITE(Q,26)TT,X,AA,PHI,EX,XV,XLAM,DWN,PLNK,PLNK1,XWAVENO
      WRITE(Q,36) TEMPP,ZCM
   36 FORMAT(/*  TEMPP=*F10.3/*  ZCM DEPTH =*F10.3 )
   35 CONTINUE

      PLNK=PLNK/PLNK1
      SUM=SUM+(PLNK*EX)

      IF(.NOT. DBUG) GO TO 37
      WRITE(Q,38) PLNK,SUM
```

```
 38  FORMAT(/*  PLNK NORMALIZED =*E12.5/*  VALUE OF SUM INSIDE DEPTH LO
    *OP =*E12.5 )
 37  CONTINUE

 19  CONTINUE
 64  CONTINUE
     IF(.NOT. DBUG) GO TO 67
     WRITE(Q,66) KK
 66  FORMAT(*  THE NUMBER OF TIMES DEPTH LOOP COMPLETED BEFORE EXIT IS *I4)
    **I4)
 67  CONTINUE
     TERM3=2.*SUM

     IF(.NOT. DBUG) GO TO 39
     WRITE(Q,40) TERM3
 40  FORMAT(/
    *  50X,  *  TERM3 =*E12.5 )
 39  CONTINUE


C     NEXT FIND TERM4
C     TERM4 = 4*SUM OF FUNCTION(2I-1) FOR I=1,2,.....M
C     WHEN DEPTH INDEX GOES FROM ZERO TO 2M, M8 GOES 1 TO M2P1
C     THUS TERM4 = 4*SUM OF FUNCTION(2J) FOR J=1,2,.....M

     SUM=0.0
     EXX=0.0
     DO 20 J=1,M
     KK=J
     M8=2*J
     IZTEMP= IFIX(Z4)
     CALL DEPTMP(M8,TEMPS-M2,IZTEMP,TEMPP,ZCM)
     ZCM=ZCM/ZA
     CALL THICK(TT,F,OS,ZCM,DENS)
     EX=EXP(-TT*PHI)
C     SAVE THE FIRST EX IN EXX FOR COMPARISON TO LATER VALUES
     CALL PLANCK(TEMPP,XV, 2, PLNK)

     IF(.NOT. DBUG) GO TO 41
     WRITE(Q,26)TT,X,AA,PHI,EX,XV,XLAM,DWN,PLNK,PLNK1,XWAVENO
     WRITE(Q,36)  TEMPP,ZCM
 41  CONTINUE

     PLNK=PLNK/PLNK1
     SUM=SUM+(PLNK*EX)

     IF(.NOT. DBUG) GO TO 42
     WRITE(Q,38)PLNK,SUM
 42  CONTINUE

 20  CONTINUE
 65  CONTINUE
     IF(.NOT. DBUG) GO TO 68
     WRITE(Q,66) KK
 68  CONTINUE
```

```
      TERM4=4.*SUM
      IF(.NOT. DBUG) GO TO 43
      WRITE(Q,44) TERM4
   44 FORMAT(/
     * 60X,   *  TERM4 =*E12.5  )
   43 CONTINUE

C      NEXT FIND INTEGRAL
C      INTEGRAL = (H/3)*(TERM1 + TERM2 + TERM3 + TERM4 )
C      H=(B-A)/2M
      H=(Z-0.)/FLOAT(M2)
C      IN OUR PROBLEM, WE WE SET BOUNDARY A TO ZERO.
C      SUM = INTEGRAL
      SUM=0.0
      SUM=(H /3.)*(TERM1 + TERM2 + TERM3 + TERM4 )
C      EMERGENT INTENSITY EINT FOR FREQUENCY IN THIS LOOP FOLLOWS
      EINT(JJJ) = PHI*SUM

      IF(.NOT. DBUG) GO TO 45
      WRITE(Q,46)TERM1,TERM2,TERM3,TERM4,SUM,PHI,EINT(JJJ)
   46 FORMAT(/*  TERM1 =*E12.5/*  TERM2 =*E12.5/*  TERM3 =*E12.5/
     * *  TERM4 =*E12.5/*  SUM THE INTEGRAL =*E12.5/
     *  *  PHI =*E12.5 /*  EMERGENT INTENSITY =*E12.5,///// )
   45 CONTINUE

  999 CONTINUE
C      WE HAVE COMPLETED COMPUTATION FOR A GIVEN FREQUENCY
C      NEXT WE INDEX FREQUENCY DO LOOP AND REPEAT


C                        WRITE THE OUTPUT
C      XV3 CONTAINS WAVELENGTH IN ANGSTROMS.
C      XVV IS EQUIVALENCED WITH XV3.
      WRITE(Q,11)

C      PLNK2 IS PLANCK VALUE AT CENTER FREQUENCY XLAM AND TEMPERATURE
C      TEMPS(ZHP1) TO WHICH MAXIMUM OF EMERGENT POWER IS NORMALIZED.
C       LATER.  SEE BELOW.
      TEM=TEMPS(ZHP1)
      CALL PLANCK( TEM,XLAM, 2, PLNK2)

C      INTEGRATE THE SPECTRUM AND WRITE THE VALUE.
      VAL=0.
      NFQM1=NFREQ-1
      DO 95 J=1,NFQM1
   95 VAL=(((EINT(J)+EINT(J+1))/2.)*(XVV(J+1)-XVV(J)))+VAL
      WRITE(Q,96) XVV(1),XVV(NFREQ), VAL
   96 FORMAT(/*  THE EMERGENT POWER INTEGRAL ..  ..AUR NON-NORMALIZED)
     *AS ORIGINALLY COMPUTED, FROM*
     *       /F12.3* ANGSTROMS  TO* F12.3* ANGSTROMS IS* E12.5)
      WRITE(Q,102)
  102 FORMAT(*   POWER VALUES AS COMPUTED. NOT NORMALIZED*)
      WRITE(Q,85)
```

```
 85  FORMAT(//*      EMERGENT INTENSITY*)
     WRITE(Q,47)(((XVV(J),EINT(J)),J=1,NFREQ))
 47  FORMAT(//(5(2X,F12.3,F12.5)))

C                PLOT OUTPUT
C      NORMALIZE MAXIMUM OF EINT TO UNITY SO WE CAN PLOT
     YMAX=EINT(1)
     DO 58 J=2,NFREQ
     IF(EINT(J) .GT. YMAX) YMAX=EINT(J)
 58  CONTINUE
C      NOW YMAX CONTAINS THE NORMALIZATION CONSTANT FOR EINT

C      NEXT FINDS NCARDS THE NUMBER OF DATA CARDS IN A SET.
     AKKM=FLOAT(NFREQ)
     AKKKM=AKKM/4.
     NFREQ4=NFREQ/4
     IF(ABS(AKKKM-NFREQ4) .LT. 0.2) 104,105
104  NCARDS=NFREQ4
     GO TO 106
105  NCARDS=NFREQ4+1
106  CONTINUE

C      A1 IS AA TIMES TORR/760
     A1=(AA*TORR)/760.

C      NEXT DO LOOP PUNCHES NDUPS SETS OF CARDS
     IF(PUNCH1)107,108
107  CONTINUE
     DO 103 KA=1,NDUPS
     JTT=4
     JBB=1
     PUNCH 109,DM,YE,Z,DENS,A1,GROUP,TORR
109  FORMAT(1X,A10,A2,*Z=*F3.1,*DENS=*E12.5,* AA=*F7.5,* GROUP*I3,
    * F6.0,*TORR RADIANT*)
     PUNCH 110,VAL, XVV(1),XVV(NFREQ), YMAX,TEM,PLNK2,NFREQ,NCARDS
110  FORMAT(1X,E12.5,2F9.3,E12.5,F6.0,E12.5,2I5 )
C      INTEGRAL VALUE HERE IS NOT  NORMALIZED.
C      DATA HERE ARE AS COMPUTED
     DO 111 L=1,NCARDS
     PUNCH 112,L, ((XVV(J),EINT(J)),J=JBB,JTT)
112  FORMAT( I4,4(F7.2,E12.5))
     JBB=JBB+4
     JTT=JTT+4
111  CONTINUE
     PUNCH 113, ZZ
113  FORMAT(A1)
103  CONTINUE
108  CONTINUE

C      NEXT DO THE NORMALIZATION
     DO 61 J=1,NFREQ
     EINT(J)=EINT(J)/YMAX
 61  CONTINUE
     IF( .NOT. PLOT1 ) GO TO 57
C      EINT IS NORMALIZED AND IS READY FOR PLOT
```

```
      WRITE(Q,11)
      WRITE(Q,59)
   59 FORMAT(1H1,50X, *  FROM PROGRAM LTE4 *)
      WRITE(Q,63) DM,YE,IHR,MIN,ISEC
     *  ,GROUP,TORR
      WRITE(Q,24)H,Z,F,OS,DENS,AA,NFREQ,TEMPL,DWN,XLAM,DBUG,STEP,PLOT1
      WRITE(Q,81)OS1,OS2,XLAM1,XLAM2
      WRITE(Q,89) TEMPS(1), TEMPS(ZMP1)
   89 FORMAT(*  BOUNDARY TEMPERATURE IS*F7.0,8X,* CENTER TEMPERATURE IS*
     *  F7.0)
      WRITE(Q,10) O62,(TEMPS(J),J=1,ZP1)
      WRITE(Q,22) F, DWN,AHW
      WRITE(Q,23) XLAM,PLNK1
C      PLNK2 IS PLANCK VALUE AT CENTER FREQUENCY XLAM AND TEMPERATURE
C      TEMPS(ZMP1) TO WHICH MAXIMUM OF EMERGENT POWER IS NORMALIZED.
C       SEE BELOW.
      WRITE(Q,98) PLNK2, XLAM, TEM
   98 FORMAT(*  PLANCK VALUE IS* E12.5*  AT CENTER FREQUENCY* F12.3/
     * *    AND AT  CENTER TEMPERATURE* F12.3 *DEGREES KELVIN.*/
     **        TO WHICH MAXIMUM OF EMERGENT POWER IS NORMALIZED.* )
      WRITE(Q,60) YMAX,DUM
   60 FORMAT(*  YMAX THE NORMALIZATION CONSTANT FOR EINT IS*E12.5,/
     * *  THE OPTICAL THICKNESS (TOTAL) IS*E12.5)
      CALL PLOT(EINT,XVV,NFREQ)
   57 CONTINUE

C       NEXT NORMALIZE TO PLNK2 VALUE
      DO 97 J=1,NFREQ
C      INTEGRATE NEXT
   97 EINT(J)= EINT(J) * PLNK2
      VAL=0.
      NFQM1=NFREQ-1
      DO 100  J=1,NFQM1
  100 VAL=(((EINT(J)+EINT(J+1))/2.)*(XVV(J+1)-XVV(J)))+VAL
      WRITE(Q,11)
      WRITE(Q,98) PLNK2, XLAM, TEM
      WRITE(Q,99) XVV(1),XVV(NFREQ), VAL
   99 FORMAT(  /*  THE EMERGENT POWER (MAXIMUM NORMALIZED TO PLANCK) FRO
     *OM* F12.3*ANGSTROMS TO *F12.3* ANGSTROMS*/
     *  *    IS*E12.5  )
      WRITE(Q,101)
  101 FORMAT(*   POWER NORMALIZED TO PLANCK VALUE FOLLOWS*)
      WRITE(Q,85)
      WRITE(Q,47)(((XVV(J),EINT(J)),J=1,NFREQ))

C      PUNCH2 NEXT
C      NEXT DO LOOP PUNCHES NDUPS SETS OF CARDS
      IF(PUNCH2)114,115
  114 CONTINUE
      DO 116 KA=1,NDUPS
      JTT=4
      JRR=1
      PUNCH 109,DM,YE,Z,DENS,A1,GROUP,TORR
      PUNCH 110,XVV(1),XVV(NFREQ), YMAX,TEM,PLNK2,NFREQ,NCARDS
C      INTEGRAL VALUE IS AFTER NORMALIZATION TO PLNK2.
```

```
C      DATA ARE NORMALIZED TO PLNK2.
      DO 117 L=1,NCARDS
      PUNCH 112,L, ((XVV(J),EINT(J)),J=JBB,JTT)
      JBB=JBB+4
      JTT=JTT+4
 117  CONTINUE
      PUNCH 113, ZZ
 116  CONTINUE
 115  CONTINUE

C      REUSE XV1 STORAGE TO HOLD WAVELENGTHS FROM EYEBAL
      CALL EYEBAL (XV1,392)

C     NOW PUT A2 IN COMMON/B6/ INTO PHI1 STORAGE
      DO 119 J=1,392
      PHI1(J)=A2(J)
 119  CONTINUE

      CALL COREKT(EINT,XVV,NFREQ,PHI1,XV1,392,1,PHI2)
C
C      PUT CORRECTED DATA FROM PHI2 INTO EINT
      DO 120 J=1,NFREQ
      EINT(J)=PHI2(J)
 120  CONTINUE
C
C      INTEGRATE THE LUMINOUS VALUE AND WRITE THE VALUE
      VAL=0.
      NFOM1=NFREQ-1
      DO 129 J=1,NFOM1
 129  VAL=(((EINT(J)+EINT(J+1))/2.)*(XVV(J+1)-XVV(J)))+VAL
      WRITE(0,130)XVV(1),XVV(NFREQ), VAL
 130  FORMAT(/*  THE LUMINOUS POWER INTEGRA.(MAXIMUM NON-NORMALIZED)
     *AS ORIGINALLY COMPUTED, FROM*
     *       /F12.3* ANGSTROMS  TO* F12.3* ANGSTROMS "S* E12.5)

C      FIND MAX OF EINT  LUMINOUS ENERGY
      YMAX=EINT(1)
      DO 121 J=2,NFREQ
      IF(EINT(J) .GT. YMAX) YMAX=EINT(J)
 121  CONTINUE
C      NOW YMAX CONTAINS NORMALIZATION CONSTANT OF LUMINOUS POWER  EINT
C
      WRITE(0,123)
 123  FORMAT(///*   RELATIVE LUMINOUS POWER  NOT NORMALIZED*)
      WRITE(0,47)(((XVV(J),EINT(J)),J=1,NFREQ))
C
C      NEXT NORMALIZE EINT TO UNITY
      DO 122 J=1,NFREQ
      EINT(J)=EINT(J)/YMAX
 122  CONTINUE
C
C      PUNCH3 HERE
C      THIS IS LUMINOUS POW. NORMALIZED TO UNITY
C      NEXT DO LOOP PUNCHES NDUPS SETS OF CARDS
      IF(PUNCH3)125,126
```

```
 125  CONTINUE
      DO 127 KA=1,NDUPS
      JTT=4
      JBB=1
      PUNCH 124,DM,YE,Z,DENS,A1,GROUP,TORR
 124  FORMAT(1X,A10,A2,*Z=*F3.1,*DENS=*E12.5,* AA=*F7.5,* GROUP*I3,
     *  F6.0,*TORR LUMINOUS*)
      PUNCH 110,VAL, XVV(1),XVV(NFREQ), YMAX,TEM,PLN<2,NFREQ,NCARDS
C      INTEGRAL VALUE VAL IS LUMINOUS BEFORE NORMALIZATION.
      DO 128 L=1,NCARDS
      PUNCH 112,L, ((XVV(J),EINT(J)),J=JBB,JTT)
      JBB=JBB+4
      JTT=JTT+4
 128  CONTINUE
      PUNCH 113, ZZ
 127  CONTINUE
 126  CONTINUE
      WRITE(Q,49)
  49  FORMAT(1H1,10(/),50X,*  END OF CASE* )
      GO TO 1
      END
```

```
      SUBROUTINE PLOT(EINT,XVV,NFREQ)
C   WRITTEN BY B E DOUDA 4 SEPT 1969

      DIMENSION LINE(132),EINT(2000),XVV(2000)
      INTEGER Q
      DATA Q/6/
      DATA(BLANK=1H ), (DOL=1H$), (X=1HX), ( Y=1H*), ( Z=1HO)
      TYPE INTEGER BLANK, DOL, X,Y, Z
C
      WRITE(Q,9)
    9 FORMAT(/45X38HRELATIVE POWER (NORMALIZED)
     */,16X3H0.022X4H0.2521X3H0.522X4H0.7521X3H1.0 )
C
C   PRINT A LINE OF DOL TO MAKE VERTICAL AXIS
      DO 10 J=1,132
   10 LINE(J)=BLANK
      DO 20 J=16,119
   20 LINE(J) = DOL
      WRITE(Q,30)(LINE(J),J=16,119)
   30 FORMAT (4X9HANGSIROMS2X104A1)
C
C  BLANK THE LINE
      DO 40 J=17,118
   40 LINE(J) = BLANK
      NFR=NFREQ
      DO 70 N=1,NFR
C
C  PUT X IN SELECTED LOCATION
      IF( EINT(N) .LT. 0. .OR. EINT(N) .GT. 1. ) GO TO 120
      J=100. * EINT(N) + 18.5
      LINE(J) = X
   50  CONTINUE
      WRITE(Q,60) N,XVV(N),(LINE(L),L=16,119)
  60  FORMAT(I5,1X,F8.2,1X,104A1)
C
C  PUT A  BLANK BACK IN THE LOCATION WHERE X WAS
      LINE(J) = BLANK
   70 CONTINUE
      DO 80 J=1,132
   80 LINE(J)=BLANK
      DO 90 J=16,119
   90 LINE(J) = DOL
C
      WRITE(Q,100)( LINE(J),J=16,119)
  100 FORMAT(15X104A1)
      RETURN
C
 120  WRITE(Q,130)
  130 FORMAT(//1X,*EINT    IS NEGATIVE OR GREATER THAN 1.0.  IF NEGATIVE
     *, LOOK FOR ERROR IN PROGRAM.*/*  IF GREATER THAN ONE,
     *  CHECK NORMALIZATION*//)
      RETURN
      END
```

```
      SUBROUTINE PLANCK (T,X,N,R)
C      PROGRAMMED BY B E DOUDA.  OCT 1970.   RUNS ON CDC6600.
C      T=TEMPERATURE, X=WAVELENGTH IN ANGSTROMS, R=RADIANT EXITANCE
C      N DETERMINES UNITS ASSIGNED TO R
C      C1=3.7415E-5 CM**2 ERG/SEC = 3.7415E11 A**2 ERG/SEC
C      C1=3.7415E4 A**2 J/SEC = W A**2   C1=2*PI*H*C*C*
C      C2=1.43879 CM K = 1.43879E8 A K
C      R = WATTS/A**2/A     R VALUES ARE PER HEMISPHERE.
C      R*1.E20 = WATTS/CM**2/MICRON  WHEN N=2
C      THERE ARE 1E+8 ANGSTROMS/CM
C      ONE MICRON = 1E+4 ANGSTROMS
C      R = PLANCK POWER
      DATA (C1=3.7415E4), (C2=1.43879E8)
      E = EXP( C2/(X*T))
      R = C1/( (X**5.) * (E-1.))
      IF(N .EQ. 2 )R=R*1.E20
      RETURN
      END
```

```
      SUBROUTINE DEPTMP(M8,TEMPS,M2,Z,TEMPP,ZCM)
C      B E DOUDA 25MARCH 1972
      DIMENSION TEMPS(201)
      INTEGER Z
       INTEGER ZP1
C      FIND DEPTH CALLED SIZE FOR EACH SIMPSON INTERVAL
      SIZE=FLOAT(Z)/FLOAT(M2)
      ZCM=(M8-1) * SIZE
C      ZCM, THE DEPTH IN CM AT M8, IS RETURNED TO MAIN PROGRAM
C      NEXT FIND TEMPP AT M8
       ZP1=Z+1
      M2P1=M2+1
C      HERE SIZE IS THE NUMBER OF SIMPSON RULE INTERVALS/CM DEPTH
      SIZE=FLOAT(M2)/FLOAT(Z)
      IF(M8 .EQ. 1) GO TO 30
      IF(M8 .EQ. M2P1) GO TO 40
      DO 10 J=2,ZP1
      K=J
      X=(J-1)*SIZE
      IF(X .GT. (M8-1)) GO TO 20
   10 CONTINUE
   20 DIFF=X-(M8-1)
      FRAC=DIFF/SIZE
      DIFF=TEMPS(K) - TEMPS(K-1)
      SIZE=FRAC*DIFF
      TEMPP = TEMPS(K) - SIZE
      RETURN

   30 TEMPP = TEMPS(1)
      RETURN

   40 TEMPP = TEMPS(ZP1 )
      RETURN
      END
```

```
      FUNCTION VOIGT(X,A)
C     PROGRAM WRITTEN BY G. RYBICKI
C     COMPUTES VOIGT FUNCTION FOR ANY VALUE OF X AND ANY
C     POSITIVE VALUE OF A.  BEFORE CALLING FIRST TIME
C     ENTER COFVOI WITH THE STATEMENT
C     DUMMY1=COFVOI(DUMMY2,DUMMY3)
      DIMENSION C(31)
      TYPE COMPLEX Z
      IF(A.EQ.0.0)GO TO 50
      A1=3.*A
      A2=A*A
      IF(A.LT.0.1)GO TO 10
      Z=CEXP(-9.424777960769 38*A,9.424777960769 38*X)
      VOIGT=0.0
      GO TO 20
   10 Z=CCOS(9.424777960769 38*X,9.424777960769 38*A)
      VOIGT=0.564189583547756*EXP(A2-X*X)*COS(2.*A*X)
   20 B1=(1.-REAL(Z))*A*1.5
      B2=-AIMAG(Z)
      S=-B.-1.5*X
      T=S*S+2.25*A2
      DO 40 N=1,31
      T=T+S+0.25
      S=S+0.5
      B1=A1-B1
      B2=-B2
      IF(T.GT.2.5E-12)GO TO 30
      VOIGT=VOIGT-C(N)*A*.333333333333333
      GO TO 40
   30 VOIGT=VOIGT+C(N)*(B1+B2*S)/T
   40 CONTINUE
      RETURN
   50 VOIGT=0.564189583547756*EXP(-X*X)
      RETURN
      ENTRY COFVOI
      K=-16
      DO 60 N=1,31
      K=K+1
   60 C(N)=0.0897935610625833*EXP(-FLOAT(K*K)/9.)
      RETURN
      END
```

```
      SUBROUTINE THICK(TT,F,OS,Z,DENS)
C      INPUT F, OS, Z, DENS
C      OUTPUT TOTAL OPTICAL THICKNESS TT AT DEPTH Z
C      B. E. DOUDA 20 MARCH 72

      DATA(P=3.141592654),(E=4.80298E-010),(RM=9.1091E-028)
      DATA(C=2.997925E+010)
C     DATA(TTC=6.000E+007)

C      TT= TOTAL OPTICAL THICKNESS= DIMENSIONLESS
C      P= PI
C      E= ELECTROSTATIC CHARGE (CM**1.5) (G**.5) (S**-1)
C      Z= PHYSICAL DEPTH OF ATMOSPHERE CM
C      F= DOPPLER HALF WIDTH IN FREQUENCY UNITS (S**-1)
C      RM= ELECTRON REST MASS G
C      C= SPEED OF LIGHT (CM) (S**-1)
C      DENS= N12= PARTICLES/CC IN ATOMSPHERE
C      OS= OSCILLATOR STRENGTH OF LINE, DIMENSIONLESS
C      H= PLANCK CONSTANT ERG S
C      V= CENTER FREQUENCY OF LINE 1/S
C      ERG= DYNE CM DYNE= GM CM/SEC**2
C      B12= EINSTEIN COEFFICIENT = (OS*4*P*P*E*E)/(F*RM*C)
C     ABOVE B12 IS FORM WHEN N12 IS IN DENSITY UNITS
C      TT= (H*V) / (4*P*F) * (N12 * B12 - N21 * B21) * Z
C      N21 * B21 IS NEGLIGIBLE

      TT = (DENS*OS    *P * E * E * Z ) / ( F * RM * C )


C      DENSC= DENSITY AT SPECIFIED THICKNESS , TTC
C     DENSC = (TTC*F*RM*C)/(OS    *P*E*E*Z)
C     WRITE (61,10) DENSC, TTC
C  10 FORMAT (1H1,2E21.14)

      RETURN
      END
```

```
      SUBROUTINE DOPPLER(XLAM,NK,TEMP,FHWIDTH,DWN ,AHW )
C     COMPUTES DOPPLER HALFWIDTH OF ATOMIC LINE AT SOME TEMPERATURE
C     WRITTEN BY F E DOUDA 25 AUG 1969

C     TEMP IS DEGREES KELVIN, XMASS IS WEIGHT PER MOLE,AND
C     XLAMBDA IS THE CENTER OF THE RESONANCE LINE IN ANGSTROMS.
C
      DIMENSION ANG(  1,1),XLAMBDA(2),AHWIDTH(3),DWAVENO(3)
      DIMENSION FREQ(  1)
      TYPE REAL LAMBDAP, LAMBDAM
      IF (NK .NE. 0 ) GO TO 10
      XMASS    2.9898

C     XLAMBDA(2) = 5895.9236
C     XLAMBDA(1) = 5889.9504
C     XLAMBDA(1)=5893.
C     XLAMBDA(2)=5893.

      K=1
      XLAMBDA(K)=XLAM
C     XLAM = LINE CENTER IN ANGSTROMS.
      BOLTZ=1.38054E-016
      SPEEDLI =2.997925E010
      AVAGAD=6.02252E023
      CONSTAN =2.0*SQRT(2.0*BOLTZ)*SQRT(ALOG(2.0))*SQRT(AVAGAD)/SPEEDLI

C     FHWIDTH IS DOPPLER HALFWIDTH IN FREQUENCY UNITS

      FHWIDTH=(CONSTAN*SPEEDLI/(XLAMBDA(K)*1.0E-8))*SQRT(TEMP/XMASS)
      XWAVENO =1.0/(XLAMBDA(K) * 1.0E-8)

      DWAVENO(K)=FHWIDTH/SPEEDLI
C      DWN = DOPPLER WIDTH IN WAVENUMBERS.
      DWN=DWAVENO(K)

      HWAVENO= DWAVENO(K)/2.0
      LAMBDAP=1.0E+8/ (XWAVENO + HWAVENO)
      LAMBDAM=1.0E+8/ (XWAVENO - HWAVENO)
C
C     AHWIDTH IS DOPPLER HALFWIDTH IN ANGSTROMS
      AHWIDTH(K) = LAMBDAM - LAMBDAP
      AHW = AHWIDTH(K)

      RETURN
   10 CONTINUE
      NF1=NFREQ-1
      DO 20 I=1,NFREQ
      ID=NFREQ-I+1
      ANG(I+NF1,K) = 1.0E+8 / (XWAVENO - (DWAVENO(K) * FREQ(I)))
      ANG(ID,K) = 1.0E+8 / (XWAVENO + (DWAVENO(K) * FREQ(I)))
   20 CONTINUE
      AHWIDTH(3)=AHWIDTH(2)
      J=K

      DWAVENO(3) = DWAVENO(2)
C     CALL PRINT(4)
      RETURN
      END
```

```
      SUBROUTINE COREKT (A,XA,KA,B,XB,KB,M,C)
C      PROGRAMMED BY B E DOUDA.  OCT 1970.   RUNS ON CDC6600.
C     DIMENSION    A(1000),XA(1000),   B(1000),XB(1000),     C(1000)
C     DIMENSION    A(4000),XA(4000),   B(4000),XB(4000),     C(4000)
      DIMENSION    A(2000),XA(2000),   B(2000),XB(2000),     C(2000)
C      INPUT. A(KA) ARE INTENSITIES TO BE CORRECTED AT KA POINTS
C      INPUT. XA(KA) ARE WAVELENGTHS ASSIGNED TO A
C      INPUT. B(KB) ARE DATA THAT CORRECT A.
C      INPUT. XB(KB) ARE WAVELENGTHS ASSIGNED TO B
C      INPUT. KA IS NUMBER OF A, KB IS THE NUMBER OF B
C      M SETS TYPE OF CORRECTION
C      DOES A/B=C AT WAVELENGTHS ASSIGNED TO A WHEN M=0
C      DOES A*B=C AT WAVELENGTHS ASSIGNED TO A WHEN M=1
C      OUTPUT. C(KA) ARE THE CORRECTED DATA AT KA POINTS AND
C       AT WAVELENGTH XA.
      IF(XA(1).LT.XB(1).OR.XA(KA).GT.XB(KB)) WRITE(6,1)
    1 FORMAT(//,* CHECK RANGE OF B IN SUBROUTINE COREKT FOR ADEQUACY*//)
      KBM=KB-1
      DO 3 J=1,KA
      DO 3 K=1,KBM
      KP=K+1
      IF(.NOT.(XB(K).LE.XA(J).AND.XB(KP).GE.XA(J))) GO TO 3
      D=XB(KP)-XB(K)
      E=XA(J)-XB(K)
      F=B(K)+((E/D)*(B(KP)-B(K)))
      IF(M.EQ.1) GO TO 5
      C(J)=A(J)/F
      GO TO 3
    5 C(J)=A(J)*F
    3 CONTINUE
      RETURN
      END
```

```
      BLOCK DATA EYEB
      COMMON/B6/A1(392)
C      A1 IS EYE RESPONSE TABLE USED IN EYEBAL.
      DATA((A1(J),J=1,102)=
     *0.00004000,0.00004499,0.00004947,0.00005588,0.00005866,0.00006425,
     *0.00007110,0.00007966,0.00009037,0.00010367,0.00012000,0.00013760,
     *0.00015490,0.00017290,0.00019260,0.00021500,0.00024100,0.00027150,
     *0.00030750,0.00035000,0.00040000,0.00044990,0.00049470,0.00053880,
     *0.00058660,0.00064250,0.00071100,0.00079660,0.00090370,0.00103670,
     *0.00120000,0.00137740,0.00155520,0.00174180,0.00194560,0.00217500,
     *0.00243840,0.00274420,0.00310080,0.00351660,0.00400000,0.00454850,
     *0.00515200,0.00580750,0.00651200,0.00726250,0.00805600,0.00888050,
     *0.00976000,0.01066450,0.01160000,0.01256990,0.01357920,0.01462730,
     *0.01571360,0.01683750,0.01799840,0.01919570,0.02042880,0.02169710,
     *0.02300000,0.02432270,0.02565760,0.02701490,0.02840480,0.02983750,
     *0.03132320,0.03287210,0.03449400,0.03620630,0.03800000,0.03987600,
     *0.04180800,0.04380200,0.04586400,0.04800000,0.05021500,0.05251800,
     *0.05491240,0.05740400,0.06000000,0.06265897,0.06535196,0.06810296,
     *0.07093596,0.07387495,0.07694399,0.08016700,0.08356796,0.08717096,
     *0.09099996,0.09501696,0.09917599,0.10348898,0.10796797,0.11262494,
     *0.11747199,0.12252098,0.12778395,0.13327295,0.13900000,0.14494245)
      DATA((A1(J),J=103,204)=
     *0.15071994,0.15670747,0.16287994,0.16931248,0.17607999,0.18325746,
     *0.19092000,0.19914246,0.20799994,0.21737446,0.22701597,0.23707145,
     *0.24756795,0.25856245,0.27011198,0.28227347,0.29510337,0.30866045,
     *0.32299995,0.33823997,0.35440999,0.37137997,0.38901997,0.40724999,
     *0.42593999,0.44496000,0.46422994,0.48361999,0.50299996,0.52285999,
     *0.54354995,0.56483996,0.58649999,0.60824996,0.62985998,0.65109998,
     *0.67168999,0.69139999,0.70999998,0.72770000,0.74487996,0.76154000,
     *0.77763999,0.79218994,0.80815995,0.82253999,0.83631998,0.84947997,
     *0.86199999,0.87385994,0.88505995,0.89561999,0.90556997,0.91494000,
     *0.92374998,0.93203996,0.93981999,0.94713998,0.95400000,0.96036998,
     *0.96611995,0.97133994,0.97603998,0.98024994,0.98399997,0.98731995,
     *0.99023998,0.99278996,0.99499995,0.99688395,0.99831200,0.99936795,
     *1.00001526,1.00024996,1.00006390,0.99945199,0.99840796,0.99692995,
     *0.99499995,0.99261999,0.98977995,0.98648995,0.98276997,0.97862995,
     *0.97406995,0.96912998,0.96377999,0.95807994,0.95199996,0.94551998,
     *0.93858999,0.93124998,0.92349994,0.91537994,0.90689999,0.89810997,
     *0.88900995,0.87963998,0.86999995,0.86001998,0.84958994,0.83877999)
      DATA((A1(J),J=205,306)=
     *0.82765996,0.81624997,0.80461997,0.79283994,0.78092998,0.76896000,
     *0.75699997,0.74493998,0.73286000,0.72021997,0.70762998,0.69493997,
     *0.68216997,0.66935998,0.65653993,0.64374000,0.63099998,0.61824995,
     *0.60542995,0.59255999,0.57966000,0.56674999,0.55385995,0.54101998,
     *0.52824998,0.51555997,0.50299996,0.49052995,0.47811997,0.46576995,
     *0.45347995,0.44124997,0.42907995,0.41696995,0.40491998,0.39291996,
     *0.38099998,0.36903995,0.35699999,0.34493995,0.33291995,0.32099998,
     *0.30923998,0.29769999,0.28643994,0.27551997,0.26499999,0.25484997,
     *0.24497998,0.23539996,0.22609999,0.21699995,0.20817000,0.19955999,
     *0.19117999,0.18296995,0.17499995,0.16720998,0.15963995,0.15228999,
     *0.14515996,0.13824999,0.13155997,0.12508994,0.11883998,0.11280996,
     *0.10699999,0.10143995,0.09612000,0.09104997,0.08620000,0.08155998,
     *0.07711995,0.07285994,0.06875998,0.06481999,0.06100000,0.05735000,
     *0.05389000,0.05060000,0.04750000,0.04456000,0.04178000,0.03914000,
```

```
*0.03663000,0.03426000,0.03200000,0.02990000,0.02800000,0.02628000,
*0.02470000,0.02324000,0.02188000,0.02060000,0.01938000,0.01818000,
*0.01700000,0.01584700,0.01476800,0.01375600,0.01280800,0.01191800)
 DATA((AI(J),J=307,392)=
*0.01108400,0.01030000,0.00956000,0.00886100,0.00820000,0.00759000,
*0.00704600,0.00655800,0.00612100,0.00572500,0.00536300,0.00502800,
*0.00471000,0.00440400,0.00410000,0.00381058,0.00355040,0.00331572,
*0.00310320,0.00290938,0.00273080,0.00256402,0.00240560,0.00225208,
*0.00210000,0.00195418,0.00182088,0.00169880,0.00158664,0.00148312,
*0.00138696,0.00129688,0.00121152,0.00112966,0.00105000,0.00097477,
*0.00090656,0.00084459,0.00078808,0.00073625,0.00068832,0.00064351,
*0.00060104,0.00056013,0.00052000,0.00048184,0.00044712,0.00041548,
*0.00038656,0.00036000,0.00033544,0.00031252,0.00029088,0.00027016,
*0.00025000,0.00023102,0.00021392,0.00019850,0.00018456,0.00017188,
*0.00016024,0.00014944,0.00013928,0.00012954,0.00012000,0.00011103,
*0.00010304,0.00009591,0.00008952,0.00008375,0.00007848,0.00007359,
*0.00006896,0.00006447,0.00006000,0.00005572,0.00005184,0.00004832,
*0.00004512,0.00004219,0.00003948,0.00003695,0.00003456,0.00003226,
*0.00003000,0.0        )
 END
```

```
      SUBROUTINE EYEBAL (X,N)
C      REV 22MAR71 TO USE WITH BLOCK DATA EYEB
C      PROGRAMMED BY B E DOUDA.  OCT 1970.   RUNS ON CDC6600.
C      A1 IS EYE RESPONSE TABLE. X IS CORRESPONDING WAVELENGTH. ANGSTROM
C      N  IS NUMBER OF POINTS .  X(1)=3800.   X(392)=7710.
      DIMENSION          X(392)
C      A1 TABLE IS IN BLOCK DATA EYEB.
      COMMON/B6/A1(392)
      N=392
      X(1)=3800.
      DO  2 J=2,N
      JM1=J-1
    2 X(J)= X(JM1)+10.
C     WRITE(6,3) (X(J),A1(J),J=1,N)
C 3   FORMAT(/A( 6(1X,F6.0,E14.7)))
C      NORMALIZE MAXIMUM POINT TO 1.0
      AN=A1(176)
      DO 4 J=1,N
    4 A1(J)=A1(J)/AN
C     WRITE(6,3) (X(J),A1(J),J=1,N)
      RETURN
      END
```

VITA

Bernard Edward Douda

Place and Date of Birth

Lonsdale, Minnesota, 22 May 1930

Education

Primary School, Lonsdale, Minnesota, 1935-1943
High School, Faribault, Minnesota, 1943-1947
Cornell College, Mount Vernon, Iowa, 1947-1951 (A.B. 1951)
Indiana University, Bloomington, Indiana, 1964-1973 (M.S. 1969)

Honorary and Professional Societies

American Chemical Society
Optical Society of America
American Institute of Physics
Sigma Xi
Phi Lambda Upsilon

Positions

Chemical Engineer, NAD Crane, Indiana, 1956-1971

Manager, Chemical Sciences Division, Research and Development Department, Naval Ammunition Depot, Crane, Indiana, 1971-1973

Publications

Application of Radiative Transfer Theory to Illuminating-Flare Flames, Bull. Am. Phys. Soc. 15, 1526 (1970).

Visible Radiation from Illuminating-Flare Flames: Strong Emission Features (with R. M. Blunt and E. J. Bair), J. Opt. Soc. Am. 60, 1116 (1970).

Visible Radiation from Illuminating-Flare Flames. II. Formation of the Sodium Resonance Continuum (with E. J. Bair), J. Opt. Soc. Am. 60, 1257 (1970).

Red Highway Flare Spectrum, Am. J. Optom. and Arch. Am. Acad. Optom. 49, 415 (1972).

Emission Studies of Selected Pyrotechnic Flames, J. Opt. Soc. Am. 55, 787 (1955).

U.S. Patents

White Smoke Composition, 3,625,855, Class 252/305 (7 December 1971).

Device for Producing White Smoke by Imploding Red Phosphorus, 3,625,155, Class 102/90 (7 December 1971), Coinventor with Roscoe D. Dwiggins.

White Smoke Composition Containing Red Phosphorus, 3,607,472, Class 149/19 (21 September 1971).

Aircraft Parachute Flare, 3,499,385, Class 102/35 (10 March 1970).

Illuminating Flare Composition Composed of Magnesium, Sodium Nitrate, and a Vinyl Terminated Polysiloxane Binder, 3,411,964, Class 149/19 (19 November 1963).

Illuminating Flare Composition Composed of Magnesium, Sodium Nitrate, and an Epoxy Resin-Polyglycol Resin Binder, 3,411,963, Class 149/19 (10 November 1968).

Process for Polymerizing Acrylic Monomers with Strontium Perchlorate for Pyrotechnics and Propellants, 3,369,946, Class 149/83 (20 February 1968).

Pyrotechnic Compound Tris(Glycine) Strontium (II) Perchlorate and Method for Making Same, 3,296,045, Class 149/75 (3 January 1967).

Plastic Pyrotechnic Compositions Containing Strontium Perchlorate and Acrylic Polymer, 3,258,373, Class 149/19 (28 June 1966).